2022

LIPOSOMAL TECHNOLOGIES TO IMPROVE GENE DELIVERY

David Nardo Padron
University of Kentucky, dna235@uky.edu
Author ORCID Identifier:
https://orcid.org/ 0000-0003-3009-7686
Digital Object Identifier: https://doi.org/10.13023/etd.2022.280

STUDENT AGREEMENT:

I represent that my thesis or dissertation and abstract are my original work. Proper attribution has been given to all outside sources. I understand that I am solely responsible for obtaining any needed copyright permissions. I have obtained needed written permission statement(s) from the owner(s) of each third-party copyrighted matter to be included in my work, allowing electronic distribution (if such use is not permitted by the fair use doctrine) which will be submitted to UKnowledge as Additional File.

I hereby grant to The University of Kentucky and its agents the irrevocable, non-exclusive, and royalty-free license to archive and make accessible my work in whole or in part in all forms of media, now or hereafter known. I agree that the document mentioned above may be made available immediately for worldwide access unless an embargo applies.

I retain all other ownership rights to the copyright of my work. I also retain the right to use in future works (such as articles or books) all or part of my work. I understand that I am free to register the copyright to my work.

REVIEW, APPROVAL AND ACCEPTANCE

The document mentioned above has been reviewed and accepted by the student's advisor, on behalf of the advisory committee, and by the Director of Graduate Studies (DGS), on behalf of the program; we verify that this is the final, approved version of the student's thesis including all changes required by the advisory committee. The undersigned agree to abide by the statements above.

David Nardo Padron, Student

Vincent J. Venditto, Major Professor

David J. Feola, Director of Graduate Studies

LIPOSOMAL TECHNOLOGIES TO IMPROVE GENE DELIVERY

DISSERTATION

A dissertation submitted in partial fulfillment of the
requirements for the degree of Doctor of Philosophy in the
College of Pharmacy
at the University of Kentucky

By

David Nardo Padron

Lexington, Kentucky

Co- Directors: Dr. Vincent J. Venditto, Assistant Professor of Pharmaceutical Sciences

and Dr. David J. Feola, Professor of Pharmacy Practice and Science

Lexington, Kentucky

2022

https://orcid.org/ 0000-0003-3009-7686

ABSTRACT OF DISSERTATION

LIPOSOMAL TECHNOLOGIES TO IMPROVE GENE DELIVERY

Lipid based nanoparticles (LBNs) are used in myriad applications in medicine from small molecule drug delivery to mRNA vaccines. A major contributing factor to the development of the field has been the ongoing development of novel compounds that retain the functionality of natural lipids but expand upon them through inclusion of functional moieties that can be applied to specific scientific and biomedical questions. In the body of this dissertation, an extensive overview of LBNs is provided, focusing primarily on their use in immune modulation. The research presented herein begins with the synthesis of a novel class of lipids based on the triazine (TZ) cyanuric chloride. Twelve compounds were synthesized and assessed for their biophysical behavior and ability to form LBNs. Of the 12 compounds, 10 were able to form nanoparticles and these were assessed for in vitro toxicity. The toxicity of the nanoparticles differs based on the nanoparticle charge and approximate that observed for similarly charged compounds. The cationic TZ lipids were then tested in vitro for their ability to deliver plasmid DNA into cells where they showed improved efficacy compared with the cationic lipid DOTMA, and similar toxicity. Finally, TZ lipids were used to lipidate peptides in a liposomal peptide vaccine where they induced similar anti-peptide titers as a CHEMS conjugate. Following these experiments, the in vivo toxicity and potential for plasmid delivery was evaluated for the cationic TZ lipids. TZ lipids led to toxicity similar to other cationic lipids. Of note, the PEG length in the nanoparticles was studied for its effect on transfection efficiency as was the effect of the helper lipid in the formulation. These experiments showed improved transfection efficiency with DOPE and with shorter length PEG chains on the nanoparticle surface. Evaluation of immune responses toward the transgene studied showed a similar titer response as the free protein. However, when the protein was delivered with a cationic lipid as control, titers increased significantly, particularly for the TZ lipid used, which increased titers 1000-fold. These data provide evidence for continued evaluation of TZ lipids as gene delivery vectors and as potential vaccine adjuvants. Finally, in continuing the evaluation of LBNs to improve gene therapy, an LBN based system was evaluated to deplete anti-AAV8 antibodies. As one of the most promising strategies to deliver transgenes since AAV provides an excellent platform that is unfortunately affected by the presence of anti-viral antibodies. This system, using doxorubicin liposomes coated with recombinant VP1 protein bound to DGS-NTA-Ni lipid or DSPE-PEG_{2000}-Maleimide, failed to deplete circulating antibodies to AAV. However, the results of the experiments carried out shed light on how this strategy might be improved upon at a later time. Finally, in an attempt to better understand the immune targets on AAV, the antibody response toward AAV8 was tested in human samples from deidentified blood donors and compared with that of mice and monkeys treated with the virus. Serum from these species was scrutinized for its ability to neutralize the virus in vitro and evaluated using a peptide array for targets against the viral capsid protein VP1. Collectively, the studies presented in the body of this dissertation

demonstrate the utility of LBNs in gene delivery, both as vectors and as aids for viral delivery.

KEYWORDS: Drug delivery, Gene delivery, Immune modulation, Liposome, Vaccines.

David Nardo Padron

[06/17/2022]

Date

LIPOSOMAL TECHNOLOGIES TO IMPROVE GENE DELIVERY

By
David Nardo Padron

Vincent J. Venditto
Co-Director of Dissertation

David J. Feola
Co-Director of Dissertation

David J. Feola
Director of Graduate Studies

[06/17/2022]
Date

ACKNOWLEDGMENTS

I would like to express my utmost gratitude to my lab members, both past and present, who have been instrumental in my daily work and success as a scientist. Particularly, I'd like to acknowledge Dr. Michelle G. Pitts, who has been an invaluable mentor and friend throughout my years in Lexington, as well as Dr. David M. Henson who helped me begin my journey into the world of liposomes and whose presence in my life made me a better researcher. My undergraduate students, Cierra M. Isom, Jason T. Spaude, and Nick E. Cheung, who not only helped my work progress but helped me grow as a mentor and a scientist. I would also like to thank my peers, especially Rupinder Kaur, who has been the best colleague and friend that I could ever have hoped for.

I would like to acknowledge of my research mentor, Dr. Vincent J. Venditto, whose guidance, while sometimes challenging to follow, has allowed me to arrive where I proudly am today. I'd also like to thank as my graduate committee, Dr. David Feola, Dr. Daniel Pack and Dr. Jerold Woodward, who have guided me throughout my research journey, pushed me to expand the boundaries of my knowledge and allowed me to succeed as a student researcher. Additionally, I would also like to thank Dr. Esther Penni Black for her guidance and mentorship during my time as a clinical and experimental therapeutics student, and Catina Rossoll whose friendship and guidance has been essential to my success.

In addition to the aforementioned individuals, I'd like to thank the UK COP NMR Core, Dr. Steven van Lanen's laboratory and Dr. Minakshi Bhadwaj for their help in acquiring mass spectroscopy, the PPS Core Lab for providing much of the instrumentation necessary for my work, Dr. Gregory Graf's lab, Dr. Sylvie Garneau-Tsodikova's lab, and Dr. Barbara Knutson and Dr. Steven Rankin lab in the Department of Chemical Engineering. Furthermore, the work presented herein would not have been possible without the guidance of Dr. Nishad Thamblan Chandrika and Tanya Myers-Morales who helped guide me through specific portions of my research.

Finally, I'd like to acknowledge my family, who have supported me all my life and without whom I wouldn't be who or where I am today.

TABLE OF CONTENTS

LIST OF TABLES

LIST OF FIGURES

CHAPTER 1: INTRODUCTION TO LIPID NANOPARTICLES AND THEIR UTILITY IN MODULATING IMMUNE RESPONSES[203]

1.1 Introduction

As the field of immunobiology evolves and the immune system's role in disease is better understood, there's a need to develop tools to modulate immunity. Lipid nanoparticles (LNPs), first described in 1964, are structures formed by natural or synthetic lipids when placed in an aqueous environment and range in size from 20-1000 nm in diameter. Due to the pliability and applicability of these structures, LNPs provide a tool for modulating disease and possess great potential for improving outcomes in immunological diseases.[203] LNPs can be optimized to encapsulate both lipophilic and hydrophilic therapeutics, including biomolecules, like proteins and nucleic acids. LNP therapies containing small molecules have been approved for anti-cancer, anti-fungal, and anti-angiogenic applications, paving the way for their study in modulating immune responses. More recently, LNP therapies have been approved for siRNA delivery, as well as mRNA vaccine vectors, demonstrating how far the field has come and how much potential this strategy has for improving human health. In this chapter, the use of LNP based therapies is evaluated, focusing primarily on their role in modulating immune responses.

1.1.1 Principles of lipid-based nanoparticles

The term LNP is used to describe several lipid based structures, including micelles, oil-in-water emulsions, drug-lipid complexes, cochleates and liposomes.[204] Liposomes, which are the primary focus of this chapter, are spherical vesicles composed of a single or multiple lamellar bilayers that encapsulate an aqueous core. The primary units of liposomes are lipids that naturally conform to bilayers when placed in aqueous solutions. These include lipids like phosphatidylcholine, phosphatidylethanolamine, phosphatidylserine, phosphatidic acid, phosphatidylinositol, phosphatidylglycerol and cardiolipin (Figure 1.1). Since first described by Bangham and Horne in 1964, liposomes have been evaluated for applications like drug delivery, gene transfection, imaging, immunizations, as well as to study biological processes.[205-207]

LNPs used in therapeutic delivery are made with both natural and synthetic lipids, taking advantage of the properties conferred by the hydrophilic head group and a hydrophobic tails of the lipids, as well as different preparation techniques, all of which can affect the nanoparticle structure and functionality (Figure 1.2).[204, 205, 208] Generally, liposomes are made primarily with cylindrical lipids, as these provide a more stable bilayer structure.[203] However, other lipids are used to alter structural characteristics, such as size or charge, that improve therapeutic delivery and can alter the interaction of the LNP with their target biological system.[204, 209] For example, dendritic cells will generally take up smaller, unilamellar liposomes, while macrophages tend to take up larger particles and when used for protein vaccines, LNPs larger than 100 nm skew the response toward T_H1-

dependent responses, while smaller and multilamellar liposomes skew the response toward T_H2-dependent responses.[210]

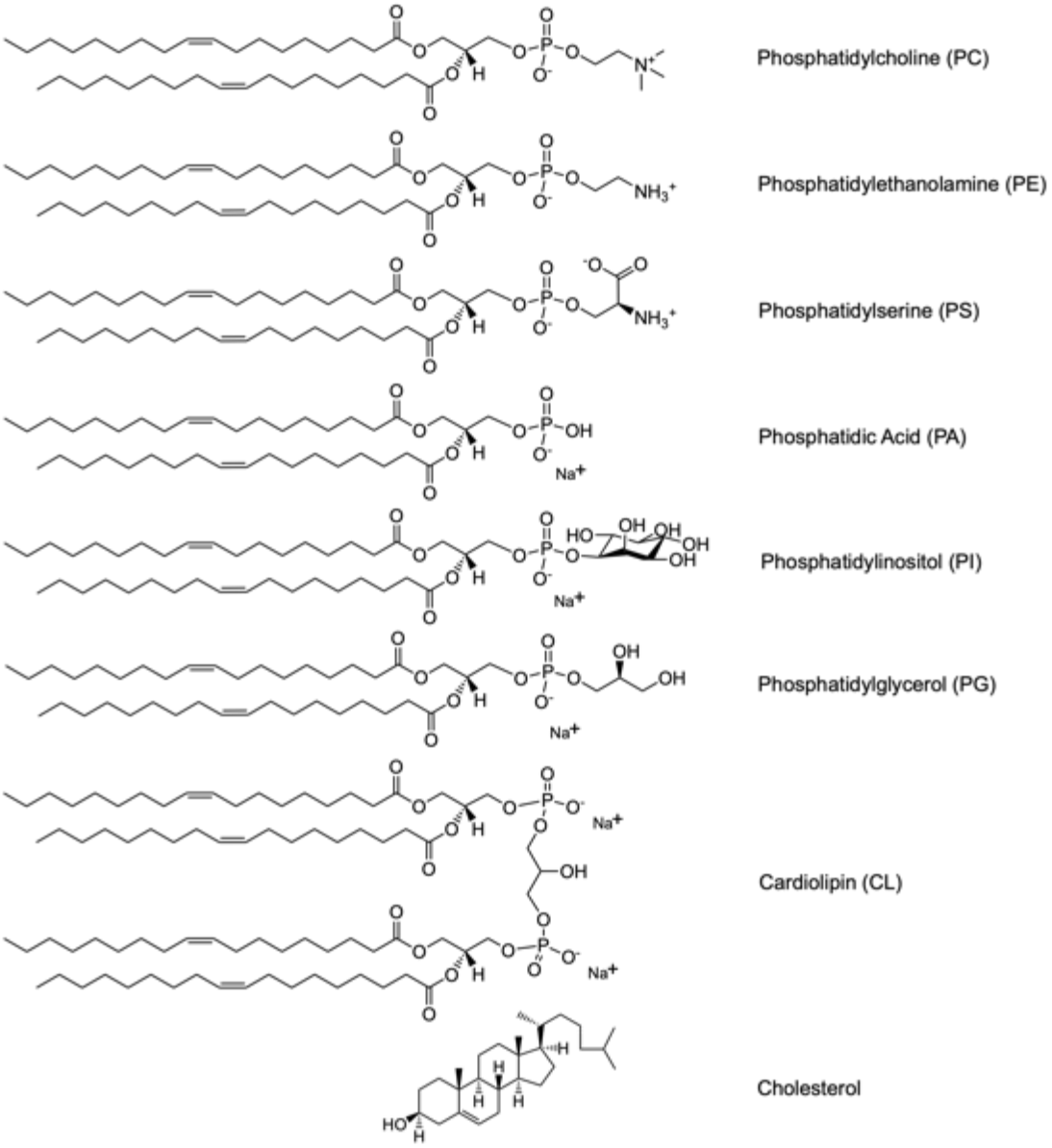

Figure 0.1 Natural phospholipids displayed with 1,2-dioleoyl-sn-glycero (DO) lipid tails. These lipids also exist in various other forms, such as dimyristoyl (DM - C14), dipalmitoyl (DP – C16) and distearoyl (DS – C18), among others. Cholesterol is included in many formulations to improve the fluidity of the LNPs.

In drug delivery, the formulation size also determines the pharmacokinetics of LNPs, as smaller particles move freely between compartments, while larger ones can be used as depots in certain tissues.[211] In protein vaccines, the fluidity of liposomal vesicles,

which can be increased by using smaller or unsaturated lipid tails or by adding cholesterol, elicits stronger responses compared with more rigid structures made with stearoyl tails.[210] Surface charge also plays a role in immunogenicity as cationic particles interact more easily with cells to induce stronger immune responses and enhance the depot effect of liposomes.[211 212] Moreover, inclusion of bioactive lipids can activate specific cellular responses. For example, sphingosine-1-phosphate (S1P) can engage with S1P receptors to mediate vascular and immune function, while eicosanoids can be used in LNPs to regulate physiological processes mediated by these metabolites.[213-217]

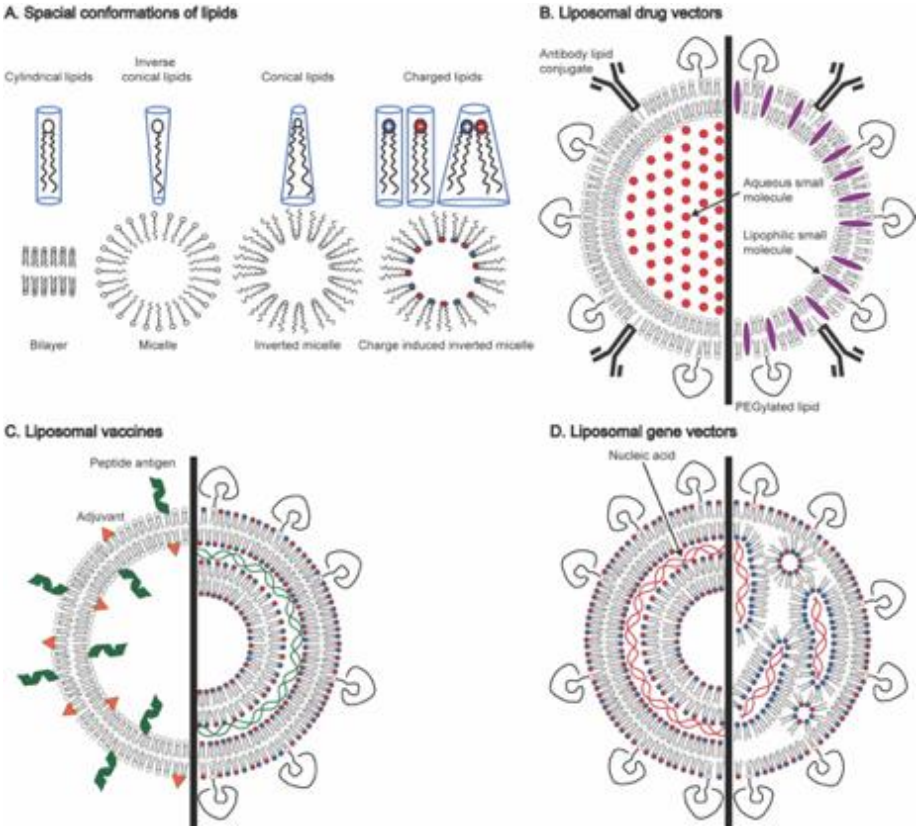

Figure 1.2: Lipid nanoparticle characteristics and biological activity can be optimized by altering the lipids used in a formulation. (A) Lipid structure (cylindrical, inverted conical, conical) dictates LNP architecture (bilayer, micelle, inverted micelles, respectively). Interactions between lipids, such as ionic interactions between headgroups, can also alter LNP architecture. (B) Small molecule delivery of water-soluble dugs (hexagons) or lipophilic drugs can be achieved by encapsulating drugs inside the nanoparticle or the bilayer itself. Further optimization can be achieved through addition of polymers that enhance pharmacokinetics (i.e. polyethylene glycol) or targeting (i.e. antibodies). (C) Liposomal vaccines can be made with both protein immunogens (helical structures) and adjuvants (triangles), as well as with nucleic acids that encode for immunogenic proteins. (D) Gene delivery has been made possible with the synthesis of cationic lipids that form lipoplexes or lipid nanoparticles that entrap nucleic acids.

1.1.2 Basics of the immune system

Modulating immune responses requires a basic understanding of the immune system and its role in disease. A crucial aspect of the immune system is to distinguish self from non-self. This function is dependent on cellular receptors that recognize pathogen associated molecular patterns (innate immunity) or highly specific targets on pathogens that can lead to immunological memory when activated (adaptive immunity).

Innate immune cells recognize pathogens through activation of pattern recognition receptors (PRRs), such as toll-like receptors (TLRs), often through the help of antigen presenting cells (APCs) like macrophages and dendritic cells. PRRs recognize pathogen associated molecular patterns (PAMPs), which are proteins, lipids, glycolipids or nucleic acids characteristic of pathogens.[218] Upon activation, PRRs initiate signaling cascades that induce the release of cytokines and chemokines to activate and recruit immune cells. Following activation, APCs upregulate the presentation of pathogen derived peptides, to activate helper T (T_H) cells and cytotoxic T lymphocytes (CTLs). While activated CTLs induce apoptosis in infected and defective (i.e. oncogenic) cells, T_H cells help to enhance immunity in several ways, including engagement with activated B cells to proliferate, promote affinity maturation of the antibody variable region, and antibody class switching from IgM and IgD to IgA, IgE and IgG.[218] In addition to responding to pathogens, the immune system also has mechanisms to inhibit responses against self-antigens and resolve immune responses after pathogens clearance. These mechanisms take advantage of inhibitory cytokines like IL-10 and TGF-beta, as well as direct cellular responses with regulatory T cells (T_{regs}).[218]

Because of the nuanced complexity of the immune system, LNPs offer an obvious mechanism for immune modulation due to the granular nature of these vehicles, which allows for highly tailorable design. In this context, the inclusion of small molecule therapeutics, nucleic acids, and immunogens can provide different ways to target specific immune responses.[219-222] This chapter will highlight advances made in the field of LNP development focused on modulating the immune system with three types of LNPs: 1) LNPs as small molecule drug carriers; 2) LNPs as vaccines; and 3) LNPs as gene delivery vehicles. Special attention will be given to the clinical utility of LNPs with lessons learned from currently approved LNP-based therapeutics that can guide future development of LNPs with targeted immunomodulatory properties.

1.2 Liposomal vaccines

When considering liposomal immune modulation, especially following the COVID-19 pandemic, the most obvious clinical examples are liposomal vaccines, which have started to become a mainstay of modern medicine.[223] Research on liposome based vaccines against diphtheria and mycobacterium were first reported in 1974.[224] Since then,

efforts in this field have led to two clinically approved virosomal vaccines against influenza and hepatitis A, and more recently, two mRNA based vaccines against COVID-19 (Table 1.2).[223, 225-227] As vaccine vectors, liposomes provide an ideal platform to tailor immune responses against antigens by incorporating adjuvants that can modulate the immune response (see figure 1.1), along with antigenic targets.[223, 225, 226]

LNP vaccines depend on the ability of antigen presenting cells to ingest liposomes and elicit the activation of immunity toward the targeted antigen, either directly, in the case of protein based vaccines, or after transduction, with nucleic acid vaccines. [228] With protein vaccines, processing of liposomal contents by APCs results in activation of PRRs by liposomal adjuvants and antigen presentation on MHC-II. Professional APCs like macrophages and dendritic cells are responsible for most liposomal uptake, however B cells can also act as APCs for encapsulated antigens.[213, 228] With nucleic acid vaccines, protein expression is achieved following transfection of cells, resulting primarily in MHC-I presentation and has been associated with CTL activation.[229-231]

Both antigens and adjuvants can be bound to liposomes via electrostatic interaction to the lipid surface, covalent and non-covalent anchoring to lipids, and encapsulation within the lipid bilayer. [213] While all these methods can be optimized to achieve adequate delivery, the method used can affect the vaccine efficacy. For example, liposomal encapsulation within the aqueous core protects molecules from degradation, which is crucial in nucleic acid vaccines and vaccines made with rapidly degrading proteins.[228, 232-235] However, with protein based vaccines, covalently anchoring antigens to the surface of the LNP bilayer can significantly enhance antigen immunogenicity. [213] In general, antibody based responses are stronger when antigens are conjugated to the surface of the nanoparticle, rather than encapsulated, although cytotoxic T lymphocyte (CTL) responses are similar with either method. [213]

The success of the COVID-19 mRNA vaccines were achieved thanks to many advances made in liposomal gene delivery, which have allowed for the possibility for creating vaccines against pathogens and tumors.[227, 236, 237] With nucleic acid based vaccines, antigens are transcribed and processed for presentation on MHC-I to activate a CTL responses, while the nucleic acid and cationic lipids in the vaccine can activate various TLRs to enhance the immune response.[227, 230, 238-241] DNA vaccines with various cationic lipids have been engineered against herpes simplex virus 1 (HSV1) and influenza A virus. [237, 242] [223, 243] Additionally, the liposomal system Vaxfectin has been used in animal models to enhance immunity against herpes simplex type 2, measles, influenza, malaria and simian immunodeficiency virus. [244-248]

Early literature on liposomal nucleic acid vaccines focuses primarily on DNA delivery.[229, 230, 249] However, research showed that mRNA delivery leads to both increased transfection efficiency, as well as immunogenic potential. mRNA formulations have been tested in various animal models of melanoma, pancreatic cancer and lung cancer, viral infections, including Ebola virus and of course, COVID-19. [227, 238, 250-252] mRNA produces robust immune responses because of its ability to target various PRRs (i.e.: TLR 7, TLR8

etc.) and induce protein production without nuclear translocation. Additionally, the transient nature of mRNA expression makes it an ideal candidate for vaccine therapy, where transfection can last long enough to induce an immune response without lasting expression that could lead to toxicity.[253, 254]

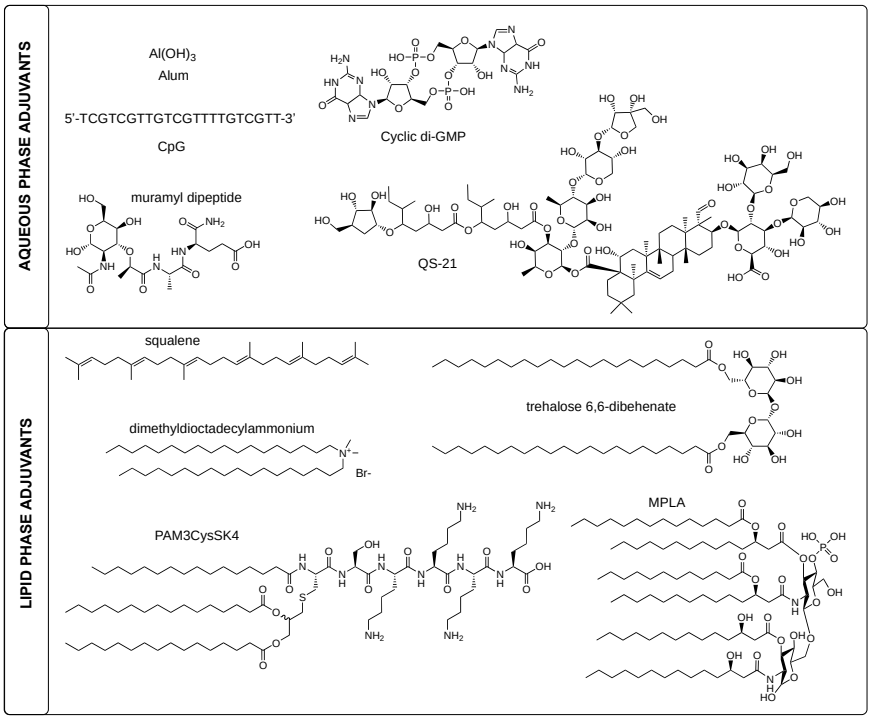

Figure 1.3: Adjuvants used in liposomal vaccines to enhance the cellular and humoral immune responses toward pathogens.

1.3 Liposomal immune modulation with small molecule therapeutics

Small molecule therapeutics can be encapsulated in the aqueous interior (in the case of water soluble drugs) or incorporated in the bilayer of LNPs (in the case of lipophilic drugs) (Figure 1.3).[255, 256] In LNPs, small molecule therapeutics display increased half-lives and reduced toxicity, which add to the appeal of this delivery strategy.[257] Currently, several LNP therapeutics have been approved for cancer therapy, fungal disease, analgesia, as well as photodynamic therapy (Figure 1.3 and Table 1.2).[255, 257-259]

1.3.1 Principles of liposomal pharmacology based on Doxil

The first liposomal therapeutic approved by the FDA was Doxil, a nanoparticle consisting of doxorubicin encapsulated hydrogenated soy phosphatidylcholine bilayer, surrounded by a polyethylene glycol (PEG) corona.[259] As with many drugs now delivered through liposomes, free doxorubicin has an extensive adverse effect profile and poor pharmacokinetics, despite having great clinical potential. Through years of collaborative

research, Doxil showed a blood area under the curve increase of 609 mg/hr/L compared to 1 mg/hr/L for free drug.[260] Additionally, in the first successful clinical trial to evaluate its use, Doxil administration led to a 5- to 11-fold increase in tumor drug levels, reduced toxicity, and increased patient tolerance.[261, 262] These findings highlight two of the main reasons behind the use of liposomal delivery, improved pharmacokinetics and reduced toxicity. One of the crucial points learned from the development of Doxil was the fact that liposomes are largely targeted and removed by the reticuloendothelial system, an issue that was resolved through the incorporation of PEG conjugated lipids that extend circulation half-life from hours to days.

1.3.2 Immune modulation using small molecule therapeutics

Doxil also provides a great example of how LNPs can be used to modulate immunity. One issue observed following administration with PEGylated therapeutics is the development of anti-PEG antibodies that can result in opsonization and accelerated blood clearance of subsequent doses.[263-266] These antibodies are the result of PEG recognizing B cells that elicit a T cell independent response against the polymer.[266] In PEGylated doxorubicin liposomes, however, the anti-PEG response fails to develop due to cytotoxicity of doxorubicin on PEG targeting B cells.[267] This strategy for immunosuppression has been explored using ovalbumin, with successful inhibition of antibodies to the immunogenic protein[268, 269] and removal of pre-existing anti-ovalbumin antibodies.[270] Methotrexate, a therapeutic used in cancer and autoimmune conditions, has also been shown to inhibit immunity toward co-administered proteins when given in a liposomal formulation.[271]

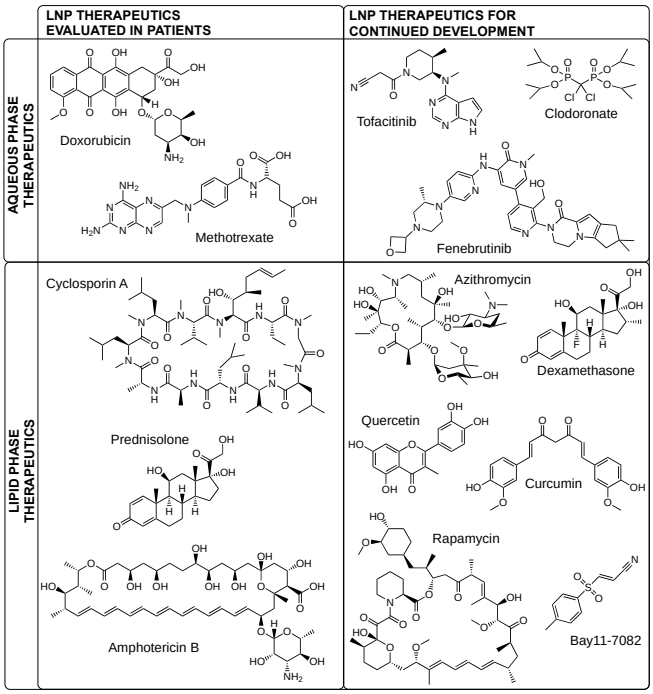

Figure 1.4: Small molecules approved or studied for liposomal delivery.

Another commonly used liposomal agent is clodronate. Liposomal clodronate, particularly without PEG, is rapidly taken up by phagocytic cells and leads to their death, providing a tool to study the role of these cells in various pathologies.[272 273] Clodronate liposomes have also been shown to reduce the severity of thrombocytopenic purpera,[274] autoimmune hemolytic anemia,[275] and arthritis in mouse and rat models.[276, 277] Mannosylation of clodronate liposomes, which improves macrophage targeting, has also been shown to decrease the severity of the experimental autoimmune encephalomyelitis (EAE) rat model of multiple sclerosis.[278] While most clinically available liposomal drugs are not tissue specific, LNPs can also be targeted to specific cell receptors through conjugation with antibodies or other targeting ligands attached to the nanoparticle surface.[279]

1.4 Modulation of immune responses through gene delivery vectors

A more complex, but more nuanced way to target and modulate immune responses is through gene delivery. Without many remarkable advances made in liposomal gene delivery and the contributions of countless researchers, the mRNA vaccines that helped to normalize the COVID-19 pandemic would not have been possible. Gene therapy, in a general sense, seeks to introduce missing/faulty genes or remove/decrease faulty genes directly or through RNA interference (RNAi).[280] In August of 2018, after demonstrating efficacy in phase III clinical trials, the FDA approved Patisiran, a LNP-based therapy for the treatment of transthyretin induced amyloidosis (Table 1.3).[281] In addition to Patisiran, the N-acetylgalactosamine based siRNA agent, Givlaari, was approved in 2019 for treating acute hepatic porphyria and several other siRNA agents are being studied for cancer, hepatitis, atherosclerosis and other systemic conditions, many using LNP vectors.[209, 282-286]

1.4.1 Principles of Liposomal Gene Delivery

The simplest strategy of achieving gene therapy is to introduce genes systemically, with the goal that they will be taken up by cells. However, naked nucleic acids are rapidly degraded in circulation and yield poor outcomes, especially *in vivo*. As a result, viral and non-viral vectors are used to enhance delivery.[287-289] Viral vectors use the natural structures of viruses to insert genes to the host cell/animal. Vectors like adeno-associated virus (AAV) have acceptable efficacy and safety parameters but also have significant limitations.[290, 291] One of the drawbacks of viral vectors is difficulty associated with their production and purification. *In vivo*, viruses also elicit systemic reactions that can lead to host toxicity and to neutralizing antibody production against the vector, which limits continued use of gene therapy.[287]

Non-viral gene delivery encompasses delivery with LNPs, peptides, polymers, dendrimers, and other nanoparticle strategies.[292, 293] Non-viral therapies employ cationic moieties, such as cationic lipid headgroups (Figure 1.4), to ionically pair with anionic phosphates on nucleic acids. LNPs achieve this through interaction of pre-formed liposomes with nucleic acids to form lipoplexes, or encapsulation of nucleic acids within

the liposome interior to generate what current literature refers to formally as LNPs.[209] As in other areas of liposome research, the efficacy of gene delivery depends on the particle size (ideally ~100 nm), stability and surface charge of the nanoparticle.[209, 290, 294] Some major contributions to the field are the development of ionizable cationic lipids and the ethanol loading procedure (and later microfluidic preparation), which improved the viability of LNPs, yielding higher loading efficiency and reduced toxicity.[209] Other strategies to enhance liposomal gene delivery focus on altering the nucleic acid molecules. For example, Andrew Gael demonstrated the ability of self-amplifying mRNA to overcome the limitations of vector molecules by increasing the mRNA bioavailability in cells, while the work of Drew Weissman and Katalin Kariko demonstrated the role of modified nucleotides (particularly N1-methyl-pseudouridine) in reducing mRNA immunogenicity and improving transfection.[238, 295-297] Other groups have focused on modifying RNA to improve the activity, half-life and specificity of these molecules.[298, 299]

1.4.2 Biology of liposomal gene delivery

Liposomal uptake into cells is cell type dependent. While clathrin- and caveolae-mediated endocytosis are the primary mechanisms of lipoplex uptake, other mechanisms, including macropinocytosis, phagocytosis, receptor mediated endocytosis and fusion with the cell membrane can contribute to their uptake.[232, 291, 300-303] Following endocytosis, nucleic acids can be degraded once the endosome fuses with a lysosome, an obstacle that can be overcome through the microfluidic mixing techniques described above, which can help to produce hexagonal (H_{II}) phase structures (Figure 1.2). around the nucleic acid and help the nucleic acid escape into the cytosol. [209, 291, 304-306] Once in the cytoplasm, nucleic acids can act directly on their target proteins (for siRNAs and mRNAs) or be transported to their final destinations in the nucleus (in the case of DNA).[209, 221]

Formulation optimization in gene delivery is crucial to delivery in several ways. For example, addition of dioleoyl phosphatidylethanolamine (DOPE) to a formulation can improve LNP escape from endosomes.[291, 307, 308] PEGylated lipoplexes, which can improve in vivo delivery by increasing circulation half-life, can also improve endosomal escape when exchangeable PEG-lipid analogs or cleavable pH sensitive PEG analogs are used in the formulation.[300]

Liposomal gene delivery is further complicated in vivo, where nanoparticles must bypass immune responses, protein adsorption, and biological processes in addition to the myriad cellular obstacles described above. One positive aspect of LNP delivery is propensity of LNPs to associate with lipid trafficking proteins like apolipoprotein E (ApoE), which helps to target LNPs to hepatocytes and neuronal tissues.[209] While circulating lipids cannot cross the blood brain barrier, ApoE is capable of transporting brain-derived lipids to neurons, improving delivery in this setting. Another major target of LNPs are the phagocytic cells of the immune system, highlighting the potential therapeutic utility of LNP therapies in inflammatory and immune mediated diseases.[209, 309]

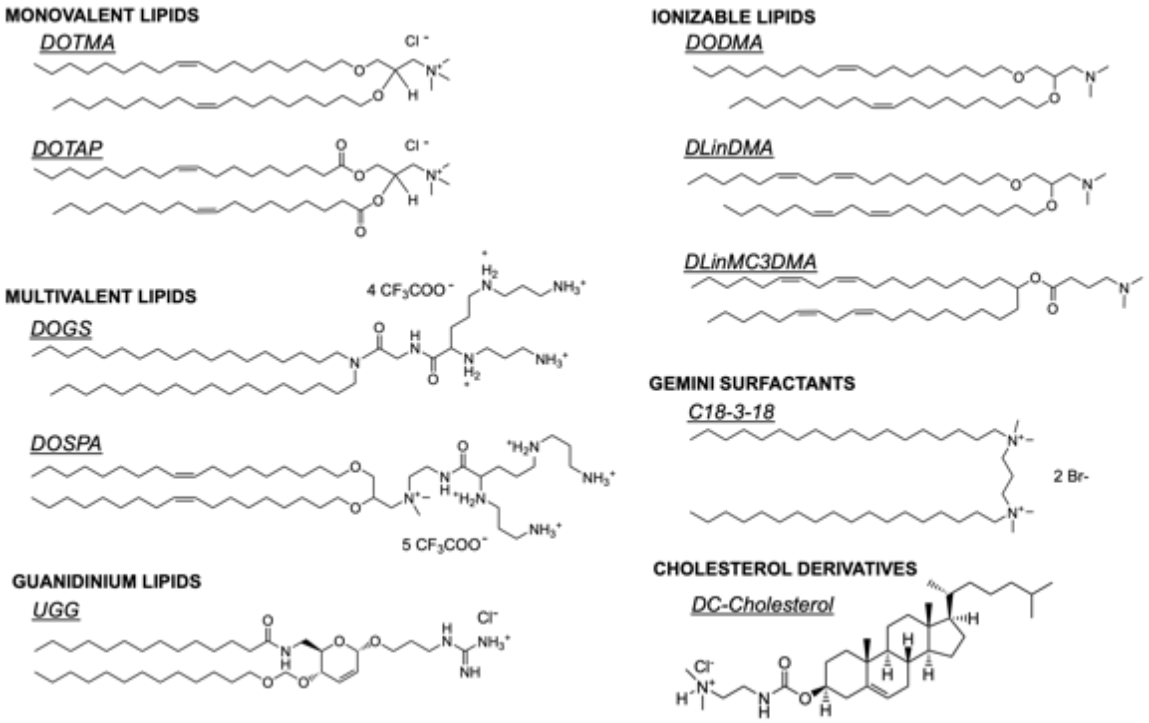

Figure 1.5: Cationic lipids used for gene delivery can be described in six general classes. Examples of each class are shown above: monovalent lipids (DOTMA, DOTAP), multivalent lipids (DOGS, DOSPA), guanidinium-containing lipids (UGG), ionizable lipids (DODMA, DLinDMA, DLinMC3DMA), gemini surfactants (C18-3-18), and cholesterol analogues (DC-cholesterol).

Targeting specific tissues can also be improved by using antibodies or other surface molecules. For example, addition of cyclic arginine-glycine-aspartic acid (cRGD) to an siRNA based formulation helped target the nanoparticles to $\alpha_V\beta_3$ integrin on A549 lung cancer cells.[310] Targeted delivery of lipoplexes has also been achieved using Listeriolysin O to target HER2 expressing cells using the luciferase reporter gene on a DNA plasmid.[311] Despite their relative safety, a major downside to cationic lipids is their propensity to induce cell lysis. To reduce cytotoxicity, cationic lipids are often mixed with helper lipids, like cholesterol and other natural lipids that increase the stability of these formulations.[312] The damage resulting from cell lysis during LNP gene delivery can ultimately lead to activation of the immune system.[287] Immunosuppressants like dexamethasone are often used in the clinical setting to attenuate LNP toxicity.[209, 291]

1.4.3 Immune modulation using liposomal gene vectors

LNPs provide a highly tailorable vector to modify the immune response of cells at a genetic level. An example of such a platform involves suppression of TNFα, a major cytokine involved in various inflammatory processes where TNFα siRNA was delivered to reduce inflammation in LPS induced sepsis,[313] and in inflammatory bowel disease.[314]

Aldayel et al. also published a study demonstrating the ability of DOTAP based LNPs to deliver TNFα siRNA and reduce inflammation in mouse models of collagen-induced arthritis and in methotrexate resistant, anti-collagen-induced arthritis.[315] The cell cycle protein, cyclin D1, is a regulatory molecule involved in the proliferation of lymphocytes during inflammation. In 2008, Peer et al. developed an LNP containing anti-cyclin D1 siRNA with a β_7 integrin antibody in a mouse model of colitis. In this study, cyclin D1 reduction led to a decline in inflammation mediated damage to the colon.[316] Another interesting study by Katakowski, et al. showed that delivery of siRNA targeting CD40, CD80 and CD86 to dendritic cells can inhibit T and B cell activation.[317]

Like siRNA, miRNA can inhibit the transduction of proteins and have been used in LNP based systems to target immune responses.[285, 318-321] Lipofectamine RNAiMAX delivery of hsa-miR-199a-3p and hsa-miR590-3p into mice by Lesizza et al. improved recovery from myocardial infarction compared with untreated mice.[322] miR-210, which can repress mitochondrial metabolism and attenuate keratinocyte proliferation, has been evaluated by Ghatak, et al. using antiphypoxamiR functionalized gramicidin LNPs following ischemic injury and showed that countering miR-210 improved healing.[323]

Although much of the research on LNP for immune modulation has focused on smaller nucleic acids, due to their efficacy and stability, LNPs can also be used to deliver DNA in the context of immunotherapy. Using mannose or galactosyl complexed LNPs encapsulating NFκB oligonucleotide, Dinh et al. was able to inhibit osteoclastogenesis in macrophages,[324] while Wijagkanalan et al. found reduced levels of TNF-α, IL-1β, CINC-1, and decreased neutrophil infiltration in a rat model of lung inflammation.[325] In 2001, Iwata, et al. delivered LNPs containing an endothelial nitric oxide synthase (eNOS) plasmid to show that eNOS upregulation reduced ischemic damage to rat transplant allografts, following NFκB inhibition and reduction of leukocyte infiltration. [326-328] LNPs containing DNA for interleukin 10 (IL-10) and interleukin 4 (IL-4), which play an essential role in reducing inflammation related damage and increasing reparative processes, have been evaluated for reducing inflammation, improving tissue function and prolonging survival of cardiac allografts in cellular and animal models of cardiac transplant.[329-333] IL-10 DNA can also improve outcomes in rat models of liver transplant using DOTAP based liposome formulations.[334] LNPs made with techniques such as microfluidic mixing have also been shown to enhance delivery into difficult to target cells, like mast cells, and reduce inflammation in allergic and rheumatic conditions.[335]

1.4 Conclusions

The discoveries that resulted in the optimization and approval of Doxil propelled research into other areas of liposomal research that have led to the approval of myriad other therapeutics for clinical use.[259] Extension of these strategies to vaccine and gene delivery has broadened the scope and clinical impact of LNPs, allowing LNP based mRNA vaccines and siRNA therapeutics to be used in patients.[209, 226, 336] As biomedical research delineates

the molecular mechanism of disease processes, LNP gene vectors constitute a promising treatment option to be used across many disease states. Much of the research in the field focuses on siRNA and mRNA delivery. mRNA particularly has been highly successful within the context of vaccines due to its ability to activate PRRs and to induce higher levels of antigen and anti-pathogen titers. However, within the context of gene replacement or gene therapy for immune modulation, wherein therapeutic genes should ideally avoid immune activation, mRNA may not be the best candidate. An additional challenge to liposomal gene delivery is the propensity of LNPs toward liver expression due to trafficking to this organ and to be taken up by hepatocytes, which warrants exploration into mechanisms to target to other areas.[209] Finally, as it pertains to academic research, the high cost of cationic lipids used for gene delivery makes research in this area difficult to engage in. Especially since many novel, promising compounds are inaccessible due to commercial or private patents. Throughout the body of work presented in this dissertation, I attempt to address some of these concern by developing a novel class of compounds with potential for gene therapy and evaluating their use in the context of DNA based gene delivery. Furthermore, as plasmid delivery often fails to induce the same level of gene expression seen with viral vectors, the later part of the dissertation focuses on the evaluation of a liposomal system to address the issue of immunity against viral vectors to improve viral gene delivery through liposomal suppression of B cells.

Table 1.1 Liposomal vaccines approved for clinical use

Agent	**Stage**	**Therapeutic Class**	**Therapeutic Target**	**Indication**	**REF**
Hepatitis A virosome (Epaxal)	*EMA Approved*	Virosome	Hepatitis A virus	Hepatitis A	337, 338
Influenza virosome (Inflexal V)	*EMA Approved*	Virosome	Hemagglutinin/neuraminidase	Influenza	339, 340
BNT162b2	*FDA Approved*	mRNA vaccine	COVID-19 spike protein	COVID-19	227
mRNA-1273	*FDA Approved*	mRNA vaccine	COVID-19 spike protein	COVID-19	227

Table 1.2 Liposomal small molecule therapeutics approved for clinical use

Agent	**Stage**	**Therapeutic Class**	**Therapeutic Target**	**Indication**	**REF**
Amphotericin B	*FDA Approved*	Antifungal	Ergosterol	Fungal infection	258
Anthralin	*FDA Approved*	Anthracene	Inhibition of cell proliferation	Psoriasis	341
Bupivacaine	*FDA Approved*	Opioid	Opioid Receptor	Pain relief	258
Cytarabine	*FDA Approved*	Antineoplastic	Nucleoside anti-metabolite	Neoplastic meningitis	258

Table 1.2 continued

Daunorubicin	*FDA Approved*	Antineoplastic	Topoisomerase II inhibition	AIDS related Kaposi sarcoma	258
Doxorubicin	*FDA Approved*	Antineoplastic	Topoisomerase II inhibition	Various oncologic conditions	258
Irinotecan	*FDA Approved*	Antineoplastic	Topoisomerase I inhibition	Pancreatic cancer	258
Mifamurtide	*EMA Approved*	Muramyl tripeptide	Tumor monocytes and macrophages	Osteosarcoma	258
Morphine	*FDA Approved*	Opioid	Opioid Receptor	Pain relief	258
Verteporphin	*FDA Approved*	Photosensitizer	ROS production, vessel occlusion	Choroidal neovascularization	258
Vincristine	*FDA Approved*	Antineoplastic	Microtubules	Acute lymphoblastic leukemia	258

Table 1.3 Liposomal nucleic acid therapeutics approved for clinical use

Agent	**Stage**	**Therapeutic Class**	**Therapeutic Target**	**Indication**	**REF**
Patisiran	*FDA Approved*	siRNA	Transthyretin	Transthyretin-related hereditary amyloidosis	342

CHAPTER 2: CYANURIC CHLORIDE AS THE BASIS FOR COMPOSITIONALLY DIVERSE LIPIDS

Reproduced from RSC Adv., 2021, 11, 24752-24761. (DOI: 10.1039/D1RA02425F) with permission from the Royal Society of Chemistry.[343]

2.1 Introduction

Liposomes provide an optimal vehicle for pharmaceutical delivery due to their versatility as amphipathic vectors that can be employed for delivering hydrophobic and hydrophilic agents.[217, 302] By altering the lipid composition in these nanoparticles, myriad properties can be honed to optimize their functionality. In the last few decades, liposome research has fueled the development of synthetic lipids that improve therapeutic delivery, particularly of nucleic acids.[209] However, the complexity and cost of novel lipids limits liposome research.[204, 217, 344, 345] To overcome this, various groups have developed synthetic, cationic lipid libraries with the goal of improving siRNA and mRNA delivery using cost effective and high-throughput schemes, taking advantage of specific chemical structures that allow for rapid headgroup diversification.[344-346]

In addition to their utility as gene vectors, liposomes have been investigated extensively for vaccine development using nucleic acids or proteins[295, 347] both as adjuvants,[226] and as antigen vectors.[348] Incorporating adjuvants and antigens in a single formulation also improves antigen exposure to immune cells and enhances the efficacy of liposomal vaccines.[349, 350] However, the need for synthetic lipids that serve as a platforms to generate structure immunogenicity relationships are critical to advance the field of liposomal vaccine design.

Chemical entities that facilitate efficient, cost-effective lipid synthesis provide opportunities to access diverse compositional space for therapeutic delivery. Cyanuric chloride is a heteronuclear aromatic molecule used as a chemoselective linker due to the thermally controlled reactivity of its three electrophilic carbons.[351] Previous studies have evaluated the utility of cyanuric chloride for synthesis of a variety of molecules including dendrimers and ionizable lipids for gene delivery.[352, 353] Here, it was hypothesized that by altering the functionality of the headgroup structure, cyanuric chloride could provide a simple, cost effective strategy to generate a variety of compounds with lipid-like properties that could be optimized for therapeutic applications across different areas of research.

In this chapter, cyanuric chloride was used as a linker to generate a library of triazine (TZ) based lipids with dialkylamines as tails and various small molecule head groups, chosen due to their cost effectiveness, commercial availability, and diversity in functional moieties, which provide a platform for future evaluation of an expanded library of triazine based lipids. Here we discuss the synthetic pathways used to produce these

compounds, compare some of the properties conferred by different headgroups and evaluate the biological utility of the molecules generated through this process.

2.2 Methods

2.2.1 Materials and instrumentation for synthesis of cyanuric chloride lipids and lipopeptides/lipoproteins

Beta-alanine-tert-butyl ester, cyanuric chloride, didodecylamine, diisopropylethylamine (DIPEA), 2-mercaptoethylamine HCl, morpholine, ninhydrin, N,N-dimethyl diaminopropane and trityl chloride were purchased from TCI America (Portland, OR). Dioctadecylamine was purchased from Sigma-Aldrich (Milwaukee, WI). *N*-Boc-1,3-diaminopropane was purchased from Matrix Scientific (Columbia, SC). 1,2-dimyristoyl-sn-glycero-3-phosphocholine (DMPC), 1,2-distearoyl-sn-glycero-3-phosphocholine (DSPC), 1,2-dimyristoyl-sn-glycero-3-phospho-(1'-rac-glycerol) (DMPG), 1,2-dioleoyl-sn-glycero-3-phosphoethanolamine (DOPE), 1,2-di-O-octadecenyl-3-trimethylammonium propane (DOTMA) and cholesterol were purchased from Avanti Polar Lipids, Inc. (Alabaster, AL). Solvents for reactions were purchased from various suppliers through VWR (Radnor, PA). Thin layer chromatography (TLC; Milipore Sigma, Silica gel 60 F_{254}) was visualized under UV light or with 2% ninhydrin in DMSO. Final compound purity was assessed via a Waters 2707 Autosampler, Waters 2545 Quaternary Gradient Module pump and Waters 2998 Photodiode Array Detector following injection into a Waters XBridge C18 3.5 μm column (part no. 186003034) using a water, acetonitrile and methanol mixture as described in the figures below and detected at 205 and 254 nm. ^{1}H and ^{13}C NMR spectra were recorded in deuterated chloroform using a Varian 400 MHz or Varian 500 MHz spectrometer equipped with a 5 mm OneProbe (Cambridge Isotope Laboratories, Inc.; Tewksbury, MA). HR-MS was performed on an Agilent 6230B TOF LC/MS instrument in positive ion by direct injection of the compounds. Lipopeptide purification was performed using the Waters system described above.

Two approaches were taken for the synthesis of the TZ lipids: a convergent and a divergent route. In the convergent approach, two small molecule nucleophiles with protected, ionizable moieties were reacted with cyanuric chloride through nucleophilic aromatic substitution (NAS). The resulting monochlorotriazine was then reacted with a long-chained secondary amine lipid tail (dioctadecylamine or didodecylamine) to yield the final protected lipid. In the divergent approach, the lipid tail was reacted first to form a dichlorotriazine, followed by headgroup diversification through addition of various nucleophilic small molecule moieties as headgroups. In both approaches, the first NAS was initiated on ice and allowed to stir at room temperature in chloroform for at least 4 hours. The second substituent was added at room temperature in chloroform and heated to 50 °C for at least 24 hours. The final NAS reaction was performed in xylenes or dioxane and heated from room temperature to 80 °C for at least 72 hours. In each reaction, excess nucleophile or DIPEA served as base. The reactions were monitored at each step via thin

layer chromatography and characterized by nuclear magnetic resonance and mass spectrometry. Small molecule nucleophiles with reactant pendant moieties were protected with acid labile protecting groups and deprotected as the final step in the lipid synthesis with trifluoroacetic acid in dichloromethane. Figures depicting the intermediate compounds and final lipids, as well as their NMR spectra and HPLC traces, can be found in the appendix.

Intermediate A was prepared by adding 1 equiv. of cyanuric chloride to a stirring solution of chloroform with 2.4 equiv. of beta-alanine-tert-butyl ester and 10 equiv. of DIPEA on ice. The mixture was allowed to come to room temperature, then heated overnight at 50 °C. Remaining beta-alanine-tert-butyl ester was removed by washing the dried product three times with brine. The monochlorotriazine was purified using a 0-30% ethyl acetate/ CH_2Cl_2 mixture on silica gel and the final product was eluted from the column using ethyl acetate, which was evaporated to yield intermediate A (73.8%) (30% ethyl acetate:chloroform, R_f = 0.88). ^{1}H-NMR (500 MHz, $CHCl_3$) δ 5.65-5.86 (m, 2NH), 3.56-3.68 (m, 4H), 2.47-2.52 (m, 4H), 1.42-1.48 (m, 18H); ^{13}C-NMR (125 MHz, $CHCl_3$) δ 171.18, 165.57, 156.38, 81.13, 36.58, 34.94, 28.07; HRMS MW calculated for $C_{17}H_{28}ClN_5O_4$ $(M + H)^+$: = 402.1903; found: 402.1939.

Intermediate B was prepared by adding 1 equiv. of cyanuric chloride to a stirring solution of chloroform with 2.4 equiv. of *N*-Boc-1,3-diaminopropane and 10 equiv. of DIPEA on ice. The mixture was allowed to come to room temperature, then heated overnight at 50 °C. Remaining *N*-Boc-1,3-diaminopropane was removed by washing the dried product three times with brine. The monochlorotriazine was purified using a 0-30% ethyl acetate/ CH_2Cl_2 mixture on silica gel and the final product was eluted from the column using ethyl acetate, which was evaporated to yield intermediate B (86%) (50% ethyl acetate:chloroform, R_f = 0.51). ^{1}H-NMR (500 MHz, $CHCl_3$) δ 4.96-6.51 (m, 4NH), 3.38-3.49 (m, 4H), 3.19 (m, 4H), 1.74 (m, 4H), 1.44 (m, 18H); ^{13}C-NMR (125 MHz, $CHCl_3$) δ 168.02, 165.77, 156.17, 79.23, 37.97, 37.56, 30.04, 28.39; HRMS MW calculated for $C_{19}H_{34}ClN_7O_4$ $(M + H)^+$: = 460.2434; found: 460.2505.

2-[(Triphenylmethyl)thio]ethanamine (CAS number: 1095-85-8) was prepared by an adaptation of the procedure described by Watrelot et al.[354] To a stirred solution of 2-mercaptoethylamine HCl (1.1 equiv.) in dichloromethane at 0 °C under nitrogen was added dropwise trifluoracetic acid (TFA, 3 mL) followed by dropwise addition of trityl chloride (1 equiv.). The reaction was stirred for 2.5 hours at 0 °C then concentrated and diluted in $CHCl_3$ (10 mL) and washed 3 times with 1 M NaOH and once with brine. The organic layer was then dried over magnesium sulfate and filtered and evaporated to dryness to afford the desired compound (92%) without further purification. ^{1}H-NMR (500 MHz,$CDCl_3$) δ 7.43 (m, 6H), 7.28 (m, 6H), 7.21 (m, 3H), 2.6 (t, J = 6.5 Hz, 2H), 2.32 (t, J = 6.5 Hz, 2H), 1.21 (bs, 2H, NH_2); ^{13}C-NMR (125 MHz, $CDCl_3$) δ 144.87, 129.56, 127.82, 126.61, 66.50, 41.08, 36.35.

Intermediate C was prepared by adding 1 equiv. of cyanuric chloride to a stirring solution of chloroform with 1.2 equiv. of beta-alanine-tert-butyl ester and 10 equiv. of

DIPEA on ice. The mixture was allowed to come to room temperature and reacted for 4 hours until the disappearance of cyanuric chloride was confirmed on TLC (chloroform, R_f = 0.58). To this mixture 1.1-1.5 equiv. of 2-[(triphenylmethyl)thio]ethanamine was added and stirred at room temperature for 24 hours. The final compound was dried and dissolved in ethyl acetate and then purified by washing with 0.5 M HCl three times then twice with brine. The organic phase was dried over magnesium sulfate and evaporated to yield intermediate C (97.7-99.3%). Of note, the formation of this product starting with 2-[(triphenylmethyl)thio]ethanamine yields an insoluble white solid following the addition of 2-[(triphenylmethyl)thio]ethanamine, which is extremely difficult to purify and dissolve for further reactions. ^{1}H-NMR (500 MHz, $CHCl_3$) δ 7.39 (m, 6H), 7.16-7.28 (m, 9H), 5.67-6.14 (m, 2NH), 3.51-3.66 (m, 2H), 3.14-3.30 (m, 2H), 2.39-2.50 (m, H4), 1.42-1.47 (m, 9H); ^{13}C-NMR (125 MHz, $CHCl_3$) δ 171.20, 168.31, 165.39, 146.84, 144.67, 129.45, 127.85, 127.17, 126.69, 81.09, 66.73, 39.60, 36.43, 34.86, 31.40, 28.07; HRMS MW calculated for $C_{31}H_{34}ClN_5O_4S$ $(M + H)^+$: = 576.2195; found: 576.2198.

Intermediate D was prepared by adding 1.1-1.5 equiv. of cyanuric chloride to a solution of chloroform with 1 equiv. of dioctadecylamine and 10 equiv. of DIPEA. The solution was started at -78 °C and allowed to come to 4 °C overnight. In the morning the reaction was assessed for the disappearance of the secondary amine using 2% ninhydrin in DMSO on TLC (3:2 CH_2Cl_2:hexanes, R_f = 0.95). The completed reaction was dried by rotary evaporation, then precipitated from chloroform with MeOH and filtered. This process was repeated twice, and the resulting white powder was resuspended in $CHCl_3$, dried over magnesium sulfate, filtered and evaporated to dryness to afford intermediate D (92-95%). ^{1}H-NMR (500 MHz, $CHCl_3$) δ 3.51 (t, J = 10, 4H), 1.55-1.61 (m, 4H), 1.20-1.32 (m, 60H), 0.86 (t, J = 10, 6H); ^{13}C-NMR (125 MHz, $CHCl_3$) δ 169.66, 164.16, 47.75, 31.84, 29.61, 29.58, 29.57, 29.55, 29.49, 29.40, 29.28, 29.15, 27.06, 26.59, 22.60, 14.03; HRMS MW calculated for $C_{39}H_{74}Cl_2N_4$ $(M + H)^+$: = 669.5363; found: 669.5361.

Intermediate E was prepared by adding 1.2 equiv. of beta-alanine-tert-butyl ester to a solution of chloroform with 1 equiv. of intermediate D and 10 equiv. of DIPEA. The mixture was stirred at room temperature for 2 hours then heated to 50 °C and allowed to react overnight. Remaining beta-alanine-tert-butyl ester was removed by washing the reaction mixture three times with brine. The compound was further purified on a silica gel column using a 10% ethyl acetate/chloroform mixture to yield intermediate E (51.2%) ($CHCl_3$, R_f = 0.50). ^{1}H-NMR (500 MHz, $CHCl_3$) δ 5.52-5.6 (m, NH), 3.57-3.66 (m, 2H), 3.35-3.51 (m, 4H), 2.49 (t, J = 7.5, 2H), 1.52-1.62 (m, 4H), 1.44 (s, 9H), 1.20-1.32 (m, 60H), 0.88 (t, J = 7.5, 6H); ^{13}C-NMR (125 MHz, $CHCl_3$) δ 171.13, 168.61, 165.12, 164.44, 80.90, 47.33, 47.09, 35.00, 31.83, 29.61, 29.57, 29.54, 29.49, 29.37, 29.30, 29.27, 28.02, 27.73, 26.97, 26.70, 22.60, 14.03; HRMS MW calculated for $C_{46}H_{88}ClN_5O_2$ $(M + H)^+$: = 778.6699; found: 778.6692.

Intermediate F was prepared in the same manner as intermediate D using didodecylamine with a similar product yield (93-95%). ^{1}H-NMR (500 MHz, $CHCl_3$) δ 3.51 (t, J = 9.5, 4H), 1.54-1.62 (m, 4H), 1.22-1.32 (m, 36H), 0.86 (t, J = 8.5, 6H); ^{13}C-NMR

(125 MHz, $CHCl_3$) δ 169.60, 164.08, 47.71, 31.86, 29.55, 29.26, 29.14, 27.02, 26.56, 22.63, 14.07; HRMS MW calculated for $C_{27}H_{50}Cl_2N_4$ $(M + H)^+$: = 501.3485; found: 501.3489.

Intermediate G was prepared in the same manner as described for intermediate E using intermediate F with a similar product yield (50.4%). ^{1}H-NMR (500 MHz, $CHCl_3$) δ 5.52-5.6 (t, *J* = 6.1, NH), 3.58-3.62 (m, 2H), 3.35-3.49 (m, 4H), 2.49 (t, *J* = 6.5, 2H), 1.50-1.61 (m, 4H), 1.42 (s, 9H), 1.20-1.29 (m, 36H), 0.86 (t, *J* = 7, 6H); ^{13}C-NMR (125 MHz, $CHCl_3$) δ 171.03, 168.45, 165.11, 164.38, 80.67, 47.28, 47.01, 35.02, 31.78, 29.52, 29.49, 29.48, 29.43, 29.33, 29.24, 29.21, 27.95, 27.69, 26.92, 26.64, 22.54, 13.97; HRMS MW calculated for $C_{34}H_{64}ClN_5O_2$ $(M + H)^+$: = 610.4821; found: 610.4842.

Lipid 1 was prepared by adding 1 equiv. of didodecylamine to a stirring solution of dioxane containing 2 equiv. of intermediate A and 10 equiv. of DIPEA. The solution was heated to 80 °C. After at least 48 hours (shorter reaction periods led to reduction in product yield) the reaction was evaporated using a rotary evaporator and re-dissolved in chloroform then washed three times with brine. The organic phase was then dried over magnesium sulfate, filtered, and dried in a rotary evaporator. The resulting solid was purified on a silica gel column using a chloroform to ethyl acetate mobile phase gradient (1:9 ethyl acetate:chloroform R_f = 0.5) and confirmed on NMR before being deprotected using a mixture of 1:1 TFA and dichloromethane and evaporated to dryness to yield lipid 1 (39.7-52.7%, final product).^{1}H-NMR (500 MHz, $CHCl_3$) δ 8.30 (s, 2OH), 3.60-3.70 (m, 4H), 3.44-3.54 (t, *J* = 7.5, 4H), 2.63 (t, *J* = 5, 4H), 1.56-1.64 (m, 4H), 1.23-1.32 (m, 36H), 0.87 (t, *J* = 5, 6H) ; ^{13}C-NMR (125 MHz, $CHCl_3$) δ 196.46, 175.78, 161.64, 154.61, 107.24, 48.06, 36.65, 33.71, 31.82, 29.57, 29.55, 29.53, 29.29, 29.26, 27.77, 26.95, 22.59, 14.02; HRMS MW calculated for $C_{33}H_{62}N_6O_4$ $(M + H)^+$: = 607.4905; found: 697.4904.

Lipid 2 was prepared in the same manner as compound 1 using dioctadecylamine and yielded compound 2 (21.7-27.6 %, final product). ^{1}H-NMR (400 MHz, $CHCl_3$) d 8.18 (s, 2COOH), 3.39-3.74 (m, 8H), 2.53-2.79 (m, 4H), 1.52-1.64 (m, 4H), 1.18-1.33 (m, 60H), 0.86 (t, *J* = 6, 6H); ^{13}C-NMR (100 MHz, $CHCl_3$) d 175.64, 161.67, 154.74, 48.24, 36.62, 33.44, 31.89, 29.68, 29.63, 29.60, 29.58, 29.37, 29.33, 27.84, 27.01, 22.66, 14.08; HRMS MW calculated for $C_{45}H_{86}N_6O_4$ $(M + H)^+$: = 775.6783; found: 775.6790.

Lipid 3 was prepared by adding 1 equiv. of didodecylamine to a stirring solution of dioxane containing 2 equiv. of intermediate B and 10 equiv. of DIPEA. The solution was heated to 80 °C. After at least 48 hours (shorter reaction periods led to reduction in product yield) the reaction was evaporated and dissolved in chloroform then washed three times with brine. The organic phase was then dried over magnesium sulfate, filtered, and dried using a rotary evaporator. The resulting solid was purified on a silica gel column using a chloroform to ethyl acetate mobile phase gradient (ethyl acetate R_f = 0.46) and confirmed on NMR before being deprotected using a mixture of 1:1 TFA in dichloromethane and evaporated to dryness to yield lipid 3 (32-46.0%, final product).^{1}H-NMR (500 MHz, $CHCl_3$) δ 3.28-3.48 (m, 8H), 2.77 (t, *J* = 7.5, 4H), 1.68 (t, *J* = 7.5, 4H), 1.48-1.58 (m, 4H), 1.16-1.32 (m, 36H), 0.86 (t, *J* = 7.5, 6H); ^{13}C-NMR (125 MHz, $CHCl_3$) d 164.88, 46.71,

31.90, 29.67, 29.65, 29.63, 29.53, 29.34, 28.04, 27.11, 22.66, 14.10; HRMS MW calculated for $C_{33}H_{68}N_8$ $(M + H)^+$: = 557.6540; found: 577.5639.

Lipid 4 was prepared in the same manner as compound 3 using dioctadecylamine and yielded (55.8-56%, final product). ^{1}H-NMR (500 MHz, $CHCl_3$) δ 3.31-3.49 (m, 8H), 2.82-3.04 (m, 4H), 1.72-1.92 (m, 4H), 1.48-1.58 (m, 4H), 1.17-1.34 (m, 60H), 0.86 (t, *J* = 7.5, 6H); ^{13}C-NMR (125 MHz, $CHCl_3$) d 164.54, 46.78, 31.83, 29.62, 29.56, 29.45, 29.26, 27.93, 27.05, 22.59, 14.02; HRMS MW calculated for $C_{45}H_{92}N_8$ $(M + H)^+$: = 745.7518; found: 745.7526. Of note, the peak resolution of this compound was poor and while several attempts were made to improve the quality of the spectra using various solvents alone and in combination, as well as various additives, the definition could not be improved beyond that presented here.

Lipid 5 was prepared by adding 1 equiv. of didodecylamine to a stirring solution of dioxane containing 2 equiv. of intermediate C and 10 equiv. DIPEA. The solution was heated to 80 °C. After at least 48 hours (shorter reaction periods led to reduction in product yield) the reaction was concentrated by rotary evaporation and re-dissolved in chloroform then washed three times with brine. The organic phase was then dried over magnesium sulfate, filtered, and dried using a rotary evaporator. The resulting solid was deprotected using a mixture of 1:1 TFA in dichloromethane and evaporated to dryness. The resulting solid was purified by silica gel chromatography by first eluting impurities with chloroform and ethyl acetate, then eluting the final product with methanol. The methanol fraction was dried and re-dissolved in chloroform before being filtered over magnesium sulfate to yield lipid 5 (90.6%, final product).^{1}H-NMR (500 MHz, $CHCl_3$) δ 8.40 (OH), 7.67 (s, NH), 3.47-3.70 (m, 8H), 2.62-2.75 (m, 4H), 1.55-1.66 (m, 4H), 1.42 (t, *J* = 8.6, SH), 1.23-1.33 (m, 36H), 0.87 (t, J = 7, 6H); ^{13}C-NMR (125 MHz, $CHCl_3$) d 176.27, 162.51, 161.61, 154.95, 154.41, 117.19, 114.89, 93.02, 48.19 43.93, 36.35, 33.06, 31.81, 30.91, 29.53, 29.52, 29.35, 29.29, 29.24, 27.83, 27.77, 27.61, 26.99, 26.93, 23.31, 22.58, 14.00; HRMS MW calculated for $C_{32}H_{62}N_6O_2S$ $(M + H)^+$: = 595.4728; found: 595.4735.

Lipid 6 was prepared in the same manner as compound 5 using dioctadecylamine and yielded lipid 6 (72.6%, final product). ^{1}H-NMR (500 MHz, $CHCl_3$) δ 9.01 (s, OH), 7.78 (s, NH), 3.44-3.73 (m, 8H), 2.65-2.74 (m, 4H), 1.53-1.65 (m, 4H), 1.42 (t, *J* = 8.6, SH), 1.22-1.31 (m, 6oH), 0.86 (t, *J* = 7, 6H); ^{13}C-NMR (125 MHz, $CHCl_3$) d 175.46, 162.97, 161.61, 155.09, 154.54, 117.59, 114.71, 48.32, 44.02, 36.83, 33.24, 30.89, 31.01, 29.68, 29.63, 29.59, 29.43, 29.37, 29.33, 27.91, 27.07, 27.02, 23.41, 22.66, 14.08, 13.08; HRMS MW calculated for $C_{44}H_{86}N_6O_2S$ $(M + H)^+$: = 763.6606; found: 763.6604.

Lipid 7 was prepared by adding 8 equiv. of morpholine to 1 equiv. of intermediate D dissolved in chloroform and refluxed overnight. After 48 hours, the reaction was first washed with 0.5 M NaOH, then brine and the organic phase was evaporated to yield lipid 7 (99.3%, final product) (ethyl acetate, R_f = 0.75). ^{1}H-NMR (500 MHz, $CHCl_3$) δ 3.67-3.75 (m, 16H), 3.44 (t, *J* = 7.5, 4H), 1.50-1.57 (m, 4H), 1.22-1.32 (m, 60H), 0.88 (t, *J* = 7.5, 6H); ^{13}C-NMR (125 MHz, $CHCl_3$) d 165.34, 164.96, 66.84, 46.74, 43.55, 31.84, 29.62,

29.60, 29.58, 29.57, 29.56, 29.42, 29.27, 27.84, 27.01, 22.60, 14.03; HRMS MW calculated for $C_{47}H_{90}N_6O_2$ $(M + H)^+$: = 771.7198; found: 771.7197.

Lipid 8 was prepared by adding 1 equiv. of intermediate E to 8 equiv. of morpholine in xylenes or dioxane and heating to 80 °C for 48 hours. The solvent was removed using a rotary evaporator at 80-90°C and the resulting solid was dissolved in chloroform and washed three times with 0.5 M HCl then twice with brine. The organic phase contained a number of impurities and was purified by silica gel chromatography using at 0-10% ethyl acetate:chloroform mobile phase gradient. The pure product was then confirmed on NMR before being deprotected using a mixture of 1:1 TFA in dichloromethane and evaporated to dryness to yield lipid 8 (86.6%, final product). ^{1}H-NMR (500 MHz, $CHCl_3$) δ 8.23 (m, OH), 3.66-3.88 (m, 10H), 3.32-3.52 (m, 4H), 2.57-2.75 (m, 2H), 1.50-1.62 (m, 4H), 1.22-1.32 (m, 60H), 0.86 (t, *J* = 8, 6H); ^{13}C-NMR (125 MHz, $CHCl_3$) d 171.88, 166.05, 165.33, 165.00, 80.95, 66.91, 46.80, 43.56, 36.48, 35.77, 31.90, 29.68, 29.65, 29.64, 29.64, 27.52, 29.34, 28.13, 27.09, 22.67, 14.09; HRMS MW calculated for $C_{46}H_{88}N_6O_3$ $(M + H)^+$: = 773.6991; found: 773.6991.

Lipid 9 was prepared by adding 20 equiv. of *N*,*N*-dimethyl-1,3-diaminopropane to a stirring solution of intermediate F and 10 equiv. of DIPEA in dioxane. The reaction was allowed to stir at room temperature for 24 hours then heated at 80 °C for another 48 hours. The reaction was then concentrated using a rotary evaporator and the product was dissolved in ethyl acetate and washed three times with brine. The organic phase was collected, dried over magnesium sulfate and concentrated to yield lipid 9 (92.3 %, final product). ^{1}H-NMR (500 MHz, $CHCl_3$) δ 5.15 (s, 2NH), 3.36-3.49 (m, 4H), 3.28-3.36 (m, 4H), 2.27 (t, J = 9.6, 4H), 2.16 (s, 12H), 1.59-1.76 (m, 4H), 1.45-1.57 (m, 4H), 1.17-1.28 (m, 36H), 0.83 (t, *J* = 8.6, 6H); ^{13}C-NMR (125 MHz, $CHCl_3$) d 165.90, 164.89, 57.63, 46.71, 45.44, 39.17, 31.83, 29.62, 29.61, 29.58, 29.56, 29.46, 29.27, 27.99, 27.72, 27.05, 22.59, 14.02; HRMS MW calculated for $C_{37}H_{76}N_8$ $(M + H)^+$: = 633.6266; found: 633.6270.

Lipid 10 was prepared in the same manner as compound 9 using intermediate D and yielded lipid 10 (93.4 %, final product). ^{1}H-NMR (500 MHz, $CHCl_3$) δ 5.20 (s, 2NH), 3.30-3.50 (m, 8H), 2.35 (t, *J* = 8.4, 4H), 2.22 (s, 12H), 1.64-1.78 (m, 4H), 1.46-1.59 (m, 4H), 1.18-1.32 (m, 60H), 0.83 (t, *J* = 8.6, 6H); ^{13}C-NMR (125 MHz, $CHCl_3$) d 165.42, 164.73, 57.63, 46.79, 45.37, 39.23, 31.89, 29.68, 29.53, 29.33, 28.03, 27.55, 27.11, 22.66, 14.09; HRMS MW calculated for $C_{49}H_{101}N_8$ $(M + H)^+$: = 801.8144; found: 801.8126.

Lipid 11 was prepared by adding 4-8 equiv. of *N*-Boc-1,3-diaminopropane to a stirring solution of dioxane containing 1 equiv. of intermediate G and 10 equiv. of DIPEA. The solution was stirred at 80 °C for 72 hours after which the solvent was removed using a rotary evaporator. The resulting solid was then dissolved in chloroform and washed three times with 0.5 M HCl then twice with brine. The organic phase was dried then purified by silica gel chromatography using a chloroform to ethyl acetate gradient and the product was confirmed on NMR before being deprotected using a mixture of 1:1 TFA in dichloromethane and evaporated to dryness to yield pure lipid 11 (90.3%, final product). ^{1}H-NMR (500 MHz, $CHCl_3$) δ 7.98 (s, 3NH), 7.66 (s, OH), 3.38-3.69 (m, 8H), 2.95-3.13

(m, 2H), 2.54-2.69 (m, 2H), 1.92-2.09 (m, 2H), 1.51-1.64 (m, 4H), 1.22-1.32 (m, 36H), 0.87 (t, *J* = 5, 6H); ^{13}C-NMR (125 MHz, $CHCl_3$) d 175.48, 154.54, 48.23, 31.82, 29.53, 29.26, 27.73, 27.60, 26.94, 22.59, 14.00; HRMS MW calculated for $C_{33}H_{65}N_7O_2$ $(M + H)^+$: = 592.5273; found: 592.5277.

Lipid 12 was prepared in the same manner as compound 11 using intermediate E and yielded lipid 12 (44.4%, final product). ^{1}H-NMR (500 MHz, $CHCl_3$) δ 7.92 (s, 3NH), 7.64 (s, OH), 3.30-3.72 (m, 8H), 2.92-3.20 (m, 2H), 2.51-2.72 (m, 2H), 1.89-2.15 (m, 2H), 1.53-1.63 (m, 4H), 1.20-1.34 (m, 60H), 0.87 (t, *J* = 7.5, 6H); ^{13}C-NMR (125 MHz, $CHCl_3$) d 175.51, 154.49, 48.18, 31.84, 29.63, 29.28, 27.73, 26.95, 24.78, 22.60, 14.02; HRMS MW calculated for $C_{45}H_{89}N_7O_2$ $(M + H)^+$: = 760.7151; found: 760.7159.

2.2.2 Lipopeptide synthesis

Lipidation of an ApoA-I peptide spanning the residues 141-184 of the mouse sequence (ApoA-$I_{141-184}$) was completed using intermediate D (C18 TZ linker). Resin was added to a vial, based on 22-40 mg of resin-cleaved and deprotected peptide (sequence *β*AGGLSPVAEEFRDRMRTHVDSLRTQLAPHSEQMRESLAQRLAELKSN) (Elim Biopharm, Inc.) containing 200 mg of intermediate D and 10 equiv. of DIPEA and stirred slowly at 35 °C for 72 hours (10.3-23 mg yield). After the reaction was completed, both compounds were washed extensively with chloroform to remove excess reactants and the peptide was cleaved from resin and deprotected in 4.7 mL of trifluoracetic acid, 125 µL ethanedithiol, 125 µL water and 50 µL triisopropylsilane. After 30 minutes this solution was pipetted through a glass wool filter into a conical vial containing cold diethyl ether (-20 ˚C) and left overnight at -20 ˚C. The following morning, the conical vial was centrifuged at 4000 rpm for 5 minutes and the peptide pellet was resuspended in cold ether and allowed to sit for one more day at -20 ˚C. Centrifugation was repeated and the resulting pellet was dried, weighed, and resuspended in a 1:1 mixture of water and tetrahydrofuran at 2 mg/mL. Concentration was confirmed by absorbance at 205 nm. The resulting products were further purified via HPLC using a gradient of 50 to 95% acetonitrile in water with 0.1% TFA and detected at 215 nm using the ChromeScope software provided by Waters. The reaction yielded 10.3-23.0 mg (46.8-57.5% yield) of purified final lipopeptide product.

2.2.3 Biophysical characterization of lipids and nanoparticles

Lipid nanoparticles were formed by dissolving lipids in chloroform and mixing them at the ratio described in each figure legend, then drying them into a thin lipid film by rotary evaporation before being placed under house vacuum overnight. To form liposomes, the dried lipids were rehydrated in HEPES buffered saline (20 mM HEPES, 145 mM NaCl, pH 7) (HBS) and sonicated until translucent at 60 °C. Lipoplexes were formed from liposomes by mixing liposomes and DNA at the specified ratio of positive nintrogens to negative charges phosphates (N:P ratio) in Opti-MEM (for cells) or HBS for physical characterization and incubating them at room temperature for at least 12 minutes prior to use. Nanoparticle size was determined using a Zetasizer Nano ZS (Malvern Panalytical) with the following settings: four measurements of fifteen, five second runs detected at a

backscatter angle of 173° at room temperature. The zeta potential for the liposomes was determined in a DTS1070 folded capillary zeta cell using the following settings: four measurements of at least 50 runs modelled with the Smoluchowski equation at room temperature using the automatic settings from the instrument.

2.2.4 Differential scanning calorimetry

The transition temperature (T_m) of the lipids was determined using a Multicell differential scanning calorimeter (TA Instruments). Liposomes were made with triazine lipids at a concentration of 10 mM in 20 mM HEPES buffer. These were heated to 60 °C and sonicated until the solution was translucent. For T_m determination, 250 μLs of the liposome solution were transferred into reusable Hastelloy ampoules while 250 μLs of the HEPES solution were transferred to the third ampoule, leaving the reference ampoule empty. For lipids 7 and 8, which failed to form nanoparticles, 250 μLs of the solution containing the lipid aggregate were transferred to the ampoules after sonication. Data were collected over a range of 10-110 °C at a rate of 2 °C/min in a heat-cool-heat cycle. After the run was complete, the CpCalc 2.1 software package was used to convert the raw data into a molar heat capacity and the data from the second heating cycle were processed using Microsoft Excel.

2.2.5 Carboxyfluorescein encapsulation assay

The ability of CC lipids to encapsulate molecules was tested using 5-(6)-Carboxyfluorescein (CF) purchased from Acros Organics (Pittsburg, PA), which was purified using the protocol established by Ralston *et al.* [355]. Briefly, unpurified CF was dissolved in refluxing ethanol for 3 hours in the presence of activated charcoal and filtered. The filtrate was diluted in enough distilled water to achieve a 1:2 ethanol/water ratio and crystalized at -20 °C. The crystalized CF was filtered and washed multiple times with distilled water and dried overnight. Solid CF was then dissolved in water and 5 M NaOH to a concentration of 250 mM and passed over an LH-20 Sephadex column. Five mL were purified on a 10x2 cm column by elution at room temperature with distilled water. CF eluted as a dark orange-red band that was quantified via absorbance at 492 nm using of coefficient of 6-CF (76,900 M^{-1}/cm) as described by Weinstein *et al.*[356] For the encapsulation assay, thin lipid films of CC lipids were prepared as described above. After evaporating remaining organic solvent overnight, the lipids were resuspended in a solution of 200 mM CF. Control phosphatidylcholine liposomes were then purified using a PD10 desalting column (GE Life Sciences).

2.2.6 Determination of nanoparticle pKa via TNS fluorescence

Cationic liposome pKa was determined by measuring the fluorescence of 2-(p-toluidino)-6-napthalene sulfonic acid (TNS), as described by Jayaraman, et al.[357] For this, liposomes were from the various cationic lipids were rehydrated in a solution of 10 mM HEPES, 10 mM MES, 10 mM ammonium acetate and 130 mM NaCl at a pH range of 2.5 to 12. The pH of each formulation was re-assessed to ensure that the pH had not significantly deviated from the original solution and 180 μL of each formulation was mixed

with 20 μL of 10 μM TNS in distilled water (for a final TNS concentration of 1 μM). The solutions were mixed by pipetting and incubated at room temperature for 10 minutes, before being analysed for fluorescence intensity using a 321 nm excitation and 445 nm emission wavelengths.

2.2.7 Gel shift assays using plasmid DNA

Nanoparticles consisting of a 1:1 molar ratio of cationic lipid/DOPE were rehydrated in a 20 mM HEPES solution at pH 4. The nanoparticles were mixed at equal volumes (5 μL) with plasmid DNA (5 μL) at the amine to phosphate (N:P) ratios indicated in the figure legends and incubated at room temperature for 10 minutes. For the triazine lipids the amine quantity per lipid was assumed to be 2 (one per headgroup), while DOTMA was considered to have 1 amine per lipid. After 10 minutes, 10 μL of the lipoplex was mixed with 2 μL of 6x loading dye (Boston BioProducts) and loaded onto a 1% agarose gel containing 0.5 μg/mL of ethidium bromide and run at 100 mV for 60 minutes. The gels were visualized and photographed using a Bio-Rad ChemiDoc XR system using the manufacturer's software.

2.2.8 Cells and mouse strains used for experiments

HEK293T cells, kindly donated by Dr. Gregory Graf of the University of Kentucky College of Pharmacy, while bone marrow derived macrophages were extracted from the femurs and tibias of 6-12 week old C57BL/6J female mice as described by Akbar *et al.* [358, 359] and cultured for 7 days in media containing 20 ng/ml murine M-CSF (Biolegend) [RPMI 1640 (Life Technologies no. 21870), 10% fetal bovine serum (Gemini), 2.5 mM L-glutamine, 10 mM HEPES, 0.1 mM β2-mercaptoethanol (β2-ME), 100 U/ml penicillin, 0.1 mg/ml streptomycin]. After 7 days, the cells were transferred to tissue culture 96 well plates (Corning) at a density of 100,000 in 200 μL of medium and allowed to settle overnight for subsequent assays. C57BL/6J (#000664) mice were purchased from Jackson Labs at 5-6 weeks of age and used in experiments at 7-9 weeks. Mice were sedated using isoflurane gas prior to blood collection by saphenous vein puncture or subcutaneous (s.c.) injections. Baseline plasma levels of all experimental parameters were established one week prior to injections. Blood was collected by superficial temporal vein puncture using a small animal lancet (Medipoint) into a microcentrifuge tube and centrifuged for 2 min at 13,000 *x g*. Plasma was stored at -80 °C for later assays. Mice were housed in a specific-pathogen free facility at the University of Kentucky, and all experimental procedures were approved by the University of Kentucky Institutional Animal Care and Use Committee.

2.2.9 Lactate dehydrogenase release (LDH) toxicity assay

For determination of cytotoxicity, mature bone marrow-derived macrophages (BMDM) were treated with 20 μL of the lipids (concentrations denoted in figure legend) diluted in 20 mM HEPES buffer, with HEPES buffer as negative control and 10% triton X-100 as positive control. After 24 hours, the 96 well plates were centrifuged at 200 *x g* for 5 minutes to remove debris and 100 μL of media was transferred to an untreated flat-bottom 96 well plate. Next, 100 μL of LDH reaction reagent purchased from Cayman

Chemical (Ann Arbor, MI) was added to each and allowed to sit for 30 minutes at 37 °C. Absorbance at 490 and 680 nm were measured using a BioTek Synergy H1 plate reader and the data were processed using Microsoft Excel. Mean values from triplicates are shown for one of two independent experiments.

2.2.10 Transfection of luciferase plasmid and cell viability

HeLa cells cultured in EMEM (ATCC) supplemented with 10% Fetal Bovine Serum were transferred to a 96 well plate, in quadruplicate, at a density of 20,000 cells per well and incubated for 24 hours at 37 °C in 5% CO_2. Liposomes made with a 1:1 ratio of DOPE and TZ lipid were added to a pGL3 Luciferase Reporter Vector (Promega) at N:P ratios of 2.5, 5 and 10, and incubated at 37 °C for 10 minutes before being diluted in 100 μL of non-supplemented EMEM and added to the cells. Following a four-hour incubation at 37 °C, the media was changed, and the cells were incubated for another twenty hours, at which point the cells were lysed with a cell culture lysis reagent at pH 7.8 composed of 25 mM tris-phosphate buffer, 0.7 g/L 1,2-diaminocyclohexane, 10% glycerol, 1% Triton X-100, and 1% protease inhibitor cocktail (Millipore). Total protein content was determined with a bicinchoninic acid assay (G-Biosciences) and luciferase protein expression was quantified by a luciferase assay (Promega). Cell viability was assessed using a Cell Titer Blue assay kit (Promega) based on the manufacturer's instructions. In each of the three independent experiments performed, transfection was compared with cells treated with Lipofectamine 3000 (Thermo), following the manufacturer's instructions, and with DNA treated cells.

2.2.11 Transfection of plasmid expressing human alpha-1 antitrypsin (hAAT) in vitro

HEK293-T cells were seeded, in triplicate, on 24 well plates at a density of 50,000 cells per well using D-MEM containing 10% fetal bovine serum (Gemini), 100 U/ml penicillin, 0.1 mg/ml streptomycin and 500 mcg/mL geneticin (VWR) and incubated until they reached 70-90% confluency. Lipoplexes were formed by combining TZ lipid liposomes made with a 1:1 ratio of DOPE and TZ lipid in Opti-MEM (Thermo) with human alpha-1 antitrypsin (hAAT) plasmid DNA (Addgene No. 126704) and incubating for 12 minutes in Opti-MEM, before being added to cells. After 24 hours the media was removed for evaluation of viability and replaced with fresh media. The cells were then incubated for another 72 hours and then transferred to 1.5 mL microcentrifuge tubes and centrifuged at 400 rpm for 5 minutes. The media was removed and assessed for hAAT via ELISA and the cells were lysed using RIPA buffer (Thermo) for determination of total protein concentration (Thermo). In each of the three independent experiments performed, transfection was compared with cells treated with Lipofectamine 3000 (Thermo), following the manufacturer's instructions, and with DNA treated cells.

2.2.12 Quantification of hAAT expression

For quantification of hAAT expression, 50 μL of goat anti-hAAT polyclonal antibody (R&D Systems No. AF1268-SP) were plated at a concentration of 1 μg/mL in carbonate buffer, pH 9.7, in a Greiner High Binding 96 well plate and incubated overnight

at 4 °C. The plate was then washed with 200 μL of phosphate buffered saline with 0.1% Tween-20 (PBS-T) four times and blocked with 100 μL of PBS with 0.05 % casein (Beantown Chemical, 124240; PBS-C) for 1 hour at 37 °C. The plate was then washed again, and 100 μL of fresh media from cells were plated, in duplicate, along with a standard curve made by serially diluting purified hAAT (OriGene No. RG202082) in PBS-C from 50 ng/mL to 0.048 ng/mL and incubated for 1 hour at 37 °C. The plate was then washed and 50 μL of mouse anti-hAAT monoclonal IgG2a antibody (R&D Systems No. MAB1268-SP) were plated at a concentration of 1 μg/mL and incubated at 37 °C for 1 hour. The plate was washed again, and 100 μL of HRP conjugated goat anti-mouse IgG2a (Abcam No. 98698) was added at a 1:5000 dilution and incubated for 30 minutes at 37 °C. The plate was then washed six times and binding was quantified by incubating the samples with 100 μL of tetramethylbenzidine (Rockland) for 30 minutes at room temperature, followed by quenching with 100 μL of 0.5 M H_2SO_4. Absorbance at 450 nm was recorded using a BioTek Synergy H1 microplate reader. After quantifying hAAT using the standard curve, hAAT in each well was normalized to total cell protein in respective plate, which was quantified using a Pierce BCA Assay Kit (Thermo) using the manufacturer's instructions.

2.2.13 Mouse immunizations with ApoA-I peptide

Liposomal immunizations were administered subcutaneously to three groups (n = 5 per group) of eight-week-old female C57BL/6J mice (The Jackson Laboratory) housed in a specific pathogen-free facility at the University of Kentucky. The immunization, administered at 8 and 10 weeks of age, consisted of 50 μL of a 20 mM liposomal formulation prepared with a mixture of DMPC, DMPG, cholesterol, and monophosphoryl lipid A (MPL; Sigma) at a 15:2:3:0.3 molar ratio and 0.5 mg/ml of lipid-conjugated peptide. The peptide used for these experiments was the lecithin-cholesterol acyltransferase domain of apolipoprotein A-I (sequence *β*AGGLSPVAEEFRDRMRTHVDSLRTQLAPHSEQMRESLAQRLAELKSN). As a control, the original peptide anchor (cholesteryl hemisuccinate) was used to immunize one group of mice, while two other groups were immunized with the peptide was conjugated to intermediate D and the third group was immunized with peptide free liposomes. To assess the efficacy of immunizations, blood was collected by superficial temporal vein puncture using a small animal lancet (Medipoint) into a microcentrifuge tube and centrifuged for 10 min at 21000 *x g* after standing at room temperature for 2 hr. Plasma was stored at -80 °C for later antibody detection. The mice were sedated during any procedures using isoflurane gas. All procedures were approved by the University of Kentucky Institutional Animal Care and Use Committee.

2.2.14 Apolipoprotein A-I peptide titer ELISA

Biotinylated apolipoprotein A-I peptide was diluted to a concentration 2 μg/mL in phosphate buffered saline with 0.1% Tween-20 (PBS-T) and plated in a 96-well streptavidin-coated plate (Thermo Fisher No. 05124) using a volume of 100 μL. The peptide was incubated for 2 h at 37 °C, then washed six times with 200 μL of PBS-T.

Mouse plasma (100 uL) was serially diluted in phosphate buffered saline containing 0.05% casein (PBS-C; Beantown Chemical) in duplicate, starting at 1:200 and incubated for 30 minutes at 37 °C. The wells were then washed six times and treated with 100 μL of goat anti-mouse IgG-HRP (Invitrogen No. 16066) diluted 1:2000 in PBS-C and incubated for 30 minutes at 37 °C before being washed again. Binding was quantified by incubating the samples with 100 μL of tetramethylbenzidine (Rockland) for 30 minutes at room temperature, followed by quenching with 0.5 M H_2SO_4. Absorbance at 450 nm was recorded using a BioTek Synergy H1 microplate reader. Reciprocal endpoint titers were then calculated by plotting the absorbance vs. plasma dilution and dividing the slope of the curve by two times the average of the blank (PBS-C only) wells.

2.3 Results and discussion

The thermally controlled, chemo-selective reactivity of cyanuric chloride provides a platform to add a multitude of functional headgroups and develop a wide array of synthetic lipids.[351] In general, cyanuric chloride undergoes nucleophilic aromatic substitution at 0 °C for the first substitution, 25 °C for the second, and 70 °C for the third, although reactions are influenced by the nucleophilicity and steric hinderance of the reactants. Using this framework, two dichloro-triazine molecules were generated as the basis of lipids and several small molecules were tested as headgroups (Fig. 2.1). The relative scarcity of commercially available long-chain secondary amines (tails) as compared to the abundance of potential head groups, results in a system in which compositional diversity was introduced in the headgroups rather than the tails. Therefore, a divergent approach (based on triazine dendrimer literature describing divergent and convergent synthetic routes)[351] was initially utilized for the synthesis of these compounds by adding lipid tails to prepare a dichloro-triazine that was further diversified with various headgroups. This strategy, however, was not viable for all headgroups used, particularly those with sterically hindered moieties. Therefore, a convergent strategy was attempted by initiating synthesis with the addition of headgroups to the cyanuric chloride ring to form a monochloro-triazine to which trails were then added (Fig. 2.1).[351] Using these two routes, the divergent synthesis reduces the total number of reactions needed to prepare a library of molecules by 25-33% depending on the final composition of the lipids. Synthesis of all lipids (excluding those containing morpholine) was attempted using both routes for comparison and the resulting products were characterized by NMR and HRMS. Lipids 1-4 proceeded well under both routes with similar yields for the convergent and divergent route using the beta-alanine headgroups (lipid 2: 28% and 22%) and the diaminopropane headgroups (lipid 4: 56% and 56%). This was not the case for lipids 5 and 6, which employed trityl-protected cysteamine (Trt-Cys). Divergent synthesis of lipidated dichloro-triazine molecules with Trt-Cys resulted in an insoluble compound with exceedingly low yield and could only be successfully synthesized using the convergent route with protected beta-alanine as the first substitution on cyanuric chloride.

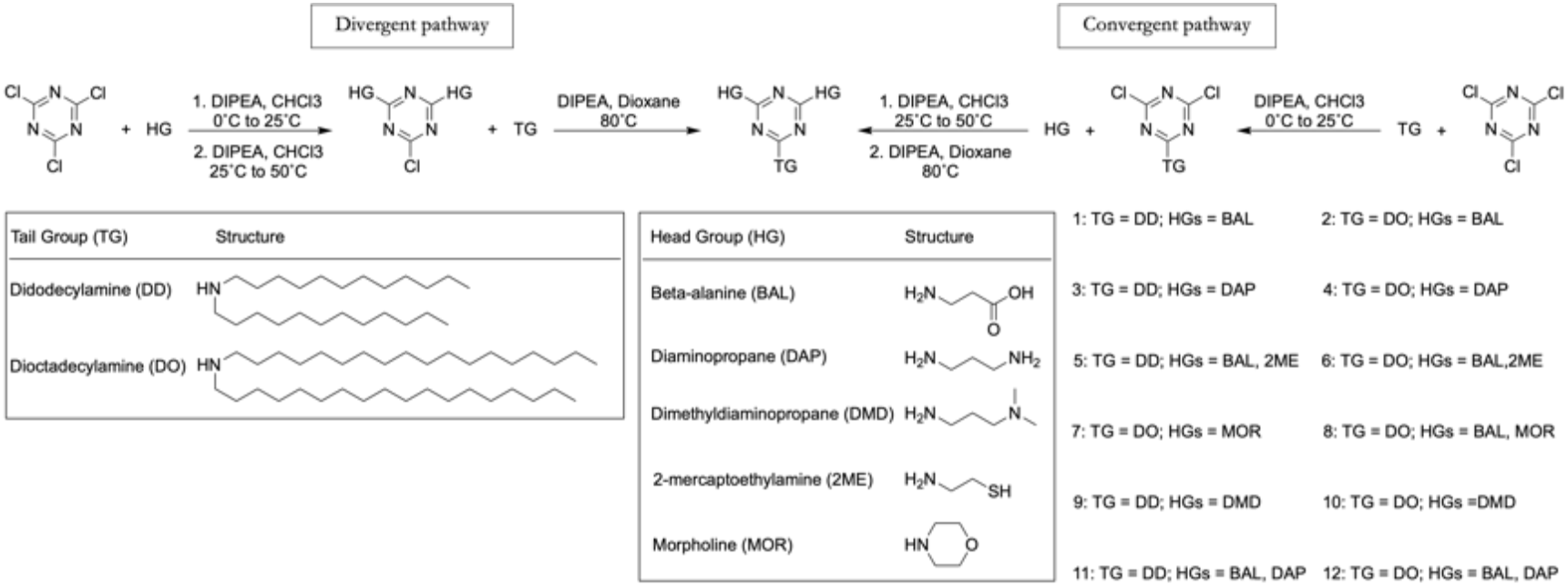

Figure 2.1 Synthetic schemes for TZ lipids depicting divergent (left) and convergent (right) schemes for triazine lipid synthesis.

Since the third addition to the TZ ring is generally more difficult to achieve, and morpholine is a strong nucleophile,[351] lipids 7 and 8 were only synthesized using the divergent route with overall yields of 91% and 80%, respectively. The divergent route was also used to synthesize lipids 9 and 10 containing N,N-dimethyldiaminopropane, as well as lipids 11 and 12 using both beta-alanine and diaminopropane in the headgroup. When using the convergent approach to synthesize these lipids, the purification of the monochlorotriazine headgroup molecules in the absence of the lipid tails was problematic requiring a slow and lengthy purification by column chromatography (>12 hours). Conversely, the divergent route facilitated synthesis and purification of the final lipids.

While some lipids resulted in similar overall yield between convergent and divergent routes, the challenges with nucleophilicity, steric hinderance and purification of intermediate molecules resulted in synthetic preference for one route over the other with certain headgroups. The divergent route results in increased compositional diversity with fewer steps and was used to overcome complications with synthesis and purification, while the convergent route serves as an important complementary role for the synthesis of certain lipids and will be considered as additional lipids in this library are synthesized.

The utility of the divergent route was then explored further by reacting the C18 dichloro-triazine compound (intermediate D, see Appendix figure 1) with the N-terminal amine of a protected peptide on rink amide resin. The utility of this reaction provides an alternative synthetic route to present lipid-anchored peptides in a liposomal bilayer for vaccination. Using the 44 amino acid sequence from apolipoprotein A-I (ApoA-I) that our group has previously investigated, we achieved improved yields as compared to previously described lipopeptide synthesis.[360, 361] The ease of lipopeptide synthesis using intermediate D provides a convenient platform for continued vaccination studies.

Next, we sought to prepare liposomal formulations using each lipid. First, the transition temperature (Tm) of each compound was determined by forming nanoparticles of pure lipid via rehydration of thin lipid films in 20 mM HEPES that were sonicated at 65 °C. The resultant nanoparticles were then transferred into Hastelloy ampules to assess the lipid transition temperature by differential scanning calorimetry. Lipids made with didodecylamine tails yielded a Tm below 10 °C, while those made with dioctadecylamine tails ranged from 28-64 °C (Fig. 2.2A and Table 2.1).

All lipids were initially formulated at pH 7 but failed to properly hydrate. Therefore, hydration of lipids 1 and 2 were tested at increasing pH and found that pH 10 was ideal for hydration. All other lipids hydrated well under acidic conditions (pH 4). Lipids 7 and 8, which contained morpholine in the headgroup, failed to form liposomes, alone or in combination with distearoyl phosphatidylcholine (DSPC) or DSPC and cholesterol from 5 to 90 mol% TZ lipid. Lipids made with isonipecotic acid headgroups also failed to form liposomes (data not shown), indicating that steric hinderance of the headgroups may preclude liposome formation. Additionally, while lipids 11 and 12 initially formed nanoparticles, they were unstable past 24 hours as determined by dynamic light scattering.

All other lipids formed nanoparticles that appear stable at one month after preparation when stored at 4 °C, based on dynamic light scattering.

The ten lipids that formed nanoparticles ranged in size from 87 to 383 nm in diameter (Table 2.1), with no clear trend between diameter and structural characteristics, such as lipid tail and charge. Lipids with cysteamine as a headgroup achieved the smallest size, while lipids 11 and 12, exhibited the largest initial diameter. The charges of each formulation also aligned with the headgroup used and ranged from -75 to 70 mV for anionic and cationic headgroups, respectively. Lipids 11 and 12, which contained beta-alanine and 1,3-diaminopropane in the headgroup, were hydrated in acidic conditions (pH 4), as they failed to form in basic conditions (pH 10), yielding a positive charge.

While TZ lipid nanoparticles remained stable for several weeks, it was unclear whether they could retain therapeutics in their aqueous core, and carboxyfluorescein (CF) encapsulation was used to test this.[356] Unfortunately, when pure TZ lipids were used to encapsulate CF, they formed a gel with the aromatic compound and future experiments to encapsulate non-aromatic molecules (i.e.: glucose) are warranted.

Two primary mechanisms of toxicity associated with lipid nanoparticles, particularly cationic ones, are cell lysis and activation of immune responses.[362, 363] Macrophages are among the primary cells responsible for the uptake of nanoparticles from circulation and are associated with the immune responses observed following *in vivo* administration, therefore these cells were chosen to test this aspect of TZ nanoparticles.[364] To assess the toxicity of TZ nanoparticles, the lipids were tested for induction of lactate dehydrogenase (LDH) release from bone marrow derived macrophages (BMDMs) from C57BL/6J mice. BMDMs were treated with TZ lipids at concentrations ranging from 31.25 to 250 nmoles/mL. As can be seen in Figure 2.2B and Table 2.1, the toxicity of the nanoparticles ranged between that of the synthetic, cationic lipid DOTMA, and the natural zwitterionic phospholipid DMPC (Table 2.1). The LD_{50} values of the cationic lipids are considerably higher than that of other lipids (132.77 and 180.38 mM for lipids 3 and 4, respectively), approximating the toxicity of DOTMA (LD_{50} = 78.45 mM). Lipids 9 and 10 also had higher toxicity than other TZ lipids (LD_{50} = 337.11 and 260.66 mM, respectively), which did not differ significantly from DMPC (LD_{50} = 968.53 mM).

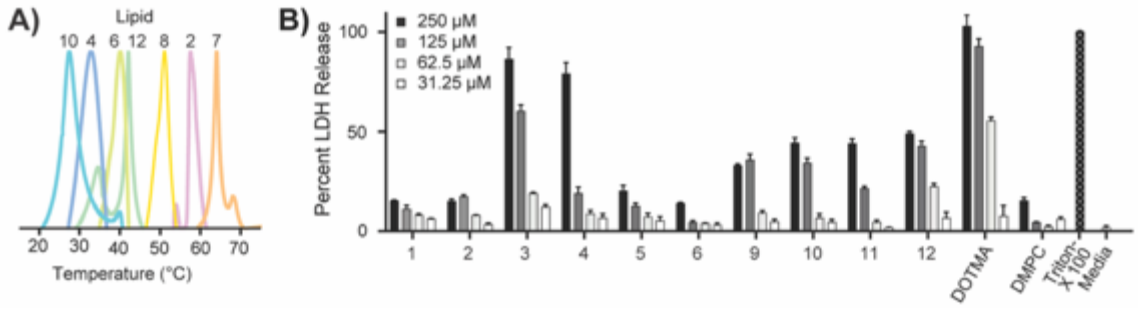

Figure 2.2. (A) Transition temperature of TZ lipids determined by DSC. (B) *In vitro* toxicity of triazine lipids. Toxicity of TZ lipids on BMDMs as compared to commercially

available cationic (DOTMA) and zwitterionic (DMPC) lipids using the lactate dehydrogenase assay. Liposomes were made by thin film hydration followed by sonication and used immediately to treat cells for 24 hours, prior to testing LDH release in cell media. Representative data from one of three independent experiments is shown; bars indicate mean values for three technical replicates of duplicate experiments +/- SEM.

Having shown great success in preclinical studies, many synthetic lipids with cationic headgroups are used in gene transfection as commercial reagents for laboratory use.[209] More recently, the first siRNA therapeutic, patisiran, was approved for clinical use by the United States FDA and two lipid-based mRNA vaccines were approved for prevention of COVID-19.[281, 365] As mentioned earlier, in 2007 Candiani et al. reported a series of cationic, reducible lipids using cyanuric chloride as a linker.[352] These were made from two single tailed triazine molecules, a cationic diaminopropane headgroup, and joined via disulphide linker. The Candiani lipids resulted in successful plasmid delivery into cells and exhibited limited toxicity, suggesting that cationic TZ lipids could be employed in this manner.[352]

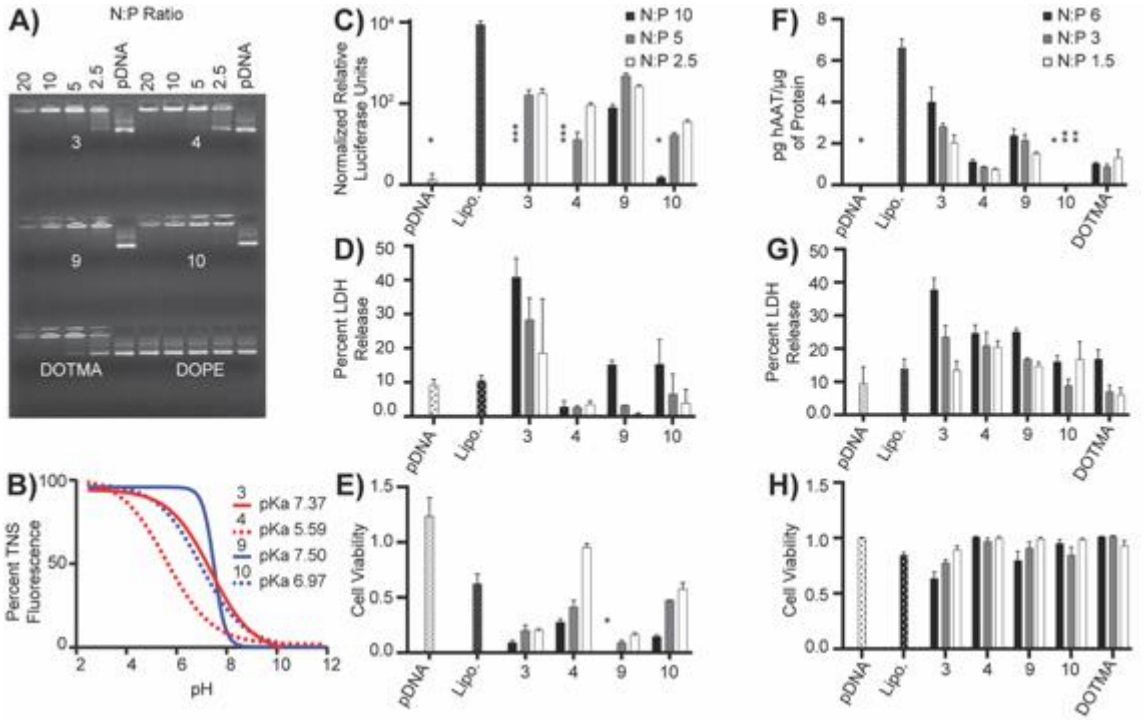

Figure 2.3. Efficacy of TZ lipids in gene transfection. (A) Gel shift assay of plasmid DNA complexed with TZ lipids. (B) pKa assessment of cationic lipids measured by TNS fluorescence at pH range 2.5 to 10. Plots represent the sigmoidal, best fit analysis of one of three independent experiments. (C-E). Transfection of HeLa cells with luciferase reporter gene using Lipofectamine 3000 or TZ lipids at an N:P ratio of 10, 5 and 2.5 (left to right). Bars represent the mean values from one of three representative experiments,

except for the LDH assay which was performed twice. (C) Luciferase expression in transfected HeLa cells. (D) LDH release from HeLa cells transfected with luciferase plasmid, 4 hours after transfection. (E) Viability of cells treated with plasmid and lipids 24 hours after transfection. (F-H) Transfection of HEK293-T cells with hAAT using Lipofectamine 3000 or TZ lipids at N:P ratios of 6, 3 and 1.5 (left to right). Bars represent the mean values from one of three representative experiments, except for the viability assay which was performed twice. (F) hAAT expression 72 hours after transfection based on ELISA and normalized to total cell protein. (G) LDH release from cells transfected with hAAT plasmid 24 hours after transfection. (H) Viability of cells treated with plasmid and lipids 48 hours after transfection. In both experiments, each treatment was compared to the Lipofectamine control using the Kruskal Wallis non-parametric test. Bars indicate mean values for triplicates +/- SEM and $p = < 0.05$.

To determine whether TZ lipids with cationic headgroups 3, 4, 9 and 10 could complex nucleic acids, nanoparticles made from a 1:1 molar ratio of cationic lipids and DOPE were incubated with plasmid DNA at increasing ratios of cationic amine (N) to anionic nucleic acid phosphate (P) and assessed for migration in an agarose gel. This 1:1 molar ratio of DOPE and cationic lipid has been extensively reported in the literature and provides a simple starting point for assessing the potential of cationic lipid formulations.[366, 367] Of note, the N content of TZ lipids are based on the distal aliphatic amines of the headgroups, but the other amines in the molecules may contribute to complexation. As shown in Fig. 2.3A, all four lipids complexed DNA at an N:P ratio of 5 or above. By comparison, DOTMA/DOPE nanoparticles inhibited DNA migration at a ratio of 10 while DOPE alone was unable to alter migration.

An important component of cationic lipids, which contributes to gene delivery is the pKa of the nanoparticles.[357, 368, 369] This property has a crucial role in the ability of liposomal nanoparticles to complex with nucleic acids and has been correlated with the efficacy of nanoparticles.[357] Particularly, ionizable lipids with a pKa ranging from 6.2 to 6.4, have been shown to achieve a high degree of efficacy when used to deliver siRNA.[209] To assess the pKa of the cationic TZ lipids, liposomes made from these lipids were rehydrated in buffered solutions ranging from pH 2.5 to 12 and mixed with TNS. Interestingly, the pKa of the TZ lipids in both sets of lipids reduced by increasing the tail length of the lipids (Fig. 2.3B), with lipids 3 and 4 varying by almost two units, despite having the same headgroup. While clear correlations are difficult to assess based on the few compounds available, the pKa of the lipids did seem to improve with reduced pKa, as described in previous literature.

The mixture of cationic TZ lipids with DOPE was then used to deliver plasmid DNA into HeLa cells using a luciferase reporter vector, comparing their efficacy with free DNA and Lipofectamine 3000.[367] As shown in figure 2.3C, all four lipids improved plasmid transfection compared with naked plasmid, with the shorter tailed lipids (3 and 9) demonstrating better efficacy than the lipids with C18 tails (4 and 10), which concurs with

the findings of Candiani et al. who reported improved transfection with shorter length tails.[352] Overall, TZ lipid transfection was only modest compared to Lipofectamine, with optimal luciferase expression reaching an average of 462 RLU/mg for lipid 9 at an N:P ratio of 5 (vs. 7937 RLU/mg for lipofectamine), and LDH release and cell viability approximating that of Lipofectamine (Fig. 2.3D-E). To confirm these findings in a more clinically relevant context, HEK293-T cells were transfected with a plasmid encoding human alpha-1 antitrypsin (hAAT) using the same lipid mixtures, and hAAT expression was assessed by ELISA. As evidenced in figures 2.3F-H, the cationic TZ lipids significantly improved transfection, except for lipid 10, and exhibited a similar toxicity profile to that of Lipofectamine.

To assess the characteristics of the lipoplexes, TZ/DOPE liposomes were mixed with hAAT plasmid DNA at N:P ratios of 0.2, 1 and 5 and their size and charge were assessed. As evidenced by table 2.2, the sizes and charges of the nanoparticles did not significantly differ from that of the free nanoparticles in most cases. However, in the case of lipid 4, there was a considerable increase in size that correlated with the DNA concentration, suggesting a potential explanation for its low efficacy and toxicity, as larger nanoparticles have been shown to display reduced uptake.

Finally, given the synthetic versatility of the divergent route to append more complex moieties, such as peptides, we compared the immunogenicity of a lipopeptide prepared with C18 TZ linker (intermediate D) with our standard cholesteryl hemisuccinate anchor in a liposomal formulation. As mentioned above, the modular design of liposomes allows for combination of antigens and adjuvants to tailor immune responses toward clinically relevant targets (Fig. 2.4A).[226] Liposomal peptide vaccines increase the bioavailability of antigens by extending their half-life and increasing their concentration in lymphatic tissues.[216] Our lab has previously developed a strategy to induce antibodies toward apolipoprotein A-I (ApoA-I) in mice, to mimic the immunity observed in humans toward this protein,[360] using a 44 amino acid peptide derived from ApoA-I. To determine whether TZ lipids can be used in this setting, formulations were prepared with the respective lipopeptides along with the TLR-4 agonist MPL. Peptides were formulated in the liposomes (20 mM) at a concentration of 1 mg/mL, or ~1000 peptides per liposome.

C57BL/6 mice were immunized twice with a liposomal vaccine containing one of the lipopeptide conjugates (Fig. 2.4B) or a control formulation without peptide and reciprocal endpoint titres (RET) toward the peptide were assessed seven days after the second immunization. RET from mice immunized with the TZ lipid anchor approximated that of CHEMS, which has been shown to serve as an optimal peptide anchor for liposomal immunization.[361] These data highlight the utility of TZ lipids as a strategy for peptide conjugation (Fig. 2.4C) onto liposomal surfaces.

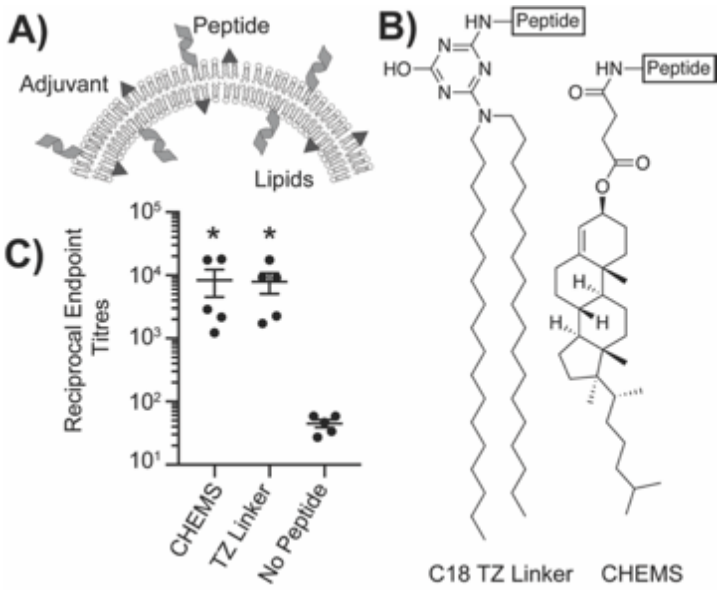

Figure 2.4. TZ lipids as peptide anchors in liposomal vaccines. (A) Liposomal vaccines can include various components, including natural phospholipids and adjuvants, to optimize responses to an immunogen. (B) Lipid linkers anchoring apolipoprotein A-I peptide to the liposomal vaccine, cholesterol hemisuccinate and intermediate D (C18 TZ). (C) Reciprocal endpoint titres 7 days after the second of two immunizations compared with no peptide immunization. Symbols correspond to individual mice and line represents mean +/- SEM and $p = < 0.05$.

2.4 Conclusions

The present work demonstrates the utility of cyanuric chloride in the development of synthetic lipids with a wide potential for therapeutic delivery, based on the properties of specific headgroups. Furthermore, this strategy provides a simple method to alter the structure of lipids to optimize lipid properties depending on the desired outcome. This work expands on previous research demonstrating the utility of this compound in the development of synthetic structures for drug delivery and provides a novel strategy to access diverse lipids with relative synthetic ease.[344, 346, 351] Furthermore, the present work supports the evaluation of triazine based compounds in in vivo models based on their improved ability to deliver genes and their toxicity profile which approximates that of the DOTMA control.

Table 2.1 Characterization of triazine lipids.

Lipid Structures	#	Tail	Yield (%)		Tm[a] (°C)	Size (nm)	PDI	Charge (mV)	LD_{50} (μM)
			Conv.	Div.					
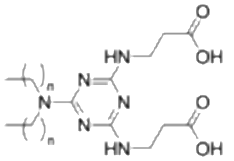	1	C12	22	49	<10	124 ± 2	0.24 ± 0.02	-63 ± 4	1098
	2	C18	20	21	58	131 ± 0	0.24 ± 0.00	-59 ± 5	894
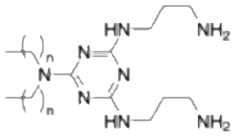	3	C12	28	43	<10	130 ± 2	0.44 ± 0.02	52 ± 3	133
	4	C18	48	53	33	126 ± 1	0.28 ± 0.00	63 ± 3	180
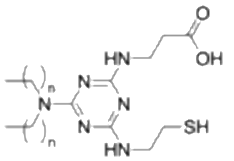	5	C12	90	ND	<10	87 ± 2	0.40 ± 0.00	-75 ± 6	679
	6	C18	72	ND	40	93 ± 2	0.27 ± 0.01	-71 ± 5	988
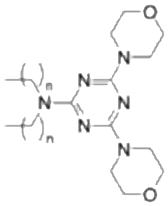	7	C18	ND	91	64	ND[b]	ND	ND	ND
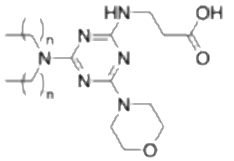	8	C18	ND	80	51	ND	ND	ND	ND
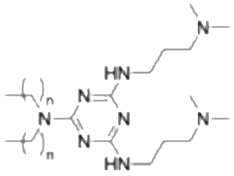	9	C12	ND	88	<10	159 ± 1	0.24 ± 0.00	45 ± 2	337
	10	C18	ND	89	28	186 ± 1	0.28 ± 0.01	47 ± 1	261
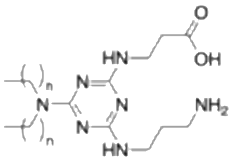	11	C12	ND	46	<10	383 ± 35	0.98 ± 0.02	42 ± 5	277
	12	C18	ND	23	42	356 ± 10	0.51 ± 0.02	70 ± 5	227

Table 2.2 Characteristics of liposomes made with DMPC, DOTMA, and various lipid combinations, as well as immunization liposomes.

Lipid	Size (nm)	PDI	Charge (mV)	LD_{50} (μM)
DMPC	277 ± 45	0.39 ± 0.01	-9 ± 0.3	969
DOTMA	105 ± 2	0.43 ± 0.06	70 ± 4	78
DOTMA:DOPE (1:1)	104 ± 5	0.28 ± 0.04	28 ± 1	ND
1:DOPE (1:1)	89 ± 1	0.45 ± 0.05	-61 ± 4	ND
2:DOPE (1:1)	85 ± 2	0.29 ± 0.04	-46 ± 2	ND
3:DOPE (1:1)	61 ± 1	0.38 ± 0.01	44 ± 2	ND
4:DOPE (1:1)	64 ± 0.2	0.28 ± 0.02	30 ± 7	ND
9:DOPE (1:1)	76 ± 4	0.57 ± 0.01	38 ± 2	ND
10:DOPE (1:1)	107 ± 2	0.23 ± 0.01	44 ± 2	ND
11:DOPE (1:1)	93 ± 5	0.24 ± 0.01	47 ± 1	ND
12:DOPE (1:1)	98 ± 1	0.34 ± 0.04	52 ± 3	ND
3 Lipoplex (N:P 1)	91 ± 3	0.45 ± 0.01	27 ± 6	ND
3 Lipoplex (N:P 5)	66 ± 1	0.25 ± 0.01	21 ± 1	ND
4 Lipoplex (N:P 1)	225 ± 7	0.39 ± 0.02	35 ± 6	ND
4 Lipoplex (N:P 5)	194 ± 5	0.22 ± 0.00	35 ± 3	ND
9 Lipoplex (N:P 1)	95 ± 4	0.46 ± 0.01	19 ± 1	ND
9 Lipoplex (N:P 5)	65 ± 2	0.35 ± 0.05	24 ± 3	ND
10 Lipoplex (N:P 1)	102 ± 4	0.55 ± 0.08	50 ± 8	ND
10 Lipoplex (N:P 5)	78 ± 1	0.44 ± 0.01	56 ± 5	ND
DOTMA Lipoplex (N:P 1)	97 ± 2	0.23 ± 0.01	34 ± 4	ND
DOTMA Lipoplex (N:P 5)	90 ± 1	0.21 ± 0.00	2 ± 0	ND
Peptide free liposome	113 ± 4	0.40 ± 0.02	ND	ND
CHEMS peptide liposome	194 ± 4	0.23 ± 0.02	ND	ND
Dioctadecylamine peptide liposome	177 ± 4	0.22 ± 0.01	ND	ND

ND = Not determined.

CHPATER 3: IN VIVO ASSESSMENT OF TRIAZINE LIPID NANOPARTICLES AS TRANSFECTION AGENTS FOR PLASMID DNA

3.1 Introduction

The ability of lipid based nanoparticles to form transfection vehicles depends on the ionic interaction between cationic lipids and nucleic acids, which allows the nanoparticle to deliver the nucleic acid payload into cells.[291] This field has been largely expanded by the work of various researchers who have elucidated the structure activity relationship of cationic lipids and have implemented design elements to optimize gene delivery.[209, 370, 371] In the previous chapter we reported the synthesis of a novel class of triazine (TZ) lipids, based on cyanuric chloride, that demonstrated potential for nucleic acid delivery due to their appended cationic moieties.[343] These compounds were similar to the dimerizable, redox-sensitive lipid reported by Candiani, et al. and the compounds published recently by Pennetta et al.[352, 372] We showed that lipoplexes (LP) formed from triazine lipids result in increased transfection efficiency *in vitro*, while also displaying comparatively reduced toxicity.[343] However, their *in vivo* characteristics have not been evaluated.

Due to the protein levels and transgene immunogenicity achieved with mRNA, versus plasmid DNA, this type of nucleic acid has become prevalent for liposomal gene delivery, particularly in the context of vaccines.[254] However, the immunogenic potential of mRNA can deter its use in other forms of gene therapy, such as gene replacement, where the development of anti-transgene antibodies can lead to clearance and failure of therapies. Plasmid delivery might therefore have an advantage in this context, since it can lead to reduced immunogenicity[373, 374] and it results in diminished immune system activation, similar to modified mRNA based nanoparticles.[231, 375]

One protein of therapeutic potential is the protease inhibitor alpha 1 antitrypsin (hAAT). While used primarily as a replacement therapy in patients who suffer from hAAT deficiency, a debilitating condition that causes severe lung damage and other sequelae, hAAT delivery has shown promising outcomes in other inflammatory diseases due to its anti-inflammatory activity.[376, 377] Like other biologics, hAAT has been shown to induce antibody responses when administered as a protein.[378-383] However, research by Song, et al. shows that this downside that can be mitigated by administering the protein via transduction with an AAV8 vector. [373, 384, 385]

Previous attempts to deliver hAAT plasmid DNA with liposomal vectors have resulted in modest outcomes in animals[386] and a phase I clinical study,[387] although in both scenarios the levels achieved were subtherapeutic.[384, 387] Due to the extensive characterization of this protein and its immunogenicity, hAAT makes an optimal candidate for research in evaluating novel cationic lipid compounds within this context. Furthermore, there are many tools available to study the protein, including plasmids and antibodies against the protein.

The studies in the present chapter were designed to assess the utility of TZ lipids in delivering hAAT plasmid *in vivo* with associated toxicity and transfection efficiency of these compounds in mice, using DOTAP as a comparison. Because our *in vitro* evaluation was based on the use of LPs we also decided to compare these to lipid nanoparticles (LNPs), as these are reported to have improved efficacy *in vivo*.[388] Formulations were developed using the lipids displayed in Figure 1 and based on standard DOTAP formulations described previously. However, further optimization of the formulations with triazine lipids was required, leading to several novel findings. Herein, we demonstrate the ability of optimized TZ lipid formulations to improve *in vivo* plasmid transfection beyond that of standard DOTAP formulations and describe the immunologic response targeting the transgenes using each formulation.

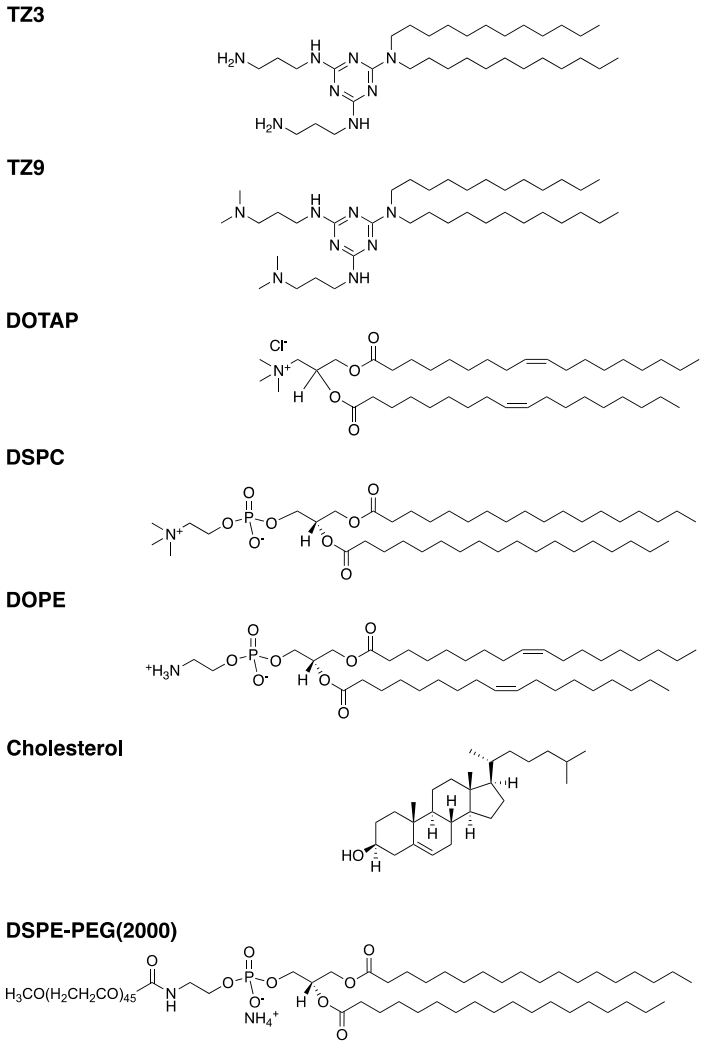

Figure 3.1. Structure of triazine lipids and other lipids used in plasmid formulations.

3.2 Experimental Methods

3.2.1 Mice and cells

Mice were purchased from Jackson Labs at 5-6 weeks of age and used in experiments at 7-9 weeks. C57BL/6J (#000664) mice were used for toxicity experiments shown in Figures 2 and S1, while BALB/cJ (#000651) were used for transfections in all other figures since the initial route of administration chosen was intravenous. Equal numbers of male and female mice were used in each experiment. Mice were sedated using isoflurane gas prior to blood collection by saphenous vein puncture or intraperitoneal (i.p.) injections. Baseline serum levels of all experimental parameters were established one week prior to injections. Mice were housed in a specific-pathogen free facility at the University of Kentucky, and all experimental procedures were approved by the University of Kentucky Institutional Animal Care and Use Committee #2020-3523. HEK293T cells, kindly donated by Dr. Gregory Graf of the University of Kentucky College of Pharmacy, J774A.1 macrophages (ATCC TIB-67) or bone marrow derived dendritic cells were used for cell experiments and maintained at 37 °C with 5% CO_2.

3.2.2 Development of bone marrow derived dendritic cells (BMDCs)

Mature murine dendritic cells were obtained by culture of bone marrow monocytes as described previously[389] using recombinant murine GM-CSF (Biolegend). On day 10 of culture, lightly adherent cells were detached with gentle washing and moved to a 96-well flat bottom cell culture plate at a density of 100,000 cells per well, in triplicate, for experiments.

3.2.3 Development of lipid nanoparticles

Two types of nanoparticles were used for experiments: liposomes and plasmid lipid nanoparticles (LNPs). In both cases, the lipids used were dissolved in chloroform, mixed at the ratio described in each figure legend, dried into a thin lipid film by rotary evaporation, and placed under house vacuum overnight before use. To form liposomes, the dried lipids were rehydrated in HEPES buffered saline (20 mM HEPES, 145 mM NaCl, pH 7) (HBS) with a pH of 4 and sonicated until translucent at 60 °C before being mixed with HBS to the final concentration and pH 7.4. Lipoplexes were formed from liposomes by mixing liposomes and DNA at a ratio of 6:1 positive to negative charges in Opti-MEM (for cells) or HBS (for mice) and incubated at room temperature for at least 12 minutes prior to administration.

To form LNPs, dried lipids were rehydrated to a concentration of 10 mM in ethanol with 10 μL of 5 M HCl per mL of ethanol and mixed with a solution of DNA at 40 ng/μL of DNA in 300 mM citric acid, pH 4. The ethanol and aqueous solutions were mixed into LNPs using the Ignite microfluidic system (Precision NanoSystems) at a ratio of 1:3 ethanol to aqueous, at a rate of 12 mL/min. The LNPs were then transferred into 3 mL Slide-A-Lyzer cassettes (ThermoFisher # PI87732) and stirred at 200 rpm in 1.5 L of a 300 mM citric acid, pH 4 solution for three hours, followed by three hours in 1.5 L of HBS

buffer, pH 4 (145 mM NaCl and 20 mM HEPES), before being moved overnight to a 1.5 L solution of HBS, pH 7.4.

3.2.4 Characterization of nanoparticles

Nanoparticle size was determined using a Zetasizer Nano ZS (Malvern Panalytical) with the following settings: four measurements of fifteen, five second runs detected at a backscatter angle of 173° at room temperature. The zeta potential for the liposomes was determined in a DTS1070 folded capillary zeta cell using the following settings: four measurements of at least 50 runs modelled with the Smoluchowski equation at room temperature using the automatic settings from the instrument. The concentration of DNA in LNPs after dialysis was quantified using an AccuClear® Ultra High Sensitivity dsDNA Quantification Kit (Biotium # 31027) and quantified on a BioTek Synergy H1 plate reader. Encapsulation efficiencies were determined by comparing the amount of DNA in the LNP solution vs. the DNA solution used to make them, after disrupting the LNPs with 0.5% C12E10 (Abcam # ab146563) and adjusting for volume differences (i.e.: excess volume added during dialysis and dilution volume during ethanol mixture).

3.2.5 Evaluation of in vivo toxicity and hAAT transfection efficiency

Mice were administered 0.1 mL of the liposomal solution i.p. Forty-eight hours later, the mice were bled for evaluation of serum creatinine (SCr; Crystal Chem no. 80350), alanine aminotransferase (ALT; AAT Bioquest no. 13803) and interleukin-6 (IL-6; Biolegend no. 431304) according to manufacturer instructions.

To assess *in vivo* hAAT transfection efficiency, mice were administered 200 µL nanoparticles or PBS vehicle i.p. at the doses indicated in the figure legend. Seventy-two hours after injection the mice were bled again for assessment of ALT levels and hAAT expression. hAAT levels were determined via ELISA using serum diluted 1:1 in PBS containing 0.05% casein (PBS-C; 124250; Beantown Chemical), as described previously.[4]

3.2.6 Flow cytometry

To measure transfection efficiency and subsequent GFP expression *in vitro*, 5×10^4 HEK293T or J774A.1 cells, or 1×10^5 mature dendritic cells, were plated in 96- well flat-bottom sterile cell culture plates and allowed to become confluent or adhere overnight. The next day, the cells were treated with 200 ng of pDNA encoding for GFP (Addgene product number 37825), delivered via nanoparticles, and incubated overnight with the nanoparticles. The media was changed at 24 hours, and after 72 total hours, cells were trypsinized briefly and transferred to a round bottom 96 well plate for flow cytometric analysis of viability and GFP expression. Live/ dead staining was performed using Zombie viability dye (Biolegend) according to manufacturer instructions. Cells were washed and resuspended in FACS buffer (Mg^{2+}/Ca^{2+}- free Hanks' balanced salt solution, 2 mM EDTA, 25 mM HEPES and 1% FBS) for fluorescence measurement. The gating schemes used for all flow cytometry are shown in Figure 3.2.

DiD liposome uptake was assessed 24 hours after liposome treatment after washing cells three times with PBS to remove free liposomes prior to trypsinization and staining as described above. Extension of this experiment to 72 hours (the optimal time for GFP transfection based on experimental data) resulted in no differences between groups due to overexposure of the cells to the nanoparticles (data not shown).

For *in vivo* evaluation of GFP transfection, mice were administered GFP plasmid (Addgene no. 37825) i.p. using LNPs or LPs at a dose of 10,000 ng of DNA or AAV8 at a dose of 2 x 10^9 genome copies per mouse (equating to approximately 200 ng of DNA) and serum was collected 3 days later to evaluate ALT levels as described above. Seven days after transfection, mice were euthanized by CO_2 inhalation and perfused with 10 mL of Ca^{2+}/Mg^{2+}-free HBSS followed by 10 mL of HBSS containing 1 mg/mL type IV collagenase (MP Biomedicals) via the hepatic portal vein. Livers were excised, diced with a scalpel, and incubated for 30 minutes at 37 °C in RPMI containing collagenase at 1 mg/mL and 50 µg/mL DNAse (MP Biomedicals). Digested liver fragments were gently pressed through a 0.22 µm mesh filter and the cells were collected, centrifuged at 50 *x g* for 3 minutes with the supernatant discarded, and then washed twice more with phosphate buffered saline. The remaining cell suspension (50 µL) from each liver was then moved to polycarbonate tubes and diluted 1:10 in FACS buffer containing anti-mouse CD16/32. After blocking, samples were incubated with fluorescent antibodies directed against mouse CD45 and CD146 for 30 minutes at 4 °C. These markers were chosen to gate out lymphoid and epithelial cells on the liver. After 30 minutes, the cells were washed twice in FACS buffer before being resuspended for fluorescence measurement.

All flow cytometry antibodies, as well as viability dyes, were purchased from Biolegend. Fluorescence measurement was performed using an Attune NxT flow cytometer (ThermoFisher).

3.2.7 Quantification of anti-hAAT antibody titers and determination of subclass ratios

To assess the presence of antibodies toward hAAT, 50 µL of hAAT (OriGene #RG202082) was plated at 2 µg/mL in carbonate buffer, pH 9.7, on a 96 well high binding plate (Greiner #82050-720) and incubated overnight at 4 °C. The next day, the plates were washed with PBS containing 0.1% Tween-20 (PBS-T) and blocked for 1 hour with PBS-C at 37 °C. After blocking, serum samples were plated at dilutions ranging from 1:100 to 1:1,000,000 and incubated at 37 °C for 2 hours. Secondary antibody (goat anti-mouse IgG HRP; Invitrogen #16066) diluted 1:2000 was applied for 30 min at 37 °C, followed by a 30 min. incubation with tetramethylbenzidine (Rockland). Absorbance at 450 nm was recorded using a BioTek Synergy H1 microplate reader. Reciprocal endpoint titers were determined by plotting A_{450} values versus known dilutions, calculating the slope of that line, and dividing the slope by two times the average of the blank (no serum) wells.

Anti-hAAT IgG subclass ratios were assessed as described above, using a single 1:100 sample dilution and the following detection antibodies: goat anti-mouse IgG1-HRP (Abcam ab98693) at 1:10,000, IgG2a-HRP (Abcam ab98698) at 1:5000, IgG2b-HRP

(Abcam ab98703) at 1:10,000 and IgG3 (Jackson 115-035-209) at 1:5000. Subclass ratios were calculated by dividing the absorbance of each subclass by that of IgG1 for each individual mouse.

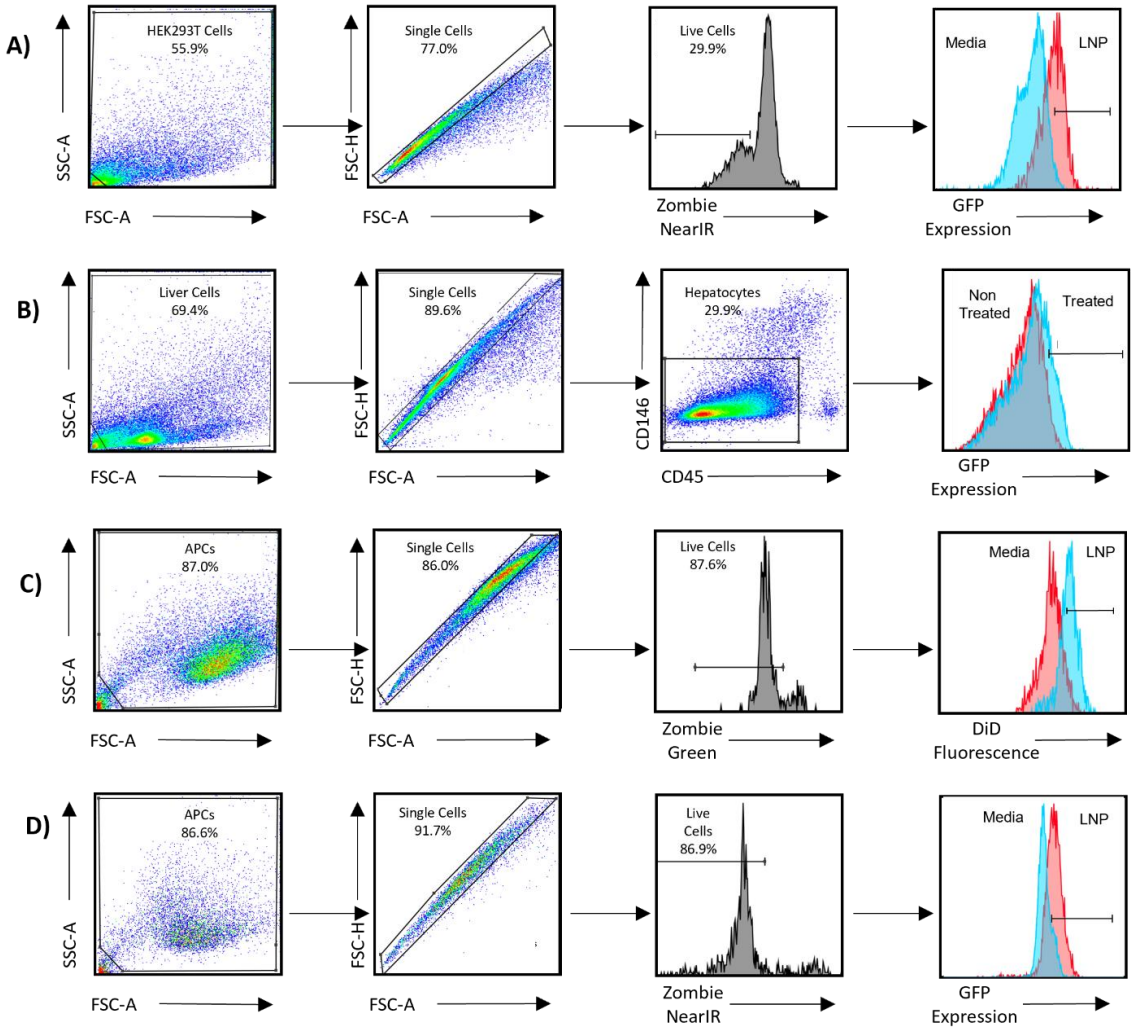

Figure 3.2. Schemes for flow cytometry analysis. A. Scheme for GFP quantification in HEK293T cells stained with Zombie NearIR Dye after transfection with GFP plasmid with LNPs. B. Scheme for GFP quantification in mouse splenocytes stained with anti-CD45-APC and anti-CD146-PE/Cy7 after transfection with GFP plasmid in nanoparticles or AAV8. C. DiD quantification in APCs stained with Zombie Green Dye after treatment with DiD liposomes. D. GFP quantification in APCs stained with Zombie NearIR Dye after treatment with GFP plasmid in nanoparticles.

3.2.8 Data analysis and statistics

Data were organized and analysed using Graph Pad Prism v.9 for Windows. Groups were compared as described in the figure legends; $*p < 0.05$; $**p < 0.01$; $***p < 0.001$; $****p < 0.0001$. In all figures, only statistically significant comparisons are shown.

3.3 Results and discussion

Prior to conducting *in vivo* transfections, the toxicity of cationic TZ lipids was assessed using the two compounds that demonstrated the highest efficacy *in vitro* (triazine lipids 3 and 9, or TZ3 and TZ9).[343] To test toxicity of TZ lipids, male and female C57BL/6J mice were administered TZ LNPs at 10 and 20 mM intraperitoneally (i.p.) in HEPES buffered saline. Seventy-two hours after administration, serum levels of alanine aminotransferase (ALT), interleukin 6 (IL-6), and creatinine (SCr) were tested and compared with baseline levels drawn one week prior (figure 3.3). Administration of LNPs formulated with 20 mM pure TZ9 lipid led to significant elevations in ALT and IL-6 and additionally, three of the ten mice in this group died. SCr levels in TZ9- treated mice were also elevated but did not reach statistical significance. ALT and IL-6 levels trended upward in mice treated with TZ3; however, neither these nor the IL-6 elevation in DOTAP-treated mice reached statistical significance. SCr levels were elevated but heterogeneous in TZ9-treated mice, while neither of the other two treatments caused SCr increases. Similarly, mice treated with 10 mM TZ9 showed statistically significant increases in ALT and IL-6, with one mouse dying in this treatment group (figure 3.3). Visual examination of internal organs at 72 hours revealed significant inflammation and swelling throughout the intestines and abdominal cavity of mice treated with TZ9 at 10 and 20 mM. The toxicity of TZ9 *in vivo* was unexpected, as *in vitro* studies indicated TZ9 to be less toxic than TZ3.[343] The discordant results between *in vitro* and *in vivo* studies suggest that the cause of toxicity is more complex than simple cytotoxicity, but the exact physiologic mechanism of toxicity is unclear. Thus, TZ3 was chosen to go forward for transfection experiments.

Lipid based nanoparticles are generally prepared with various lipids to afford a nanoparticle with specific properties, based on the desired application.[217] Earlier literature describe lipoplexes (LPs) formed by mixing cationic liposomes with nucleic acid, while more recent literature focuses on lipid nanoparticles (LNPs) made by encapsulating nucleic acid in lipids dissolved in a water miscible organic solvent.[209, 390] Much of the current literature in LNP delivery, including the literature from approved COVID vaccines, employs a formulation made with a mixture of 40-50% cationic lipid, ~10% DSPC, 30-40% cholesterol and 1-10% PEGylated lipid,[209, 357, 391-395] with some work suggesting that a 50:10:38.5:1.5 ratio is optimal for delivery of siRNA and other RNA molecules.[357, 396-398] Therefore, to evaluate TZ3 in the context of gene delivery, combinations were made with TZ3, DSPC, cholesterol and DSPE-PEG2000 at a 50:10:39:1 molar ratio, using DOTAP LNPs as a comparison. This formulation, was used to make nanoparticles by microfluidic mixing using an hAAT plasmid that ranged between 70-80 nm in diameter, with zeta potentials between 8-16 mV, and encapsulation efficiency above 70% (Table 3.1).[391] However, when administered to mice via tail vein injection, these formulations failed to elicit detectable hAAT protein levels (figure 3.4). Attempts were made to use other routes of administration (intravenous, intraperitoneal or intramuscular) or promoter used (CMV vs EF1a) but these all failed to induce expression of hAAT.

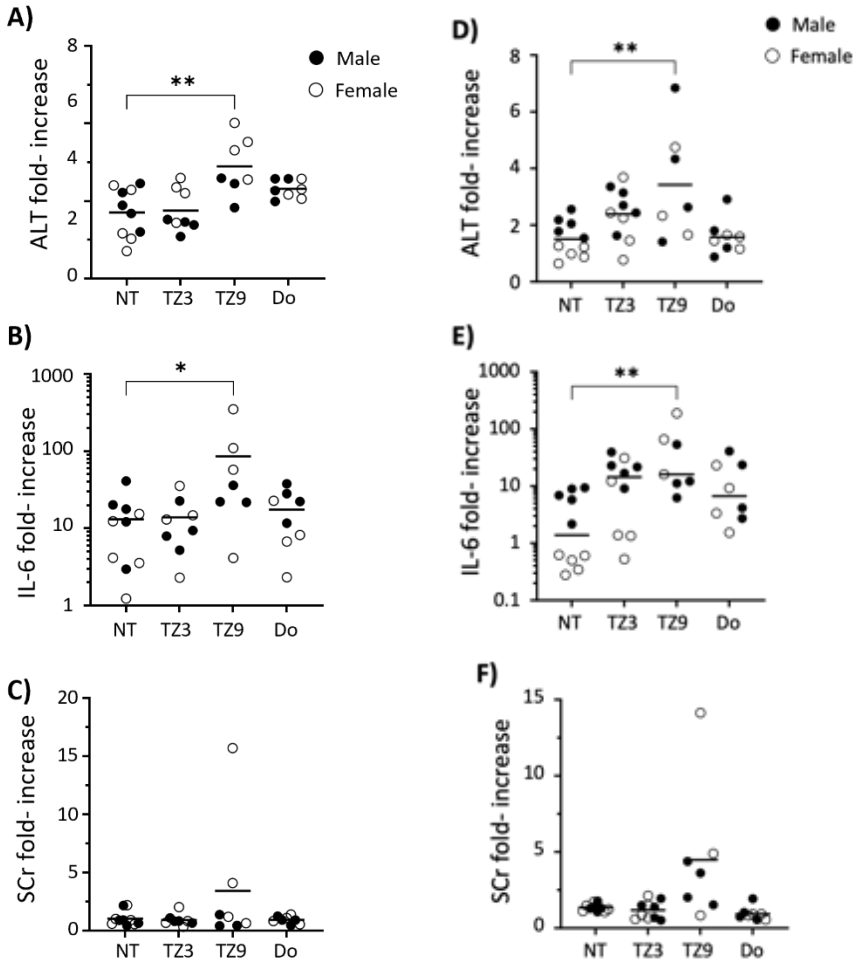

Figure 3.3. TZ3 does not result in significant *in vivo* toxicity at 10mM (A-C) or 20mM (D-F). Seven-week-old C57BL/6J mice were administered 100 µL of 10mM or 20 mM cationic lipid (TZ3, TZ9 or DOTAP (Do)) intraperitoneally in HEPES buffered saline. (A and D) Serum alanine aminotransferase (ALT), (B and E) serum creatinine (SCr), and (C and F) interleukin-6 (IL-6) levels were measured 48 hours after treatment. Fold-change from baseline measurements drawn one week prior were compared with those of untreated animals (NT). Bars and lines represent mean, and dots represent individual animals. Equal numbers of each sex were included; however, the TZ9 group represents only surviving animals. Significance was compared using one way ANOVA and Dunnett's (A) or Kruskal Wallis tests (all others); only significant comparisons are shown.

Overall, PEG content could be implicated in the poor transfection efficiency observed in figure 3.4; however, PEG has been shown to be necessary for improving circulation half-life and providing stability to nanoparticles *in vivo*. [399-403] Therefore, rather than reducing the PEG concentrations, the role of PEG length on transfection efficiency was analysed using identical lipid ratios and varying lengths of PEG polymer. These formulations were then used to prepare nanoparticles encapsulating a GFP plasmid and used to transfect HEK293T cells. As shown in figure 3.5, the length of PEG correlated with

a decrease in GFP expression. The nanoparticles made without PEG or with PEG550 yielded the highest GFP expression. However, PEG-free LNPs were unstable and formed aggregates. Consequently, formulations with PEG550 were used for further evaluation.

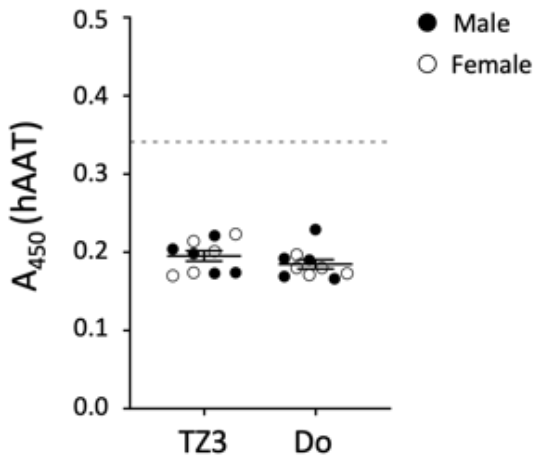

Figure 3.4. hAAT plasmid administered in cationic PEG-2000 liposomes fails to transfect mice. Eight-week-old male and female BALB/c mice were administered with 500 ng hAAT plasmid in LNPs made with 50% cationic lipid (TZ3 or DOTAP (Do)), 10% DPSC, 39% cholesterol and 1% DSPE-PEG2000. Blood was drawn 72 hours after injection and hAAT protein levels were detected by ELISA. Dotted line indicates limit of quantification.

Transfection may also be improved by using DOPE, rather than DSPC, as a helper lipid.[367, 391, 397] To further optimize transfection, the formulations containing DSPE-PEG550 were tested using DSPC or DOPE as helper lipids, with either TZ3 or DOTAP. As shown in Figure 3.5B, use of nanoparticles containing both TZ3 and DOPE significantly increased transfection efficiency, suggesting this could be the most optimal formulation.

Dynamic light scattering analysis of the nanoparticles made with PEG2000 and hAAT plasmid for the data presented in figure 3.4 exhibit similar characteristics to those described in the literature for plasmid based nanoparticles (Table 3.1).[391, 400, 404] However, the nanoparticles made with shorter PEG chains were larger and more polydisperse, a trend that has been reported previously with the reduction of PEG2000 concentration.[391, 400, 404] DOPE also increased size and polydispersity compared with DSPC. This change could possibly be attributed to the increased rigidity of the stearoyl tails of DSPC compared with DOPE's oleyl tails but has not been previously noted to the best of our knowledge. Finally, TZ3, while successful at encapsulating DNA, trended toward lower encapsulation efficiencies as compared to DOTAP, generally encapsulating 60-70% of DNA vs. DOTAP's 70-80% encapsulation. While the attributes of the nanoparticles can likely be improved by further altering multiple parameters such as cholesterol content, no additional alterations were made and further evaluation of TZ3 was pursued using PEG550 and DOPE.[405, 406]

Table 3.1. Characterization of liposomal nanoparticles used in studies. N/A = not applicable. *LNPs formulated without PEG aggregated during dialysis and had large clumps of lipid/DNA complexes.

Nanoparticle	**Size (nm)**	**PDI**	**Charge (mV)**	**DNA Encap. (%)**
TZ3 Liposomes	67.04±2.94	0.256±0.06	34.23±7.92	N/A
TZ9 Liposomes	50.53±0.73	0.256±0.02	47.95±0.21	N/A
DOTAP Liposomes	79.14±2.17	0.238±0.06	18.16±1.50	N/A
TZ3-PEG2000 hAAT LNP	78.79±1.35	0.197±0.01	8.38±1.26	74.28
DOTAP-PEG2000 hAAT LNP	70.86±0.61	0.159±0.01	15.40±0.10	79.76
TZ3-PEG550 hAAT LNP	251.93±0.91	0.139±0.02	14.70±0.44	63.62
TZ3 hAAT LP	396.63±9.82	0.390±0.09	31.33±2.40	N/A
DOTAP-PEG550 hAAT LNP	216.03±7.19	0.213±0.04	13.56±2.28	76.27
DOTAP hAAT LP	1712.67±51.21	0.488±0.17	20.35±7.85	N/A
TZ3-PEG550 GFP LNP	416.50±28.9	0.190±0.02	18.30±2.63	62.56
TZ3:DOPE Liposome	41.71±1.01	0.372±0.02	38.57±3.07	N/A
TZ3 GFP LP	157.89±3.54	0.235±0.03	33.27±8.60	N/A
DSPC:DOPE Liposomes	130.60±1.57	0.253±0.02	-7.70±1.99	N/A
No PEG LNP – GFP*	289.97±3.91	0.279±0.04	18.13±2.66	78.12
PEG550 LNP – GFP	227.93±3.93	0.188±0.04	24.77±5.03	67.18
PEG1000 LNP – GFP	196.53±8.22	0.102±0.06	25.15±1.22	68.84
PEG2000 LNP – GFP	132.73±6.99	0.264±0.05	20.07±2.04	79.22
TZ3 DSPC LNP – GFP	485.30±61.72	0.169±0.08	14.93±3.17	65.46
TZ3 DOPE LNP – GFP	649.03±129.96	0.423±0.09	15.10±0.82	59.36
DOTAP DSPC LNP – GFP	817.70±160.78	0.457±0.07	8.89±0.72	94.60
DOTAP DOPE LNP – GFP	513.47±116.92	0.491±0.15	19.57±4.05	71.01

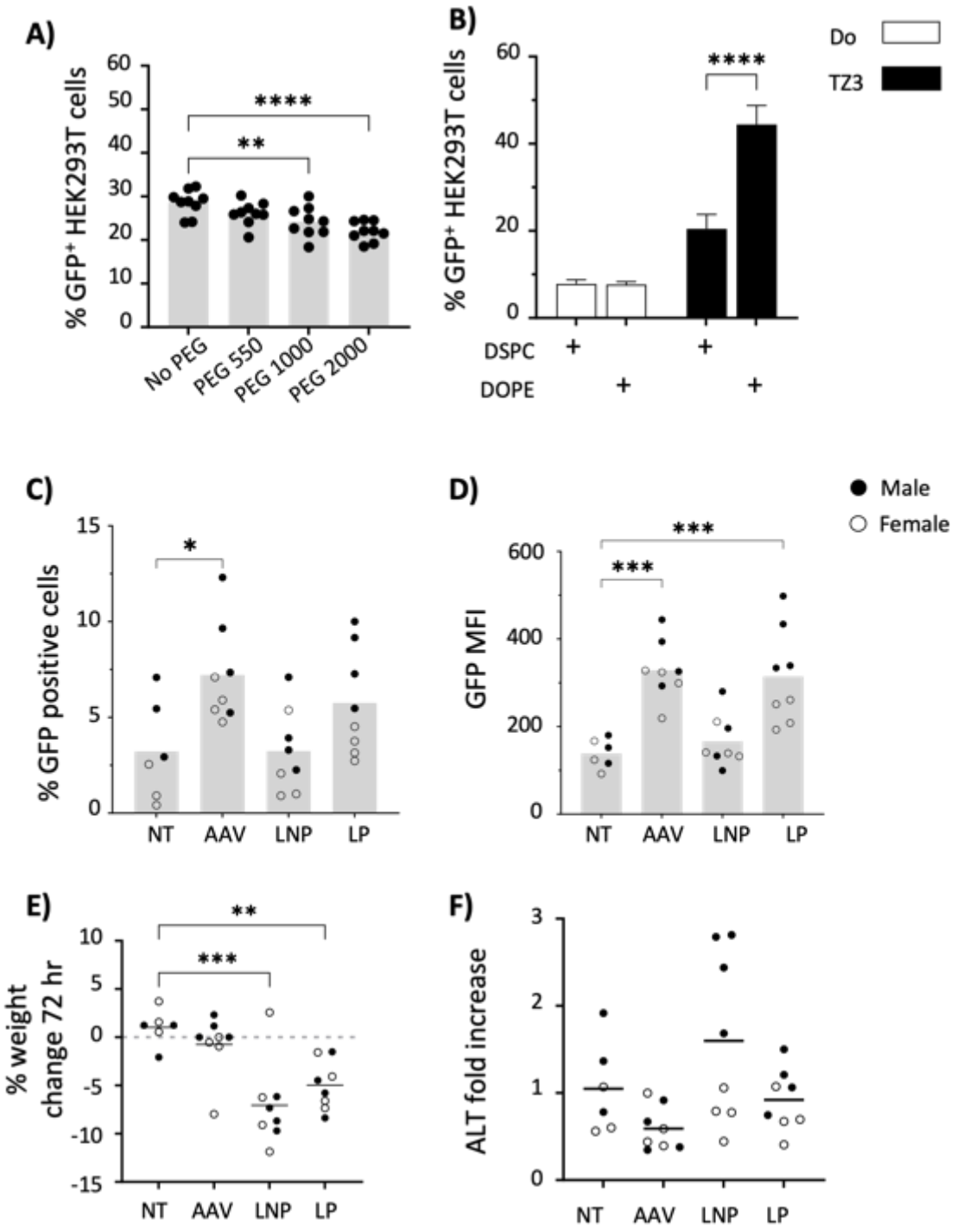

Figure 3.5. PEG550, DOPE, and TZ3 improve transfection efficiency with LNPs, but LPs exhibit improved transfection efficiency and reduced toxicity *in vivo*. (A-B) HEK293T cells were transfected with 200 ng GFP plasmid per well using LNPs and analyzed three days later for GFP expression by flow cytometry. (A) LNPs formulated with 50% TZ3, 10% DSPC, 39% cholesterol and 1% DSPE-PEG(550-2000), or 40% cholesterol and no PEG. (B) LNPs formulated with 50% DOTAP (Do) or TZ3, 10% DSPE or DOPE, 39%

cholesterol and 1% DSPE-PEG550. Pooled data from three independent experiments is shown; n = 3 transfected wells per group per experiment. (C-F) Male and female BALB/c mice were administered 1 x 10^9 genome copies of AAV8-GFP or 10 µg of GFP plasmid in either LNPs made with 50% TZ3, 10% DOPE, 39% cholesterol and 1% DSPE-PEG550 or LPs made with 50% TZ3 and 50% DOPE. One week post administration, hepatocytes were evaluated for: (C) percent GFP positive cells, or (D) mean fluorescence intensity (MFI). (E) Percent weight change and (F) serum ALT were also evaluated at the same time point. Bars indicate mean transfection efficiency +/- SD; dots represent individual transfection wells in (A) or mice in (C-F). Data were compared with one-way ANOVA and Dunnett's test in (A, C-F) or Sidak's text in (B); comparisons shown in (A) are to No PEG and in (C-F) to untreated mice (NT).

After optimization *in vitro*, the PEG550 and DOPE formulation was evaluated *in vivo* using the same GFP plasmid. Using TZ3 LNPs, 10 µg of plasmid DNA was transfected into mice and compared with the same dose of DNA delivered via LPs made from a 1:1 ratio of TZ3 and DOPE, which we previously used for *in vitro* transfection.[343] Since the resulting nanoparticles were over 200 nm in diameter, they were delivered i.p. based on the concern that intravenous (i.v.) administration could harm the animals. Additionally, previous studies have shown this route to result in similar transfection efficacy as i.v. administration.[297, 407] As shown in Figure 3.5C-D, transfection with LNPs was less efficient than that achieved using an AAV8-GFP vector, carrying the same plasmid, at a dose of 2 x 10^9 GC per mouse (~200 ng of DNA). Although transfection with LPs was heterogeneous, mean hepatocyte GFP positivity trended upward over untreated mice. Additionally, when mice were treated with the AAV8-GFP vector or LPs, GFP MFI in hepatocytes was significantly increased over untreated mice, while LNP treatment resulted in no increase over baseline (Figure 3.5D). Toxicity evaluation of these formulations showed that mice treated with LNPs and LPs lost 1-12% of their body weight at 72 hours and those treated with LNPs had slight (non-significant) elevations in ALT levels at the same timepoint (Figure 3E-F). Of note, males seemed to have higher expression of GFP compared with females treated with LPs which could be due to increased trafficking to the liver. However, this theory is not supported by existing literature to the best of our knowledge.

Based on these data we then sought to re-evaluate hAAT transfection, using TZ3 and DOTAP LNPs or LPs. The lipid formulations were made as above, and the mice received 10,000 ng of hAAT plasmid DNA. Control mice were given hAAT protein at 25 µg of protein, calculated on average observed amount of protein reported by Crepso, et al. with liposomal delivery of hAAT plasmid.[383, 408, 409] Because the lipids themselves can increase immunogenicity against proteins, separate groups of mice were administered the protein in saline or with 1 mM TZ3, DOTAP, or DMPC.[224] Following transfection, the optimized LP formulation led to detectable hAAT levels in serum in some of the mice (figure 3.6), although these were well below the values reported previously for cationic

lipid delivery.[386] As with GFP delivery, however, LP administration led to higher transfection efficiency with average hAAT levels of 9.5 ng/mL for TZ3 and 3 ng/mL for DOTAP LPs, which were closer to those observed in previous work by Crepso, et al. and Aliño, et al.[386, 408] HAAT levels persisted at 4 weeks after treatment, but only in TZ3 treated animals (figure 3.7A). In the mice given hAAT protein with individual lipids, serum hAAT levels at 72 hours were detectable but overall lower than expected based on the reported half-life;[410, 411] however, DMPC produced an intriguing protein increase in females that was not detected in males (figure 3.7B).

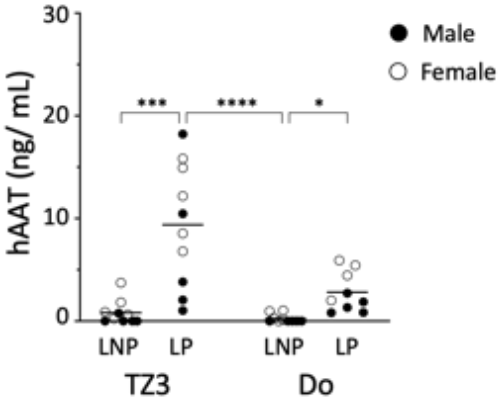

Figure 3.6. TZ3 LP transfection is more efficient *in vivo* than TZ3 LNPs or formulations made with DOTAP. BALB/c mice were administered 10 µg of hAAT DNA with LNPs made with 50% TZ3 or DOTAP (Do), 10% DOPE, 39% cholesterol and 1% DSPE-PEG550 or LPs made with 50% TZ3 and 50% DOPE. Seventy-two hours later, protein expression in the serum was assessed via ELISA. Lines represent mean hAAT concentration; dots represent individual animals. Data were compared with Kruskal-Wallis test.

As with GFP transfection, toxicity of the treatments was also assessed via ALT quantification. As shown in figure 3.7C, ALT levels rose 2-6 times above baseline at 72 hours. Conversely, in mice treated with protein, these signs of toxicity were not observed, suggesting that the toxicity is associated with liposomal transfection, not the lipids themselves.

As mentioned earlier, administration of hAAT to mice has been reported to induce anti-hAAT antibodies; therefore, anti-hAAT reciprocal endpoint titers were also assessed two weeks after hAAT transfection (day 14).[373, 412] Delivery of the transgenic protein with LNPs produced no detectable anti-hAAT IgG titers, while mice treated with LPs made using TZ3 or DOTAP showed significantly higher anti-hAAT titers than untreated mice, approximating that of the free protein in saline (figure 3.8A). While this difference could be accounted for by the difference in protein expression between the two groups (figure 3.6), previous literature shows that protein concentrations do not necessarily correlate with titer development[397] and that protein levels may not necessarily need to reach quantifiable levels for protein to induce robust immunity.[413]

Because lipids can serve as adjuvants, single lipids were also tested as above to assess the contribution of lipid to anti- hAAT immunogenicity. Administration of hAAT with DOTAP or DSPC increased titers by 10- and 100- fold, respectively. Surprisingly, TZ3 administration concurrent with hAAT protein led to an increase in titers 1000-fold higher than either of these two controls, suggesting a potential role for this compound in the setting of protein immunizations.[212, 232]

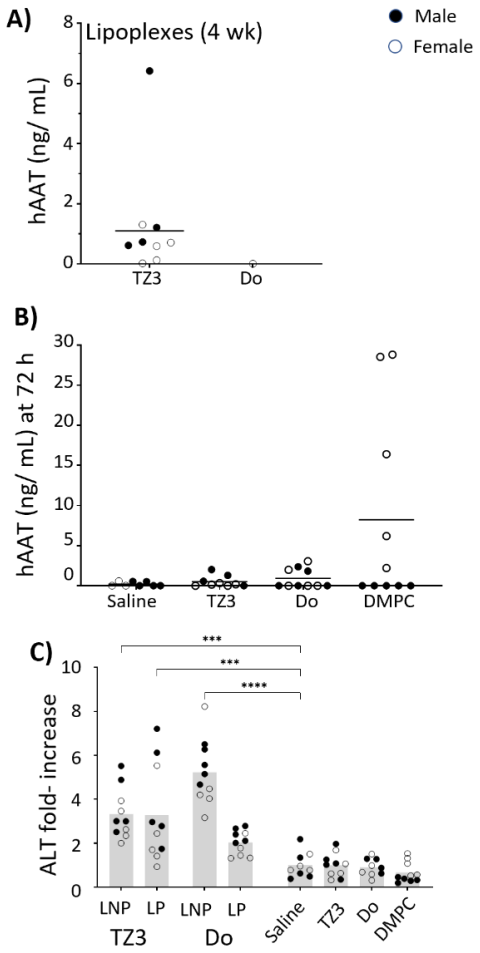

Figure 3.7. TZ3 LP transfection persists up to one-month post- delivery. BALB/c mice were administered 10 µg hAAT plasmid delivered via TZ3 or DOTAP (Do) LNP, or via lipoplex. A) Four weeks later, protein expression in the serum was assessed via ELISA. Only values above the limit of quantification are shown. B) HAAT protein concentrations at 72 hours after direct administration of 25 µg hAAT protein in either saline or with 1 mM lipid solution (indicated). C) Fold-change in serum ALT from baseline measurements at 72 hours after either transfection or protein delivery. Lines and bars represent mean; dots represent individual animals. Data in (C) were compared with one-way ANOVA and Kruskal-Wallis test; significance is as compared to protein in saline only, only significant comparisons are shown.

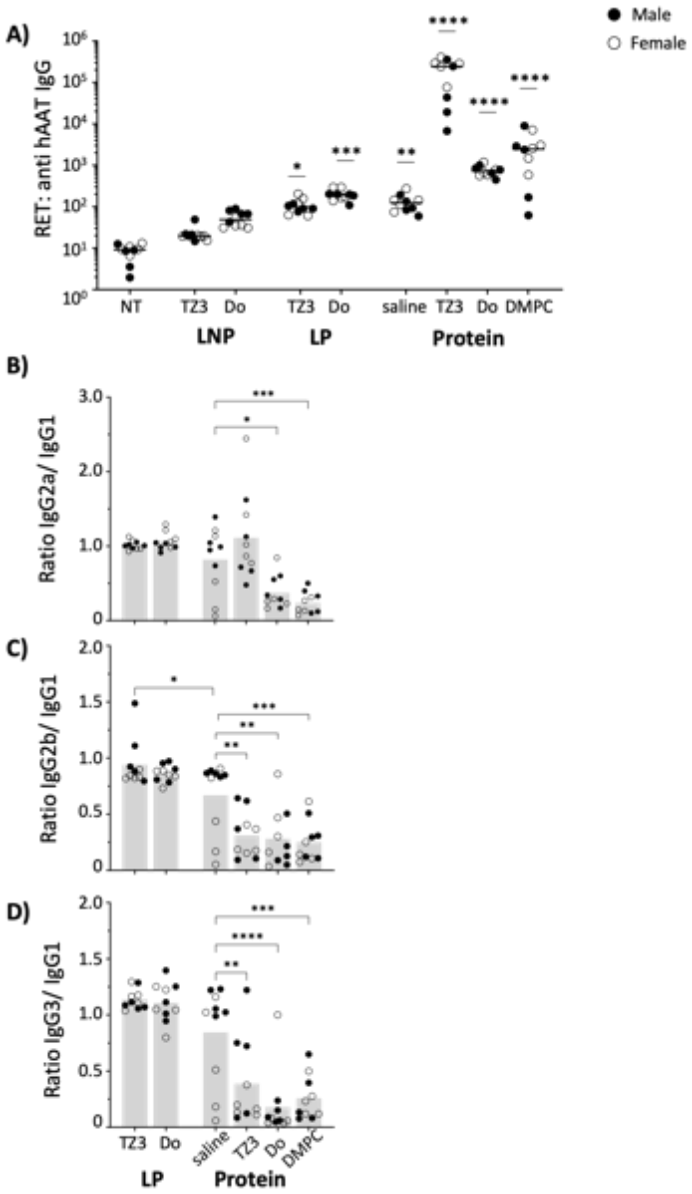

Figure 3.8. Transgene expression using TZ3 as a delivery vector elicits minimal antibody responses, while administration of hAAT protein with TZ3 results in significant immunogenicity and a Th1 bias. BALB/c mice were administered 10 µg of hAAT DNA with LNPs made with 50% TZ3 or DOTAP (Do), 10% DOPE, 39% cholesterol and 1% DSPE-PEG550 or LPs made with 50% TZ3 and 50% DOPE; or 25 µg of hAAT protein in saline or 1 mM lipid solution. (A) Fourteen days after administration, anti- hAAT IgG reciprocal endpoint titers (RET) were assessed via serum ELISA. Significance determined by Kruskal-Wallis test; comparisons made to untreated animals (NT). Ratios of IgG2a/ IgG1 (B), IgG2b/IgG1 (C), and IgG3/ IgG1 (D) were assessed at the same timepoint for treatment groups that had significantly higher RET than untreated. Bars indicate mean, while dots indicate individual animals. Significance as compared to protein delivered in saline was determined by one-way ANOVA in (B-D).

As immune biases toward a Th1- or Th2-type response following immunization can be suggestive of overall formulation immunogenicity, anti-hAAT subclass composition was also assessed via ELISA and the ratios of IgG2a, 2b and 3 to IgG1 were determined (Figure 3.8B-D) in all but LNP samples, as these did not achieve a sufficient antibody response. Transgenic hAAT delivery with both TZ3 and DOTAP led to a balanced Th1/Th2 response, as indicated by the ratios of IgG2a, 2b, and 3 over IgG1. Pure protein in saline resulted in similar responses; however, when delivered with lipids, there was a shift toward a Th2 response, indicated by ratios lower than 1.0. These data are similar to immune profile observed with Freund's incomplete adjuvant, which is known to induce a Th2 bias toward co-administered proteins.[414, 415] Additionally, this relative shift in IgG subclass responses is similar to that observed by Boyle, et al. with ovalbumin delivered via DNA vs. protein based vaccine.[230] Interestingly, hAAT protein delivered with TZ3 resulted in a more balanced IgG2a/ IgG1 ratio than DOTAP and DMPC; however, the other two subclasses did not follow suite. While the clinical relevance of this difference is difficult to assess in this non-infectious model, it may have implications that will be explored in future experiments.

A potential reason for the difference between LNP and LP titers, could perhaps be explained through previous work by Lu, et al. with AAV, which shows that expression in antigen presenting cells (APCs) is associated with the development of antibodies against hAAT.[412] Since PEGylation of nanoparticles was originally intended to bypass the reticuloendothelial system and nanoparticle removal by APCs,[416, 417] it was hypothesized that this feature of LNPs could explain the difference in antibodies developed against LNP and LP transgenes. To test this hypothesis, 5% DiD liposomes were made with or without DSPE-PEG2000 and incubated with J774 macrophages and bone marrow derived dendritic cells (DC). After 18 hours, cells were washed to remove free liposomes and assayed by flow cytometry. The addition of PEG resulted in lower DiD fluorescence in both cell types, and most prominently in DCs, which showed more than 60% less fluorescence when PEG was included as a LNP component (Figure 3.9A).

Since these LNPs were made with PEG550, which has been shown to have limited ability to inhibit APC uptake,[416] the effect of PEG on APC transfection with GFP plasmid formulations containing PEG550 was tested next. J774 macrophages and DCs were treated with either LPs, PEG free LNPs or PEG550 LNPs containing the same amount of GFP plasmid. In both cell types, transfection with PEG-free LNPs resulted in significantly higher GFP transfection than lipoplexes or LNPs containing PEG550 (figure 3.9B). In both DCs and J774 macrophages, the addition of PEG to LNPs decreased GFP positivity by more than 15%. DC expression was also slightly more efficient (~6%) with LP treatment than PEGylated LNPs; however, this pattern was not observed with J774 macrophages. These studies collectively suggest that the addition of PEG to nanoparticles may have an advantage in reducing the immunogenicity of liposomal transgenes, but also reduce the transfection efficiency when delivering plasmid DNA.

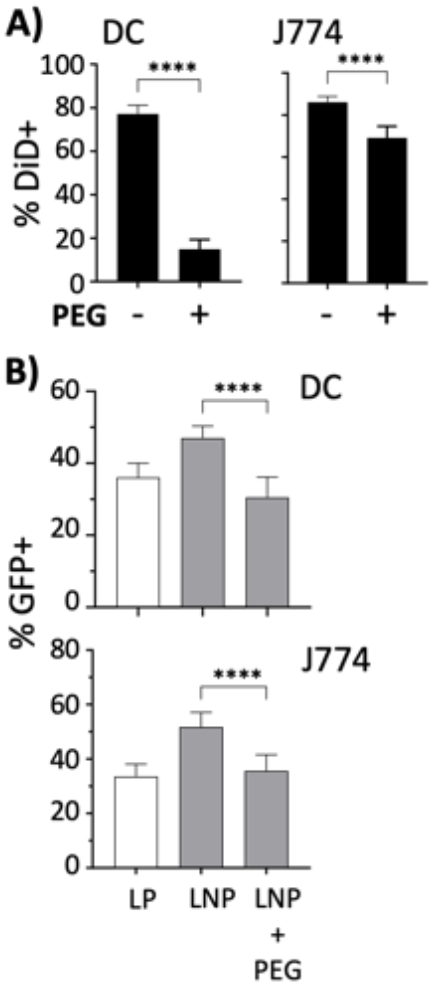

Figure 3.9. PEGylation decreases LNP uptake by antigen presenting cells. (A) Bone marrow-derived dendritic cells (DC) or J774 macrophages were incubated for 18 hours with LNPs made with 5% DiD and DSPE-PEG2000, or PEG-free liposomes. The percentage of cells positive for DiD fluorescence by flow cytometry is shown; data represent pooled results from three independent experiments, *N*= 3 wells/ treatment. (B) Bone marrow-derived dendritic cells (DC) or J774 macrophages were transfected with 200 ng of GFP DNA delivered with LPs made of 50% TZ3 and 50% DOPE; LNPs made with 50% TZ3, 10% DOPE, 40% cholesterol; or LNPs made with 50% TZ3, 10% DOPE, 39% cholesterol and 1% DSPE-PEG550. Seventy-two hours after transfection, the cells were analyzed by flow cytometry for GFP expression; data represent pooled results from three independent experiments, *N*= 3 wells/treatment. Bars indicate mean +/- SD. Only statistically significant comparisons are shown. Significance determined by one-sample T-test in (A) or one-way ANOVA in (B). ND = not determined.

3.4 Conclusions

The present manuscript highlights the utility of cationic triazine lipids as a tool for *in vivo* research. Evaluation of *in vivo* toxicity of the compounds showed, surprisingly, that TZ9 confers significant toxicity and mortality via a yet unknown mechanism, which differed from the *in vitro* toxicity observed during transfection.[343] This toxicity not only led to elevations in liver, kidney and inflammatory markers, but also to the death of several animals. However, TZ3 showed comparable toxicity to DOTAP, a commonly used cationic lipid, suggesting the need for further testing of the structure activity relationship of this cationic compound class.

The toxicity experiments were followed by evaluation of transfection with TZ3, which demonstrated increased transfection efficacy compared with DOTAP, both *in vivo* and *in vitro*. These results concur with the findings of Martinez-Negro, et al. and Candiani, et al. showing improved transfection efficacy with cationic lipids containing aromatic moieties.[352, 418] While the role of the triazine ring of the lipids described here, and their interaction with plasmid DNA have not been determined, others have indicated that the aromatic rings improve interactions with DNA base pairs through π-π stacking, and intercalation for improved binding.[419, 420] Regardless of the functional implications of the structural characteristics of triazine lipids, TZ3 serves as a leading candidate for *in vivo* transfection.

While LP transfections achieved hAAT levels similar to those reported in previous lipid literature,[386] lipid-based plasmid delivery systems were not able to achieve the levels observed with viral delivery systems.[373, 421] The hAAT plasmid used in these studies is based on a lentiviral system reported by Wilson, et al.[421] where the vector yielded protein at the microgram range, like the levels reported by Akbar, et al. with AAV.[373] While further optimization of the nanoparticle system, or use of other cationic lipid vectors, could improve transfections, it is also possible that plasmids designed for viral delivery require modifications to induce therapeutic protein levels using lipid nanoparticles. Plasmids offer certain advantages over other forms of nucleic acids, including longer stability and lower immunogenicity toward transgenes, [254, 374] theoretically making them better suited for long term expression of therapeutic transgenes. However, because DNA requires translocation into the nucleus and additional processing to achieve transfection, which ultimately leads to reduced levels of protein, other strategies, such as mRNA have dominated the field with the goal of improved hAAT expression using lipid-based systems.[254, 391]

As has been demonstrated by Gael and colleagues in vaccine studies[374] and by Huysmans, et al. in protein expression kinetic experiments,[422] mRNA confers higher protein levels and perhaps could achieve levels of hAAT within physiological levels. In fact, a previous report of mRNA by Karadagi, et al. shows that mRNA can significantly increase hAAT levels *in vitro* and possibly also *in vivo*, although the authors do not quantify circulating levels of protein after administration into mice.[423] Unfortunately, this would mean the need for continued mRNA delivery or self-replicating constructs, as opposed to the more stable expression achieved following delivery with viral vectors. One way to

remedy this could be through optimization of the plasmid delivery system, or the use of more novel systems such as CRISPR.[424, 425]

In addition to advances in mRNA delivery, much of the recent literature using LNPs for gene delivery takes advantage of ionizable lipids in formulations optimized primarily for siRNA delivery.[209, 357, 401] While these compounds are greatly successful and offer many advantages to gene delivery, we have shown here that formulations containing triazine lipids can provide a successful tool for plasmid delivery. Furthermore, we have shown that formulations containing DOPE and PEG550, rather than DSPC and PEG2000, can enhance the efficacy of plasmid delivery both in cells and in mice. Particularly interesting was the finding that LNPs, which contained PEG, reduced titers against the transgene compared with LPs without PEG. While the antibody response to hAAT is relatively low, these data suggest a need for further interrogation of the role of PEG in cationic lipid vaccines. Although we have shown that PEG can reduce nanoparticle uptake and transfection in antigen presenting cells (APCs), PEG is recognized by B cells *in vivo*,[266] which could help increase uptake and expression of antigens in B cells that recognize the polymer as an epitope and counter the reduced uptake by phagocytes. Another confounding factor for our evaluation of these findings is that, as reported by Hassett, et al., differences in nanoparticle size can affect titers generated by mRNA vaccines, a hypothesis that was not evaluated in the present manuscript.[426] This factor may potentially be crucial in the setting of immune system activation as larger nanoparticles (>200 nm) have limited ability of entering lymph nodes, compared with smaller ones.[427, 428]

In addition to the modest increase in immunogenicity toward the transgene when delivered as a lipoplex, TZ3 also resulted in robust antibody induction (RET $>10^5$) when used to deliver the hAAT protein. The ability of lipid based adjuvants is well recognized and has been reported in previous literature to surpass the titer response toward proteins, compared with DNA based vaccines, although perhaps not the CTL response, which was not evaluated here.[229, 230] Furthermore, cationic lipids are known to possess immunomodulatory properties[212, 224, 429] and serve as adjuvants,[232] but the significant induction with TZ3 was an unexpected finding. This is particularly notable given that TZ3 induced an antibody response two orders of magnitude greater than DOTAP. These data suggest that additional studies are needed to fully explore the adjuvanticity of TZ lipids when used in vaccine formulations.

Overall, these findings suggest the need for further investigation into the optimization of TZ lipid nanoparticles, as well as expansion of the current lipid repertoire to generate structure activity relationships using an expanded library of novel lipid structures for gene and vaccine delivery.

CHAPTER 4: EVALUATION OF A LIPOSOME BASED STRATEGY TO SUPPRESS ANTI-AAV ANTIBODIES

4.1 Introduction

Despite the superior transduction efficiency achieved with viral vectors in the context of gene replacement, compared with non-viral vectors, a major drawback of viral gene delivery is the immunogenicity of the vectors themselves.[430, 431] Preclinical and clinical studies show the intense cytokine storm elicited by delivery of viral vectors, with some viruses eliciting more intense immune responses than others.[431] In addition, the antibody responses generated against viral vectors create a major obstacle for their in vivo success. In patients who have had previous exposure to viral vectors, or those who have previously received viral gene therapies, neutralizing antibodies (NAbs) that inhibit viral transduction preclude the use of these therapies.[432]

Several approaches have been followed to counter the effect of anti-AAV NAbs, such as exclusion of patients with high NAb titers from clinical studies, administration of high vector doses, use of 'decoy' capsids, administration of immunosuppressants, using alternative or less common AAV serotypes, removal of NAbs via plasmapheresis or delivery of vectors directly to target tissues.[432] Because of this setback, AAV epitopes have been extensively studied in attempts to understand and modulate its immunogenicity.[430] Of the AAV therapeutics approved, voretigene neparvovec-rzyl is able to bypass systemic immunity due to direct administration into the retina.[433] While clearly effective, this approach is not feasible for all diseases due to inaccessibility of target tissues or because target cells are too diffuse throughout the body. Concomitant immunosuppression is another effective way to bypass some of these adverse effects. For example, alipogene tiparvovec, is co-administered with cyclosporine and mycophenolate mofetil, immunosuppressants that reduce virus induced immunogenicity and improve transfection rates.[434] The most recent approval, onasemnogene abeparvovec, takes advantage of immunosuppressants, in addition to being delivered in AAV9, which is much less prevalent as a naturally circulating virus.[433-435] Recently, Zhong, et al. reported that the use of CTLA4-Ig and CD40-Ig can prevent activation of T and B cells following AAV transduction and allows for repeated dosing.[436] Additionally, Selecta Biosciences has shown that the use of ImmTOR, a rapamycin containing lipid nanoparticle, can also inhibit immune activation when co-administered with AAV and allows for repeated dosing.[437, 438]

Unfortunately, many of these immunosuppressive strategies can lead to global immunosuppression, which puts patients at risk of infections and increases the risk of cancer.[439, 440] ImmTOR, in particular, has been shown to induce the development of regulatory T cells toward ovalbumin, which could be problematic in the context of viral suppression as it may lead to difficulty in staving off later infections.[441] An ideal NAb suppressing agent, in the context of AAV, should target specific B cells without affecting other aspects of the immune system and should allow for recovery of immune cells

following suppression. A phenomenon observed in the field of liposomal drug discovery is that PEGylated nanoparticles will often develop antibodies against the surface polymer.[442] However, in the presence of a cytotoxic drug, such as doxorubicin, anti-PEG antibodies fail to develop, prolonging the half-life of the nanoparticle.[443] This phenomenon has also been described in the context of ovalbumin by Oja, et al. who showed that antibodies against this protein fail to develop when doxorubicin is loaded into the liposomes that the protein is bound to.[268] More recently the Oku lab further expanded on this phenomenon by demonstrating that pre-existing anti-ovalbumin antibodies could be suppressed following immunization through the use of doxorubicin loaded liposomes, and even more effectively by using tacrolimus.[270, 444] In our lab, we have also shown the ability of such a strategy to suppress anti-peptide antibodies following immunization, and the ability of such a strategy to allow for recovery of the anti-peptide response following reimmunization.[445] In the present chapter, a liposome-based strategy is evaluated for its ability to suppress anti-AAV antibodies. To this end, doxorubicin loaded liposomes conjugated to the main surface protein of AAV8, VP1, are used to suppress B cells responsible for a pre-existing response to the virus.

4.2 Methods

4.2.1 Development of AAV8 VP1 plasmid constructs for E. coli

To produce AAV8 VP1 in prokaryotic cells, the VP1 sequence was cloned from Addgene's AAV2/8 packing plasmid (112864) using the forward primer CAGCCATATGGCTGCCGATGGTTATC and reverse primer TATAGGAATTCTTTAATGATGATGATGATGATGATGATGCAGATTACGGGTG AGGTAAC (ordered from IDT) using Platinum SuperFi II DNA Polymerase (Thermo, 12361010). The resulting amplicon was purified using NEB's Monarch PCR Cleanup Kit (T1030S), digested with NEB EcoRI-HF (R3101S) and NdeI (R0111S) restriction enzymes in CutSmart buffer for 4 hours and cleaned again. Simultaneously, a pET28a plasmid donated by Dr. Ester Penni Black at the University of Kentucky was digested with these same restriction enzymes, purified on a 1% agarose gel (VWR, 97064-250) stained with 0.5 mcg/mL of ethidium bromide (Thermo, 15585011). The larger band of ~5200 bp was extracted using NEB's Monarch Gel Extraction Kit (T1020S). The digested plasmid and amplicon were then ligated at 4 °C for 2 hours followed by overnight incubation at 16 °C using NEB's T4 Ligase in the ligase reaction buffer provided with the enzyme (M0202S). The following morning, the construct was transformed into NEB DH5 alpha competent cells (C2987H) using the accompanying protocol and assessed for the presence of the insert using the above primers and positive colonies were grown and sequenced using primers TAATACGACTCACTATAGGG, TTCCACATGGCTGGGCGACAG, and AGCGAGGAAGAAATCAAAACCAC (ACGT, Inc.). Upon confirmation of colonies, the plasmid was extracted from the DH5 alpha cells and transformed into BL21(DH3) competent cells (NEB, C2527H).

4.2.2 Induction and verification of VP1 protein production

To determine whether the developed constructs were successful, BL21(DH3) cells transformed with the VP1 plasmid were induced using 0.5 mM IPTG for 5 hours in 18 °C, followed by 13 hours at 18 °C, after reaching an OD600 of 0.6. This method is a modified version of the workflow used by Le, et al.[446] for producing AAV capsid protein in E. coli. As the authors suggest, the protein becomes aggregated during production in these cells, therefore the cells were spun down at 4000 *x g* at 4 °C for 15 minutes and resuspended in 0.5% Tween-20, 50 mM NaH_2PO_4, 300 mM NaCl, pH 8 containing 1 tablet of protease inhibitor cocktail (Thermo, A32963) per 50 mL. Following resuspension, the cells were sonicated using a cell homogenizer on ice and spun for 30 minutes at 14,000 *x g* at 4 °C.

The cell lysate supernatant was then collected, and the pellet was resuspended in 0.5% Tween-20 in 20 mM Tris-HCl, 8 M Urea, pH 8 containing a tablet of protease inhibitor cocktail per 50 mL and vortexed until solubilized. Both the insoluble and soluble portions were evaluated by western blot after mixing with 2x Laemni buffer (4% SDS, 10% 2-mercaptoethanol, 20% glycerol, 0.004% bromophenol blue and 0.125 M Tris HCl at pH 6.8) and heating to 95 °C for 5 minutes. The samples were loaded onto a 4-20% polyacrylamide gradient gel (Bio-Rad 4561095) using a VP1 construct made for eukaryotic cells as a control. The gel was submerged in running buffer (25 mM Tris, 192 mM glycine, 0.1% SDS) for 1 hour at 100 V and then transferred in transfer buffer (25 mM Tris and 192 mM glycine), at 4 °C for 45 minutes and 100 V to a PVDF membrane previously soaked in methanol (Cytiva 10600029).

After transferring, the membrane was blocked with 5% non-fat dry milk (MP Biosciences 902887) in TBS-T (0.2% Tween 20, 200 mM Tris 1.37 M NaCl, pH 7.6) for 30 minutes at room temperature and then incubated overnight in 1% non-fat dry milk containing 0.1 mcg of mouse anti-AAV VP1 antibody clone A1 (Progen, 61056). The following day the antibody was removed, and the membrane was washed three times with TBS-T with 5-minute incubations in between washes. Goat anti-mouse IgG2a-HRP (Abcam, 98698), diluted 1:5000 was then incubated for 30 minutes at room temperature and the membrane was developed using ECL reagent (Thermo, 32209). As suggested by Le, et al. most of the protein was contained within the insoluble pellet (figure 4.1).[446]

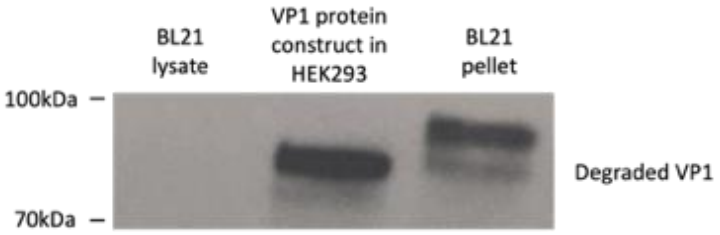

Figure 4.1 Western blot of VP1 protein in cell lysate and pellet, with eukaryotic derived protein as a control (middle).

4.2.3 Isolation of VP1 protein

VP1 isolation from the resuspended pellet was achieved using an NTA(Ni) purification kit (Thermo, 88228) by gravity. The column was washed with water 5 times and equilibrated five times with 0.5% Tween-20 in 20 mM Tris-HCl, 8 M Urea, pH 8, containing 5 mM imidazole. The protein was loaded and washed with equilibration buffer, followed by 20 mM and then 40 mM imidazole. Finally, the protein was eluted using 500 mM imidazole and dialyzed at 4 °C with PBS, pH 8 for a total of 24 hours with 4 buffer changes during that time. The resulting protein was then frozen at -80 °C and stored for later use.

4.2.4 Preparation of lipoproteins for immunization and suppression liposomes

Conjugation of VP1 to NTA(Ni) lipid was achieved by making liposomes from a 57:38:5 DSPC, cholesterol NTA(Ni)-DGS (Avanti, 790404P) formulation at a 10 mM liposome concentration. To these, VP1 protein was added at 5, 10, 20 and 40 NTA lipid to protein ratio, the mixture was incubated at room temperature for 30 minutes, and the formed nanoparticles were eluted through a PD-10 desalting column and assessed for size and protein concentration. For both suppression and immunization, the 40:1 ratio was chosen due to improved retention.

Conjugation to maleimide lipid was completed by placing VP1 in a pH 6.5 PBS solution at 0.4 mg/mL and mixing in 3.75 mg of DSPE-PEG_{2000}-Maleimide (Avanti, 880126C) at 1 mg/mL in DMSO (this is roughly 1.27 µmoles of lipid to 0.0046 µmoles of protein, or a 1 to 277 lipid to protein ratio). The reaction was covered with nitrogen gas and allowed to stir overnight at room temperature. The following day, the reaction was placed in 10 volume equivalents of ether and incubated overnight at -20 °C to precipitate protein. After overnight precipitation the protein was centrifuged at 4000 *x g* and the ether was discarded. The protein was washed again with ether to remove remaining maleimide lipid and the final protein quantification was determined by BCA.

4.2.5 Development of suppressive doxorubicin liposomes[447, 448]

Liposomes made with a 62:38 molar ratio of DSPC and cholesterol were dried into a thin lipid film from chloroform solutions and hydrated in 300 mM ammonium sulfate and sonicated at 65 °C until opalescent. For suppression with NTA-Ni liposomes 5% of the DSPC was replaced with 5% NTA(Ni)-DGS (Avanti, 790404P), while the liposomes containing maleimide bound VP1 had 50 µg of the protein added to the formulation. After hydration, the liposomes were cooled to room temperature and eluted through a PD10 desalting column (Cytiva, 17085101) equilibrated with 150 mM NaCl at pH 5.5. For the NTA-Ni containing liposomes, 25 mM MES was added to the equilibration buffer. After collecting the liposomes from the PD-10 column, they were sized and the amount of protein was quantified, in the case of the maleimide-VP1 liposomes, since these were formulated with protein, while the NTA liposomes were conjugated to protein after remote loading doxorubicin. At this point, 2.5 mg of doxorubicin were added per mL of 10 mM liposome solution and the samples were incubated at 58 °C for 45 minutes with the container cap

open. After 45 minutes incubation, the samples were moved to 4 °C for 15 minutes and added to 10 kDa MWCO dialysis cassettes (Thermo, 87730) and dialyzed overnight in pH7 PBS at 4 °C. The next day, remaining doxorubicin was removed by running the samples through a PD-10 column calibrated with PBS and encapsulated doxorubicin was quantified on a microplate reader at 490 nm using a standard curve made from free drug in PBS after diluting all samples 1:1 in 1% Triton X-100. Encapsulation efficiency was determined from the total doxorubicin in the final set of samples compared with the 2.5 mg added initially. For the NTA(Ni) liposomes, the day of injection, VP1 was added to the liposomes at a 40:1 NTA(Ni) lipid to protein and incubated on ice for 30 minutes, prior to administration.

Table 4.1 Characteristics of liposomes used to immunize or suppress against AAV8

Formulation	**Composition**	**Size**	**PDI**	**Protein/Drug Concentration**
Base DSPC formulation	DSPC:Chol. 62:38	102.37±2.00	0.298±0.02	20 ug VP1 protein
NTA(Ni)*	DSPC: Chol., NTA(Ni)-DGS 57:38:5	101.13±1.96	0.385±0.06	32.44±7.02% doxorubicin
NTA(Ni)-VP1	DSPC: Chol., NTA(Ni)-DGS 57:38:5 with VP1 protein	See above	See above	N/A
- 5:1 NTA to VP1		657.37±486.93	0.615±0.34	28.99% VP1
- 10:1 NTA to VP1		160.77±2.79	0.187±0.03	52.61% VP1
- 20:1 NTA to VP1		161.13±1.33	0.199±0.04	62.32% VP1
- 40:1 NTA to VP1*		161.93±0.93	0.218±0.02	64.48% VP1
Maleimide	DSPC: Chol., DSPE-PEG(2000)-Mal. 57:38:5	114.45±2.25	0.245±0.01	N/A
Maleimide-VP1*	DSPC: Chol., DSPE-PEG(2000)-Mal. 57:38 and Mal. VP1 50 ug	156.47±24.83	0.337±0.03	82.75±12.69% doxorubicin 64.40±17.29% VP1

*Used for doxorubicin-based suppression experiments.

4.2.6 Mouse experiments

Assessment of the in vivo effects of our suppression strategy was completed with C57BL/6J (#000664) mice purchased from Jackson Labs at 5-6 weeks of age and used in

experiments at 7-9 weeks. For all experiments, mice were sedated with isoflurane gas. Baseline plasma levels of all experimental parameters were established on day 1, prior to administration of any therapies. Blood samples were collected by superficial temporal vein puncture using a small animal lancet (Medipoint) into a microcentrifuge tube and centrifuged for 2 min at 13,000 *x g*, prior to storage -80 °C for later assays. All mice were housed in a specific-pathogen free facility at the University of Kentucky, and all experimental procedures were approved by the University of Kentucky IACUC.

To assess the liposomal doxorubicin suppression strategy, mice were immunized on day 1 with 50 µg of ovalbumin (Thermo, 77120) in 10% Freund's complete adjuvant (Thermo, 77140) at a total volume of 50 µL. Mice also received 1x10^9 genome copies of AAV8-GFP (Addgene, 37825-AAV8) to generate an immune response against the virus, except for control mice. On day 7, the mice received a second ovalbumin immunization with Freund's incomplete adjuvant (Thermo, 77145) made in the same manner as above. On day 21, the mice were given liposomal doxorubicin bound to VP1 through maleimide or NTA, to compare the two conjugation systems, protein free liposomal doxorubicin, or no suppression. The dose of doxorubicin used was 8 µg/g based on an average of 20 g for females and 25 g for males, the amount of protein given in the formulations was 1 µg/g. On day 35, the animals were given AAV8-TdTomato (Addgene, 59462-AAV8)[449] at 1x10^12 viral genome copies intraperitoneally (ip), and they were assessed for protein expression in the liver two weeks later. On days 1, 14, 28 and 42, blood was collected from each animal to assess antibody expression levels.

4.2.7 Interference with human neutralizing antibody assay for AAV8-GFP using HEK 293 cells measured by flow cytometry[450]

VP1 protein was serially diluted in serum free DMEM starting at a concentration of 1 mg/mL. Plasma was then diluted in DMEM without FBS down the plate starting at 1:80. Plasma was plated at 50 µL in all but the last well, to serve as a AAV8 VP1 free control, and samples were incubated at 4 °C. After two hours AAV-GFP was diluted to 4.4x10^10 GCs in DMEM, 50 µL were added to each well and the samples were incubated for another 2 hours at 4 °C. During sample incubation, HEK293T cells (henceforth cells) were plated at a density of 2x10^4 cells in a 96 well plate in triplicate and placed in an incubator at 37 °C with 5% CO_2 until samples incubated for the 2 hours, at which point 45 µL of the AAV-serum-VP1 mixture were added to each set of cells in triplicate. After 72 hours, the cells were processed for GFP expression as shown in figure 4.2.

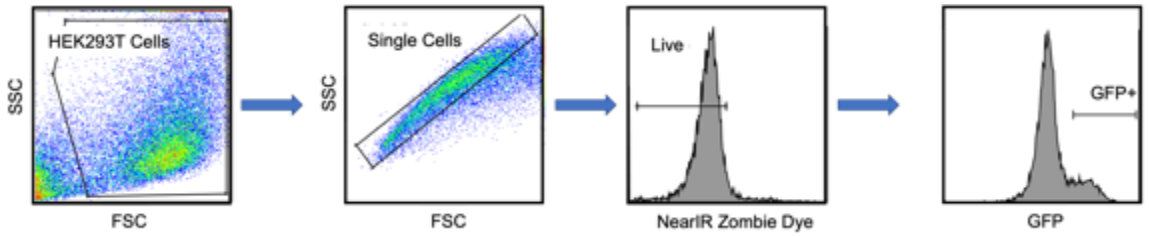

Figure 4.2. Scheme for quantification of GFP expression in HEK293T cells after interference with NAb pre-treated AAV8 in the presence or absence of VP1.

4.2.8 Evaluation of splenocyte populations following suppression treatment

Evaluation of the effects of doxorubicin liposomes on immune cell populations was completed after treating mice with suppression nanoparticles above, two weeks after treatment with AAV8. After 14 days following the administration of doxorubicin liposomes, the mice were euthanized and their spleens were mashed through a 0.45 µm filter into 50 mL tubes. The cells were centrifuged at 350 rpm and resuspended in 6 mL of 0.2% NaCl to lyse red blood cells, followed promptly by addition of 1.6% NaCl to neutralize the osmolarity of the solution. The cells were centrifuged one more time and washed in PBS before being counted in a 1:10 dilution with trypan blue. One million cells were moved to FACS tubes, in duplicate, and washed once with FACS buffer (Mg^{2+}/Ca^{2+}-free Hanks' balanced salt solution, 2 mM EDTA, 25 mM HEPES and 1% FBS) and resuspended in 100 µL of mouse Fc block (Biolegend, 101320) at 1 µg per sample. The cells were incubated for 20 minutes at 4 °C prior to addition of antibodies, which were added for 30 minutes. After this, the cells were washed twice in 500 µL of FACS buffer and resuspended in 500 µL again, before being processed using an Attune Nxt flow cytometer. Two panels were used for assessing splenocytes. For lymphocyte assessment the panel consisted of anti-mouse CD3-PerCP (Biolegend, 100325), anti-mouse CD19-PE/Cy7 (Abcam, ab210210) and Alexa Fluor 647 (Abcam, ab269823) conjugated to VP1 using the manufacturer's instructions. For assessment of antigen presenting cell populations the panel consisted of anti-mouse MHCII-APC (Biolegend 107614), anti-mouse CD11c-PerCP/Cy5.5 (Biolegend, 117327) and anti-mouse-F4/80-PE (Biolegend, 123110). The scheme used for each panel is show in figure 4.3.

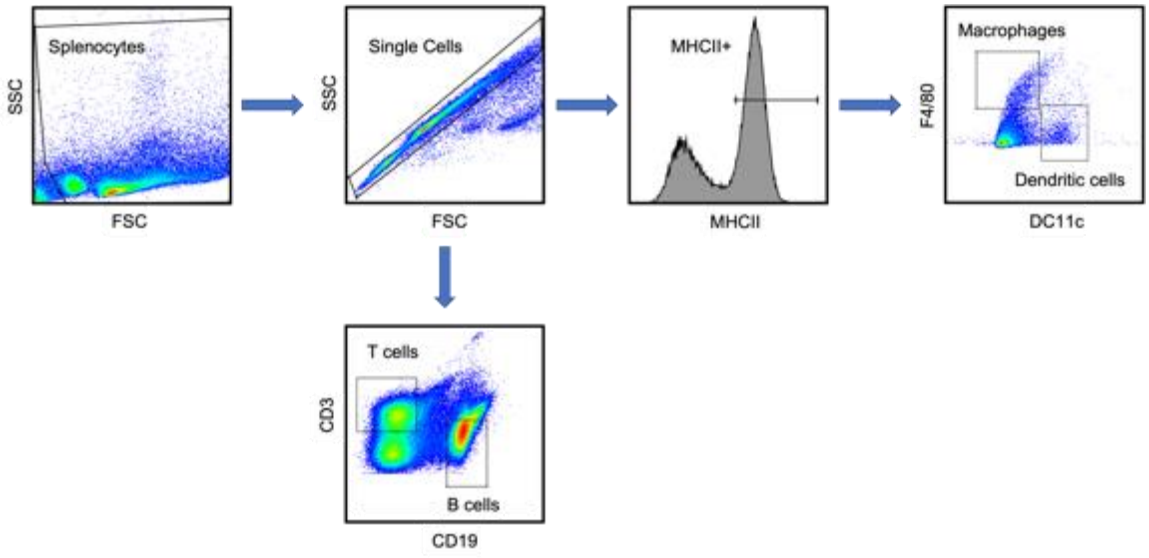

Figure 4.3 Scheme for splenocyte cell populations after liposomal doxorubicin treatment.

4.2.9 Detection of antibodies via ELISA

For detection of anti-AAV8 antibodies, 50 µL of AAV8-GFP (Addgene, 37825-AAV8) were plated on a high protein binding plate using a concentration 1x10^10 GC per

mL in pH 9.7 carbonate buffer and incubated at 4 °C overnight. The following day the plate was washed four times with 200 µL of 0.1% PBS-T, after which the PBS-T was discarded, and the plate was dried by blotting on paper towel (henceforth "washed"). The plate was then blocked with 200 µL of PBS with 0.1% casein (PBS-C) per well and incubated at 37 °C for 1 hour. Plasma samples were diluted to 1:200 using PBS-C on a round bottom transfer plate and after washing off the blocking buffer, 100 µL of samples were added, in duplicate and incubated at 37 °C for 1 hour. After sample incubation, the plates were washed and 100 µL of goat anti-mouse IgG HRP were added at a 1:2000 dilution (Invitrogen, 16066) and incubated at 37 °C for 30 minutes prior to washing and adding 100 µL of TMB for another 30 minutes, at room temperature, in the dark. After half an hour, the TMB reaction was quenched with 100 µL of 0.5 M sulfuric acid and the absorbance at 450 nm was determined using a microplate reader. Detection of anti-albumin antibodies was completed as above, using 50 µL of ovalbumin at 2 µg/mL (Thermo, 77120) and anti-ApoA-I antibody detection was completed with 50 µL of ApoA-I (Mybiosource, MBS2888749) at 1 µg/mL.

4.2.10 TdTomato Quantification

For determining fluorescence, the animals were euthanized, and their livers were collected and placed on a 24 well plate in PBS. Fluorescence was determined using an IVIS Spectrum equipped with an XGI-8 Anesthesia System using the Living Image Acquisition/Analysis Software Package. Fluorescence was determined using a 570 nm excitation filter and 640 emission filter with a 0.5 second exposure time.

4.2.11 Data analysis and statistics

Data were organized and analyzed using Graph Pad Prism v.8 or v.9 for Windows. Groups were assessed for normality and compared as described in the figure legends; *p*-*, $P < 0.05$; **, $P < 0.01$; ***, $P < 0.001$; ****, $P < 0.0001$. In all figures, only statistically significant comparisons are shown.

4.3 Results and discussion

The viral capsid of AAV is made from the protein VP1 and its two splice variants, VP2 and VP3.[430, 451] To investigate the ability of our liposome-based strategy to suppress AAV8 targeting B cells, the VP1 protein of AAV8 was synthesized in BL21 *E. coli* by subcloning the protein from an AAV8 packing plasmid into a PET28a vector with an N and C terminal hexahistidine sequence (His tag). Initial attempts were made to clone the protein into a plasmid containing the human alpha-1 antitrypsin gene, leaving the protein's signal peptide intact, to produce VP1 extracellularly. However, this approach failed, despite several attempts at optimization. In *E. coli*, the protein proved difficult to isolate, due to aggregation within the insoluble portion of the bacterial pellet. This phenomenon has been previously reported by Le, et al. who concluded that, while changing vectors can improve protein concentration in the soluble portion of the bacterial lysate, the yield was

ultimately too low and suggested that production of the protein in a BL21 vector yielded the best results, despite issues with protein degradation.[446] Although difficulties in purifying VP1 persisted, the methods from Le, et al. yielded a considerable amount of protein (~15 mg in 400 mL of culture). The isolated protein, while slightly degraded could also be confirmed by Western blot, suggesting that production of VP1 in bacteria allows for appropriate protein folding (figure 4.1).

The liposomes used in the present suppression strategy were formed using a combination of DSPC and cholesterol described extensively in the literature with the addition of 5% NTA(Ni)-DGS (abbreviated NTA) or DSPE-PEG_{2000}-Maleimide (abbreviated maleimide or mal.).[448] As described by Nielsen, et al. the use of NTA in the liposome bilayer significantly reduced the encapsulation efficiency of doxorubicin (~32%) compared with the maleimide liposomes (~82%).[447] When conjugated to VP1, both sets of liposomes yielded nanoparticles of about 150-160 nm in diameter, an increase from 100-115 nm before the incorporation of the protein (see table 4.2). For the maleimide liposomes, the protein was conjugated to maleimide prior to incorporation to the liposomes. Despite this, only ~64% of the protein was recovered after all the processing was completed (rehydration, sonication, and size exclusion chromatography). For the NTA liposomes, the addition of protein was performed after remote loading of doxorubicin using four different protein to NTA(Ni) lipid ratios (5:1, 10:1, 20:1, 40:1). While the size of the nanoparticles increased with all four protein to NTA(Ni) ratios, only the 20:1 and 40:1 protein:NTA(Ni) ratios led to a ~60% protein recovery ratio. Therefore, further experiments were performed with a ratio of 40:1.

To determine the translational potential of VP1 conjugated suppression liposomes, the VP1 protein isolated from BL21 cells was used in an in vitro interference assay with serum from five human samples that were positive for anti-AAV8 antibodies (see Chapter 5 for details). VP1 was incubated with patient serum, prior to incubation with AAV8-GFP and transduction efficiency was assessed via flow cytometry. As evidenced in figure 4.4, the presence of VP1 at concentrations ranging from 7.5 to 120 μg/mL led to considerable improvement in transduction. However, this varied significantly from sample to sample, highlighting the interpersonal variability of immune responses. The reason behind this is potentially related to the interindividual responses in patients, but impossible to fully assess due to the nature of these samples being from a fully de-identified population.

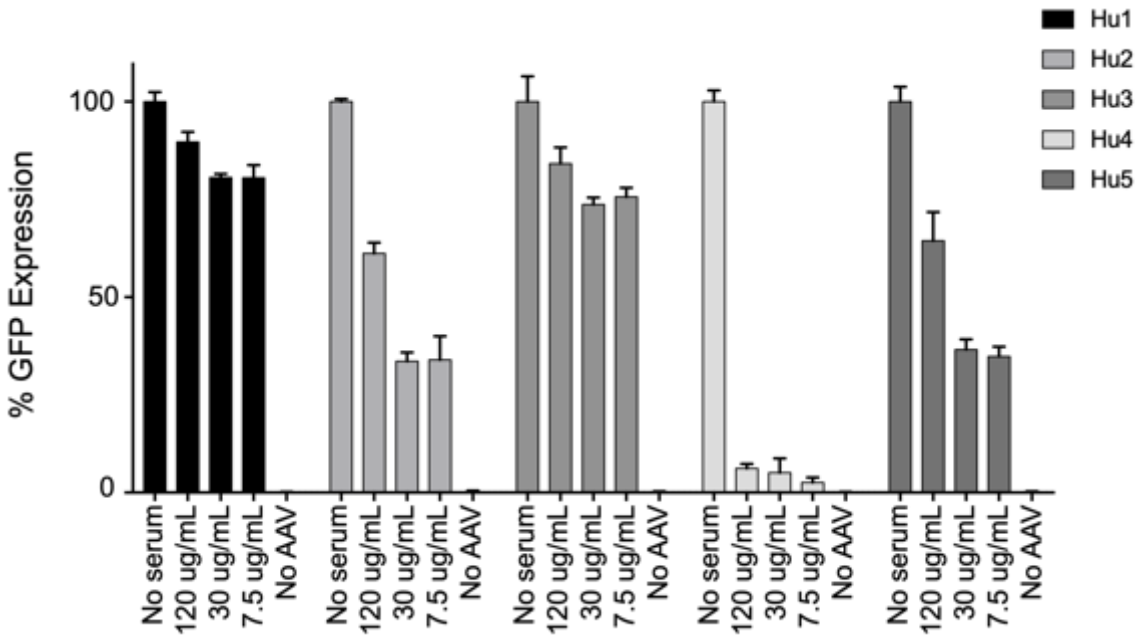

Figure 4.4. Evaluation of translational potential of VP1 based suppression. Serum from five human serum samples with antibodies to AAV8 was incubated with VP1 protein, followed by incubation with AAV8-GFP. The samples were then used to treat HEK293T cells for 72 hours and the GFP expression was quantified via flow cytometry.

To assess the toxicity of the liposomal suppression strategy, mice were treated with doxorubicin liposomes bound to the VP1 protein. Two weeks after administration, the splenocyte populations were evaluated via flow cytometry as in figure 4.3 and cell counts were determined with FlowJo. As shown in figure 4.5A, significant decreases were observed among macrophages and B cells, as would be expected following treatment with cytotoxic liposomes. By comparison, no changes were seen in the untreated animals compared with untreated, AAV8 naïve mice (data not shown). The T cell population was significantly elevated, perhaps due to inflammation resulting from the drug treatment. Attempts were made to evaluate the VP1 specific cell population by conjugating the purified protein to an AF647 fluorophore (Abcam ab269823). As can be evidenced on the last panel of figure 4.5A, there was a very clear decline in the cells binding to VP1-AF647. However, given the high background seen with control AF-647 (figure 4.5B), it is difficult to assess this difference with certainty. It is more than likely that the reduction in total cell count is due to the reduction in total B cells, rather than an actual reduction in the epitope specific population, suggesting that further optimization of the assay is needed to assess differences in the epitope specific population.

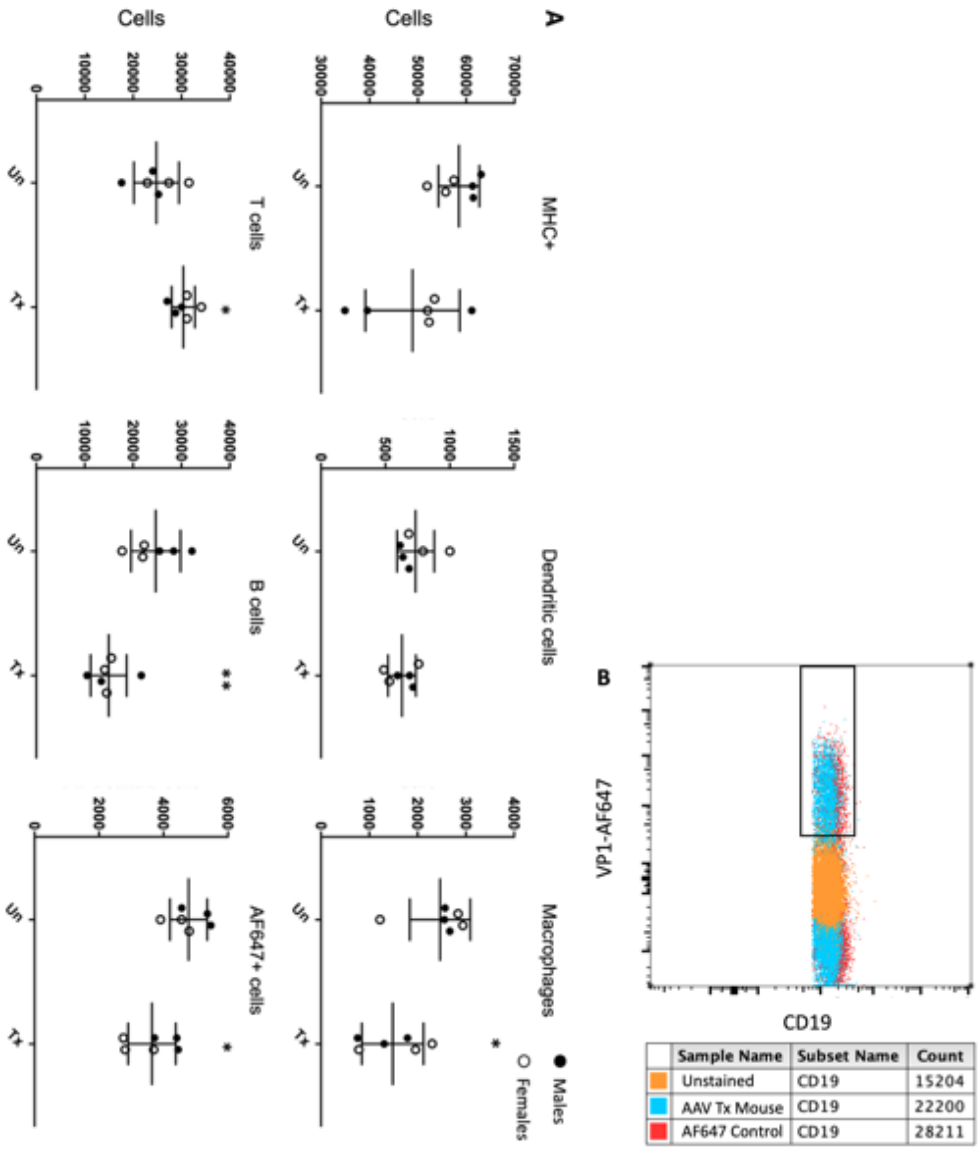

Figure 4.5. A. Evaluation of spleen myeloid cells (top) and lymphoid cells (bottom) in mice treated with suppressive liposomes. Mice (n=3/sex) were given AAV8-GFP and then treated with liposomes before being evaluated two weeks later for spleen cell populations were studied by flow cytometry. Treated mice were compared with untreated mice at the same timepoint. Groups were analyzed by T test. B. FlowJo plot of B cells treated with AF647 conjugated VP1, to determine changes in the antigen specific cell population, show considerable background noise among cells, suggesting the presence of non-specific recognition against the viral protein or diffusion of the fluorophore into non-specific cells.

Next, to determine the ability of liposomal doxorubicin suppression to selectively suppress the antibody response to AAV, mice were bled on day one for assessment of anti-AAV8, ovalbumin (OVA) and ApoA-I antibodies (see figure 4.6). Here OVA was used as an immunization control and ApoA-I was used as a control of the intrinsic mouse immune responses, as antibodies against this protein have been previously reported to naturally

occur in C57BL/6J mice.[360] After bleeding, the mice were immunized with OVA in Freund's complete adjuvant (FCA) subcutaneously and given 1x10^9 genome copies of AAV8-GFP. The following week, the mice received another dose of OVA with Freund's incomplete adjuvant (FIA) and the immune responses were reassessed on day 14. At this point, a clear elevation of anti-AAV8, and to a lesser extent OVA can be seen in treated animals (figure 4.7A and B). As expected, the anti-ApoA-I response was largely variable among mice.

Following suppression with either liposomal doxorubicin (L-Dox.) by itself or conjugated to AAV8 VP1 with either NTA(Ni)-DGS or DSPE-PEG_{2000}-Maleimide, the mice were assessed once more for antibody expression and given AAV8-TdTomato at 1x10^12 genome copies per mouse. Throughout the duration of the experiments, the anti-AAV8 response did not change in the mice treated with AAV8-GFP, suggesting a failure of the suppression experiment (Figure 4.7A). Interestingly, the mice suppressed with maleimide bound VP1 failed to respond to the third OVA immunization, although the response did not decrease from that seen in previous weeks (figure 4.7B). A small reduction in the anti-OVA response was also observed in the other two groups treated with L-Dox and NTA liposomes, although to a non-significant extent. This effect of the maleimide liposomes on the OVA response is likely due to the extended exposure to PEGylated liposomal doxorubicin on the antigen presenting cell population in these nanoparticles. These findings suggest that this method may have off target effects on new immune responses induced while the nanoparticles are circulating, but not on pre-existing ones. To add to this notion, the response to ApoA-I was also unchanged from previous weeks among all groups (figure 4.7C). More than likely, as suggested by the findings of Oja, et al. liposomal doxorubicin-based immunosuppression is mediated through suppression of antigen presenting cells, which would be further suppressed following treatment with the PEGylated maleimide liposomes. To test this further, we investigated the titers to AAV8 following the treatment with AAV8-TdTomato, as titers can provide a clearer picture of the immune response and since our absorbance values were saturated at the 1:200 serum dilution used. By looking at titers in figure 4.7D, we were able to observe a very distinct reduction in the immune response to AAV8 after administration of maleimide liposomes, even though the response was not diminished entirely.

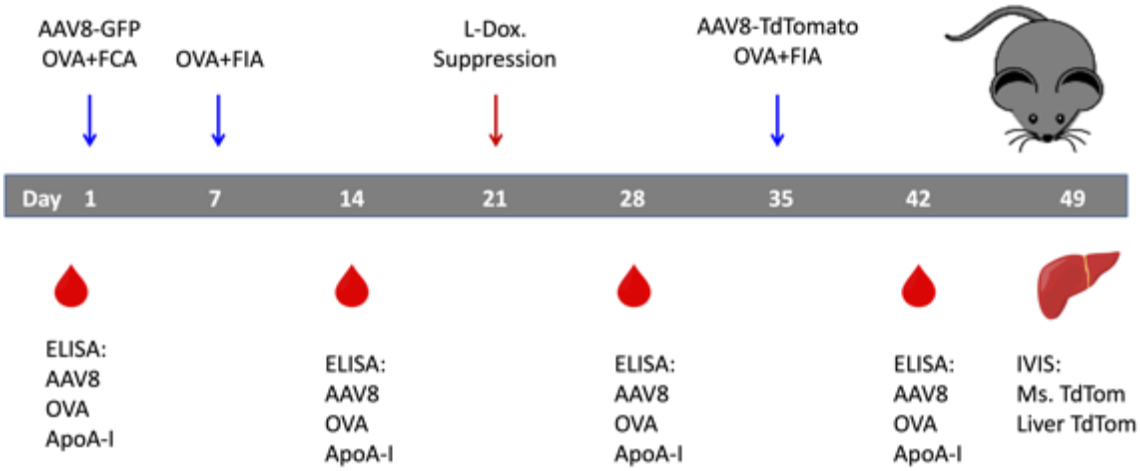

Figure 4.6. Scheme for evaluation of liposomal doxorubicin suppression (either liposomal drug by itself or conjugated to VP1) strategy on antibody responses and TdTomato expression.

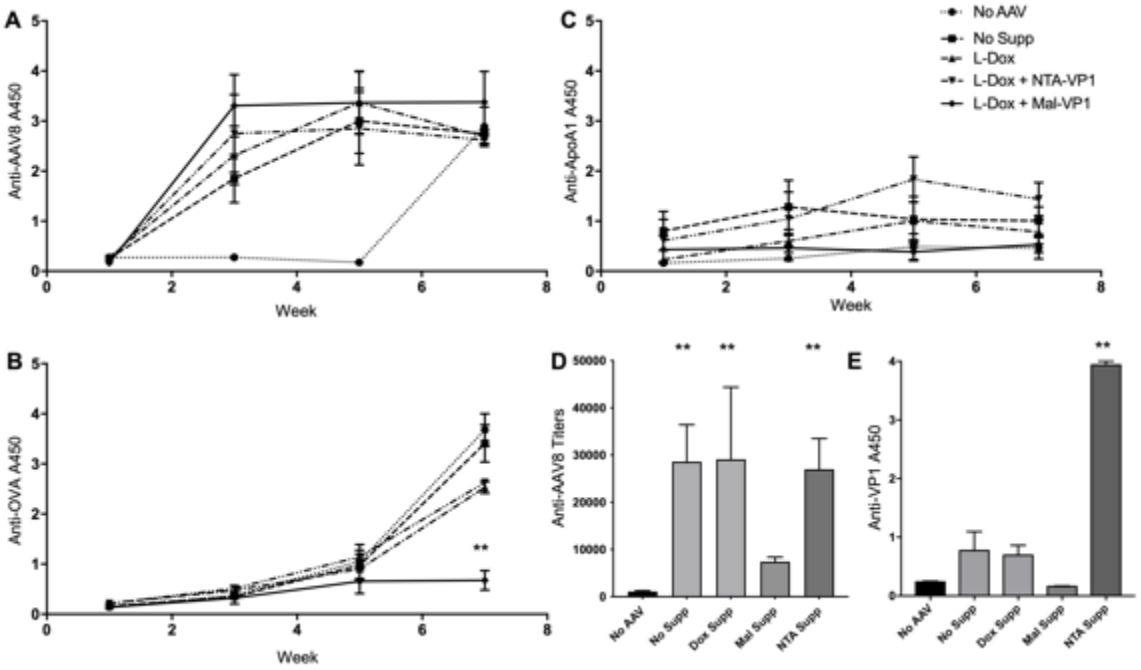

Figure 4.7. Effect of suppression on immune responses. Mice (n=3/sex) were immunized with OVA and AAV8-GFP, followed by suppression with L-Dox. and treatment with AAV8-TdTomato and describe in figure 4.6. Results show the mean+/- SEM over the course of the experiment for AAV8 (A), OVA (B) and ApoA-I (C). D. Anti-VP1 antibody response among groups one week after AAV8-TdTomato administration (week 7). E. Anti-AAV8 titers at week 7, after administration of AAV8-TdTomato. Bars show mean +/- SEM. Responses at week 7 were compared against the no AAV group by Krustal-Wallis.

Based on the antibody responses observed, it is evident that the suppression strategy failed to suppress pre-existing antibodies to AAV. However, it was unclear whether this was due to the nanoparticles themselves, or to the complexity of the anti-AAV response compared with VP1. Therefore, we decided to determine whether the suppressive strategy had any effect on the anti-VP1 response after suppression. As evidenced in figure 4.7E, the responses to VP1 following suppression were considerably diminished by maleimide conjugated VP1 suppression. However, the NTA conjugated protein led to a considerably increased response toward the protein. This finding, while unexpected, could be attributed to the transient nature of the NTA(Ni) conjugation to histidine residues on proteins. For example, Chen et al. reported only ~47% lipid recovery following size-exclusion chromatography with up to 5% NTA(Ni)-DGS liposomes.[452] The transient nature of this ionic interaction likely resulted in separation of the suppressive liposomes and the VP1 protein and led to an enhancement of the anti-VP1 response. Interestingly, neither the unsuppressed group, nor the L-Dox. suppressed group, had a very strong response to the VP1 protein, compared with the obvious response to AAV8 in figure 4.7A. Overall, these findings suggest that the anti-VP1 response differs from that of the antiviral response. Finally, two weeks after treatment with AAV8-TdTomato, the mice were evaluated for expression of the protein in the liver using an IVIS Spectrum imager and the expression was quantified and normalized to liver weight (figure 4.8). As expected from the immune responses, none of the AAV8-GFP treated mice had quantifiable expression of TdTomato, unlike the untreated mice.

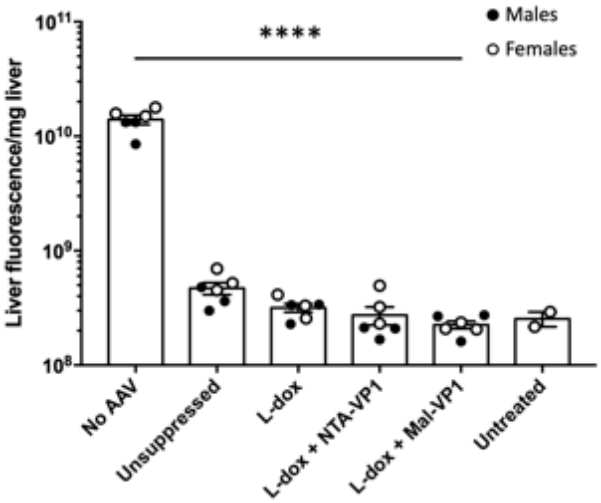

Figure 4.8. Expression of liver fluorescence in mouse livers following TdTomato delivery with AAV8. Mice (n=3/sex) previously treated with AAV8-GFP followed by suppression with liposomal doxorubicin were treated with AAV8-TdTomato and liver expression was assessed 14 days later. Groups were compared by ANOVA against the no AAV group. Two untreated (no AAV8-TdTomato) animals were used as a comparison in the expression assay, as a comparison, but not included in the statistical analysis.

4.4 Conclusions

Liposome based strategies for immunosuppression, as suggested by the work of Naoko Oku and the work by Selecta Biosciences provide a tentative strategy for epitope specific suppression.[268, 437, 438] Particularly the development of immunosuppressive nanoparticles, containing drugs such as doxorubicin, rapamycin, tacrolimus, or others in combination with linker structures, such as NTA(Ni) or maleimide, could provide a simple strategy to suppress antibodies against target proteins, either therapeutics like AAVs or biologic drugs, as well as the protein targets of autoimmune responses.

Here an attempt was made to use liposomal nanoparticles to suppress the immune response to AAV8. This approach employed liposomes loaded with the chemotherapeutic doxorubicin and bound to the VP1 protein of AAV8 with two different linkers, NTA(Ni) and maleimide. Unfortunately, this strategy failed to suppress the immune response to the virus and in the case of the maleimide nanoparticles it also enhanced the immune response to the VP1 protein itself, possibly due to displacement of the protein from the nanoparticles in circulation, resulting in immunization toward VP1. Based on this enhancement of the anti-VP1 response, compared with AAV8 treated animals, it is likely that while there is some overlap between the immune response to the protein, VP1 itself fails to recapitulate the antibody responses toward the virus. Future evaluation of this suppression strategy to AAV should consider the difference between the response to virus and protein alone and employ either entire empty capsid or attempt to recreate the external viral architecture on the liposomal surface. Additionally, such experiments should take into account the localization of the cysteines on AAV, as these may no longer be present on the viral surface, although this could be overcome through chemical modifications such as the use of SATA.[453] Furthermore, in the present experiments, the protein was assumed to bind to maleimide after addition of excess lipid and washing of the protein. It is recommended that future experiments should involve more proper characterization of the conjugation and quantification of the addition.

One unexpected finding from these studies was that the liposomes conjugated to maleimide, were likely still circulating during the third administration of OVA and of AAV8-TdTomato due to the presence of polyethylene glycol on their surface (half-life of PEGylated liposomal doxorubicin is ~46h vs. 26h for liposomal doxorubicin), and also suppressed the immune response to ovalbumin when administered after the nanoparticles.[454] This finding highlights the effect of suppression of the reticuloendothelial system on concomitant immune responses and suggests that conjugation of the target protein may not be necessary for suppression. It is also recommended that future experiments explore the distribution and uptake of the nanoparticles by cells, following administration. This includes evaluation of liposome uptake following in vivo delivery, as well as ex vivo uptake of the nanoparticles by splenocytes and isolated B cells that include evaluation of the toxic potential of the nanoparticles.

While the present work has focused on suppression of pre-existing anti-AAV8 antibodies, the present strategy holds promise for other areas of research, particularly

within the context of allergy and autoimmunity, or utilizing other immunosuppressive drugs. Maldonado et al. also showed that a similar approach using rapamycin can shift the immune response of T cells from a CD4/CD8 response to a Treg response, creating immune tolerance to ovalbumin.[455] More recently, Pan et al. showed that dexamethasone treatment, followed by immunization with peptides from the protein HMGB1, can result in immune tolerance toward HMGB1.[456] These studies, along with those mentioned earlier in this chapter suggest the need for further evaluation of liposomal immunosuppression as a strategy. Furthermore, a strategy that may prove useful in AAV studies is the inhibition of anti-AAV antibodies through coadministration of the virus with PEGylated doxorubicin, which may help to improve transfection and allow for cumulative gene therapy in patients receiving this virus.

CHAPTER 5: CHARACTERIZATION OF AAV8 PEPTIDES TO DEVELOP A PEPTIDE BASED APPROACH FOR SUPPRESSION

5.1 Introduction

In evaluating the liposomal suppression in chapter 4, it is evident that VP1-based suppression failed due to the differences between the anti-AAV response compared with the anti-VP1 response. As such, two approaches could be pursued in subsequent experiments by either attempting suppression using the entire AAV8 capsid, or reconstructing the viral structure on a liposomal surface with relevant peptides that extend outside of the viral capsid surface and recapitulate the viral capsid. As shown in chapter 4, this latter peptide-based approach could be successful. To develop such an approach, an evaluation of the literature was conducted to identify antibody targets on AAV that could be used in a liposomal strategy. A search was conducted using the terms "AAV" or "adeno associated virus" and "peptide" or "antibody target" or "epitopes". The results of this search yielded several peptide sequences, many of which protrude from the viral capsid and could serve in developing a liposomal suppression strategy (figure 5.1). Among the peptides found, Boutin, et al. reported epitopes from AAV8 and AAV1 that result in functional expansion of CD8+ T cells that are indistinguishable from those of AAV2, however, these were excluded, as many of these lie within the viral capsid.[457] As early as 2000, Wobus, et al. (magenta) and Moskalenko, et al., reported various antibody targets along AAV, that have been corroborated by later researchers.[458, 459] Gurda, et al reported aa586-591 as a target of the MAb ADK8 (teal).[460] Guiles also reported the region encompassing aa588-593 as an AAV9 epitope, along with aa496-498, as targets for the antibody PAV9.1 (teal).[461] Hui, et al. reported several MHC class I epitopes conserved across AAV serotypes via IFN-γ ELISPOT from expanded lymphocytes (green).[462] These include SADNNNSEY, which overlaps with previously reported epitopes,[458, 460, 461] LIDQYLYYL, VPQYGYLTL,[458, 463] TTSTRTWAL, YHLNGRDSL,[458] SQAVDRSSF, VPANPSTTF, FPQSGVLIF, YFDFNRFHCHFSPRD, QFSQAGASDIRDQSR, GASDIRQSRNWLP, GNRQAATADVNTQGV,[460] and SLDRLMNPL. Sabatino (blue) reported YHLNGRNSLANPGIA, NGRNSLANPGIAMAT, NLANPGISLANPGIAMATHKD, LTSEEEIKTTNPVAT,[458] and IPQYGYLTL[458, 463] Tellez, et al. reported epitopes contained within the beta barrel of the viral capsid, however, since these are not expressed on the outer surface of the viral capsid properly displayed on a lipid bilayer, they were not further investigated.[464] Finally, Govindasamy, et al. reported an AAV4 epitope on variable region IX of the virus (red) that is displayed on the outside of the surface of the viral capsid.[465] In the present chapter, four peptide sequences reported in the literature were used as targets in an immunization strategy to determine their ability to induce antibodies to AAV8. Furthermore, an evaluation of antibody targets was conducted, using peptide array, to elucidate more potential targets that could be used in this strategy.

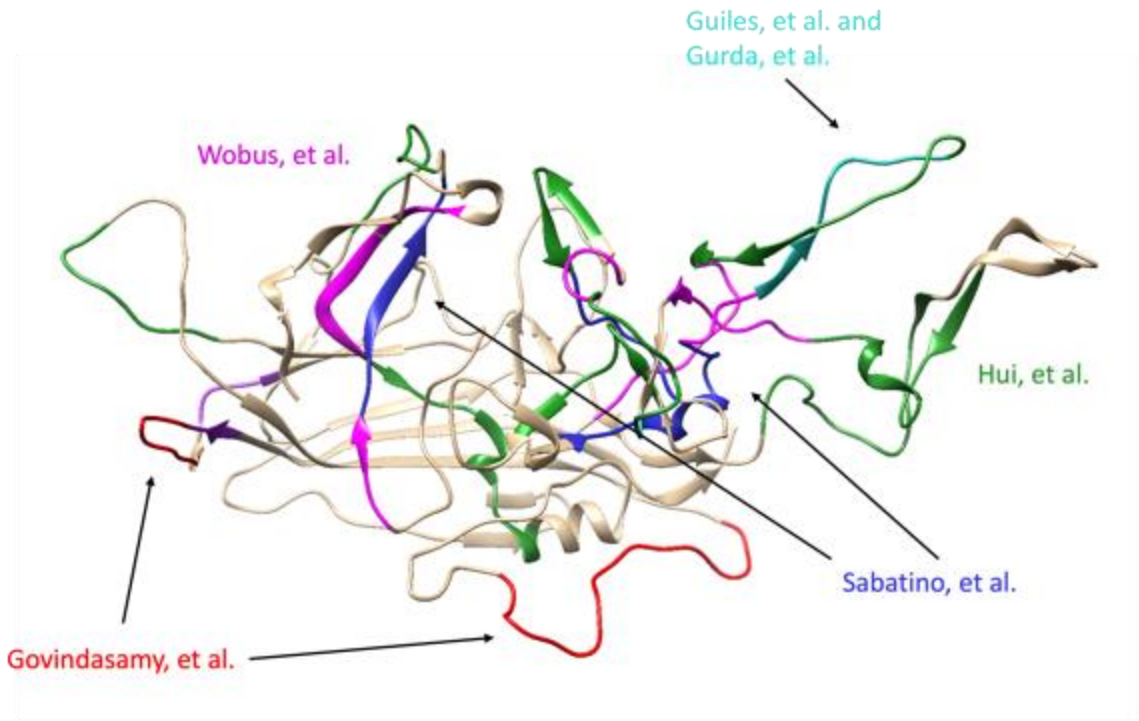

Figure 5.1. Antibody targets along the AAV capsid protein, VP1, reported by different authors. Image generated using UCSF Chimera using UniProt Q8JQF8 as a template.

5.2 Methods

5.2.1 Peptide conjugation to maleimide lipids

The four peptides above were purchased from Elim Biopharm as crude peptide on resin and deprotected for four hours using a mixture of 2.5% water, 2.5% methyl sulfide, 2.5% 3,6-dioxa-1,8-octanedithiol, 2.5% tri-isopropyl silane and 90% trifluoroacetic acid. The peptides were all designed with a cysteine on the C terminus to provide a simple binding structure and were bound to liposomes containing 5% DSPE-PEG2000-Maleimide. The peptides were added, individually, at a 10 to 1 peptide to maleimide lipid to pre-formed liposomes in PBS, pH7. After overnight incubation under N_2, the liposomes were washed three times of free peptide using a 30 kDa spin filter and the peptide concentration was determined using a BCA quantification kit (Thermo, 23225). Upon confirmation of the concentrations, the liposomes were mixed at a 1:1:1:1 ratio of each peptide and sonicated for 1 hour in a vial containing the equivalent of 0.3 mole percent of MPL to the final liposome concentration. These formulations were then used for immunization of mice, as described below.

5.2.2 Development of AAV8 VP1 plasmid constructs for E. coli

The VP1 protein for AAV8 was produced as described in chapter 4. Briefly, the VP1 sequence was cloned from Addgene's AAV2/8 packing plasmid (112864) using the

forward primer CAGCCATATGGCTGCCGATGGTTATC and reverse primer TATAGGAATTCTTTAATGATGATGATGATGATGATGATGCAGATTACGGGTG AGGTAAC and subcloned into a pET28a plasmid. This plasmid was then transformed into BL21(DH3) cells and VP1 production was induced with 0.5 mM IPTG for 5 hours in 18 °C, followed by 13 hours at 18 °C, after reaching an OD600 of 0.6. Following induction, the protein was purified from the insoluble portion of the bacteria using a an NTA(Ni) purification kit (Thermo, 88228) by gravity with the buffer systems recommended by Le, et al.[446] and stored at -80 °C in PBS, pH 9.

5.2.3 Preparation of lipoproteins for immunization and suppression liposomes

Conjugation of VP1 to NTA(Ni) lipid was achieved by making liposomes from a 57:38:5 DSPC, cholesterol, NTA(Ni)-DGS (Avanti, 790404P) formulation at a 10 mM lipid concentration. To these, VP1 protein was added at NTA lipid to protein ratio of 40:1, the mixture was incubated at room temperature for 30 minutes before being eluted through a PD-10 desalting column and assessing size and protein concentration.

Conjugation to maleimide lipid was done by placing VP1 in a pH 6.5 PBS solution at 0.4 mg/mL and mixing in 3.75 mg of DSPE-PEG(2000)-Maleimide (Avanti, 880126C) at 1 mg/mL in DMSO (this is roughly 1.27 μmoles of lipid to 0.0046 μmoles of protein, or a 277 lipid to protein ratio). The reaction was covered with nitrogen gas and allowed to stir overnight at room temperature. The following day, the reaction was placed in 10 volume equivalents of ether and incubated overnight at -20 °C to precipitate protein. After overnight precipitation the protein was spun down at 4000 *x g* and the ether was discarded. The protein was washed again with ether to remove remaining maleimide lipid and the final protein quantification was determined by BCA.

5.2.4 Mouse experiments

Assessment of the in vivo effects of our suppression strategy was completed using C57BL/6J (#000664) mice purchased from Jackson Labs at 5-6 weeks of age and used in experiments at 7-9 weeks. For all experiments, mice were sedated with isoflurane gas. Baseline plasma levels of all experimental parameters were established on day 1, prior to administration of any therapies. Blood samples were collected by superficial temporal vein puncture using a small animal lancet (Medipoint) into a microcentrifuge tube and centrifuged for 2 min at 13,000 *x g*, prior to storage -80 °C for later assays. All mice were housed in a specific-pathogen free facility at the University of Kentucky, and all experimental procedures were approved by the University of Kentucky Institutional Animal Care and Use Committee. Immunizations with AAV peptide (1.2 mg peptide 1, 1.58 mg peptide 2, 1.97 mg peptide 3 and 2.78 mg peptide 4, as quantified by BCA assay, either as free peptide or conjugated to maleimide lipid) or VP1 protein (20 μg protein, as quantified by BCA assay, given alone, at a ratio of 40:1 NTA lipid to protein, or conjugated to maleimide lipid) were administered twice, one week apart, prior to assessment of anti-AAV8 antibodies on day 21. Peptide immunizations were administered with liposomes made from 15:2:3:0.3 DMPC, DMPG, cholesterol, MPL, while protein liposomes were

made from 62:38 DSPC and cholesterol. At this point, the mice were given AAV8-TdTomato (Addgene, 59462-AAV8)[449] at 1x10^6 viral genome copies intraperitoneally (ip), and assessed on day 35 for TdTomato expression.

5.2.5 TdTomato Quantification

To assess TdTomato transduction, the animals were euthanized, and their livers were collected and placed on a 24 well plate in PBS. Fluorescence was determined using an IVIS Spectrum equipped with an XGI-8 Anesthesia System using the Living Image Acquisition/Analysis Software Package. Fluorescence was determined using a 570 nm excitation filter and 640 emission filter with a 0.5 second exposure time.

Table 5.1 Characteristics of liposomes used to immunize against AAV8

Formulation	Composition	Size	PDI	Protein/Drug Concentration
Peptide immunization	DMPC: Chol.: DSPG: MPL 15:3:2:0.3 + free peptides	74.19±6.22	0.221±0.05	1.2 mg peptide 1, 1.58 mg peptide 2, 1.97 mg peptide 3 and 2.78 mg peptide 4
Peptide immunization with maleimide peptides	DMPC: Chol.: DSPG: MPL 15:3:2:0.3 + mal-peptides	161.97±4.63	0.219±0.02	0.87 mg peptide 1, 1.24 mg peptide 2, 1.52 mg peptide 3 and 1.87 mg peptide 4
Base DSPC formulation	DSPC: Chol. 62:38	102.37±2.00	0.298±0.02	20 ug VP1 protein
NTA(Ni)-VP1*	DSPC: Chol.: NTA(Ni)-DGS 57:38:5 + VP1 protein	161.93±0.93	0.218±0.02	64.48% VP1
Maleimide-VP1*	DSPC: Chol., DSPE-PEG(2000)-Mal. 57:38 and Mal. VP1 50 ug	156.47±24.83	0.337±0.03	82.75±12.69% doxorubicin 64.40±17.29% VP1

*Used for doxorubicin based suppression experiments.

5.2.6 Detection of anti-AAV8 antibodies via ELISA[464, 466, 467]

Fifty µL of AAV8-GFP (Addgene, 37825-AAV8) were plated on a high protein binding plate using a concentration of 1e10 GC per mL in carbonate buffer and incubated at 4 °C overnight. The following day the plate was washed four times with 200 µL of 0.1% PBS-T, after which the PBS-T was discarded, and the plate was dried by blotting on paper towel (henceforth "washed"). The plate was then blocked with 200 µL of 5% non-fat dry milk (NFDM) per well and incubated at 37 °C for 60 minutes. For each set of samples, a separate plate was prepared using only blocking buffer, to determine background signal in each sample. Plasma samples were diluted to 1:100 using 1% NFDM on a round bottom transfer plate and after washing off the blocking buffer, 100 µL of samples were added, in duplicate, to AAV or control plates and incubated at 37 °C for 1 hour. After sample incubation the plates were washed and 100 µL of species-specific antibody HRP conjugate was added to each plate using goat anti-mouse IgG HRP (Invitrogen # 16066 at 1:2000), goat anti-monkey IgG HRP (Abcam 112767 at 1:4000) or goat anti-human IgG HRP (Abcam 7153 at 1:5000). The detection antibodies were incubated at 37 °C for 30 minutes prior to washing and adding 100 µL of TMB for another 30 minutes, at room temperature in the dark. After half an hour, the TMB reaction was quenched with 100 µL of 0.5 M sulfuric acid and the absorbance at 450 nm was measured using a microplate reader. The absorbance of the control plate was then subtracted from that of the AAV8 coated plate and samples were considered positive when they were 2 times over the average of the AAV free plate. For titer evaluation, the same procedure was followed, except that samples were serially diluted 6 times starting with 1:100.

5.2.7 Confirmation of anti-AAV8 antibody activity by neutralization antibody assay[450]

To a 96-well tissue culture treated plate, HEK293T cells were added at a density of 50,000 cells per well in 200 µL of media (DMEM, supplemented with 10% FBS, 1% penicillin/streptomycin and 500 µg/mL G418). The cells were then placed in an incubator at 37 °C with 5% CO_2 and allowed to attach. Plasma from AAV8 seropositive subjects was then diluted to 100 µL with DMEM in a sterile, round bottom, 96 well plate, to a concentration of 1:5 for monkey and human samples and to 1:20 for mouse samples. The plasma was then serially diluted five times in 50 µL of DMEM. On the 7th row 50 µL of DMEM was added and 100 µL to the bottom row. AAV8-GFP was diluted to 4.4e10 GCs in DMEM and 50 µL were added to the first 7 wells. The mixture was incubated for 3 hours at 4 °C[450] after which 30 µL were added to cells. Seventy-two hours later, the cell plates were centrifuged, and the media was removed. The cells were detached from their plate using 50 µL TripLE for 5 minutes and moved to a round bottom 96 well plate. PBS was added to wash the cells and they were stained with 100 µL of NearIR Zombie dye (Biolegend 423105) diluted to 1:2000 in PBS for 20 minutes, at room temperature, in the dark. After staining, the cells were washed twice in FACS buffer (HBSS without magnesium or calcium, 25 mM HEPES, 5 mM EDTA and 1% FBS) and resuspended in 200 µL of FACS buffer before being analyzed on an Attune NxT flow cytometer equipped

with an autosampler. FCS files were then analyzed using FlowJo, as in chapter 4 and the percent fluorescence, based on the plasma free and non-AAV treated cells was plotted using Prism.

5.2.8 Peptide microarray for plasma profiling of anti-AAV8 antibodies

JPT Peptide Technologies' PepStar™ peptide microarrays comprise purified synthetic peptides derived from antigens (figure 5.2A) or other sources that are chemoselectively and covalently immobilized on the glass surface. An optimized hydrophilic linker moiety is inserted between the glass surface and the antigen derived peptide sequence to avoid false negatives caused by steric hindrance. For technical reasons all peptides contain a C-terminal glycine. Each assay is performed on microarray slides (figure 5.2B) containing 21 peptide mini-arrays (figure 5.2C), which represent three replicates of the whole peptide library and where each spot represents an individual peptide. At all steps of the manufacturing and assay, quality controls are completed and stored by JPT.

Peptides comprising the AAV8 VP1 protein (Table 2.2) were immobilized on glass plates modified with a Ttds linker (figure 5.2D) and blocked using SuperBlock™ T20 (PBS) Blocking Buffer (Thermo, # 37516). The serum samples were diluted 1:200 (all samples) or 1:300 (only mice) in blocking buffer and applied to JPT peptide microarrays (batch no. 3388) for 1 h at 30 °C using a Multiwell incubation chamber. Following incubation, the samples were washed using 50 mM TBS-buffer including 0.1% Tween20 (JPT), pH 7.2 and incubated with secondary antibody diluted in blocking buffer for 1 h at 30 °C. The antibodies used were anti-human IgG Alexa Flour 657 (JIT 109-605-098, at 0.1 µg/mL); anti-monkey IgG biotin (Fitzgerald, at 1:5000); and anti-mouse IgG Dylight 650 (Thermo 84545, at 1 µg/mL). For the monkey samples, a tertiary incubation with Cy-5 labeled streptavidin (JIR, 016-170-084) was added at 0.1 µg/mL for 1 h at 30 °C. After secondary incubation, microarrays were dried and analyzed on an Axon Genepix Scanner 4300 SL50 using GenePix for spot-recognition of fluorescence at 635 nm and processed on Microsoft Excel. For each spot, the mean signal intensity was extracted (between 0 and 65535 arbitrary units). For further data evaluation, the so called MMC2 values were determined. The MMC2 equals the mean value of all three instances on the microarray except when the coefficient of variation (CV) – standard-deviation divided by the mean value – is larger than 0.5. In this case the mean of the two values closest to each other (MC2) is assigned to MMC2.

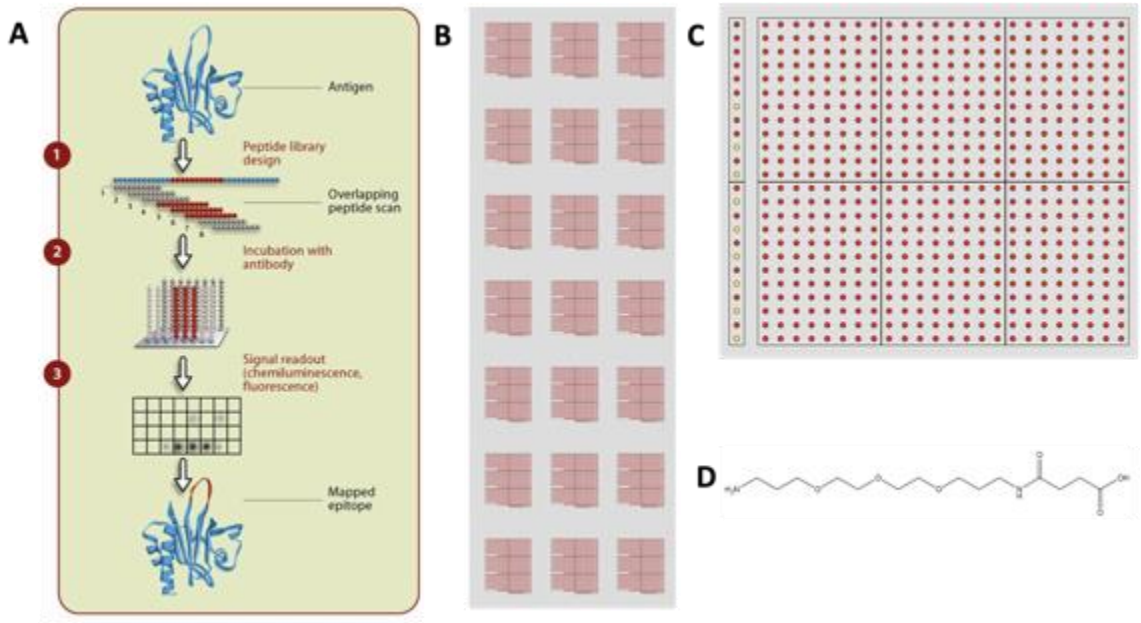

Figure 5.2. Design of JPT peptide array. A. General principle of epitope identification using overlapping peptide scans. Each spot in the microarray represents a single individual peptide. After incubation of the peptide microarray with plasma or antibody samples, bound antibodies or proteins can be detected using fluorescently labeled secondary antibodies. B. General Multiwell microarray layout. C. Mini-array layout: peptide spots are represented by red dots. Full length protein spots are printed in a separate row beneath the library. Monkey IgG, mouse IgG and human IgG control proteins (in triplicates from right to left) are highlighted by yellow color. D. Ttds linker used to attach peptides to glass plates.

Table 5.2 Peptide library of peptide array slides*

No.	Sequence	No.	Sequence	No.	Sequence
1	MAADGYLPDWLEDNL	62	TRTWALPTYNNHLYK	122	CYRQQRVSTTTGQNN
2	GYLPDWLEDNLSEGI	63	ALPTYNNHLYKQISN	123	QRVSTTTGQNNNSNF
3	DWLEDNLSEGIREWW	64	YNNHLYKQISNGTSG	124	TTTGQNNNSNFAWTA
4	DNLSEGIREWWALKP	65	LYKQISNGTSGGATN	125	QNNNSNFAWTAGTKY
5	EGIREWWALKPGAPK	66	ISNGTSGGATNDNTY	126	SNFAWTAGTKYHLNG
6	EWWALKPGAPKPKAN	67	TSGGATNDNTYFGYS	127	WTAGTKYHLNGRNSL
7	LKPGAPKPKANQQKQ	68	ATNDNTYFGYSTPWG	128	TKYHLNGRNSLANPG
8	APKPKANQQKQDDGR	69	NTYFGYSTPWGYFDF	129	LNGRNSLANPGIAMA

Table 5.2 continued

9	KANQQKQDDGRGLVL	70	GYSTPWGYFDFNRFH	130	NSLANPGIAMATHKD
10	QKQDDGRGLVLPGYK	71	PWGYFDFNRFHCHFS	131	NPGIAMATHKDDEER
11	DGRGLVLPGYKYLGP	72	FDFNRFHCHFSPRDW	132	AMATHKDDEERFFPS
12	LVLPGYKYLGPFNGL	73	RFHCHFSPRDWQRLI	133	HKDDEERFFPSNGIL
13	GYKYLGPFNGLDKGE	74	HFSPRDWQRLINNNW	134	EERFFPSNGILIFGK
14	LGPFNGLDKGEPVNA	75	RDWQRLINNNWGFRP	135	FPSNGILIFGKQNAA
15	NGLDKGEPVNAADAA	76	RLINNNWGFRPKRLS	136	GILIFGKQNAARDNA
16	KGEPVNAADAAALEH	77	NNWGFRPKRLSFKLF	137	FGKQNAARDNADYSD
17	VNAADAAALEHDKAY	78	FRPKRLSFKLFNIQV	138	NAARDNADYSDVMLT
18	DAAALEHDKAYDQQL	79	RLSFKLFNIQVKEVT	139	DNADYSDVMLTSEEE
19	LEHDKAYDQQLQAGD	80	KLFNIQVKEVTQNEG	140	YSDVMLTSEEEIKTT
20	KAYDQQLQAGDNPYL	81	IQVKEVTQNEGTKTI	141	MLTSEEEIKTTNPVA
21	QQLQAGDNPYLRYNH	82	EVTQNEGTKTIANNL	142	EEEIKTTNPVATEEY
22	AGDNPYLRYNHADAE	83	NEGTKTIANNLTSTI	143	KTTNPVATEEYGIVA
23	PYLRYNHADAEFQER	84	KTIANNLTSTIQVFT	144	PVATEEYGIVADNLQ
24	YNHADAEFQERLQED	85	NNLTSTIQVFTDSEY	145	EEYGIVADNLQQQNT
25	DAEFQERLQEDTSFG	86	STIQVFTDSEYQLPY	146	IVADNLQQQNTAPQI
26	QERLQEDTSFGGNLG	87	VFTDSEYQLPYVLGS	147	NLQQQNTAPQIGTVN
27	QEDTSFGGNLGRAVF	88	SEYQLPYVLGSAHQG	148	QNTAPQIGTVNSQGA
28	SFGGNLGRAVFQAKK	89	LPYVLGSAHQGCLPP	149	PQIGTVNSQGALPGM
29	NLGRAVFQAKKRVLE	90	LGSAHQGCLPPFPAD	150	TVNSQGALPGMVWQN
30	AVFQAKKRVLEPLGL	91	HQGCLPPFPADVFMI	151	QGALPGMVWQNRDVY
31	AKKRVLEPLGLVEEG	92	LPPFPADVFMIPQYG	152	PGMVWQNRDVYLQGP
32	VLEPLGLVEEGAKTA	93	PADVFMIPQYGYLTL	153	WQNRDVYLQGPIWAK
33	LGLVEEGAKTAPGKK	94	FMIPQYGYLTLNNGS	154	DVYLQGPIWAKIPHT
34	EEGAKTAPGKKRPVE	95	QYGYLTLNNGSQAVG	155	QGPIWAKIPHTDGNF
35	KTAPGKKRPVEPSPQ	96	LTLNNGSQAVGRSSF	156	WAKIPHTDGNFHPSP
36	GKKRPVEPSPQRSPD	97	NGSQAVGRSSFYCLE	157	PHTDGNFHPSPLMGG
37	PVEPSPQRSPDSSTG	98	AVGRSSFYCLEYFPS	158	GNFHPSPLMGGFGLK

Table 5.2 continued

38	SPQRSPDSSTGIGKK	99	SSFYCLEYFPSQMLR	159	PSPLMGGFGLKHPPP
39	SPDSSTGIGKKGQQP	100	CLEYFPSQMLRTGNN	160	MGGFGLKHPPPQILI
40	STGIGKKGQQPARKR	101	FPSQMLRTGNNFQFT	161	GLKHPPPQILIKNTP
41	GKKGQQPARKRLNFG	102	MLRTGNNFQFTYTFE	162	PPPQILIKNTPVPAD
42	QQPARKRLNFGQTGD	103	GNNFQFTYTFEDVPF	163	ILIKNTPVPADPPTT
43	RKRLNFGQTGDSESV	104	QFTYTFEDVPFHSSY	164	NTPVPADPPTTFNQS
44	NFGQTGDSESVPDPQ	105	TFEDVPFHSSYAHSQ	165	PADPPTTFNQSKLNS
45	TGDSESVPDPQPLGE	96	LTLNNGSQAVGRSSF	166	PTTFNQSKLNSFITQ
46	ESVPDPQPLGEPPAA	106	VPFHSSYAHSQSLDR	167	NQSKLNSFITQYSTG
47	DPQPLGEPPAAPSGV	107	SSYAHSQSLDRLMNP	168	LNSFITQYSTGQVSV
48	LGEPPAAPSGVGPNT	108	HSQSLDRLMNPLIDQ	169	ITQYSTGQVSVEIEW
49	PAAPSGVGPNTMAAG	109	LDRLMNPLIDQYLYY	170	STGQVSVEIEWELQK
50	SGVGPNTMAAGGGAP	110	MNPLIDQYLYYLSRT	171	VSVEIEWELQKENSK
51	PNTMAAGGGAPMADN	111	IDQYLYYLSRTQTTG	172	IEWELQKENSKRWNP
52	AAGGGAPMADNNEGA	112	LYYLSRTQTTGGTAN	173	LQKENSKRWNPEIQY
53	GAPMADNNEGADGVG	113	SRTQTTGGTANTQTL	174	NSKRWNPEIQYTSNY
54	ADNNEGADGVGSSSG	114	TTGGTANTQTLGFSQ	175	WNPEIQYTSNYYKST
55	EGADGVGSSSGNWHC	115	TANTQTLGFSQGGPN	176	IQYTSNYYKSTSVDF
56	GVGSSSGNWHCDSTW	116	QTLGFSQGGPNTMAN	177	SNYYKSTSVDFAVNT
57	SSGNWHCDSTWLGDR	117	FSQGGPNTMANQAKN	178	KSTSVDFAVNTEGVY
58	WHCDSTWLGDRVITT	118	GPNTMANQAKNWLPG	179	VDFAVNTEGVYSEPR
59	STWLGDRVITTSTRT	119	MANQAKNWLPGPCYR	180	VNTEGVYSEPRPIGT
60	GDRVITTSTRTWALP	120	AKNWLPGPCYRQQRV	181	GVYSEPRPIGTRYLT
61	ITTSTRTWALPTYNN	121	LPGPCYRQQRVSTTT	182	SEPRPIGTRYLTRNL

*Peptide array based on AAV8 VP1 sequence:

MAADGYLPDWLEDNLSEGIREWWALKPGAPKPKANQQKQDDGRGLVLPGYKY
LGPFNGLDKGEPVNAADAAALEHDKAYDQQLQAGDNPYLRYNHADAEFQERL
QEDTSFGGNLGRAVFQAKKRVLEPLGLVEEGAKTAPGKKRPVEPSPQRSPDSST
GIGKKGQQPARKRLNFGQTGDSESVPDPQPLGEPPAAPSGVGPNTMAAGGGAP
MADNNEGADGVGSSSGNWHCDSTWLGDRVITTSTRTWALPTYNNHLYKQISNG
TSGGATNDNTYFGYSTPWGYFDFNRFHCHFSPRDWQRLINNNWGFRPKRLSFKL

FNIQVKEVTQNEGTKTIANNLTSTIQVFTDSEYQLPYVLGSAHQGCLPPFPADVF
MIPQYGYLTLNNGSQAVGRSSFYCLEYFPSQMLRTGNNFQFTYTFEDVPFHSSYA
HSQSLDRLMNPLIDQYLYYLSRTQTTGGTANTQTLGFSQGGPNTMANQAKNWL
PGPCYRQQRVSTTTGQNNNSNFAWTAGTKYHLNGRNSLANPGIAMATHKDDEE
RFFPSNGILIFGKQNAARDNADYSDVMLTSEEEIKTTNPVATEEYGIVADNLQQQ
NTAPQIGTVNSQGALPGMVWQNRDVYLQGPIWAKIPHTDGNFHPSPLMGGFGL
KHPPPQILIKNTPVPADPPTTFNQSKLNSFITQYSTGQVSVEIEWELQKENSKRWN
PEIQYTSNYYKSTSVDFAVNTEGVYSEPRPIGTRYLTRNL

(>TR|Q8JQF8|Q8JQF8_9VIRUCAPSIDPROTEINOS=ADENO-ASSOCIATEDVIRUS-8OX=202813PE=1SV=1)

5.3 Results and discussion

Evaluating the existing body of literature for antibody targets along AAV8 showed that many of the targets on AAV are looped peptide segments that protrude outside the viral capsid as variable regions, therefore 3 peptides were purchased from Elim Bio based on this notion, variable region VIII (GGYGIVADNLQQQNTAPQIGTVNGC), II (GGVKEVTQNEGTKTIANNGC) and IV (GGYYLSRTQTTGGTANTQTLGFSQGGPNTMANQGC). These peptides were chosen, in addition to their relevance based on existing literature, due to their looped structure that could be recapitulated on a liposome surface through use of the triazine lipids containing a beta-alanine and cysteamine headgroup (see chapter 2). As such, the peptides have two extra glycines on the N terminus, and a glycine and cysteine on the C terminus. One other peptide, encompassing the broader variable region IX (GGTPVPADPPTTFNGC),[430] was chosen as a control. While the initial goal was to generate lipopeptides with triazine lipids, the complexity of synthesis and purification required abandoning this strategy for the simpler conjugation to a maleimide lipid. After formulation of nanoparticles containing either free or maleimide conjugated peptides and the TLR4 agonist MPL, mice were immunized twice and then injected with AAV8-TdTomato to assess for transduction efficiency.[360]

Following immunization, the mice treated with free peptide to display a quantifiable antibody response against AAV8, as did unimmunized controls (figure 5.3A). By comparison, free VP1, without MPL, did achieve some immunogenicity. Unlike free peptides, however, maleimide linked peptides induced an anti-AAV response approximating that of free VP1. Liposome bound VP1, linked to both DGS-NTA and maleimide lipid, while not able to achieve the antibody response with actual AAV8 (from the mice in the non-suppressed group in chapter 4), did considerably increase the antibody response against AAV8. Furthermore, the mice immunized with VP1 had a considerable reduction in TdTomato expression (figure 5.3B). Interestingly, even though no anti-AAV8 antibodies could be detected in mice immunized with unbound AAV peptides, there was still a reduction TdTomato expression, suggesting that either the unquantifiable B cell response to the peptides was sufficient to suppress transduction, or that a memory T cell response to the peptides helped suppress transduction.

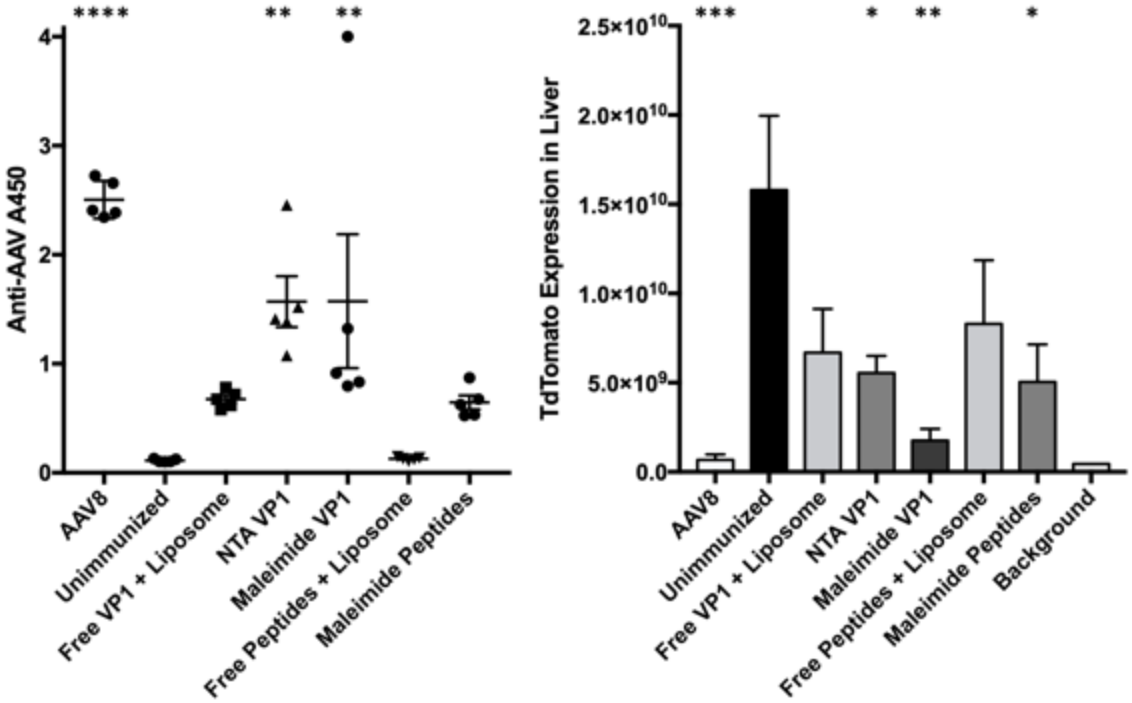

Figure 5.3. Response to literature-based peptides from AAV8. A. Immune response to AAV following immunization with peptides or VP1 protein, alone or conjugated to a liposome surface with different lipids. B. TdTomato expression following transduction with AAV8-TdTomato (1e11 gc/mouse), in mice previously immunized with peptides or VP1. The responses from the mice are compared with untreated animals, or animals treated with AAV8 in chapter 4. In A, lines represent mean +/- SEM and dots represent individual animals (n=5, except control mice from chapter 4, in B, two untreated mice were used as background controls, which were excluded from treatment assessment); in B, bars represent mean and lines represent SEM. Data were compared by ANOVA against the unimmunized group (*p*-*, *P* <0.05; **, *P* <0.01; ***, *P* < 0.001; ****, *P* <0.0001).

Because the peptides chosen failed to completely suppress transduction with AAV, we decided to undertake an evaluation of peptides that could be added to our repertoire. First, using plasma from C57BL/6J mice treated with AAV, an ELISA was developed to detect the presence of antibodies against AAV8. This assay was then used to detect anti-AAV8 antibodies in cynomolgus monkeys treated with AAV8, using plasma donated by Dr. Ryan Temel from a cohort of 12 animals transduced with the virus. Finally, to find epitopes that could have a greater translational component, 165 plasma samples from deidentified blood donors obtained through the Kentucky Blood Center were assessed for the presence of antibodies against the virus using this same assay. As evidenced in figure 5.4A, all mice previously treated with AAV8, had varying responses to the virus via ELISA. Some of the monkeys, however, did not display anti-AAV responses despite

previous exposure to the virus, suggesting either issues with administration, or allelic differences among the individual animals that resulted in poor immune responses. Among the 165 human samples assayed, 18.2% had levels of anti-AAV8 antibodies above background. This value is higher than that reported by Calcedo, et al. but lower than that reported more recently by Kruzik, et al. for populations in the United States.[466, 468] Unfortunately, due to the anonymous nature of our samples and the specificity of their location (Lexington, KY), it is difficult to assess the relevance of this number in a greater clinical scheme. To further confirm the presence of these antibodies, reciprocal endpoint titers (RETs) were performed on the highest mouse and monkey samples, and the 8 highest human samples. RETs demonstrated that the samples chosen did, in fact, have antibodies to AAV8, particularly in the mouse samples (figure 5.4B).

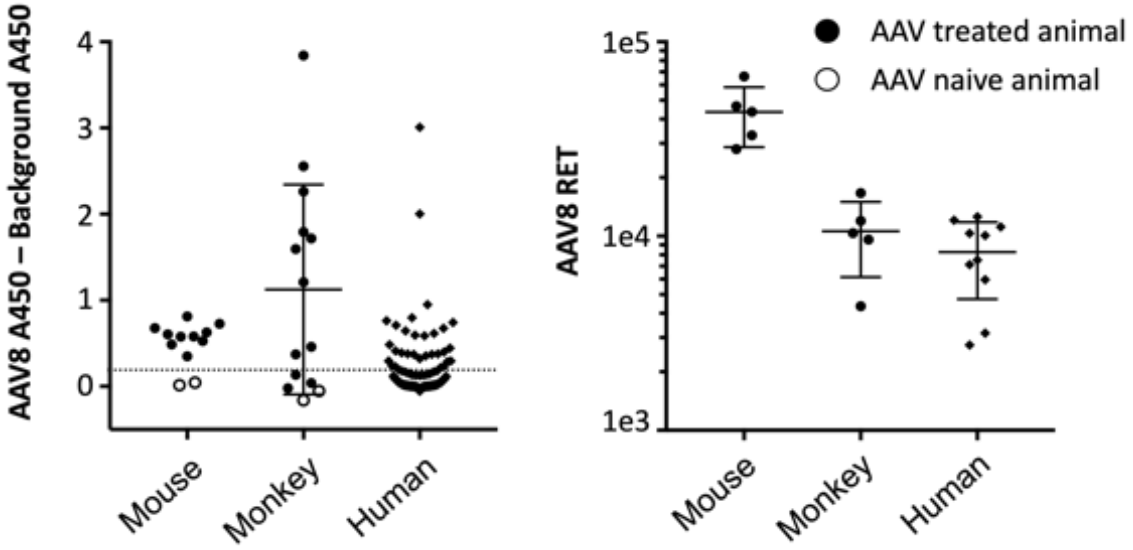

Figure 5.4. Evaluation of antibodies toward AAV8 via ELISA. A. ELISA of serum samples from mice and monkeys treated with AAV8, and human blood donors. B. Anti-AAV8 titers among highest positive samples across all three species. As the assays performed across the three species used different species-specific antibodies, statistical analysis could not be performed in these experiments. Of note, the initial experiments using mouse serum (left) were carried out using an older aliquot of AAV8, which yielded lower absorbances in these samples. But as evidenced by the titer and later neutralizing antibody experiments, these samples actually had a much stronger response than the other two species. The ELISAs for the mice were not repeated using new AAV due to low availability of samples, which were needed for titers and neutralization experiments.

Next, to determine whether these antibodies could deter AAV transduction, a neutralizing antibody (NAb) assay was developed using HEK293T cells and AAV8-GFP. The samples used for RET assessment were incubated with AAV8-GFP prior to transducing cells. For mice, the plasma from three bleeds was pooled for each individual

mouse, to yield better homogeneity when performing biological replicates of HEK293 transductions. As seen in figure 5.5A all five mice had a strong NAb response to AAV. For the monkey samples, combining samples was not necessary, due to the volume available for each timepoint. Therefore, monkey plasma was assayed for NAbs at 7 and 14 days after transfection, which showed no significant difference in the response, suggesting a strong memory response to AAV, following treatment (figures 5.4B-C). However, unlike with the mice, monkey serum had to be much more concentrated, as assays had to be started at a 1:5 dilution, rather than 1:20. For the human samples, both serum and plasma samples were available for each patient. Therefore, both tissue types were evaluated for NAbs, which showed no difference (figure 5.5D). Furthermore, since several human samples demonstrated high absorbance in the AAV8 ELISA and the control plate (false positives responding to possible blocking solution in ELISA), some of these samples were also assessed and were found, in fact, to have no neutralizing antibodies against AAV (figure 5.5E). In looking at the human samples chosen for their high absorbance in ELISA (1-3 and 5-10), the NAb responses observed were variable, as in the monkey samples, but there was nevertheless a strong neutralizing response in the samples that were positive in the ELISA experiments (figure 5.5F).

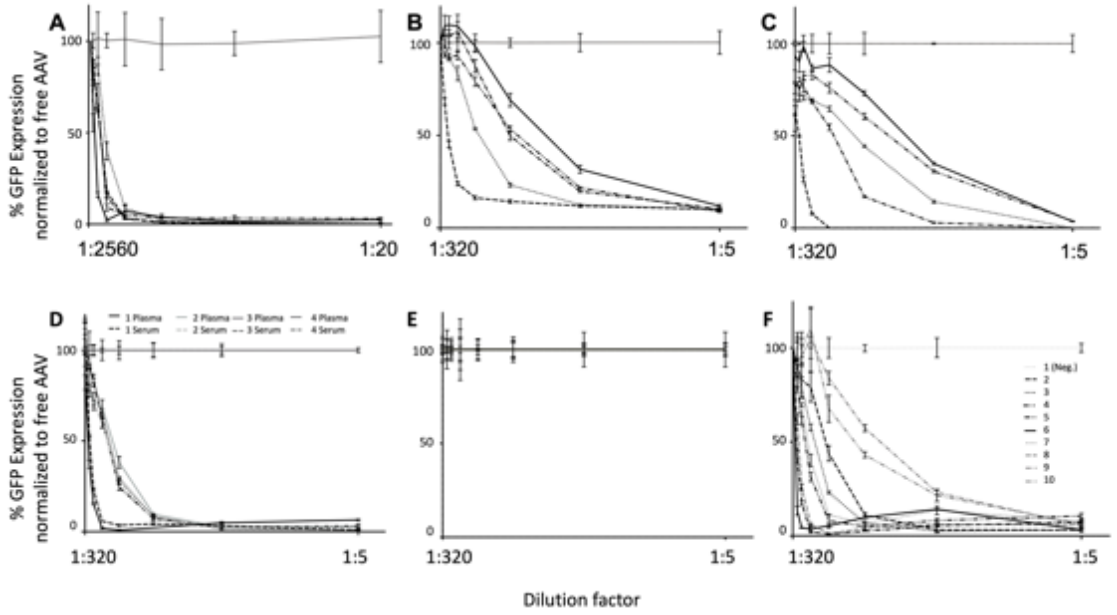

Figure 5.5. Neutralizing antibody (NAb) assay to confirm functionality of antibodies to AAV8. A. NAb assay of mice starting at a 1:10 dilution, compared with untreated mouse. B-C. NAb assay of monkeys treated with AAV8, and one untreated control, at 7 (B) and 14 (C) days after transduction, starting with a 1:5 dilution of serum. D-E. Evaluation of NAbs in human serum vs. plasma (D) and of false positive samples in ELISA (E). F. Evaluation of NAb response in human samples, using one negative sample and starting with a 1:5 serum dilution. Lines represent GFP expression across multiple dilutions for one

of three experimental replicates of individual samples across, error bars indicate mean+/-SEM of three cell replicates.

Following confirmation of the neutralizing capacity of the antibody response in the available samples, 5 mouse, 5 monkey and 8 human samples were sent to JPT Peptide Technologies (Berlin, Germany) for evaluation of capsid targets via peptide array. The following results and figures are part of the report generated by JPT based on the assay run by Dr. Maren Eckey, at JPT (order number 45318 (PO#27221). An example of a fluorescence readout image of a mini array reflecting typical microarray incubation of human plasma is shown in figure 5.6. Co-immobilized human IgG showed an interaction indicating that the assay worked as expected (bottom row of signals in the figure). In addition, monkey IgG also gave rise to strong signals which were generated by known cross-reactivity of the secondary antibody between species.

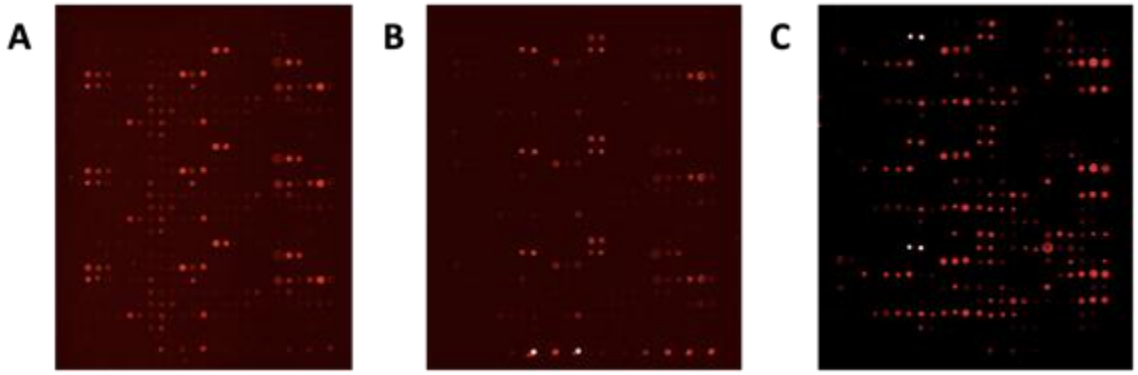

Figure 5.6. Results of peptide array of AAV8 VP1. A-C. Representative image of a mini-array incubated with the sample Human-6 diluted 1 to 200 (A), Monkey-5 diluted 1 to 200 (B) and Mouse-5 diluted 1 to 300 (C). Colors: black – no signal, shades of red – increasing intensity of detected signal, and white – detector saturation (=65535 light units).

Evaluation of anti-peptide across species yielded a relatively homogenous response across the three species, suggesting some degree of homogeneity in the B cell responses among species (figure 5.7). The response in the mice, as noted in the titer evaluation, as NAb assays, were much higher and these samples required higher dilution compared with monkey and human samples. Apart from still a lot of weak signals all over the library, a few medium to strong signals could be detected. As noted, by Dr. Eckey in her report, there were considerable differences in the background and number of strong specific interactions among species. Human sample 1 had particularly high background staining, while peptides 73 and 74 yielded strong signals in the absence of any primary antibody.

The high background response in the control samples, while discouraging, warrants further evaluation, as the samples across species seem to correlate with that of mice, where no significant background was noted. While further processing of data could clarify whether these responses in monkey and human samples are false negatives, it has been previously suggested that further processing can introduce errors.[469] High background in peptide arrays has been previously attributed to binding of detection antibodies to different components of the assay plate, often due to hydrophobic interaction, a phenomenon that has also been seen more frequently with human samples, than experimental animals.[470, 471] While the present set of data on these peptide epitopes need to be evaluated via other methods, such as ELISA,[472] to determine whether these targets are false positives or negatives, the location of these epitopes suggest novel targets on VP1 (table 5.3 and figure 5.8) that could serve to improve our suppression strategies toward AAV.

Table 5.3. Amino acid regions on AAV8 identified as antibody targets by peptide array

Protein region (aa)	Combined sequences
41-67	DGRGLVLPGYKYLGPFNGLDKGEPVNA
241-284	KTAPGKKRPVEPSPQRSPDSSTGIGKKGQQPARKRLNFGQTGD
285-324	DPQPLGEPPAAPSGVGPNTMAAGGGAPMADNNEGADGVG
328-363	WHCDSTWLGDRVITTSTRTWALPTYNNHLYKQISN
373-416	NTYFGYSTPWGYFDFNRFHCHFSPRDWQRLINNNWGFRPKRLS
444-495	VFTDSEYQLPYVLGSAHQGCLPPFPADVFMIPQYGYLTLNNGSQA VGRSSF
492-551	SSFYCLEYFPSQMLRTGNNFQFTYTFEDVPFHSSYAHSQSLDRLM NPLIDQLIDQYLYY
569-628	GPNTMANQAKNWLPGPCYRQQRVSTTTGQNNNSNFAWTAGTK YHLNGRNSLANPGIAMA
657-696	YSDVMLTSEEEIKTTNPVATEEYGIVADNLQQQNTAPQI
693-752	PQIGTVNSQGALPGMVWQNRDVYLQGPIWAKIPHTDGNFHPSPL MGGFGLKHPPPQILI
780-811	VSVEIEWELQKENSKRWNPEIQYTSNYYKST
812-838	VDFAVNTEGVYSEPRPIGTRYLTRNL

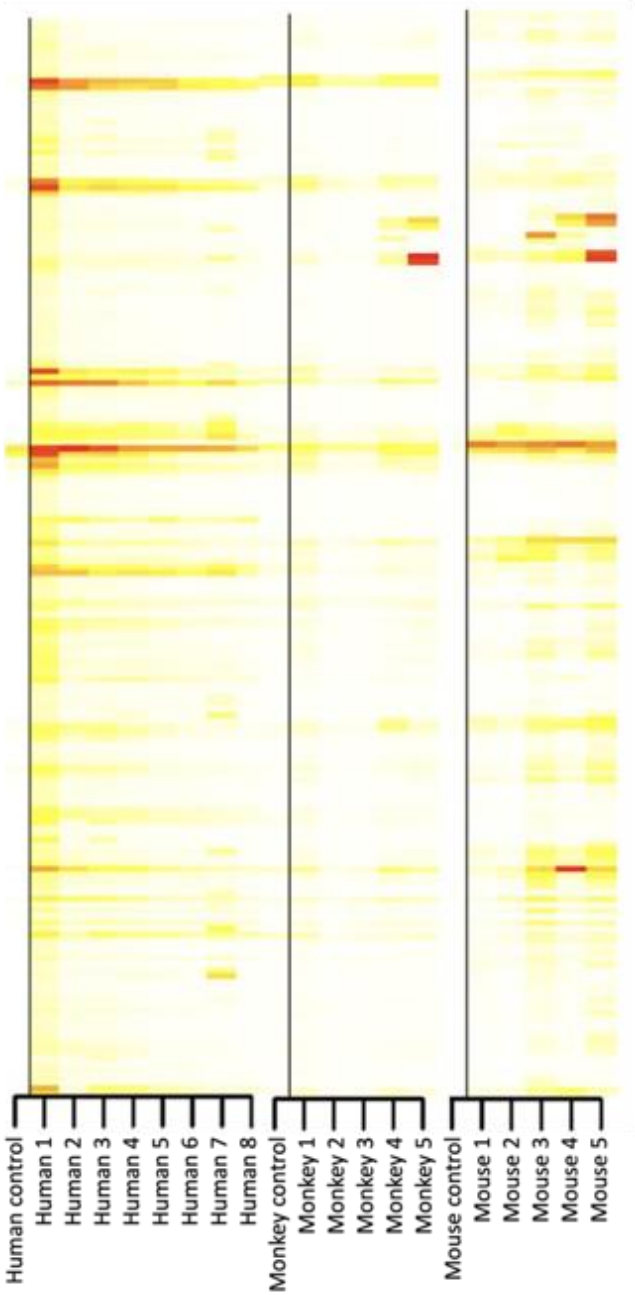

Figure 5.7. Heatmap of antibody responses in serum of mice and monkeys treated with AAV8, as well as human samples with anti-AAV8 antibodies. Heatmap diagram showing results from plasma sample incubations for all immobilized peptides. For human and monkey samples, serum was diluted 1 to 200, while for mice a 1 to 300 dilution was used. Each line represents a peptide, in the order specified in table 5.2. The MMC2 values are shown as color coded ranging from white (low intensity) over yellow (middle intensity) to red (high intensity, highest MMC2 value). A black line on each heatmap separates the control incubations performed on the same slides applying detection antibody -or detection system respectively- alone.

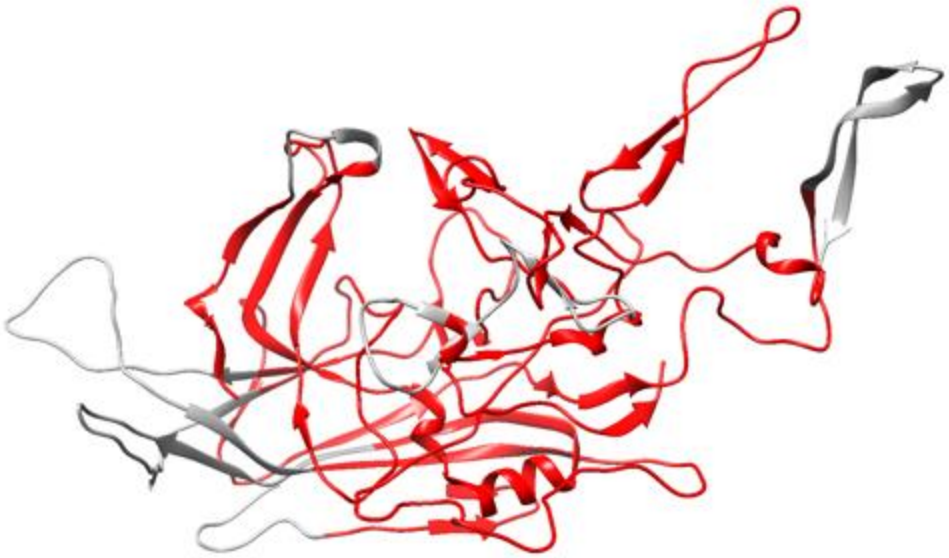

Figure 5.8. Display of epitopes on AAV8 VP1 targeted by peptide array, in red. Image generated using UCSF Chimera using UniProt Q8JQF8 as a template. The first three sequences identified the peptide array is not included, as the protein structure provided by UniProt begins later in the protein sequence.

5.4 Conclusions

To generate a consensus of peptides that could recapitulate the immune response to the AAV capsid on the surface of a lipid nanoparticle, for later evaluation of suppression, we have first studied literature reported peptide targets. The peptides used from the literature, while producing a considerable reduction in AAV transduction, did not fully achieve the suppression of viral transduction in the liver. Because of this, we attempted to improve upon this strategy through evaluation of a peptide array against the virus, using plasma from mice, monkeys and humans. The samples used encompass both antibodies formed either through AAV8 treatment, in mice or monkeys, or naturally, in humans. The ability of these antibodies to recognize AAV8 differed somewhat across the three species, with mice seemingly having the highest response in both ELISA and NAb assays, while the other two species had much more variable responses. These differences could perhaps be due to the genetic prolife of the mice vs. other species, as well as the environmental differences encountered by each of these. Interestingly, in the human samples, which reflect the most natural immune system among the three studies species, the antibody response observed via ELISA was confounded, in several patients, by the presence of antibodies reacting with the non-fat dry milk blocking buffer. The presence of these antibodies highlights the need for strenuous scrutinization of antibody responses in human assays, which was previously discussed by Dr. David Henson in our lab in his dissertation.[445]

Evaluation of linear epitopes via peptide array across three different species yielded very robust responses from mice, but not necessarily from either human or monkey samples warranting further evaluation to determine their role, as well as the translational potential of these peptide segments. Specifically, experiments such as NAb inhibition, immunizations for detection of anti-AAV antibodies, and suppression should be performed to determine whether these peptides could serve as valid targets for liposome-based studies of AAV. However, it is encouraging that the linear antibody epitopes found through the JPT peptide assay correspond to several of the previously reported segments along the AAV surface, including several epitopes along the beta-barrel core motif.[430] Furthermore, while immunizations with peptides or NAb interference assays may yield some information on the usefulness of liposome bound peptides in a suppressive strategy, evaluation of the three-dimensional structure of the resultant nanoparticle with crystallography or NMR may prove useful in determining the best strategy to use for such an approach.[473-475]

CHAPTER 6: SUMMARY AND CONCLUSIONS

6.1 Research overview

As discussed throughout chapter 1, lipid nanoparticles offer an outstanding tool to modulate immunity. Their versatility as amphipathic vectors, liposomes provide an optimal vehicle for pharmaceutical delivery.[217, 302] Not only can they be used to incorporate a large array of therapeutically active agents, but their composition can be altered to optimize their utility for different applications, as evidenced by the many approved agents that use liposomes as a delivery platform (see tables 1.1-1.3) in vaccine, drug, and gene delivery. In the present body of work, attempts were made to apply various types of liposomal nanoparticles to understand and improve certain shortfalls encountered in gene delivery.

Gene therapy seeks to introduce missing/faulty genes or remove/decrease faulty genes directly or through RNA interference (RNAi)[280, 287-289] and is largely divided into viral and non-viral delivery. Viral vectors take advantage of the natural mechanisms used by viruses to insert genes to the host, while non-viral gene delivery often employs cationic moieties, such as cationic lipids, to ionically bind nucleic acid and guide it into cells.[292, 293] While generally more effective, viral vectors like adeno-associated virus (AAV) have acceptable efficacy and safety parameters but elicit systemic reactions that lead to neutralizing antibody production against the vector, limiting their use.[287, 290, 291] Non-viral systems, while usually not immunogenic, struggle with their ability to circulate in vivo and to achieve tissue specific transfection, since most of them traffic to organs like the liver, spleen or lungs. Another major obstacle for gene delivery is the lack of processes that allows these nanoparticles to traffic to specific cellular compartments, like the nucleus, causing much of the field to transition into RNA delivery.[209, 238, 290, 294-299]

In the last two decades, the development of ionizable cationic lipids, which allowed for improved in vivo circulation of nanoparticles and reduced toxicity, as well as the ethanol loading procedure (or microfluidic preparation), which improved nucleic acid entrapment in nanoparticles, allowed the field to make some major strides.[209] These advances have allowed for the approval of siRNA and mRNA therapeutics, which have majorly contributed to patient health. However, the high-cost cationic lipids used for gene delivery, as well as some of the more novel technologies developed in the field, such as microfluidic devices, create obstacles for research in the field, especially because many of these technologies are locked behind patents that limit innovation from new researchers. This is also true in the field of AAV delivery, where many of the technologies used to suppress or bypass immunity toward the virus require expensive engineering or the use of patented technologies, such as the rapamycin nanoparticles from Selecta Biosciences.

In this manuscript some of the concerns associated with gene therapy were addressed. The first part focuses on the development of a novel class of compounds based on the triazine, cyanuric chloride, with potential for gene therapy. The second part focuses

on understanding the immunology of AAV8 and trying to suppress antibodies against it with the goal of improving transduction with repeated doses of the virus.

6.2 Results overview

6.2.1 Overview of results from cyanuric chloride lipids

One way to overcome the costs of synthetic cationic lipids and commercial transfection reagents is through synthesis of lipids with chemical entities like cyanuric chloride that are cost effective and allow for easy modifications to the lipid to be made.[351-353] To this end, the first portion of this manuscript describes the use of cyanuric chloride to generate a library of triazine lipids with dialkylamines as tails and various small molecule head groups. Among the compounds produced, lipids 3, 4, 9 and 10 possessed cationic headgroups and were evaluated for their toxicity and transfection efficiency in cells and mice. In HEK293T cells, nanoparticles made with TZ lipids and DOPE, at a 1:1 molar ratio, led to robust transfection particularly with the compounds made with a shorter lipid tail, which was expected based on the work of Candiani, et al.[352] Lipid 3, in addition to its in vitro efficacy, showed a tolerable toxicity profile in vivo, based on renal and hepatic function, which prompted its assessment for in vivo transfections. Using an optimized formulation, lipid 3 was then used to develop lipid nanoparticles (LNPs) using a microfluidic device and compared with lipoplexes (LPs) or AAV8 using a GFP plasmid. While LNPs led to quantifiable expression of GFP in mouse livers, the expression observed with AAV and LPs was considerably higher, which was unexpected as LPs have been reported to be less effective in vivo. To validate this finding, another plasmid was delivered, encoding for human alpha-1 antitrypsin (hAAT), with both LNPs and LPs. Unfortunately, the cost of AAV8-hAAT did not allow for this additional control to be evaluated. With hAAT, transfection was again significantly higher with LPs, which led to transfection efficiencies like those reported with liposomal delivery of this protein.

Next, since hAAT has been previously reported to induce an anti-transgene antibody response in mice, we decided to assess the immunogenic potential of antitrypsin transgenes delivered with lipids. On day 14 after administration of the nanoparticles, or of the free protein in a liposomal solution, the mice were assessed for titers against human antitrypsin. As expected, the protein administered with lipids yielded considerably higher titers, particularly in the mice given lipid 3. In the transfected mice, the titers against hAAT could not be detected in LNP treated mice. However, LPs induced titers similar to free hAAT in saline. This difference could be attributed to the reduced gene expression using the LNPs in antigen presenting cells due to PEGylation, a phenomenon that was confirmed in vitro with dendritic cells and J774 macrophages. While the findings of these studies do not clarify the role of PEG on anti-transgene immunity, they highlight the need to evaluate this aspect of PEGylated nanoparticles in immunization.

6.2.2 Overview of results from AAV8 suppression

As evidenced by existing literature and some of the results from chapter 3, viral vectors provide a more robust method for achieving gene delivery than lipid nanoparticles

in the context of plasmids.[430, 431] However, as mentioned previously, these have the drawback of being targeted by the immune system, which limits transduction.[431, 432] In the second part of this manuscript a liposome based strategy was evaluated for its ability to suppress anti-AAV antibodies using doxorubicin loaded liposomes conjugated to the main surface protein of AAV8, VP1. This strategy was evaluated for its translational potential through a neutralizing antibody interference assay using VP1 and serum from humans and was followed by experimentation in mice.

The liposomes used in the suppression strategy were formed using DSPC and cholesterol with the addition of 5% NTA(Ni)-DGS (NTA) or DSPE-PEG_{2000}-Maleimide (maleimide or mal.).[448] After remote loading of doxorubicin, addition of the protein, and characterization, the nanoparticles were administered to mice at 8 mg of doxorubicin per kg of body weight, prior to administration of AAV8-TdTomato. In mice that had been treated with AAV8-GFP prior to suppression, the antibody response remained intact, based on absorbance. However, closer evaluation of anti-AAV8 titers, showed that while the immune response to AAV8 was present in the maleimide suppression group, it did not rise as it did with other groups treated with AAV8-GFP, suggesting that the suppression strategy failed to eliminate the existing immune response, but inhibited further activation of immune responses from occurring. This phenomenon was also observed in the anti-ovalbumin response used as a control. Interestingly, while the existing anti-AAV8 response was present in the maleimide group, the anti-VP1 was slightly diminished compared with other groups treated with AAV8, suggesting that there may be differences in the anti-VP1 and full capsid responses that aren't recapitulated by VP1. While the studies conducted did show some promise regarding suppression to VP1, the overall suppression toward AAV failed, as the mice could not be properly transduced with TdTomato and there were no differences between the suppressed and unsuppressed groups.

While assessing this liposomal strategy to eliminate anti-AAV antibodies, an evaluation of AAV8 epitopes was also carried out, via peptide array, with the goal of finding the most relevant peptide epitopes on the viral surface. For this, samples from mice and cynomolgus monkeys previously treated with AAV8, and from 165 de-deidentified blood donors were assessed for antibodies to AAV8. Upon confirmation of antibodies, serum from 5 mice, 5 monkeys and 8 humans were assayed by peptide array. Evaluation of the responses to peptides across species yielded several epitopes that were positive across all three species. Unfortunately, while the response in mice was very strong, the other two species showed high levels of background noise, requiring further investigation to confirm the validity of these epitopes as clinically relevant in the anti-AAV8 response.

6.3 Conclusions and future directions

Throughout this manuscript two avenues were explored to attempt to improve outcomes in gene delivery. One was the development of a novel class of lipids, and the other was the use of a lipid-based strategy to suppress anti-AAV antibodies. As discussed in chapters 2 and 3, triazine lipids offer a useful tool for gene delivery with a relatively low toxicity profile and a transfection efficiency similar to commercially available cationic

lipids. Based on the findings presented in these chapters, further evaluation of the structure activity relationship is warranted, including evaluation of the lipid tails, as well as headgroups. Another key factor to consider is the evaluation of the pKa activity relationship of these nanoparticles, which has been previously shown to affect transfection efficiency, as well as the interaction of the triazine headgroup with nucleic acids.

As it pertains to the triazine lipids, two major areas of research that were not extensively pursued in the present body of work, but should be investigated further, were small molecule drug delivery and peptide conjugation. Initial experiments to assess drug entrapment with carboxyfluorescein resulted in formation of insoluble gels with the compounds. While the nature of this interaction is perhaps worth exploring, experiments with non-aromatic compounds could show whether triazine lipids can be used in drug delivery. In the field of immunity, evaluation of triazine lipids and peptide or protein conjugates are worth exploring. Given the results seen with ApoA-I peptide immunizations in chapter 2, it is likely that these compounds could serve to improve peptide presentation on bilayers. Furthermore, given the ability of the triazine compounds to enhance immune responses shown in chapter 3, there may be a substantial role for the use of these compounds as adjuvants.

From the perspective of liposomal gene delivery, several questions arose from the present work. These include the role of PEG on liposomal delivery, which in our studies hindered transfection when developing lipid nanoparticles, as well as the unexpected finding that lipid nanoparticles led to reduced transduction compared with lipoplexes. While many hypotheses can be theorized from these findings, including the reduction in the interaction between cells and the nanoparticles due to difference in charge or hinderance from PEG, these findings warrant further evaluation. In addition to the efficiency of transgene detection, another major area of interest should be the immunogenicity of transgenes. The studies carried out here used plasmids in hope that the immune response to the transgene would be diminished. While this was the case with nanoparticles containing PEG, lipoplexes induced a quantifiable antibody response to antitrypsin at par with free protein in saline, suggesting that while this method of delivery may be more successful, it may lead to poorer outcomes down the line. Nevertheless, the evaluation of immune responses toward non-viral vector transgenes is a field where much information is lacking, despite the advances made in this area with viral vectors.

During the second half of this dissertation a different approach was taken to improving gene delivery using lipid nanoparticles. In chapter 4 an attempt was made to develop a liposome-based strategy to suppress anti-AAV8 antibodies using the main protein that composes the viral capsid, VP1. While this strategy failed to remove the antibodies formed against the virus after an initial treatment, the presence of circulating lipid nanoparticles considerably reduced the development of new antibodies against the virus and the control ovalbumin immunization. Additionally, while difficult to assess due to the weak response generated against VP1 by AAT treatment alone, the anti-VP1 in the maleimide treated group seemed to have been reduced to pretreatment levels.

These findings collectively show that this strategy could be useful following considerable tailoring of the immunosuppressive nanoparticles. To begin with, the long circulation of the nanoparticles must be evaluated if using a protein conjugation approach that uses PEGylated lipids. Additionally, the liposomal surface must better encompass the viral capsid, by using entire capsid conjugated to the liposome or through the careful tailoring of peptides to mimic the virus surface on the liposomes. For the former, using a maleimide conjugation system, such as that used here, could provide a simple approach to link AAV to the liposomal surface. For the later, initial attempts were made to study the peptide antigens, although many of the resulting structures from the peptide array used in chapter 5 demonstrated the complexity of such an approach and would likely require extremely complex analysis and engineering of the peptides used. While this strategy would likely be unnecessarily complex, pursuing this line of work could help increase the understanding of the behavior of peptides on a liposomal surface. A simpler approach could perhaps be to evaluate the immune response against an enveloped virus, such as a lentivirus, as this may allow for the attachment of viral proteins to the liposome surface and subsequent remote loading of doxorubicin. Additionally, in continuing the present experiments, it might be useful to assess whether VP1 suppression, following administration of this protein, could lead to suppression of the anti-VP1 response. These experiments, in conjunction with ex vivo cell experiments employing lymphocytes and isolated B cells to determine whether the cells take up the nanoparticles and the nanoparticles do confer toxicity to these cells, would provide a way to assess viability of this strategy in a less complex system than using an entire AAV capsid.

As suggested by the work of Naoko Oku and by Selecta Biosciences, liposome based strategies for immunosuppression provide a tentative strategy for epitope specific suppression.[268, 437, 438] Developing immunosuppressive nanoparticles with drugs such as doxorubicin, rapamycin, tacrolimus, or others in combination with linker structures, such as NTA(Ni) or maleimide, could provide a simple strategy to suppress antibodies against target proteins, either therapeutics like AAVs or biologic drugs, as well as the protein targets of autoimmune responses. A doxorubicin-based approach, such as that described here, could prove successful upon further optimization. The evaluation of other drugs, such as glucocorticoids and other immunomodulating agents could help expand the utility of this approach, especially in autoimmune and rheumatic conditions.[476-481]

While many questions remain unanswered, the body of work presented within this dissertation highlights the utility of liposomes in the field of gene delivery, not only in non-viral delivery systems, but also through supplementary therapies in viral vector delivery. Moreover, the work presented herein opens many questions to be investigated further and improve upon current modalities of gene delivery.

APPENDIX

Figure A1 Intermediate compounds for synthesis of triazine lipids

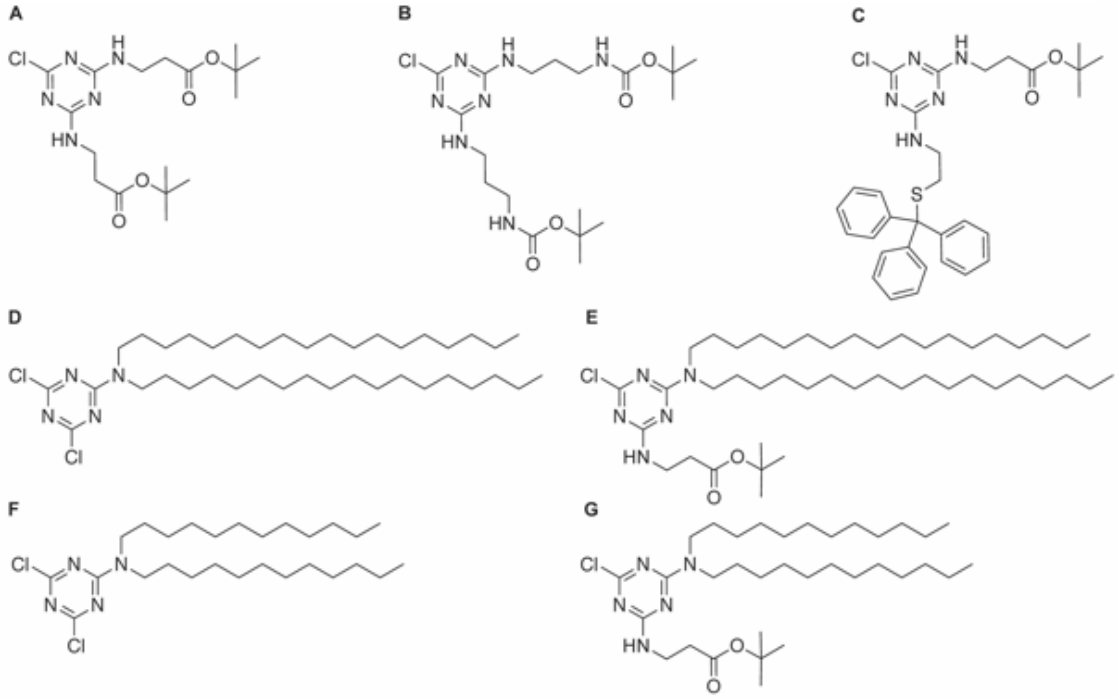

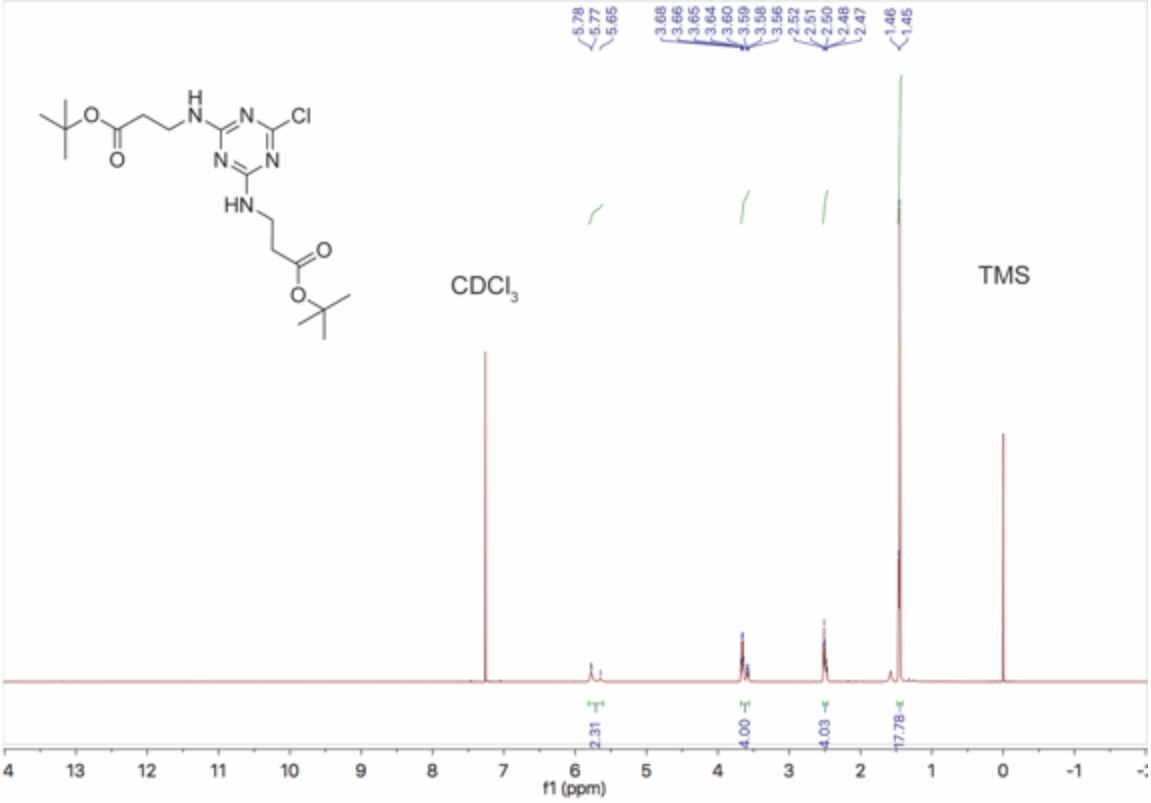

Figure A2 ^{1}H NMR of intermediate A

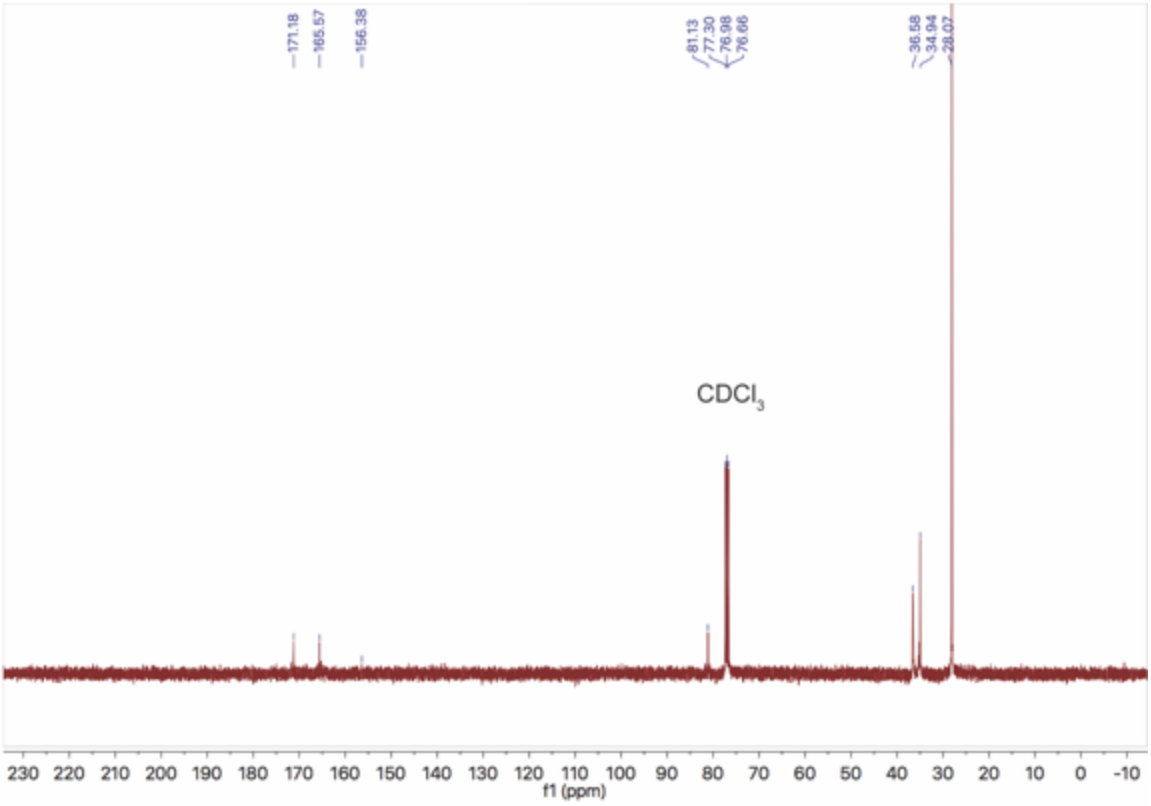

Figure A3 ^{13}C NMR of intermediate A

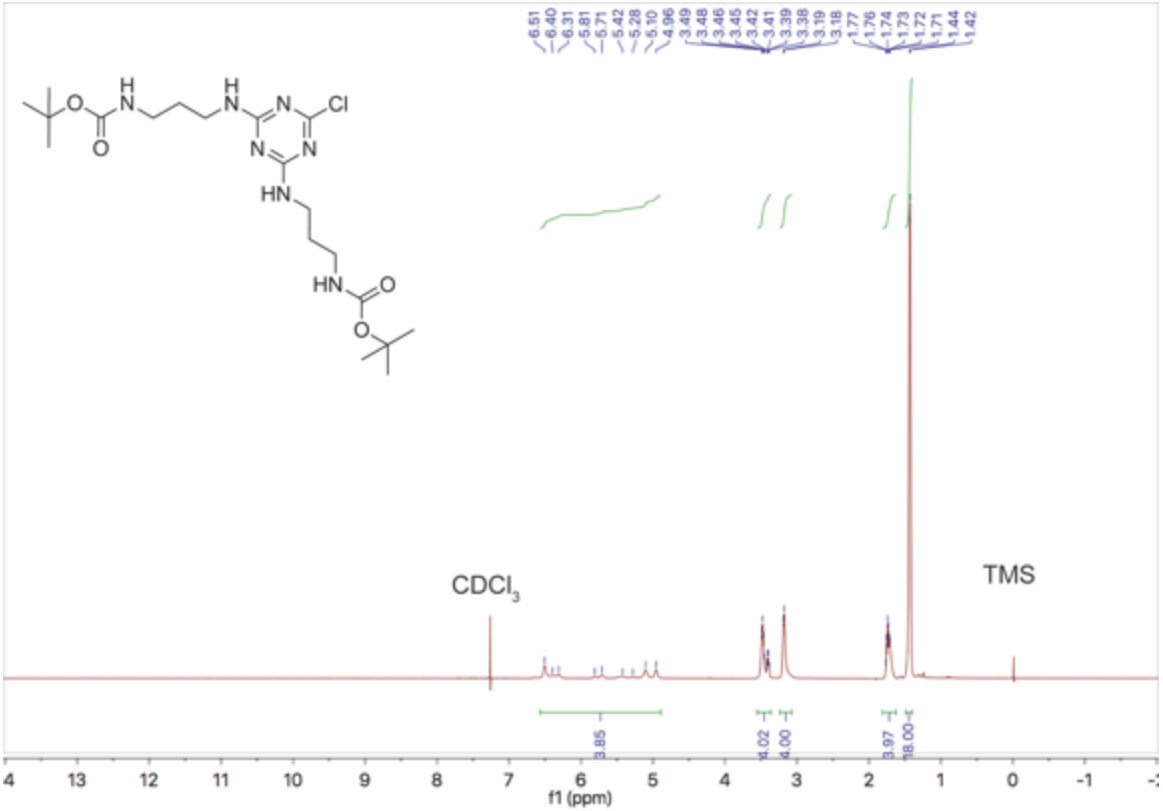

Figure A4 ^{1}H NMR of intermediate B

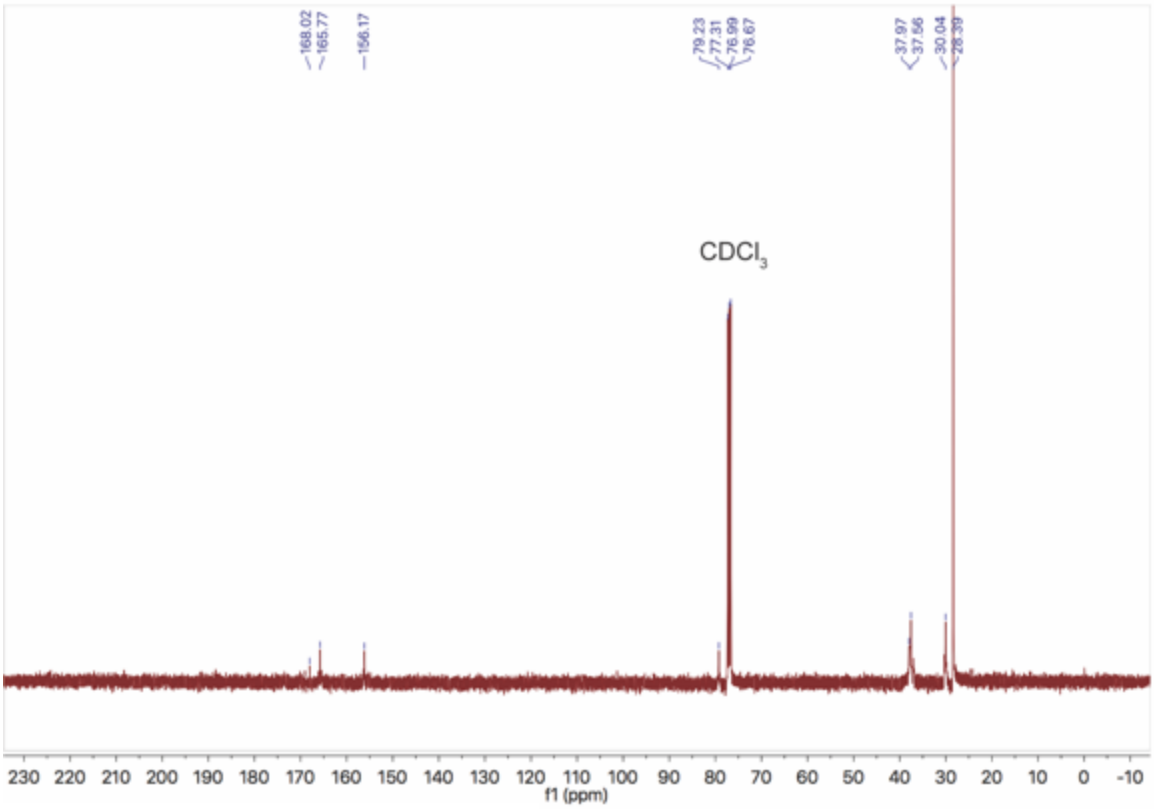

Figure A5 ^{13}C NMR of intermediate B

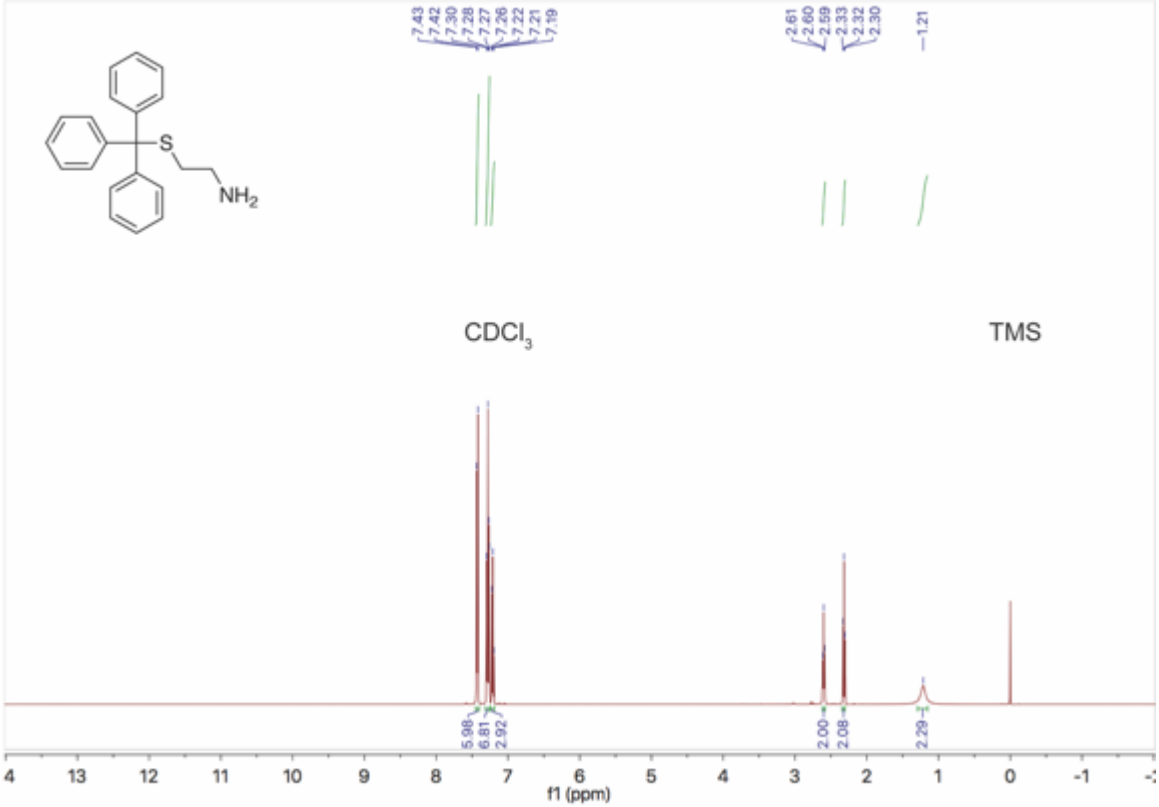

Figure A6 ^{1}H NMR of 2-[(triphenylmethyl)thio]ethanamine

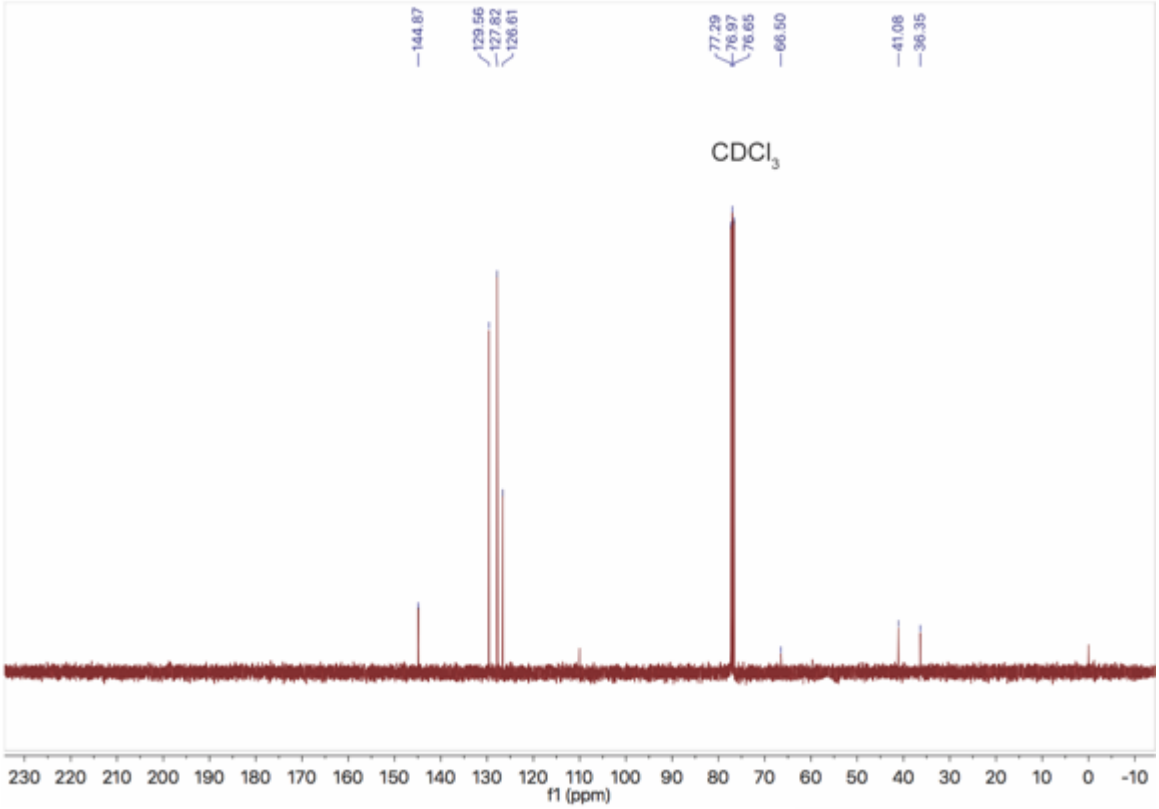

Figure A7 ^{13}C NMR of 2-[(triphenylmethyl)thio]ethanamine

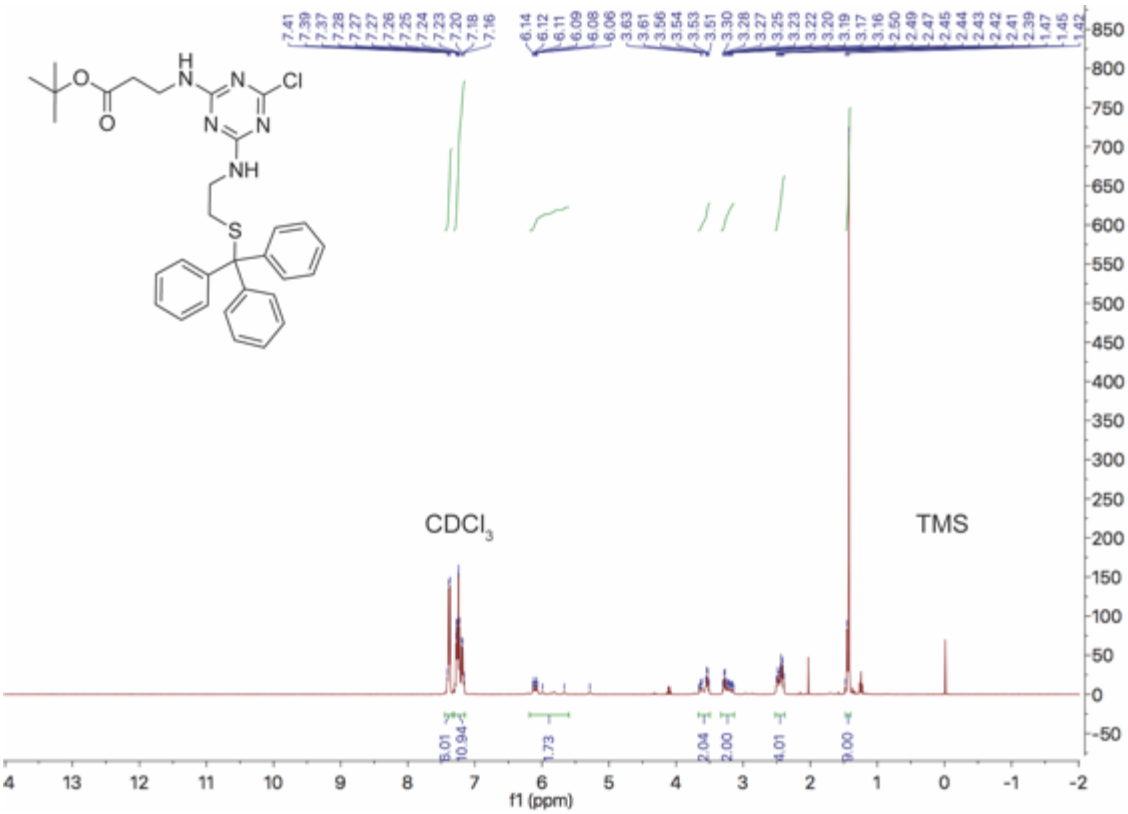

Figure A8 ^{1}H NMR of intermediate C

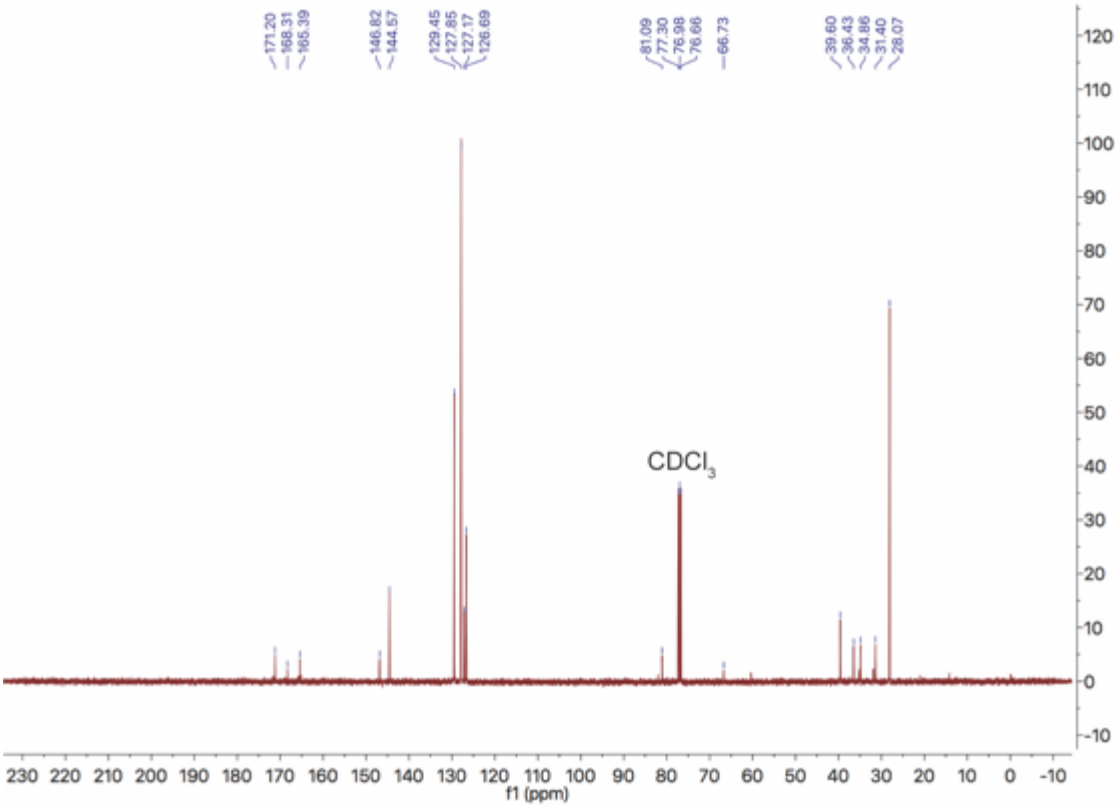

Figure A9 ^{13}C NMR of intermediate C

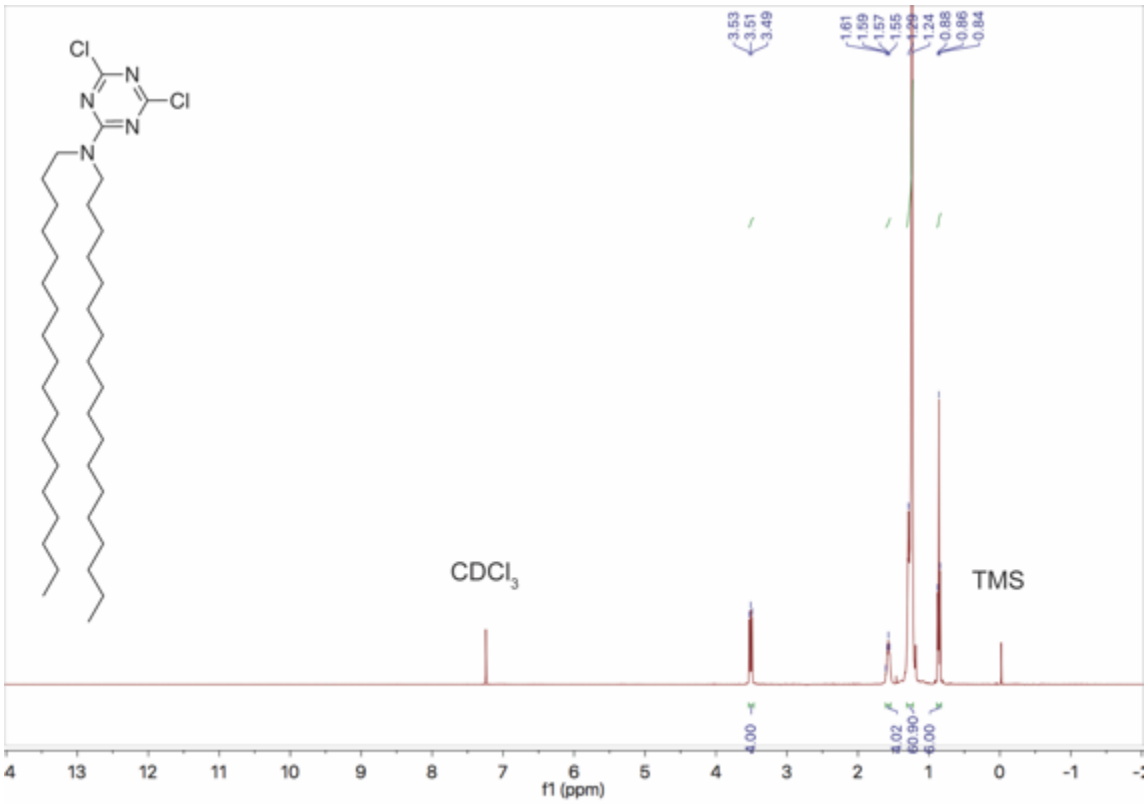

Figure A10 ^{1}H NMR of intermediate D

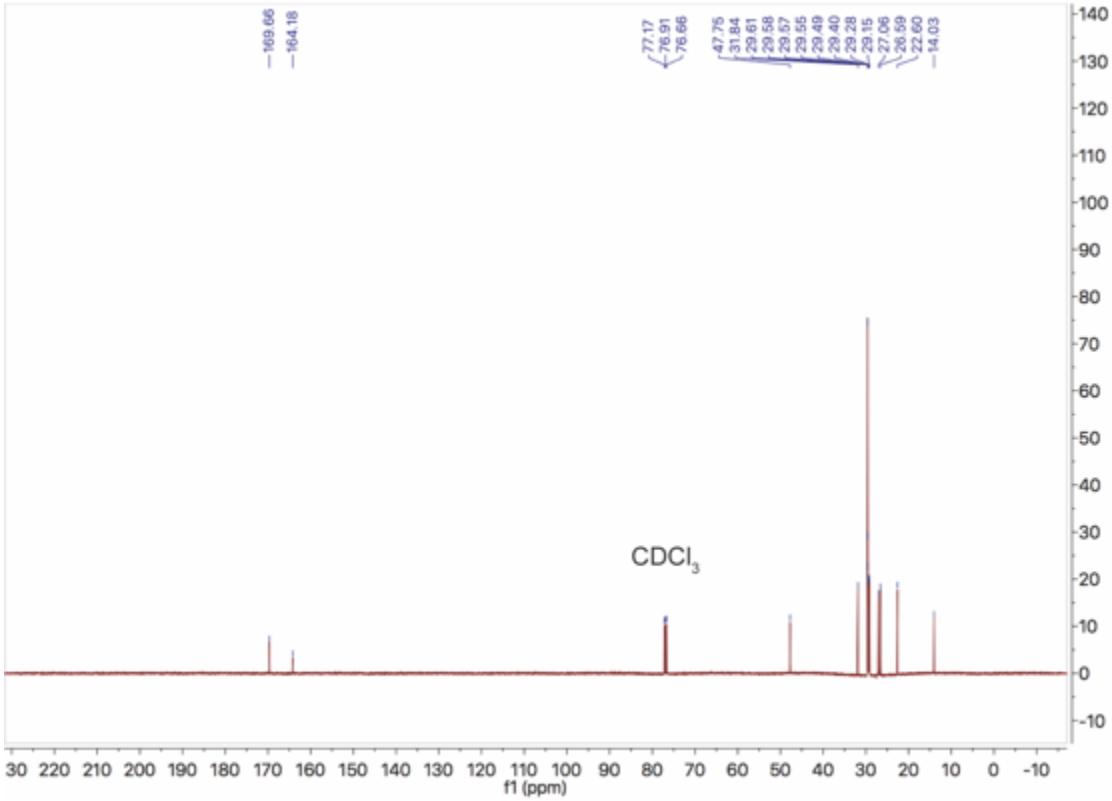

Figure A11 ^{13}C NMR of intermediate D

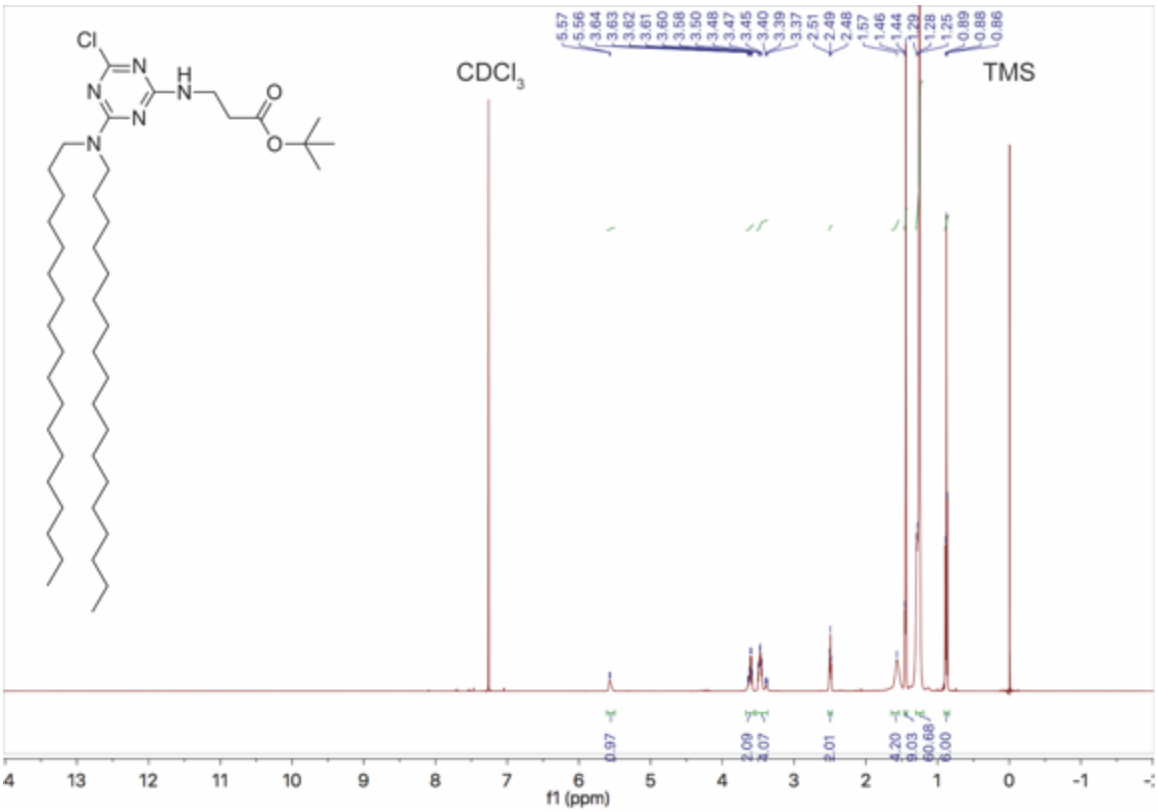

Figure A12 ^{1}H NMR of intermediate E

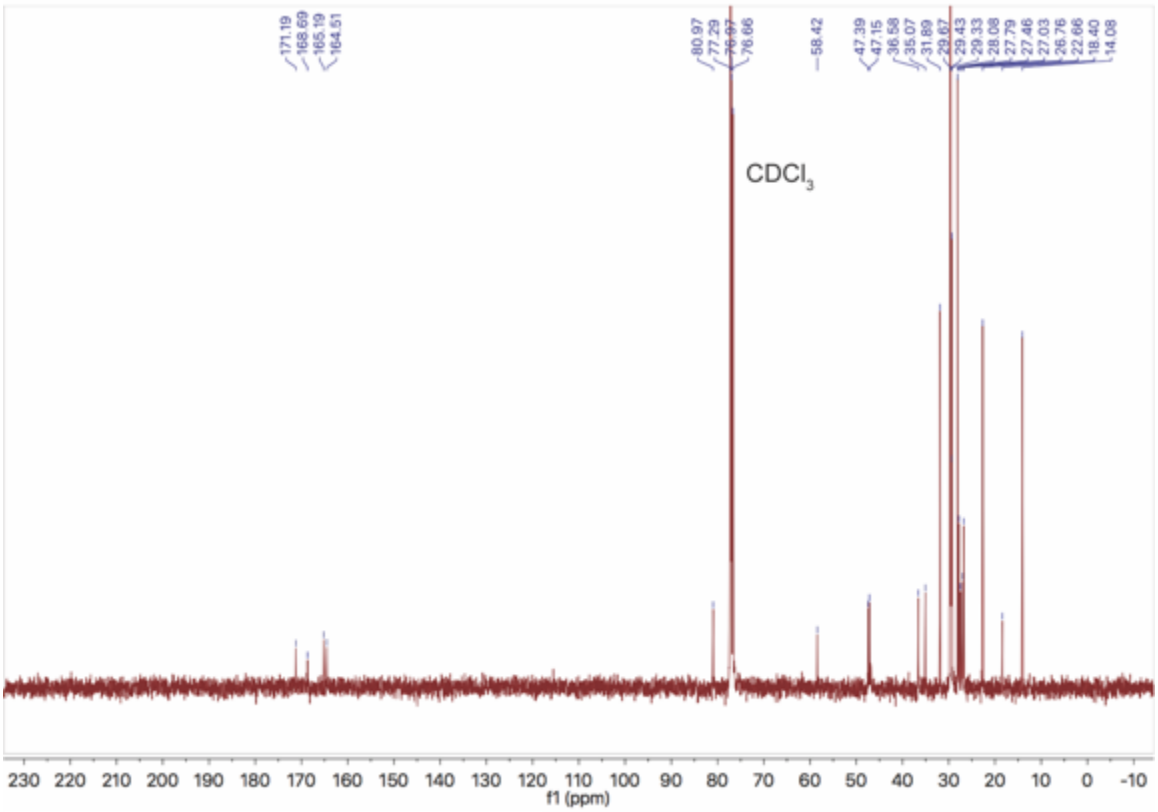

Figure A13 ^{13}C NMR of intermediate E

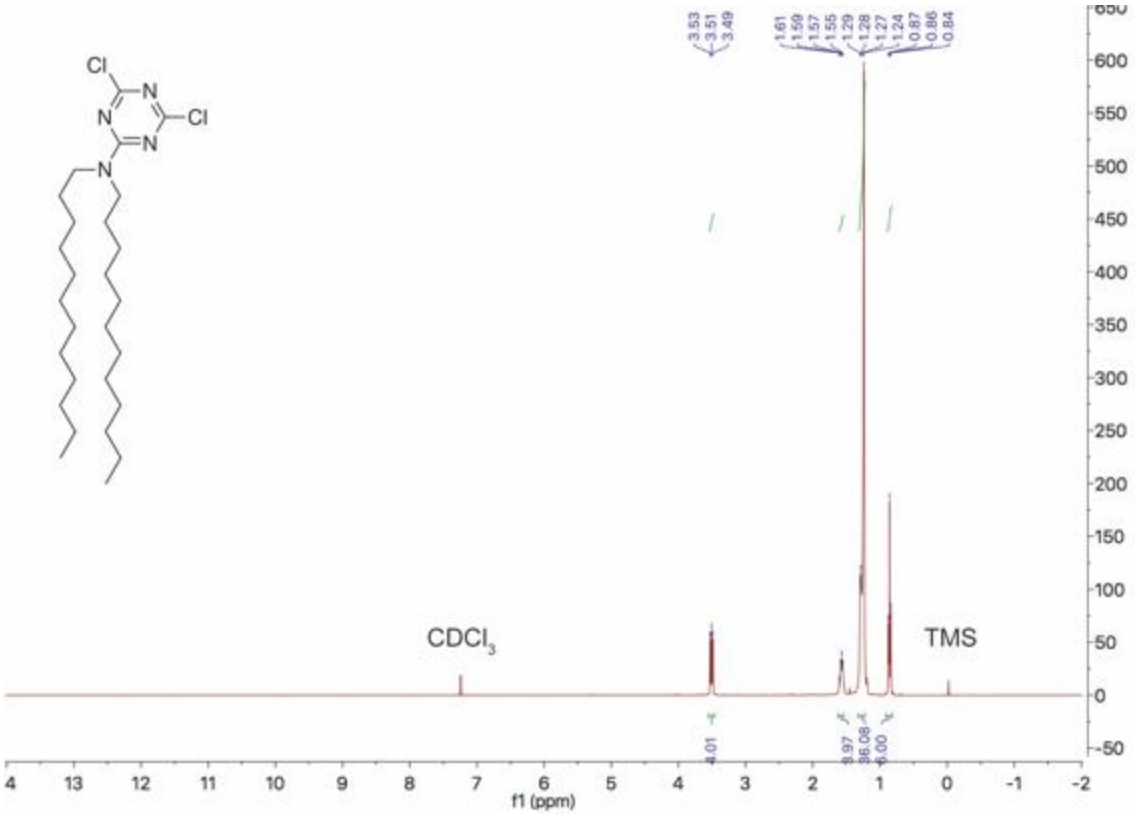

Figure A14 ^{1}H NMR of intermediate F

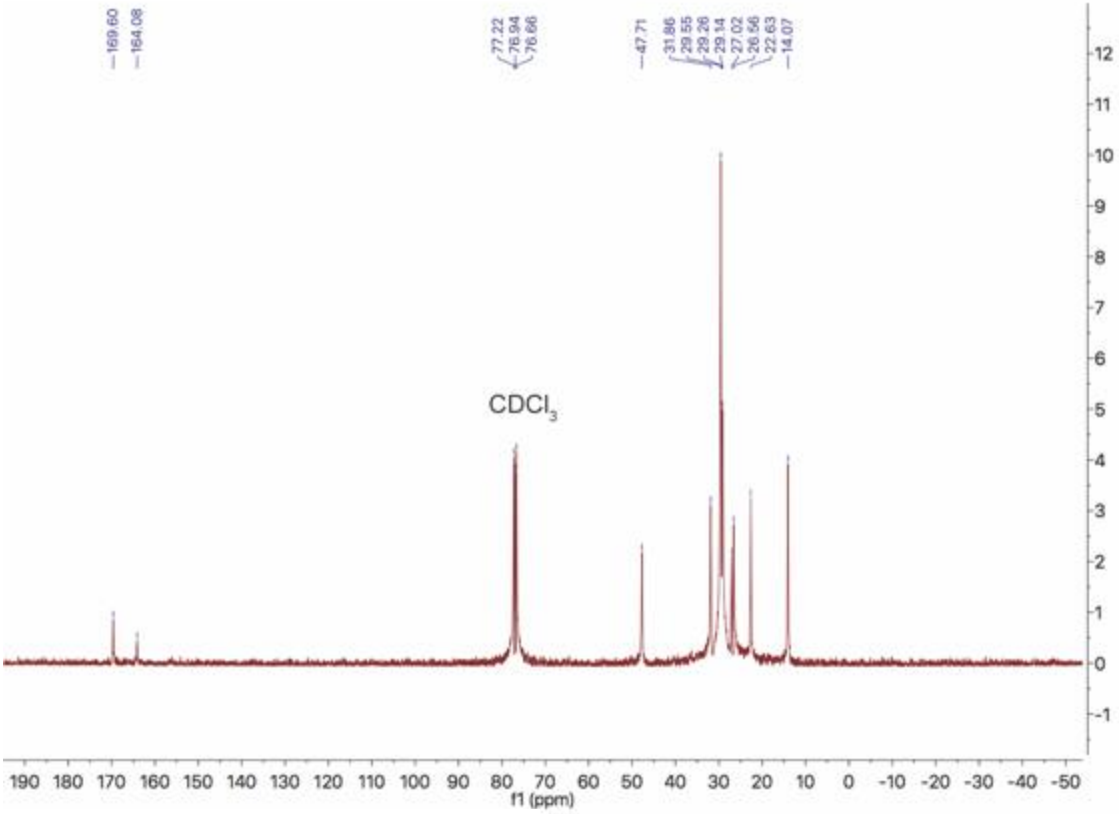

Figure A15 ^{13}C NMR of intermediate F

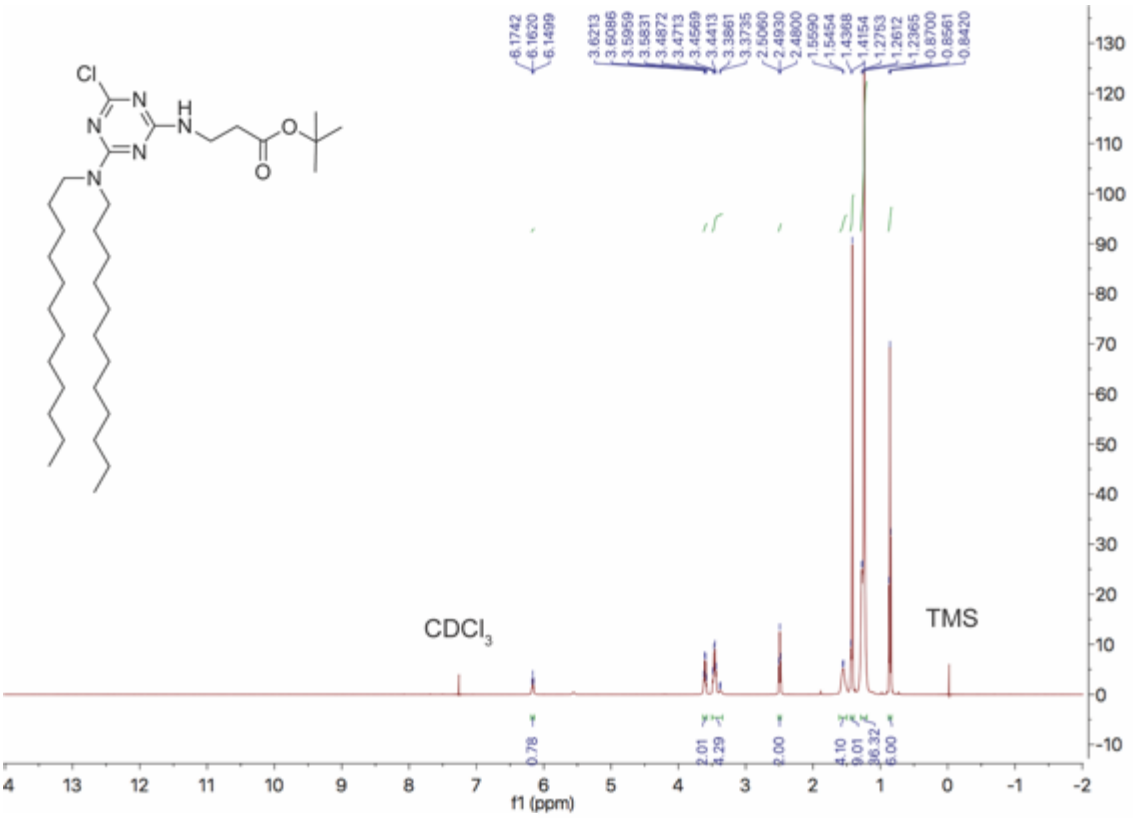

Figure A16 ^{1}H NMR of intermediate G

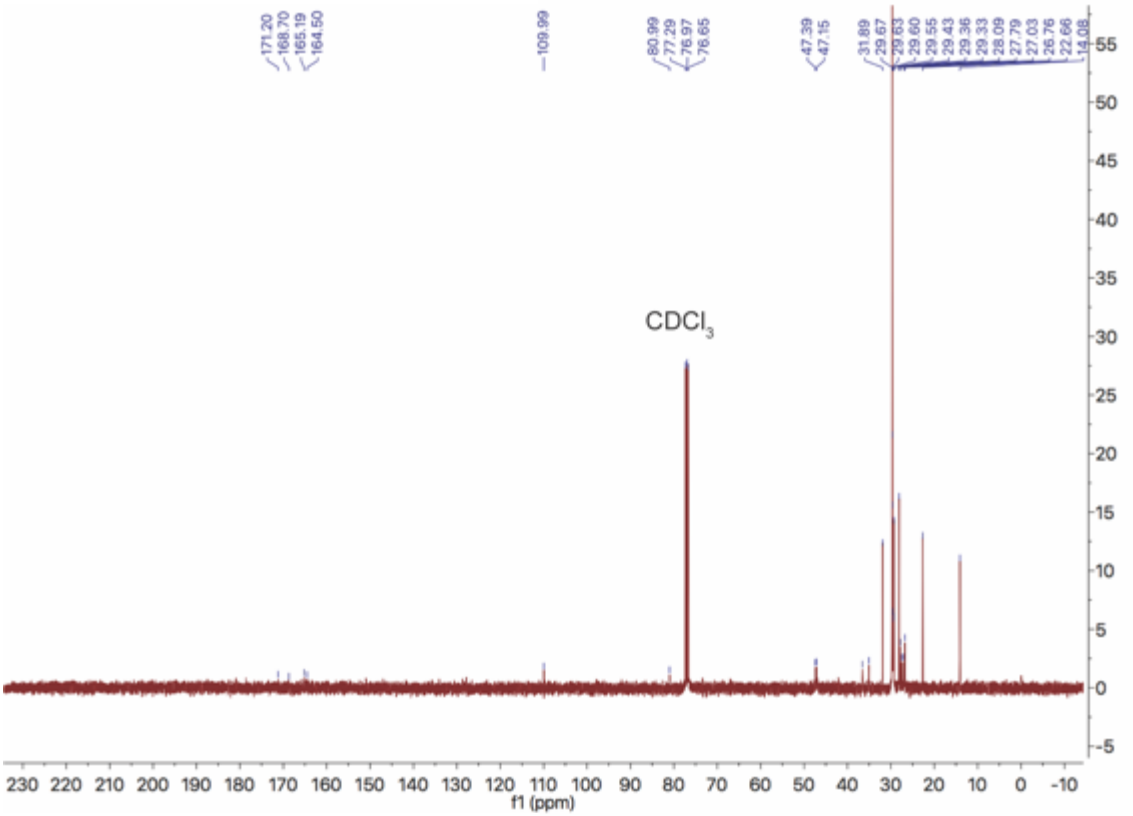

Figure A17 ^{13}C NMR of intermediate G

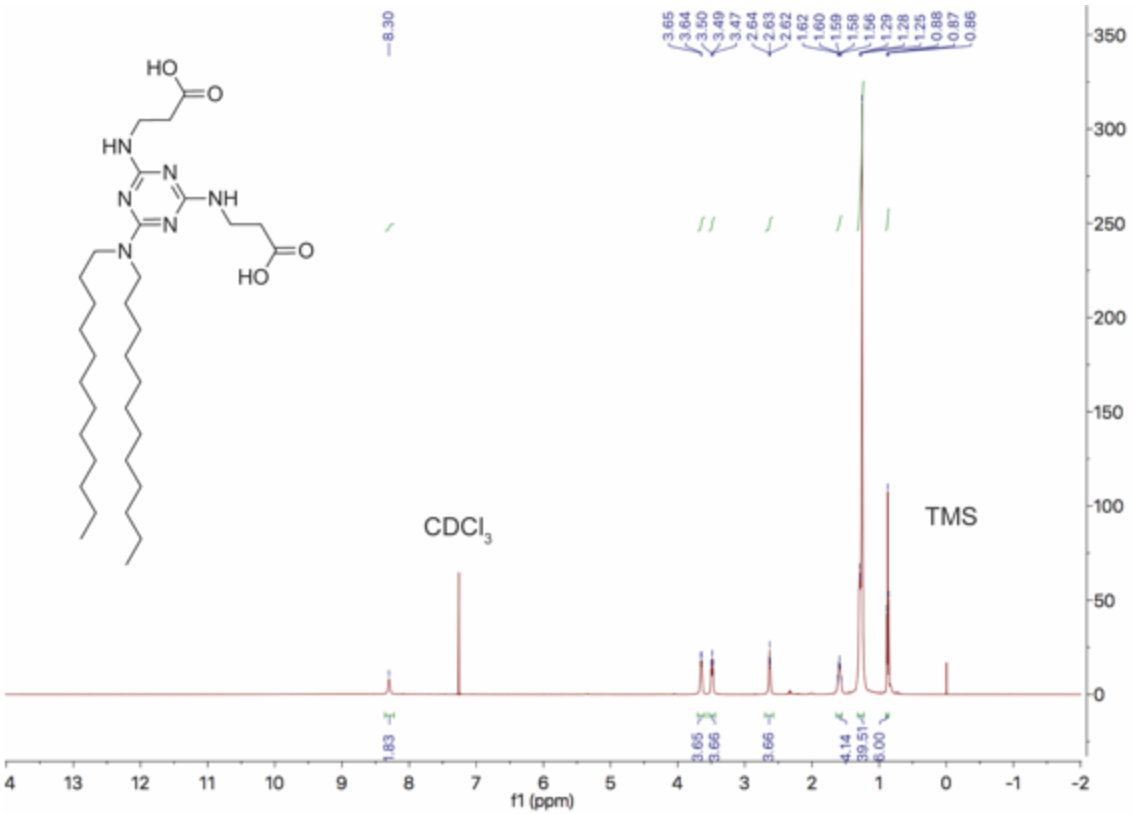

Figure A18 ^{1}H NMR of lipid 1

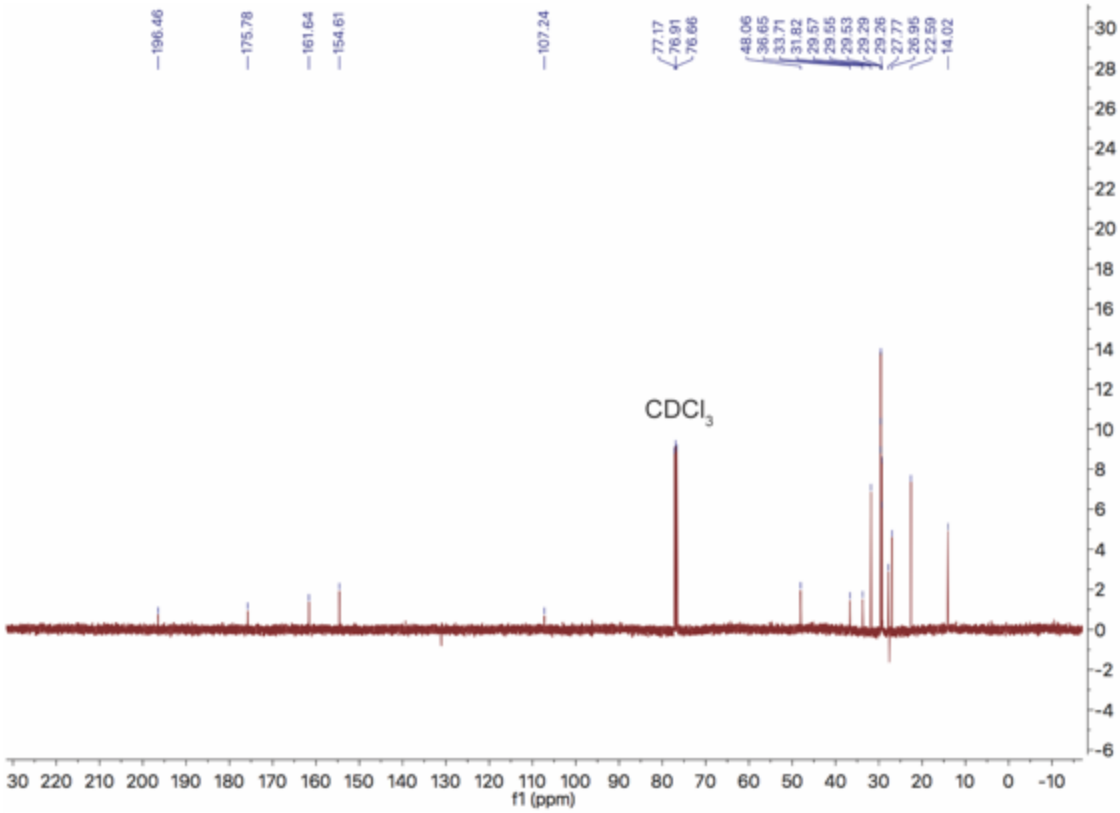

Figure A19 ^{13}C NMR of lipid 1

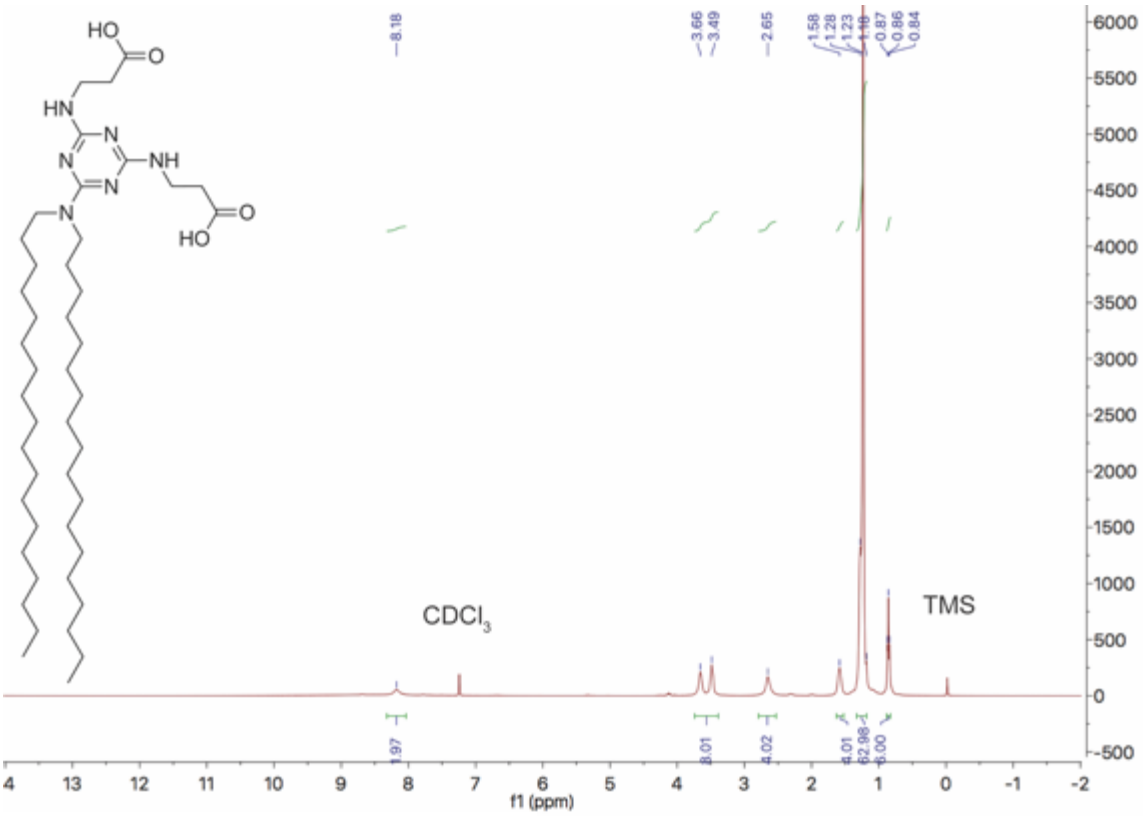

Figure A20 ^{1}H NMR of lipid 2

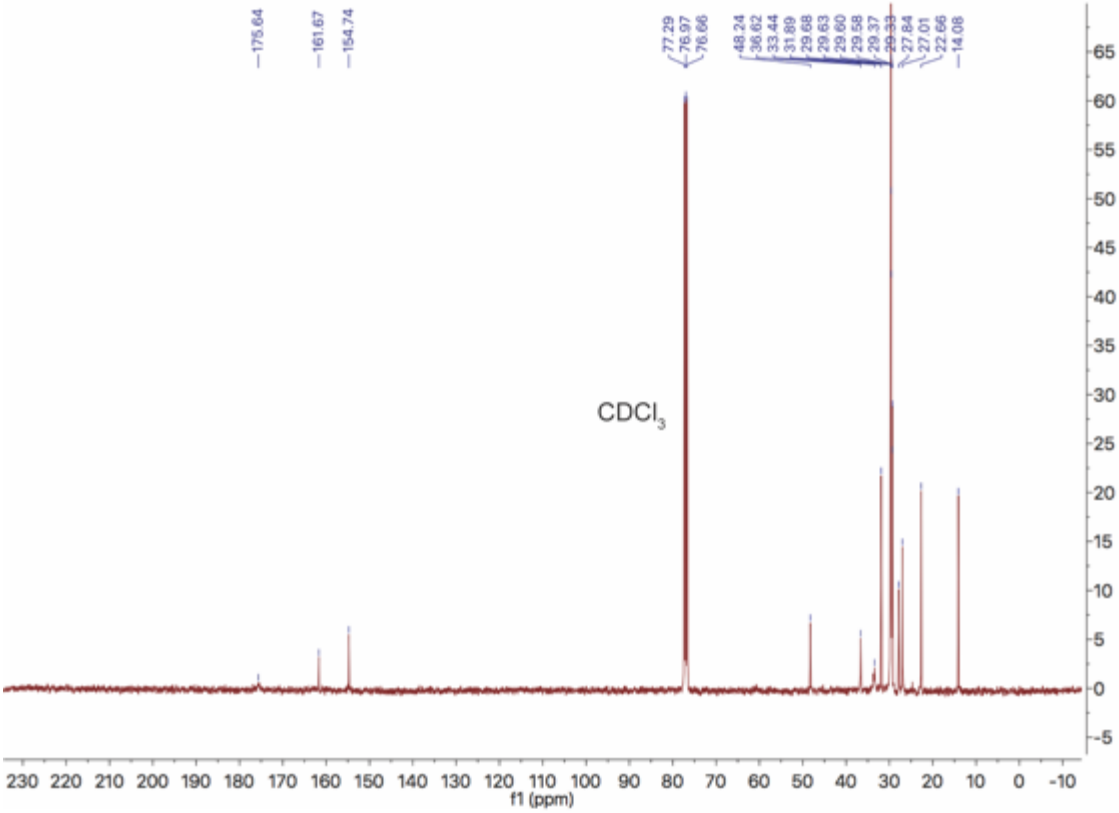

Figure A21 ^{13}C NMR of lipid 2

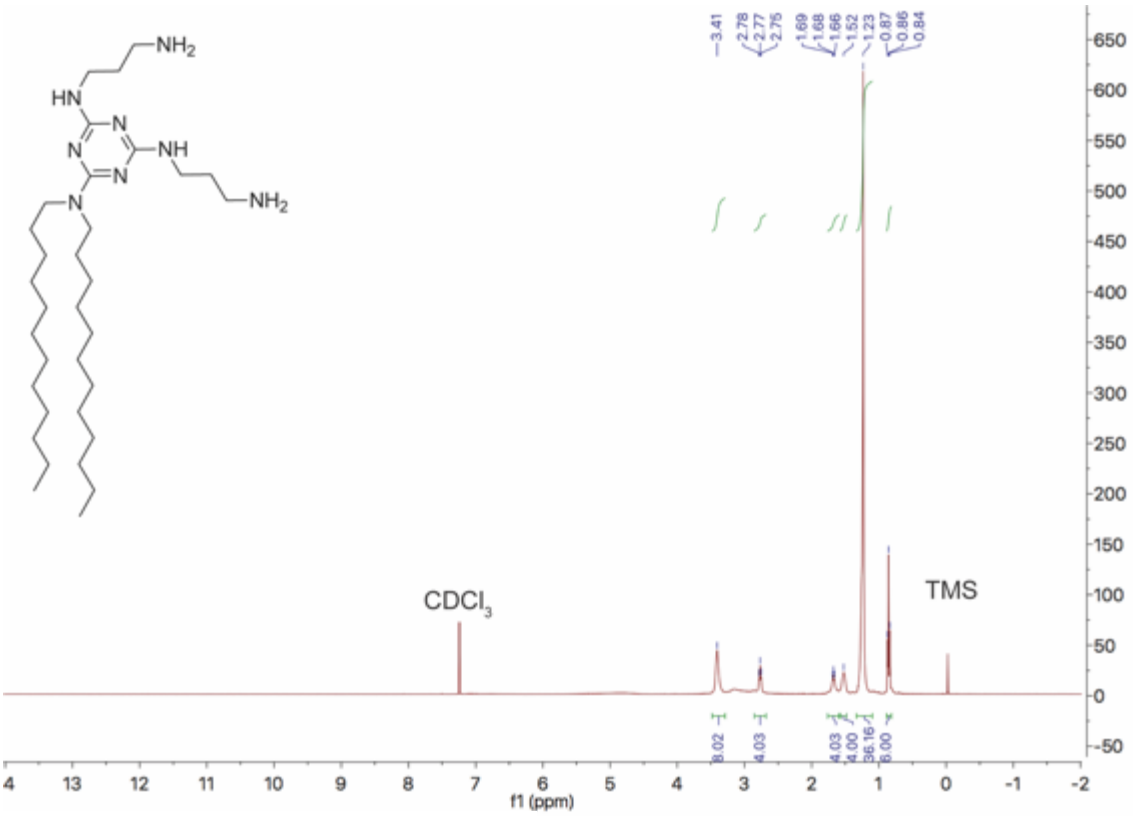

Figure A22 ^{1}H NMR of lipid 3

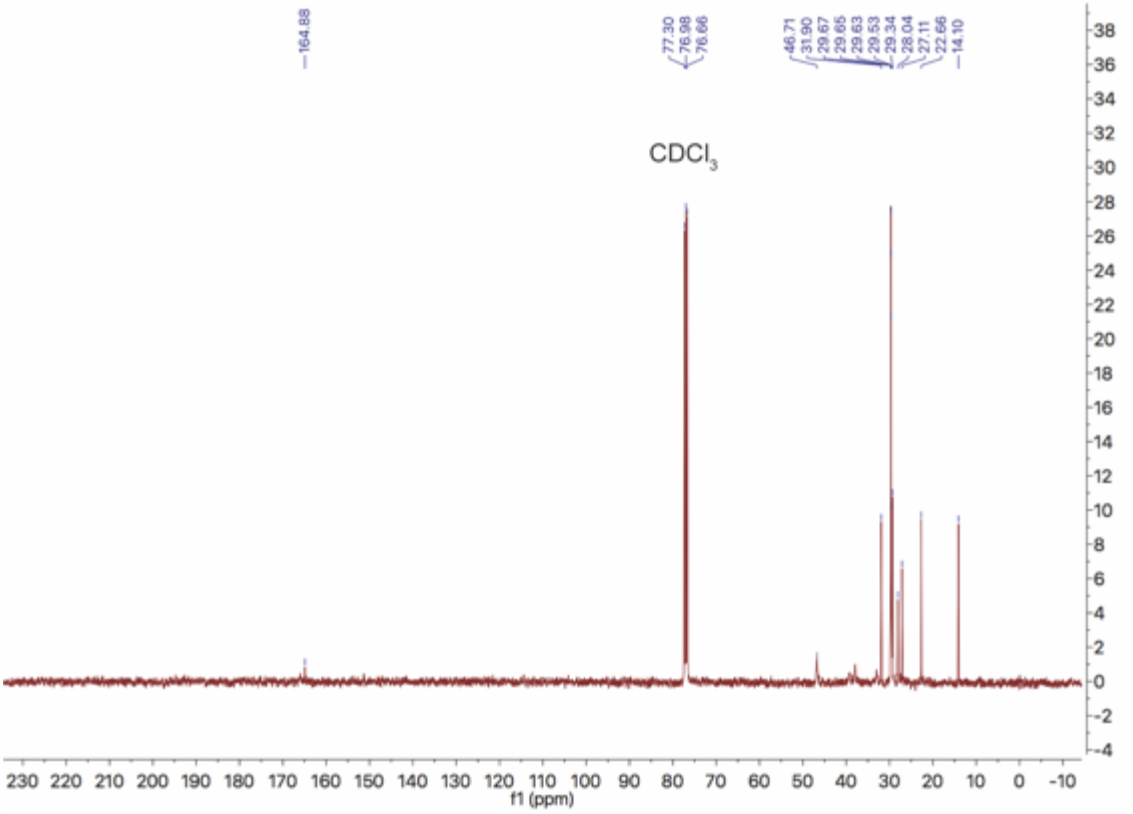

Figure A23 ^{13}C NMR of lipid 3

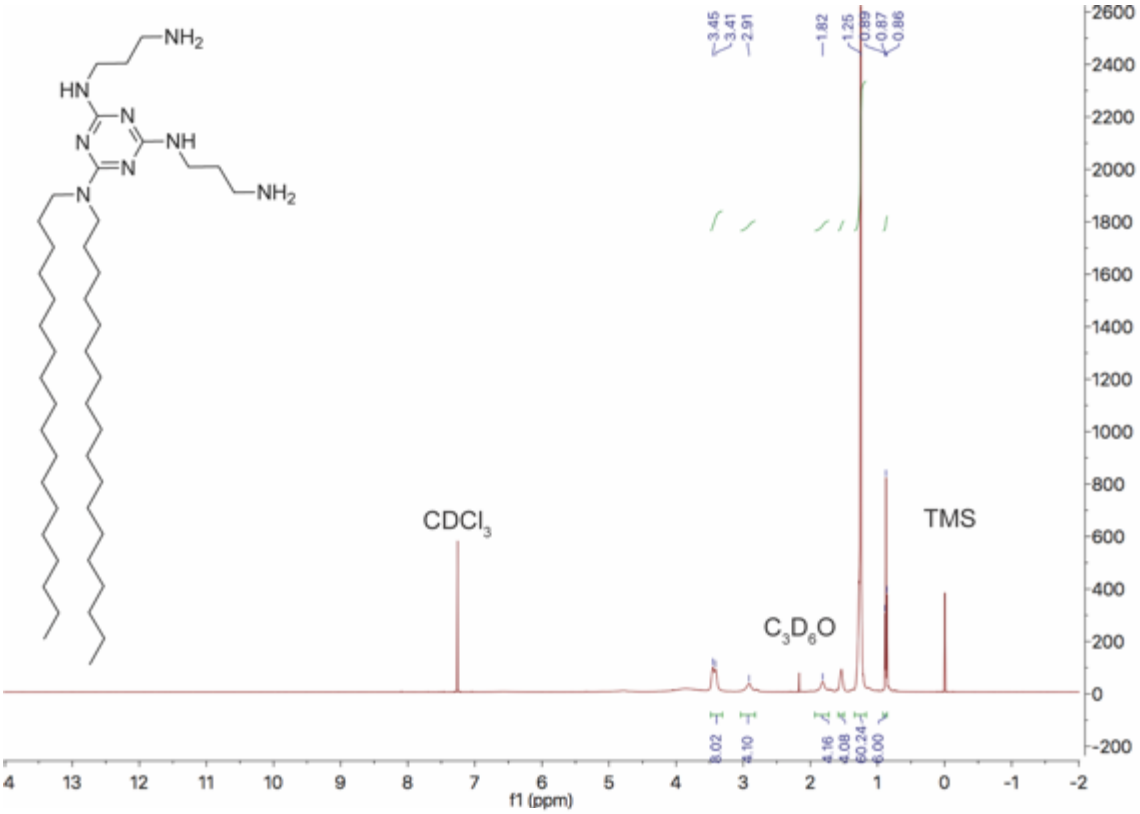

Figure A24 ^{1}H NMR of lipid 4

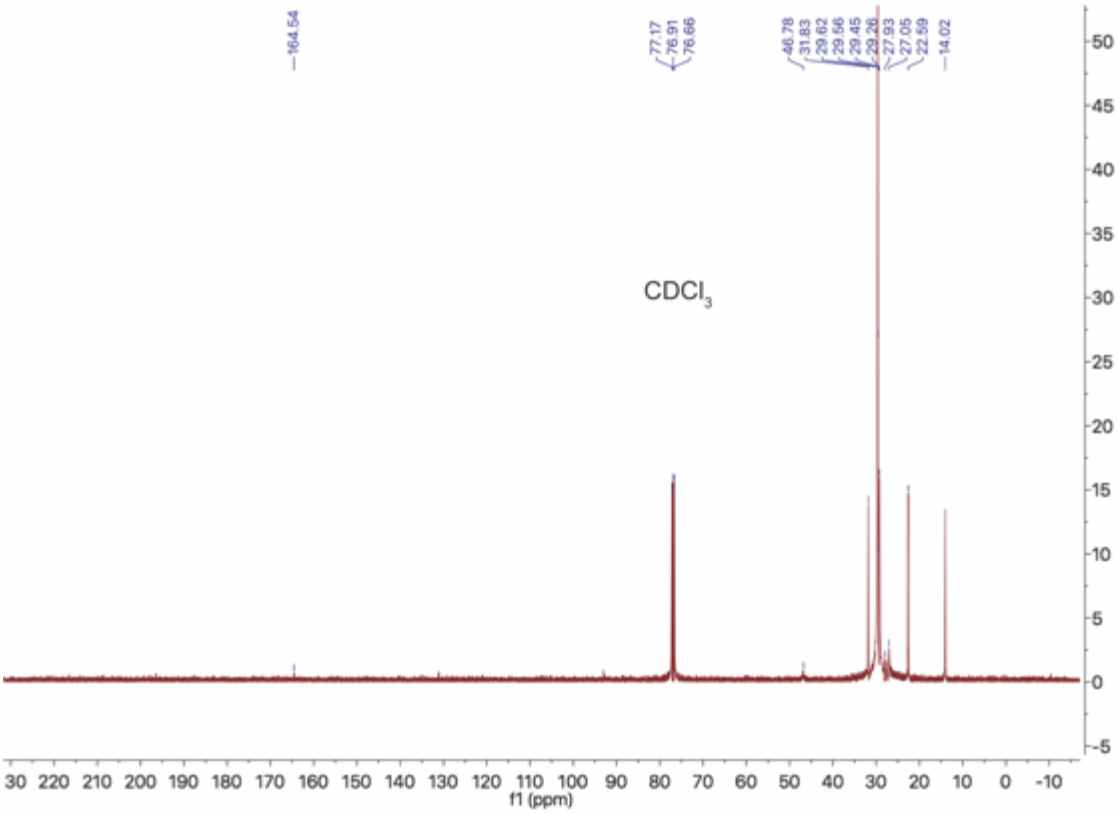

Figure A25 ^{13}C NMR of lipid 4

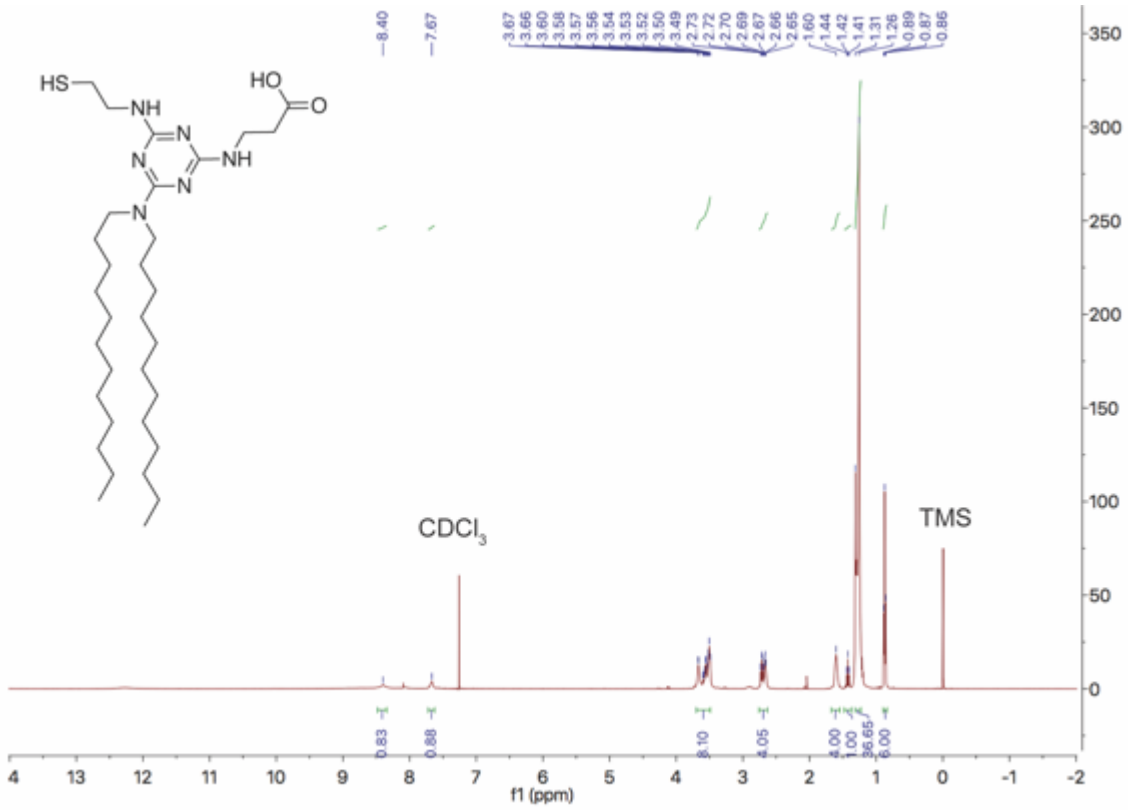

Figure 2.26 ^{1}H NMR of lipid 5

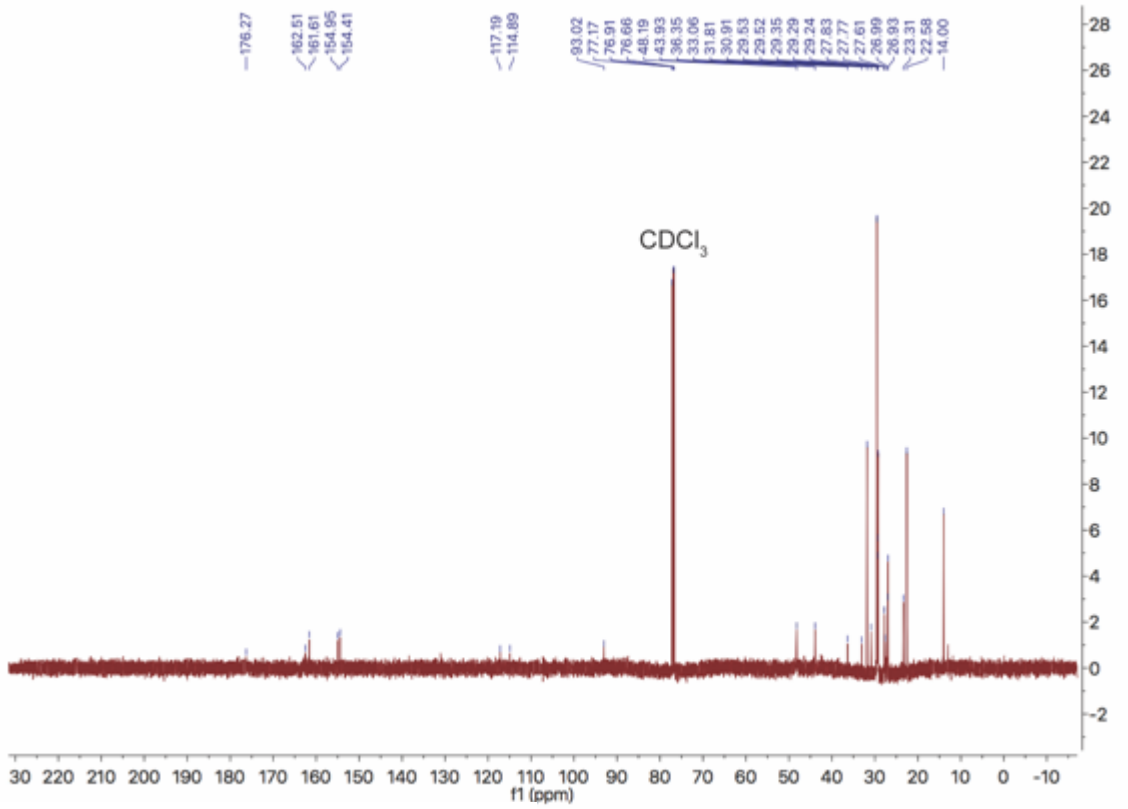

Figure A27 ^{13}C NMR of lipid 5

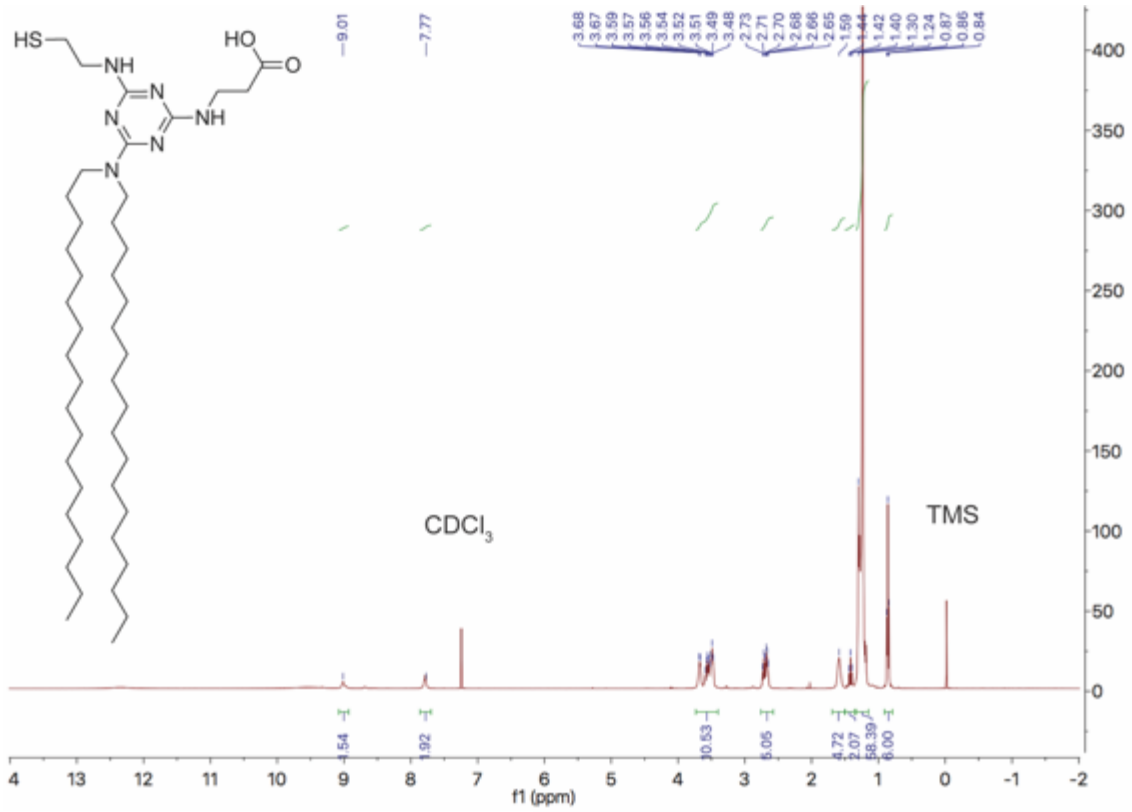

Figure A28 ^{1}H NMR of lipid 6

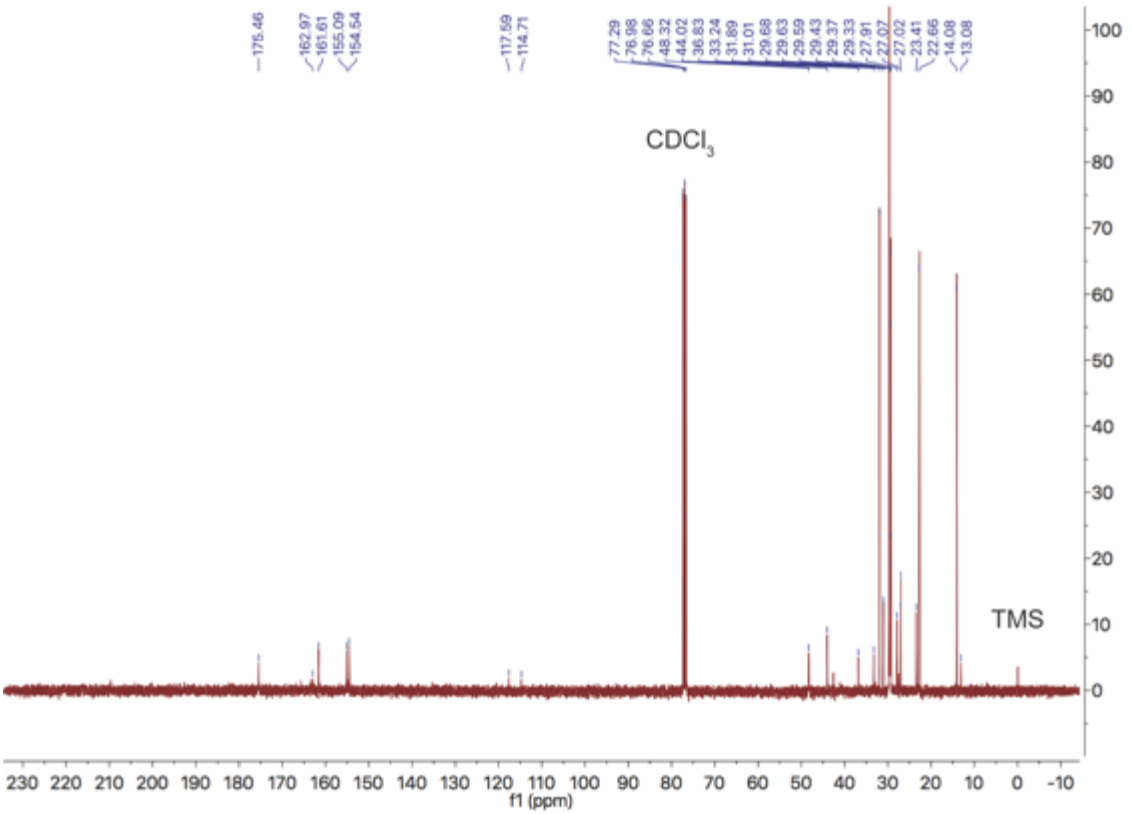

Figure A29 ^{13}C NMR of lipid 6

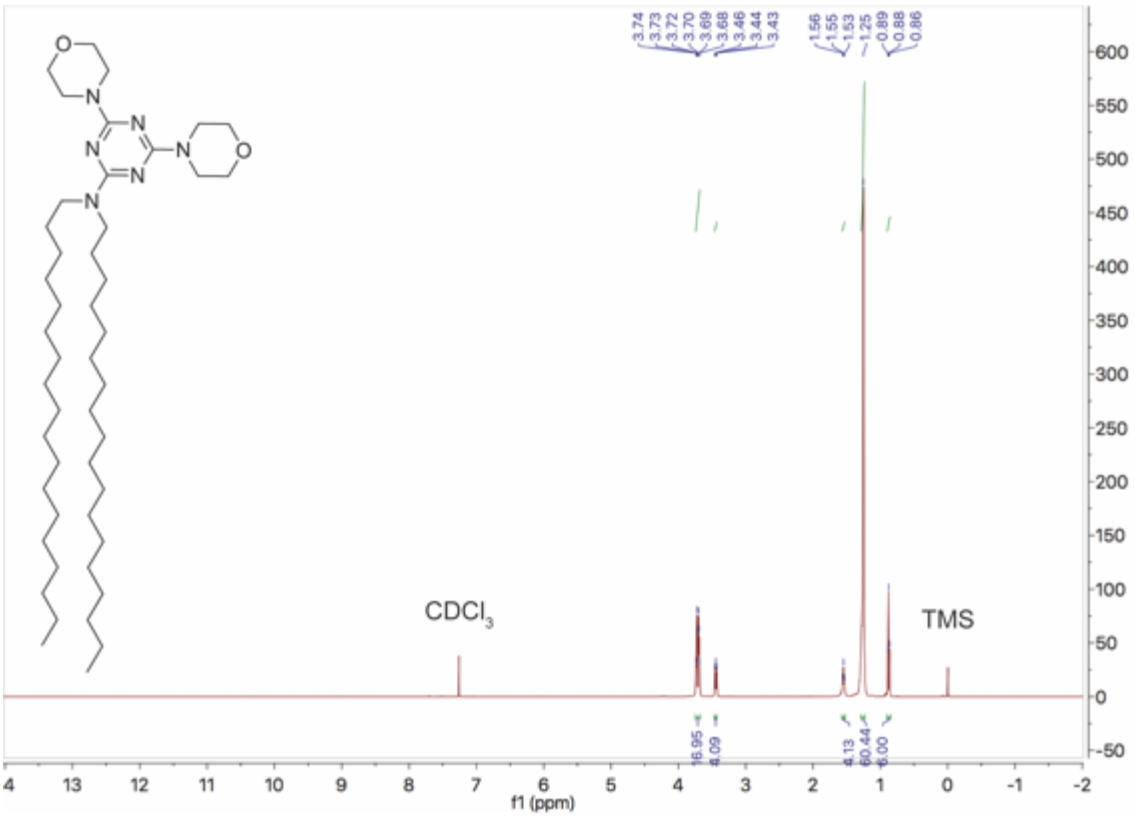

Figure A30 ^{1}H NMR of lipid 7

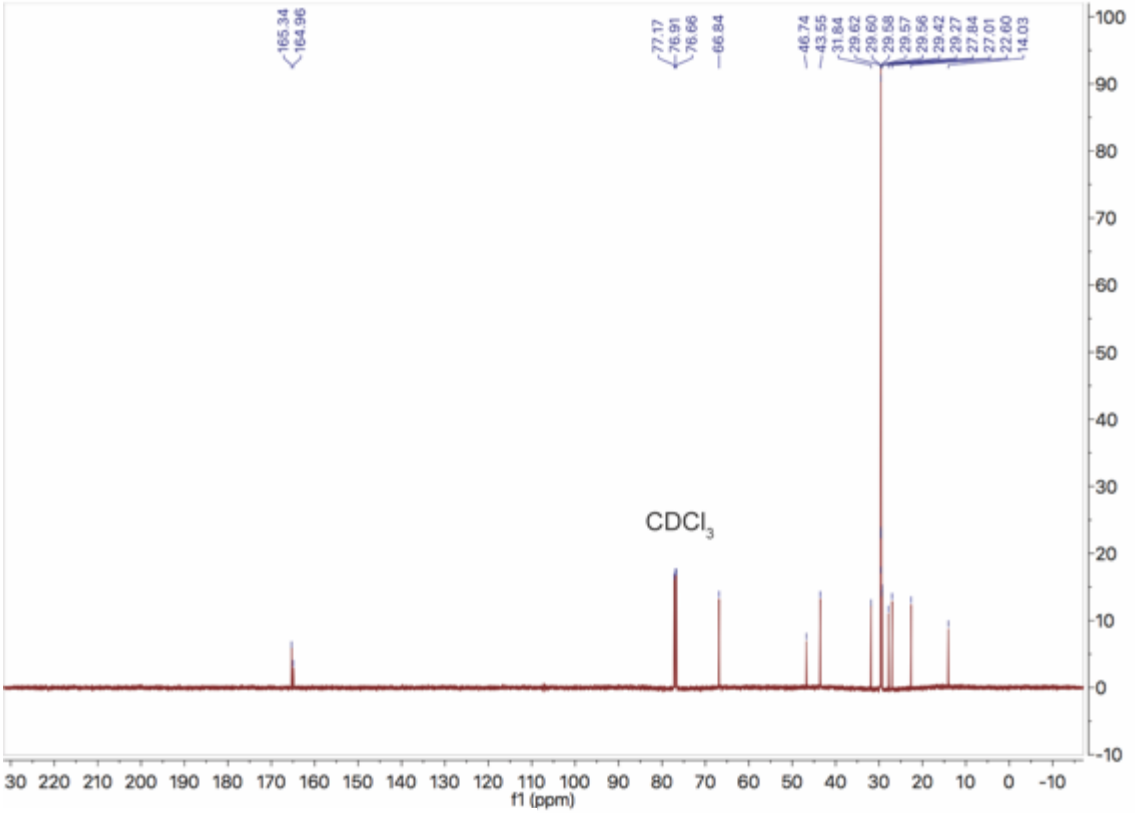

Figure A31 ^{13}C NMR of lipid 7

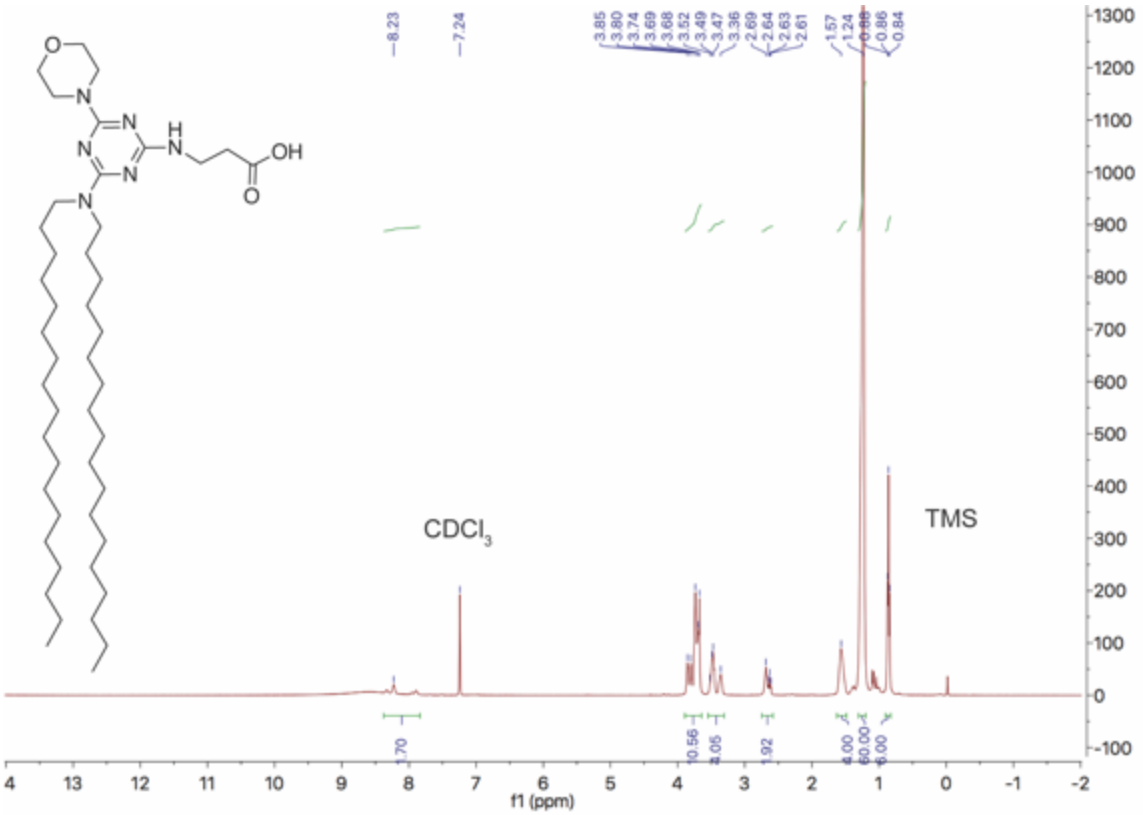

Figure A32 ^{1}H NMR of lipid

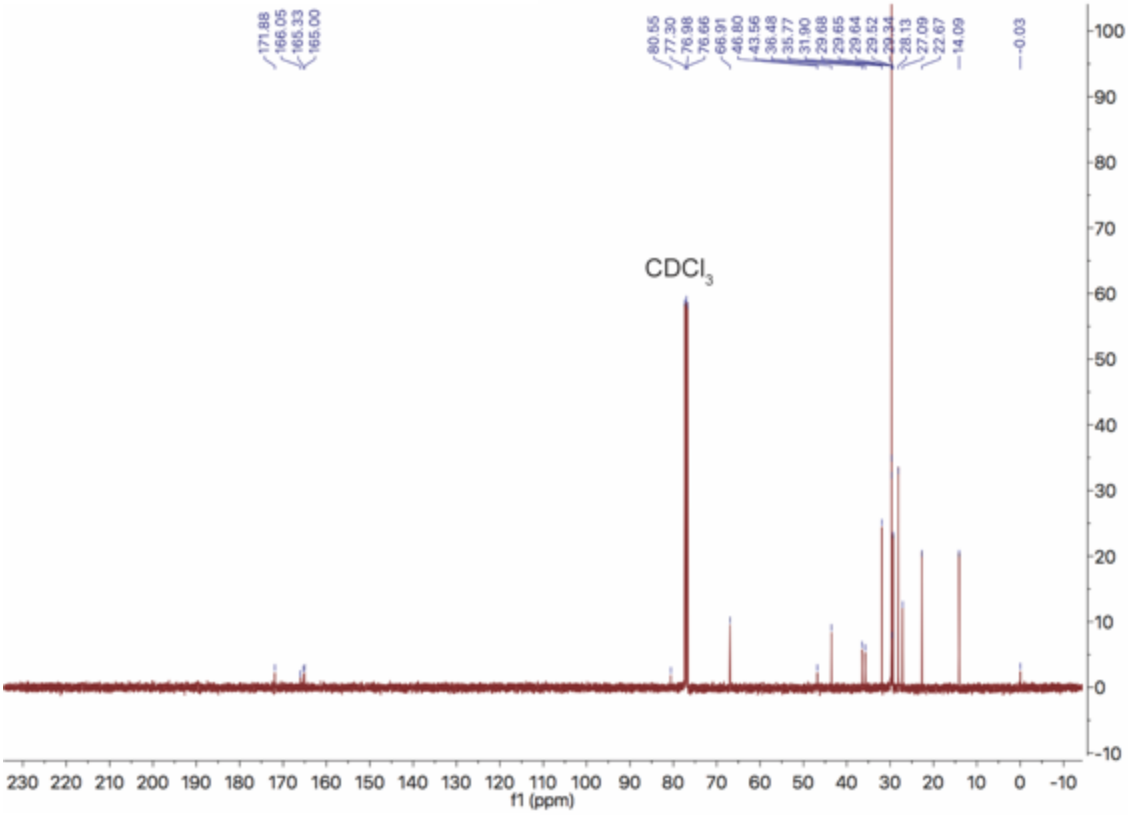

Figure A33 ^{13}C NMR of lipid 8

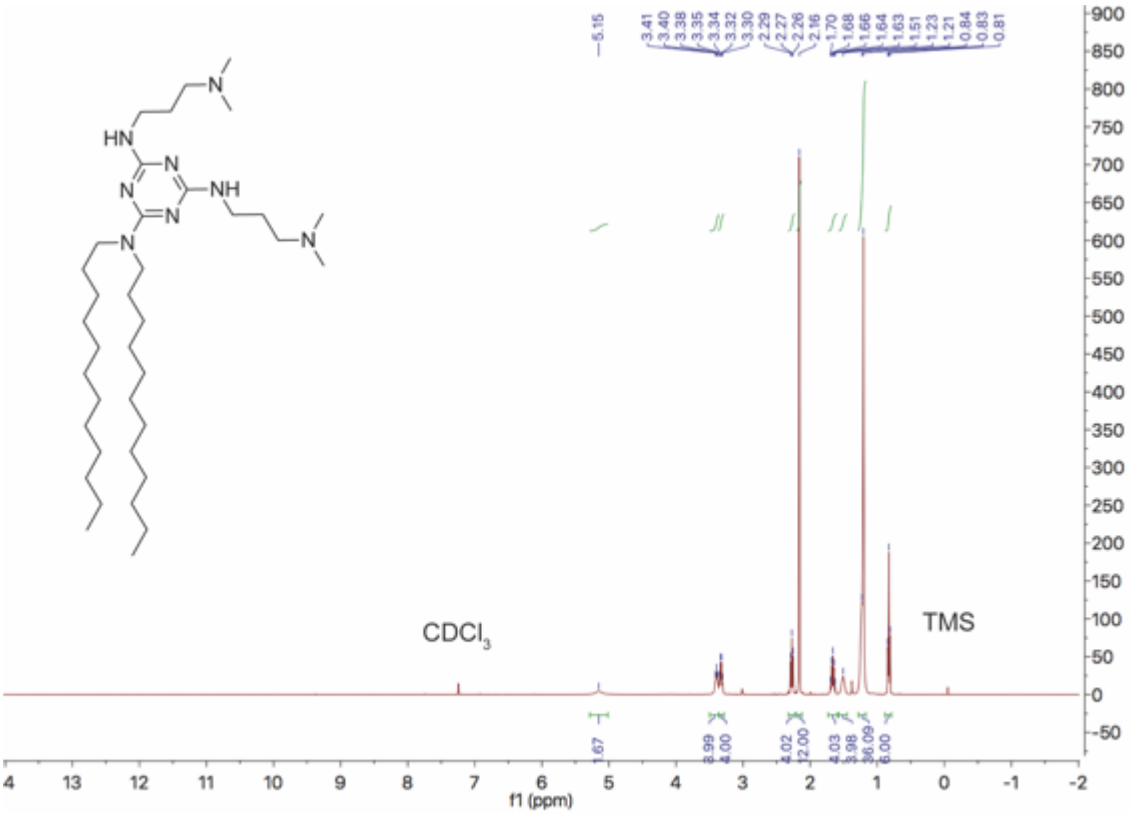

Figure A34 ^{1}H NMR of lipid 9

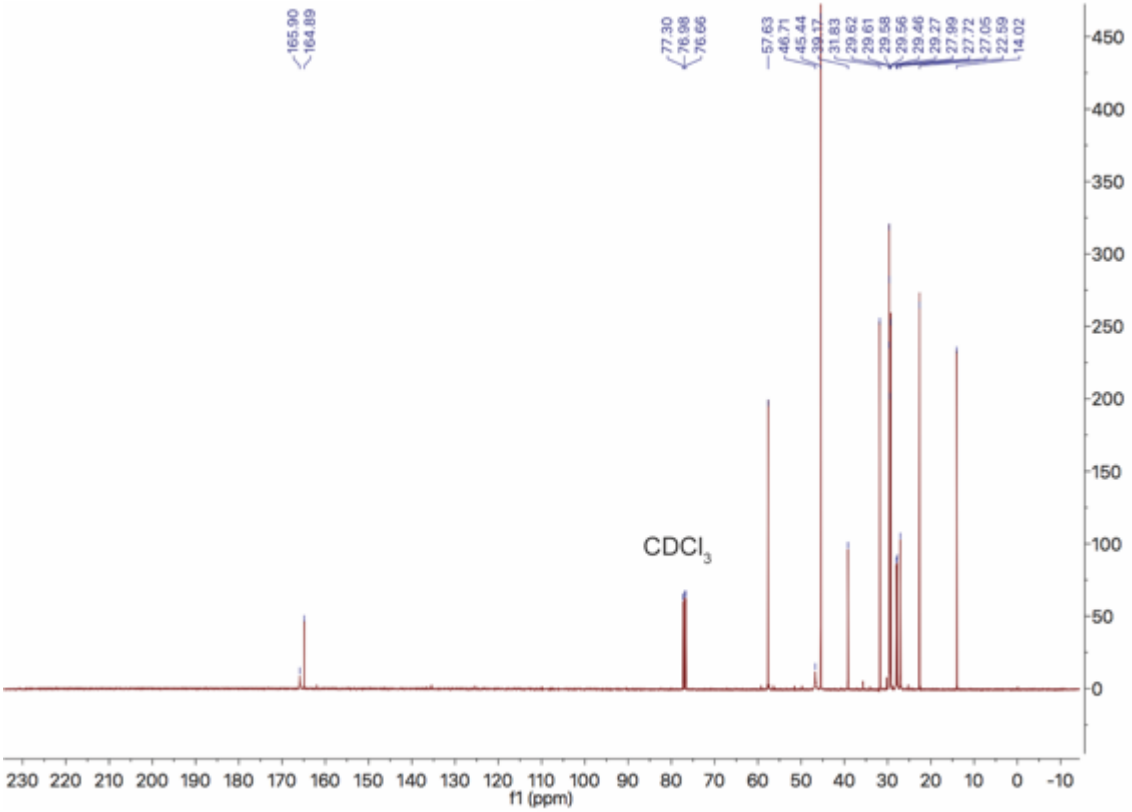

Figure A35 ^{13}C NMR of lipid 9

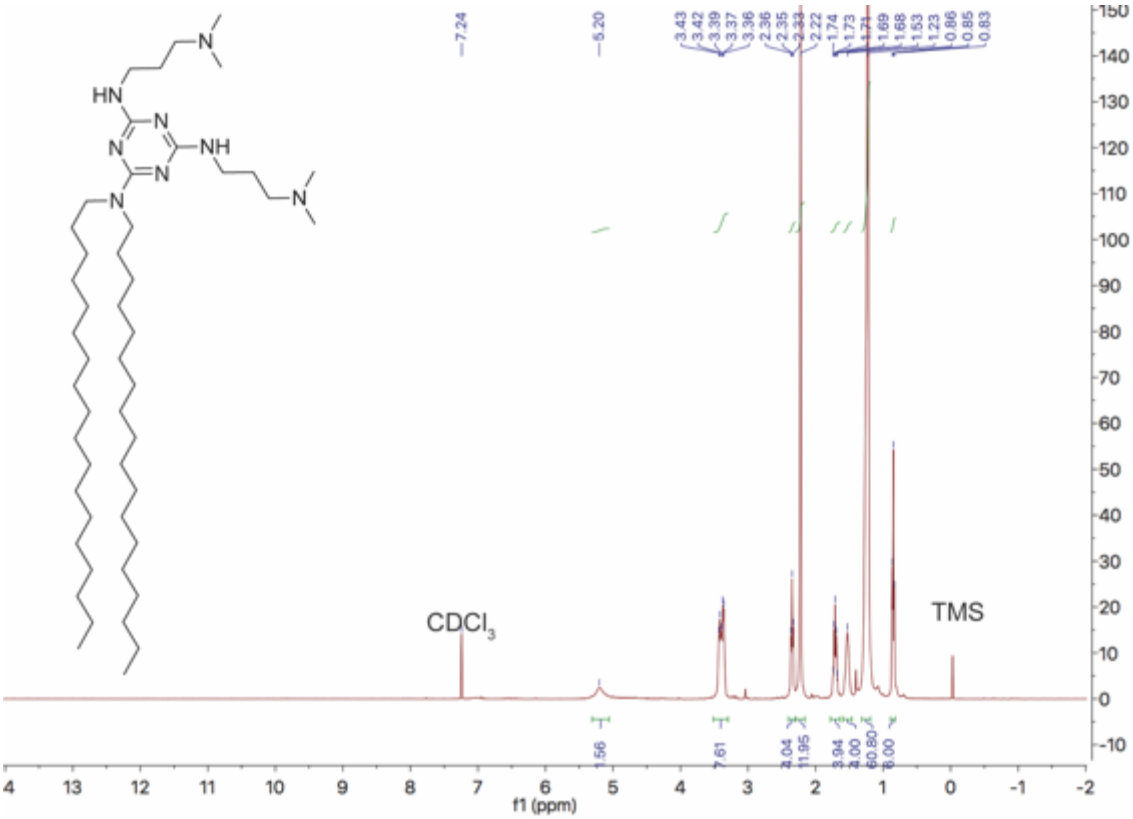

Figure A36 ^{1}H NMR of lipid 10

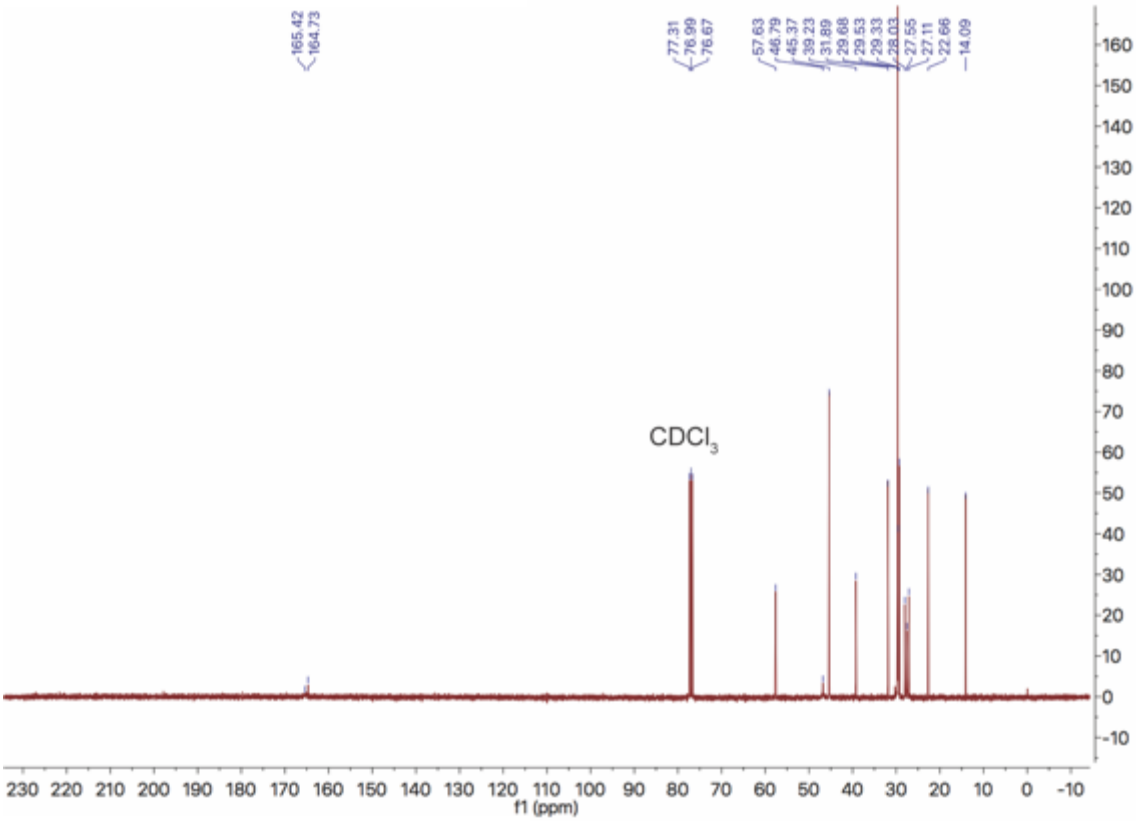

Figure A37 ^{13}C NMR of lipid 10

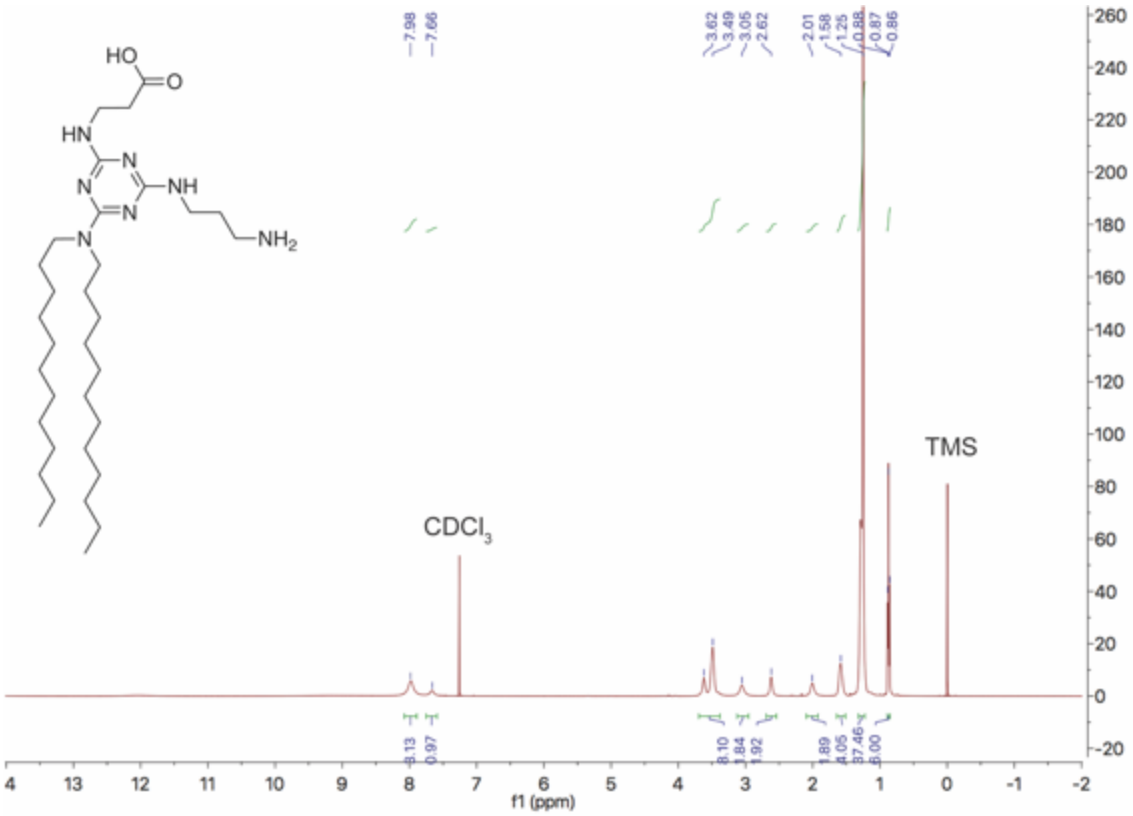

Figure A38 ^{1}H NMR of lipid 11

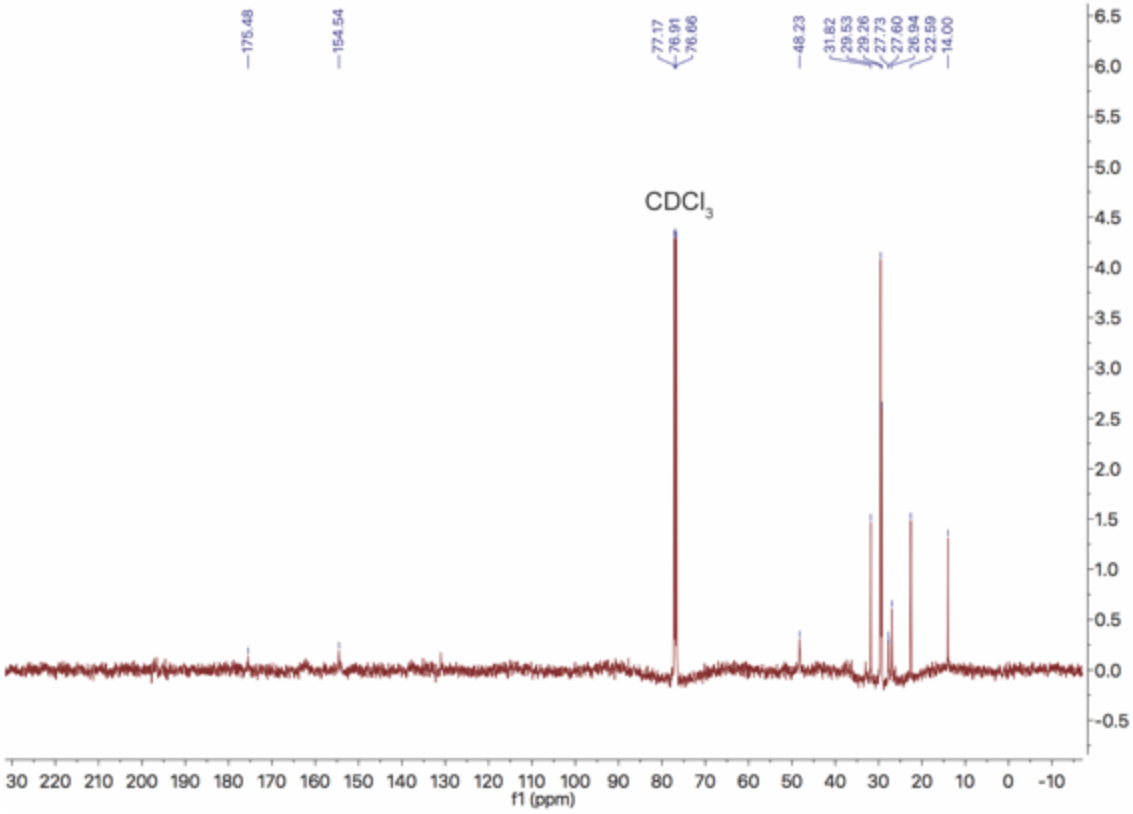

Figure A39 ^{13}C NMR of lipid 11

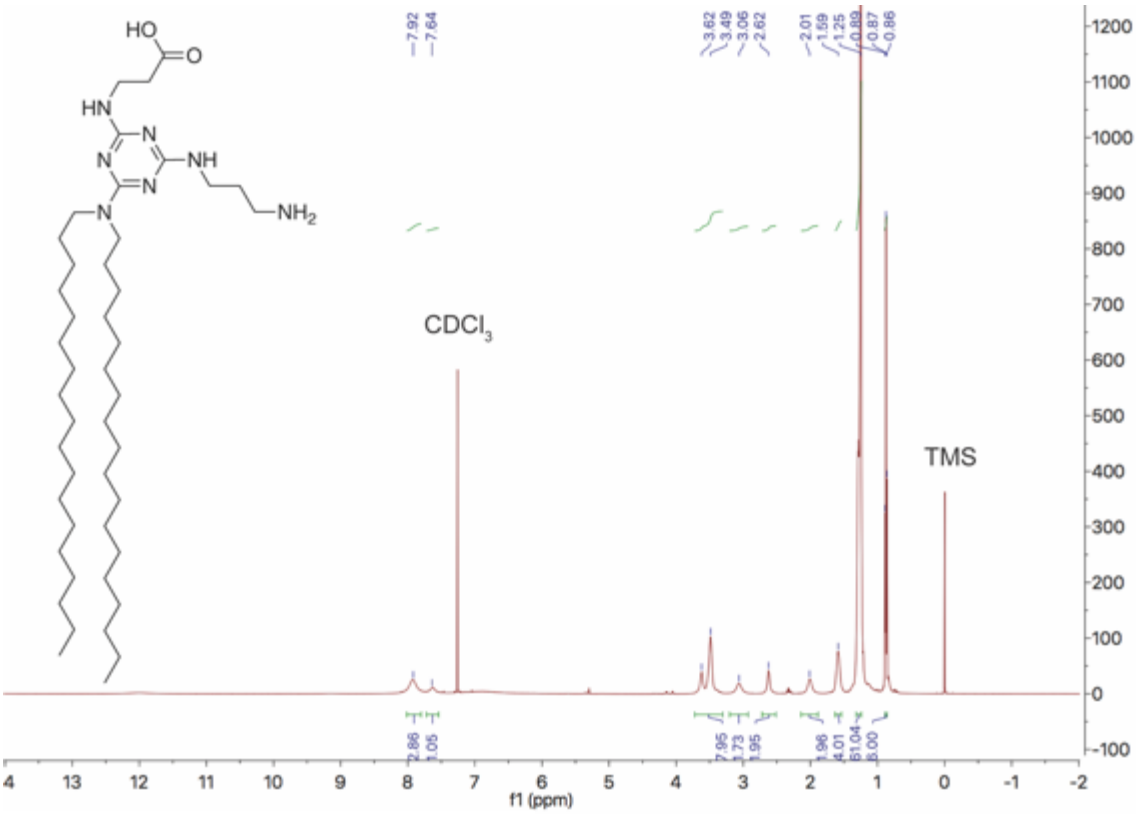

Figure A40 ^{1}H NMR of lipid 12

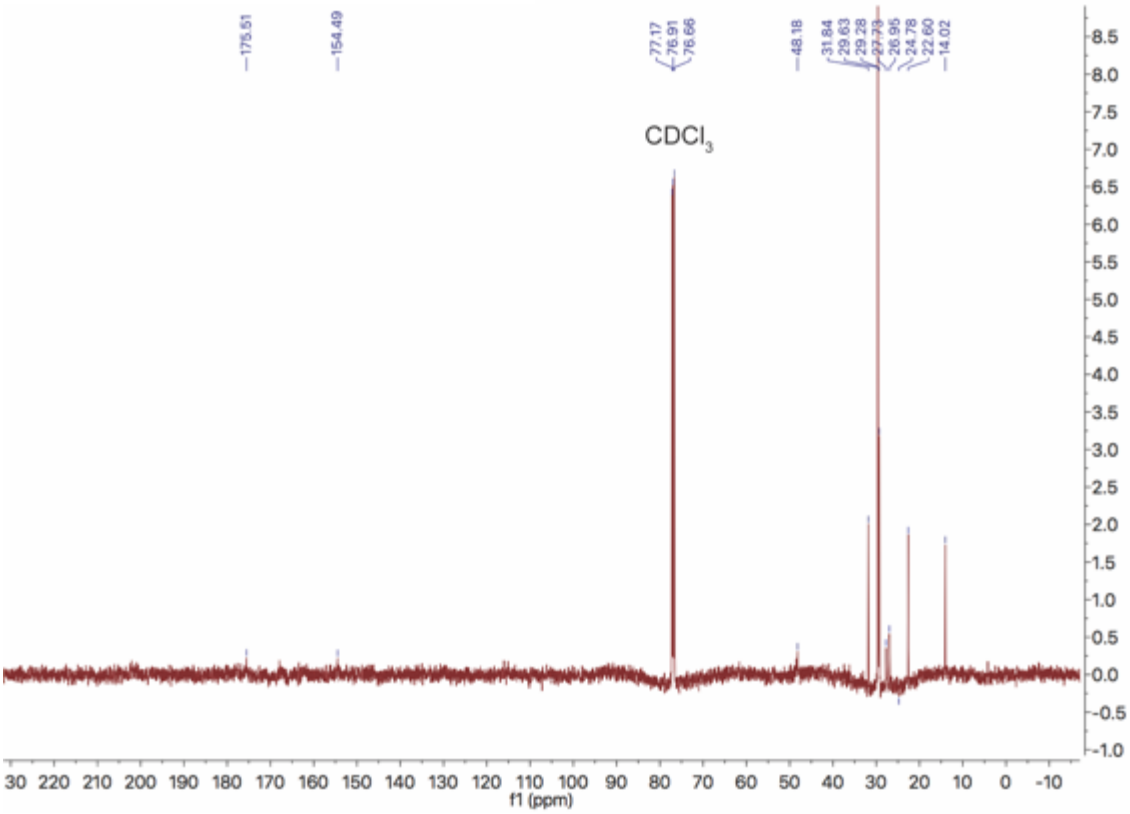

Figure A41 ^{13}C NMR of lipid 12

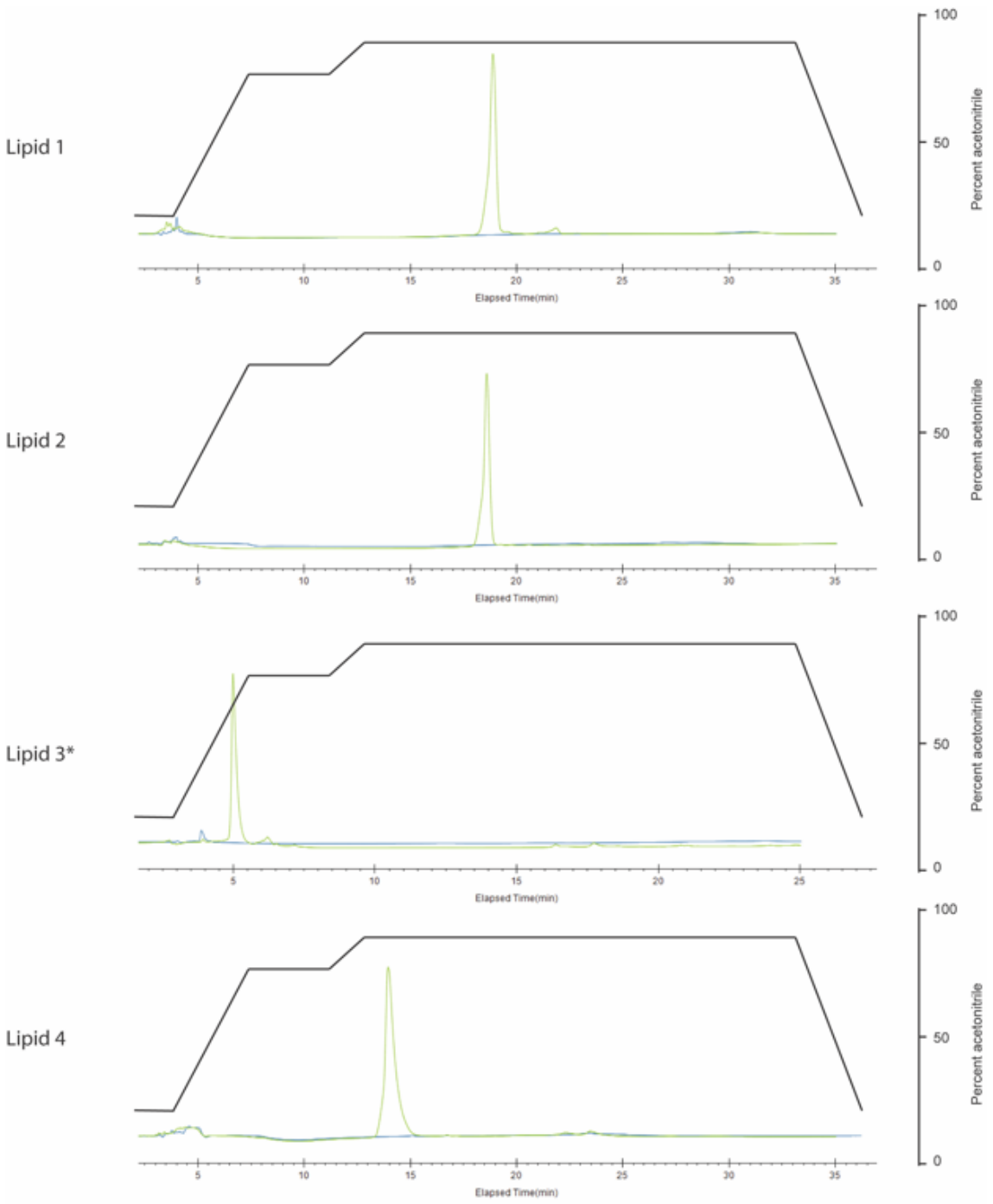

Figure A42 HPLC traces of lipids 1-4 and chloroform (used as solvent), detected at 205 and 254 (254 shown). The mobile phase was a gradient of water and acetonitrile with 0.1% trifluoroacetic acid, as indicated, and constant 5% methanol with 0.1% trifluoroacetic acid. *Shortened due to speed of compound elution.

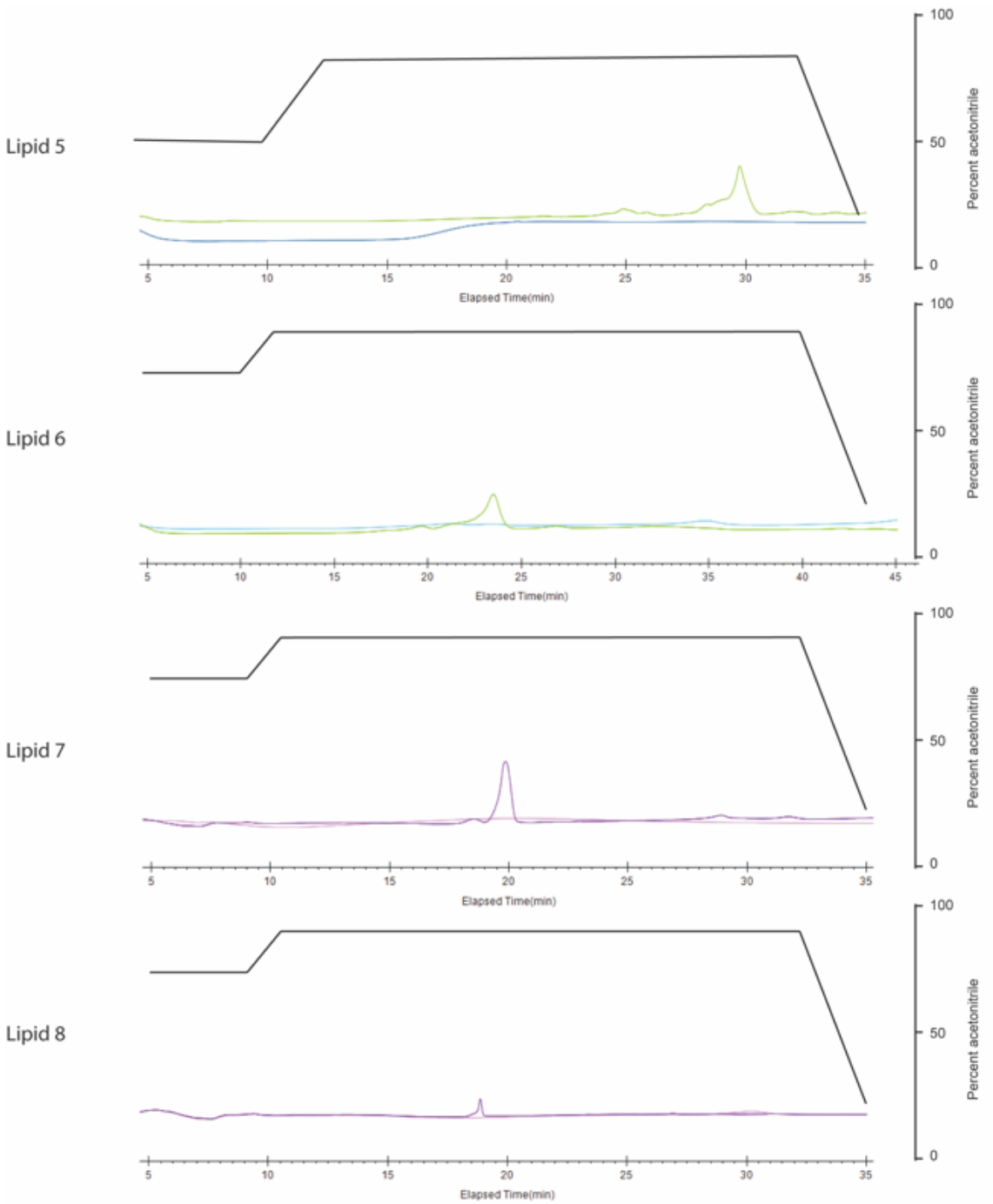

Figure A43 HPLC traces of lipids 5-8 and chloroform (used as solvent), detected at 205 and 254 (254 shown). The mobile phase was a gradient of water and acetonitrile with 0.1% trifluoroacetic acid, as indicated, and constant 5% methanol with 0.1% trifluoroacetic acid. These four compounds needed a mixture of isopropanol and chloroform for proper dissolution for HPLC.

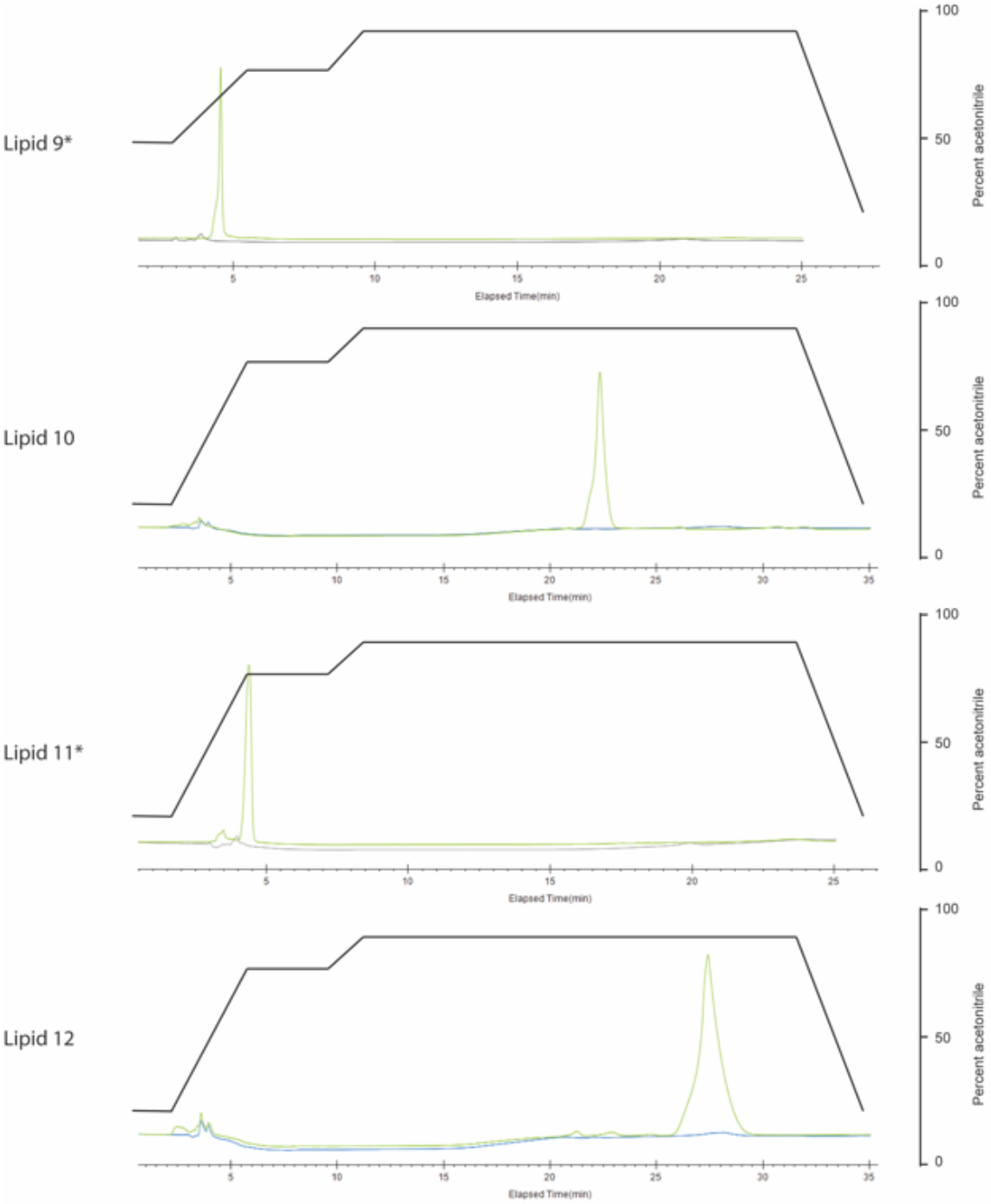

Figure A44 HPLC traces of lipids 9-12 and chloroform (used as solvent), detected at 205 and 254 (254 shown). The mobile phase was a gradient of water and acetonitrile with 0.1% trifluoroacetic acid, as indicated, and constant 5% methanol with 0.1% trifluoroacetic acid. *Shortened due to speed of compound elution.

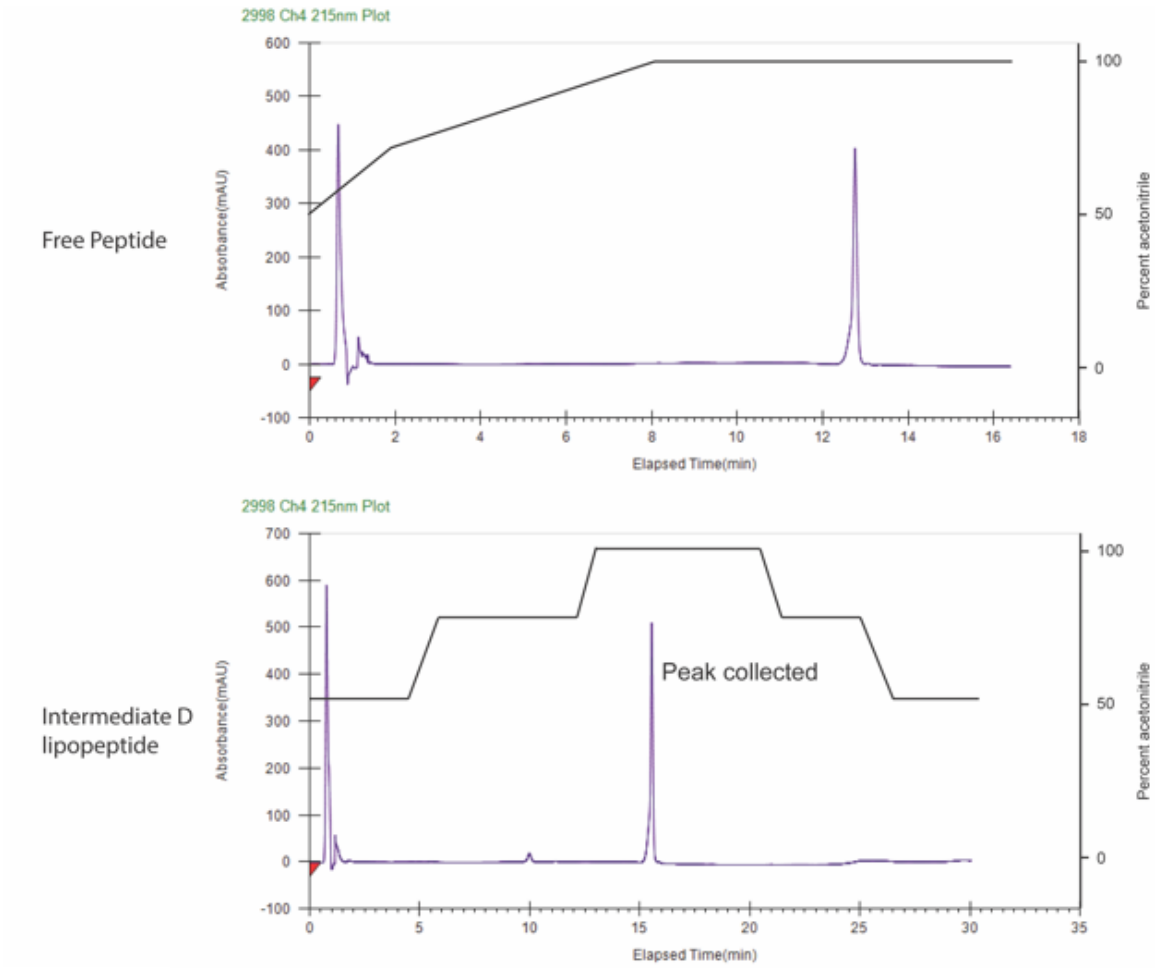

Figure A45 HPLC traces of free apolipoprotein A-I and apolipoprotein A-I lipopeptide

REFERENCES

1. Nardo, D.; Henson, D.; Springer, J. E.; Venditto, V. J., Chapter six - Modulating the immune response with liposomal delivery. In *Nanomaterials for Clinical Applications*, Pippa, N.; Demetzos, C., Eds. Elsevier: 2020; pp 159-211.
2. Li, J.; Wang, X.; Zhang, T.; Wang, C.; Huang, Z.; Luo, X.; Deng, Y., A review on phospholipids and their main applications in drug delivery systems. *Asian Journal of Pharmaceutical Sciences* **2015,** *10* (2), 81-98.
3. Daraee, H.; Etemadi, A.; Kouhi, M.; Alimirzalu, S.; Akbarzadeh, A., Application of liposomes in medicine and drug delivery. *Artificial cells, nanomedicine, and biotechnology* **2016,** *44* (1), 381-91.
4. Bangham, A. D.; Horne, R. W., Negative staining of phospholipids and their structural modification by surface-active agents as observed in the electron microscope. *Journal of Molecular Biology* **1964,** *8* (5), 660-IN10.
5. Bangham, A. D.; Hill, M. W.; Miller, N. G. A., Preparation and Use of Liposomes as Models of Biological Membranes. In *Methods in Membrane Biology: Volume 1*, Korn, E. D., Ed. Springer US: Boston, MA, 1974; pp 1-68.
6. Torchilin, V.; Weissig, V., *Liposomes : a practical approach*. 2nd ed. / ed.; Oxford ; New York : Oxford University Press: 2003.
7. Cullis, P. R.; Hope, M. J., Lipid Nanoparticle Systems for Enabling Gene Therapies. *Molecular Therapy* **2017,** *25* (7), 1467-1475.
8. Watson, D. S.; Endsley, A. N.; Huang, L., Design considerations for liposomal vaccines: influence of formulation parameters on antibody and cell-mediated immune responses to liposome associated antigens. *Vaccine* **2012,** *30* (13), 2256-2272.
9. Marasini, N.; Ghaffar, K. A.; Skwarczynski, M.; Toth, I., Chapter Twelve - Liposomes as a Vaccine Delivery System. In *Micro and Nanotechnology in Vaccine Development*, Skwarczynski, M.; Toth, I., Eds. William Andrew Publishing: 2017; pp 221-239.
10. Christensen, D.; Korsholm, K. S.; Andersen, P.; Agger, E. M., Cationic liposomes as vaccine adjuvants. *Expert Review of Vaccines* **2011,** *10* (4), 513-521.
11. Watson, D. S.; Endsley, A. N.; Huang, L., Design considerations for liposomal vaccines: influence of formulation parameters on antibody and cell-mediated immune responses to liposome associated antigens. *Vaccine* **2012,** *30* (13), 2256-72.
12. Alving, C. R.; Beck, Z.; Karasavva, N.; Matyas, G. R.; Rao, M., HIV-1, lipid rafts, and antibodies to liposomes: implications for anti-viral-neutralizing antibodies. *Molecular membrane biology* **2006,** *23* (6), 453-65.
13. Ferguson, S. W.; Nguyen, J., Exosomes as therapeutics: The implications of molecular composition and exosomal heterogeneity. *Journal of controlled release : official journal of the Controlled Release Society* **2016,** *228*, 179-190.
14. Nisini, R.; Poerio, N.; Mariotti, S.; De Santis, F.; Fraziano, M., The Multirole of Liposomes in Therapy and Prevention of Infectious Diseases. *Front Immunol* **2018,** *9*, 155.
15. Kohli, A. G.; Kierstead, P. H.; Venditto, V. J.; Walsh, C. L.; Szoka, F. C., Designer lipids for drug delivery: from heads to tails. *Journal of controlled release : official journal of the Controlled Release Society* **2014,** *190*, 274-87.
16. Murphy, K.; Weaver, C., *Janeway's Immunobiology, 9th edition*. CRC Press: 2016.

17. Karumanchi, D. K.; Skrypai, Y.; Thomas, A.; Gaillard, E. R., Rational design of liposomes for sustained release drug delivery of bevacizumab to treat ocular angiogenesis. *Journal of Drug Delivery Science and Technology* **2018,** *47*, 275-282.
18. Subramanian, N.; Atsmon-Raz, Y.; Tieleman, P. D., Characterization of the Physiochemical Interactions between LNPs and the Endosomal Lipids: A Rational Design of Gene Delivery Systems. *Biophysical Journal* **2017,** *112* (3), 43a.
19. Semple, S. C.; Akinc, A.; Chen, J.; Sandhu, A. P.; Mui, B. L.; Cho, C. K.; Sah, D. W. Y.; Stebbing, D.; Crosley, E. J.; Yaworski, E.; Hafez, I. M.; Dorkin, J. R.; Qin, J.; Lam, K.; Rajeev, K. G.; Wong, K. F.; Jeffs, L. B.; Nechev, L.; Eisenhardt, M. L.; Jayaraman, M.; Kazem, M.; Maier, M. A.; Srinivasulu, M.; Weinstein, M. J.; Chen, Q.; Alvarez, R.; Barros, S. A.; De, S.; Klimuk, S. K.; Borland, T.; Kosovrasti, V.; Cantley, W. L.; Tam, Y. K.; Manoharan, M.; Ciufolini, M. A.; Tracy, M. A.; de Fougerolles, A.; MacLachlan, I.; Cullis, P. R.; Madden, T. D.; Hope, M. J., Rational design of cationic lipids for siRNA delivery. *Nature Biotechnology* **2010,** *28*, 172.
20. Gause, K. T.; Wheatley, A. K.; Cui, J.; Yan, Y.; Kent, S. J.; Caruso, F., Immunological Principles Guiding the Rational Design of Particles for Vaccine Delivery. *ACS Nano* **2017,** *11* (1), 54-68.
21. Tazina, E.; Kostin, K.; Oborotova, N., Specific features of drug encapsulation in liposomes (A review). *Pharmaceutical Chemistry Journal* **2011,** *45* (8), 481-490.
22. Ventola, C. L., Progress in Nanomedicine: Approved and Investigational Nanodrugs. *Pharmacy and Therapeutics* **2017,** *42* (12), 742-755.
23. Song, G.; Wu, H.; Yoshino, K.; Zamboni, W. C., Factors affecting the pharmacokinetics and pharmacodynamics of liposomal drugs. *Journal of Liposome Research* **2012,** *22* (3), 177-192.
24. Bulbake, U.; Doppalapudi, S.; Kommineni, N.; Khan, W., Liposomal Formulations in Clinical Use: An Updated Review. *Pharmaceutics* **2017,** *9* (2).
25. Barenholz, Y., Doxil(R)--the first FDA-approved nano-drug: lessons learned. *Journal of controlled release : official journal of the Controlled Release Society* **2012,** *160* (2), 117-34.
26. Gabizon, A.; Catane, R.; Uziely, B.; Kaufman, B.; Safra, T.; Cohen, R.; Martin, F.; Huang, A.; Barenholz, Y., Prolonged Circulation Time and Enhanced Accumulation in Malignant Exudates of Doxorubicin Encapsulated in Polyethylene-glycol Coated Liposomes. *Cancer research* **1994,** *54* (4), 987-992.
27. Northfelt, D. W.; Martin, F. J.; Working, P.; Volberding, P. A.; Russell, J.; Newman, M.; Amantea, M. A.; Kaplan, L. D., Doxorubicin encapsulated in liposomes containing surface-bound polyethylene glycol: pharmacokinetics, tumor localization, and safety in patients with AIDS-related Kaposi's sarcoma. *Journal of clinical pharmacology* **1996,** *36* (1), 55-63.
28. Northfelt, D. W.; Dezube, B. J.; Thommes, J. A.; Miller, B. J.; Fischl, M. A.; Friedman-Kien, A.; Kaplan, L. D.; Du Mond, C.; Mamelok, R. D.; Henry, D. H., Pegylated-liposomal doxorubicin versus doxorubicin, bleomycin, and vincristine in the treatment of AIDS-related Kaposi's sarcoma: results of a randomized phase III clinical trial. *Journal of Clinical Oncology* **1998,** *16* (7), 2445-2451.
29. Kierstead, P. H.; Okochi, H.; Venditto, V. J.; Chuong, T. C.; Kivimae, S.; Frechet, J. M. J.; Szoka, F. C., The effect of polymer backbone chemistry on the induction

of the accelerated blood clearance in polymer modified liposomes. *Journal of controlled release : official journal of the Controlled Release Society* **2015,** *213,* 1-9.
30. Dams, E. T. M.; Laverman, P.; Oyen, W. J. G.; Storm, G.; Scherphof, G. L.; van der Meer, J. W. M.; Corstens, F. H. M.; Boerman, O. C., Accelerated Blood Clearance and Altered Biodistribution of Repeated Injections of Sterically Stabilized Liposomes. *Journal of Pharmacology and Experimental Therapeutics* **2000,** *292* (3), 1071.
31. Ishida, T.; Atobe, K.; Wang, X.; Kiwada, H., Accelerated blood clearance of PEGylated liposomes upon repeated injections: effect of doxorubicin-encapsulation and high-dose first injection. *Journal of controlled release : official journal of the Controlled Release Society* **2006,** *115* (3), 251-8.
32. Besin, G.; Milton, J.; Sabnis, S.; Howell, R.; Mihai, C.; Burke, K.; Benenato, K. E.; Stanton, M.; Smith, P.; Senn, J.; Hoge, S., Accelerated Blood Clearance of Lipid Nanoparticles Entails a Biphasic Humoral Response of B-1 Followed by B-2 Lymphocytes to Distinct Antigenic Moieties. *ImmunoHorizons* **2019,** *3* (7), 282.
33. Laverman, P.; Carstens, M. G.; Boerman, O. C.; Dams, E. T.; Oyen, W. J.; van Rooijen, N.; Corstens, F. H.; Storm, G., Factors affecting the accelerated blood clearance of polyethylene glycol-liposomes upon repeated injection. *The Journal of pharmacology and experimental therapeutics* **2001,** *298* (2), 607-12.
34. Oja, C.; Tardi, P.; Schutze-Redelmeier, M.; Cullis, P. R., Doxorubicin entrapped within liposome-associated antigens results in a selective inhibition of the antibody response to the linked antigen. *Biochimica et biophysica acta* **2000,** *1468* (1-2), 31-40.
35. Tardi, P. G.; Swartz, E. N.; Harasym, T. O.; Cullis, P. R.; Bally, M. B., An immune response to ovalbumin covalently coupled to liposomes is prevented when the liposomes used contain doxorubicin. *Journal of immunological methods* **1997,** *210* (2), 137-48.
36. Shimizu, K.; Miyauchi, H.; Urakami, T.; Yamamura-Ichikawa, K.; Yonezawa, S.; Asai, T.; Oku, N., Specific delivery of an immunosuppressive drug to splenic B cells by antigen-modified liposomes and its antiallergic effect. *Journal of drug targeting* **2016,** *24* (9), 890-895.
37. Shek, P. N.; Lopez, N. G.; Heath, T. D., Immune response mediated by liposome-associated protein antigens. IV. Modulation of antibody formation by vesicle-encapsulated methotrexate. *Immunology* **1986,** *57* (1), 153-7.
38. van Rooijen, N.; van Nieuwmegen, R., Elimination of phagocytic cells in the spleen after intravenous injection of liposome-encapsulated dichloromethylene diphosphonate. An enzyme-histochemical study. *Cell and tissue research* **1984,** *238* (2), 355-8.
39. Van Rooijen, N.; Sanders, A., Liposome mediated depletion of macrophages: mechanism of action, preparation of liposomes and applications. *Journal of immunological methods* **1994,** *174* (1-2), 83-93.
40. Alves-Rosa, F.; Stanganelli, C.; Cabrera, J.; van Rooijen, N.; Palermo, M. S.; Isturiz, M. A., Treatment with liposome-encapsulated clodronate as a new strategic approach in the management of immune thrombocytopenic purpura in a mouse model. *Blood* **2000,** *96* (8), 2834-40.
41. Jordan, M. B.; van Rooijen, N.; Izui, S.; Kappler, J.; Marrack, P., Liposomal clodronate as a novel agent for treating autoimmune hemolytic anemia in a mouse model. *Blood* **2003,** *101* (2), 594-601.

42. Richards, P. J.; Williams, A. S.; Goodfellow, R. M.; Williams, B. D., Liposomal clodronate eliminates synovial macrophages, reduces inflammation and ameliorates joint destruction in antigen-induced arthritis. *Rheumatology* **1999,** *38* (9), 818-825.
43. Richards, P. J.; Williams, B. D.; Williams, A. S., Suppression of chronic streptococcal cell wall-induced arthritis in Lewis rats by liposomal clodronate. *Rheumatology (Oxford, England)* **2001,** *40* (9), 978-87.
44. Huitinga, I.; van Rooijen, N.; de Groot, C. J.; Uitdehaag, B. M.; Dijkstra, C. D., Suppression of experimental allergic encephalomyelitis in Lewis rats after elimination of macrophages. *J Exp Med* **1990,** *172* (4), 1025-33.
45. Allen, T. M.; Hansen, C. B.; Guo, L. S. S., Subcutaneous administration of liposomes: a comparison with the intravenous and intraperitoneal routes of injection. *Biochimica et Biophysica Acta (BBA) - Biomembranes* **1993,** *1150* (1), 9-16.
46. Behr, J.; Zimmermann, G.; Baumgartner, R.; Leuchte, H.; Neurohr, C.; Brand, P.; Herpich, C.; Sommerer, K.; Seitz, J.; Menges, G.; Tillmanns, S.; Keller, M., Lung deposition of a liposomal cyclosporine A inhalation solution in patients after lung transplantation. *Journal of aerosol medicine and pulmonary drug delivery* **2009,** *22* (2), 121-30.
47. Clinicaltrials.gov Aerosol Liposomal Cyclosporine for Chronic Rejection in Lung Transplant Recipients. https://clinicaltrials.gov/ct2/show/NCT01650545 (accessed 12/5/18).
48. Saraswat, A.; Agarwal, R.; Katare, O. P.; Kaur, I.; Kumar, B., A randomized, double-blind, vehicle-controlled study of a novel liposomal dithranol formulation in psoriasis. *The Journal of dermatological treatment* **2007,** *18* (1), 40-5.
49. van der Velden, V. H., Glucocorticoids: mechanisms of action and anti-inflammatory potential in asthma. *Mediators of inflammation* **1998,** *7* (4), 229-237.
50. Schmidt, J.; Metselaar, J. M.; Wauben, M. H.; Toyka, K. V.; Storm, G.; Gold, R., Drug targeting by long-circulating liposomal glucocorticosteroids increases therapeutic efficacy in a model of multiple sclerosis. *Brain : a journal of neurology* **2003,** *126* (Pt 8), 1895-904.
51. Metselaar, J. M.; Wauben, M. H. M.; Wagenaar-Hilbers, J. P. A.; Boerman, O. C.; Storm, G., Complete remission of experimental arthritis by joint targeting of glucocorticoids with long-circulating liposomes. *Arthritis & Rheumatism* **2003,** *48* (7), 2059-2066.
52. Metselaar, J. M.; van den Berg, W. B.; Holthuysen, A. E. M.; Wauben, M. H. M.; Storm, G.; van Lent, P. L. E. M., Liposomal targeting of glucocorticoids to synovial lining cells strongly increases therapeutic benefit in collagen type II arthritis. *Annals of the Rheumatic Diseases* **2004,** *63* (4), 348.
53. Avnir, Y.; Ulmansky, R.; Wasserman, V.; Even-Chen, S.; Broyer, M.; Barenholz, Y.; Naparstek, Y., Amphipathic weak acid glucocorticoid prodrugs remote-loaded into sterically stabilized nanoliposomes evaluated in arthritic rats and in a Beagle dog: A novel approach to treating autoimmune arthritis. *Arthritis & Rheumatism* **2007,** *58* (1), 119-129.
54. Anderson, R.; Franch, A.; Castell, M.; Perez-Cano, F. J.; Bräuer, R.; Pohlers, D.; Gajda, M.; Siskos, A. P.; Katsila, T.; Tamvakopoulos, C.; Rauchhaus, U.; Panzner, S.; Kinne, R. W., Liposomal encapsulation enhances and prolongs the anti-inflammatory

effects of water-soluble dexamethasone phosphate in experimental adjuvant arthritis. *Arthritis research & therapy* **2010,** *12* (4), R147.
55. Clinicaltrials.gov Nanocort in Acute Exacerbation of Relapsing-Remitting Multiple Sclerosis (MS). https://clinicaltrials.gov/ct2/show/NCT01039103 (accessed 12/5/18).
56. van Assche, G.; Rutgeerts, P.; Ferrante, M.; Noman, M.; Fiddler, H.; Oldenburg, B.; Maetselaar, J.; Vermeire, S., DOP023. Safety and efficacy of a novel IV targeted pegylated liposomal prednisolone product (Nanocort): results from a phase 2a study in patients with active ulcerative colitis. *Journal of Crohn's and Colitis* **2016,** *10* (suppl_1), S39-S40.
57. Oh, Y. K.; Nix, D. E.; Straubinger, R. M., Formulation and efficacy of liposome-encapsulated antibiotics for therapy of intracellular Mycobacterium avium infection. *Antimicrobial Agents and Chemotherapy* **1995,** *39* (9), 2104-2111.
58. Murphy, B. S.; Sundareshan, V.; Cory, T. J.; Hayes, D., Jr.; Anstead, M. I.; Feola, D. J., Azithromycin alters macrophage phenotype. *The Journal of antimicrobial chemotherapy* **2008,** *61* (3), 554-60.
59. Al-Darraji, A.; Haydar, D.; Chelvarajan, L.; Tripathi, H.; Levitan, B.; Gao, E.; Venditto, V. J.; Gensel, J.; Feola, D. J.; Abdel-Latif, A., Azithromycin therapy reduces cardiac inflammation and mitigates adverse cardiac remodeling after myocardial infarction: Potential therapeutic targets in ischemic heart disease. *PLOS ONE* **2018,** *In press*.
60. Feola, D. J.; Garvy, B. A.; Cory, T. J.; Birket, S. E.; Hoy, H.; Hayes, D., Jr.; Murphy, B. S., Azithromycin alters macrophage phenotype and pulmonary compartmentalization during lung infection with Pseudomonas. *Antimicrob Agents Chemother* **2010,** *54* (6), 2437-47.
61. Zhang, B.; Bailey, W. M.; Kopper, T. J.; Orr, M. B.; Feola, D. J.; Gensel, J. C., Azithromycin drives alternative macrophage activation and improves recovery and tissue sparing in contusion spinal cord injury. *Journal of neuroinflammation* **2015,** *12*, 218.
62. Dumont, F. J.; Su, Q., Mechanism of action of the immunosuppressant rapamycin. *Life Sciences* **1995,** *58* (5), 373-395.
63. Roskoski, R., Jr., Ibrutinib inhibition of Bruton protein-tyrosine kinase (BTK) in the treatment of B cell neoplasms. *Pharmacological research* **2016,** *113* (Pt A), 395-408.
64. Crawford, J. J.; Johnson, A. R.; Misner, D. L.; Belmont, L. D.; Castanedo, G.; Choy, R.; Coraggio, M.; Dong, L.; Eigenbrot, C.; Erickson, R.; Ghilardi, N.; Hau, J.; Katewa, A.; Kohli, P. B.; Lee, W.; Lubach, J. W.; McKenzie, B. S.; Ortwine, D. F.; Schutt, L.; Tay, S.; Wei, B.; Reif, K.; Liu, L.; Wong, H.; Young, W. B., Discovery of GDC-0853: A Potent, Selective, and Noncovalent Bruton's Tyrosine Kinase Inhibitor in Early Clinical Development. *Journal of medicinal chemistry* **2018,** *61* (6), 2227-2245.
65. Spurgeon, S. E.; Coffey, G.; Fletcher, L. B.; Burke, R.; Tyner, J. W.; Druker, B. J.; Betz, A.; DeGuzman, F.; Pak, Y.; Baker, D.; Pandey, A.; Hollenbach, S. J.; Sinha, U.; Loriaux, M. M., The Selective Syk Inhibitor P505-15 (PRT062607) Inhibits B Cell Signaling and Function In Vitro and In Vivo and Augments the Activity of Fludarabine in Chronic Lymphocytic Leukemia. *Journal of Pharmacology and Experimental Therapeutics* **2013,** *344* (2), 378-387.
66. Singh, S.; Aggarwal, B. B., Activation of Transcription Factor NF-κB Is Suppressed by Curcumin (Diferuloylmethane). *Journal of Biological Chemistry* **1995,** *270* (42), 24995-25000.

67. Meyer, D. M.; Jesson, M. I.; Li, X.; Elrick, M. M.; Funckes-Shippy, C. L.; Warner, J. D.; Gross, C. J.; Dowty, M. E.; Ramaiah, S. K.; Hirsch, J. L.; Saabye, M. J.; Barks, J. L.; Kishore, N.; Morris, D. L., Anti-inflammatory activity and neutrophil reductions mediated by the JAK1/JAK3 inhibitor, CP-690,550, in rat adjuvant-induced arthritis. *Journal of inflammation (London, England)* **2010,** *7*, 41-41.
68. Schwendener, R. A., Liposomes as vaccine delivery systems: a review of the recent advances. *Therapeutic Advances in Vaccines* **2014,** *2* (6), 159-182.
69. Allison, A. G.; Gregoriadis, G., Liposomes as immunological adjuvants. *Nature* **1974,** *252* (5480), 252.
70. De Serrano, L. O.; Burkhart, D. J., Liposomal vaccine formulations as prophylactic agents: design considerations for modern vaccines. *Journal of nanobiotechnology* **2017,** *15* (1), 83-83.
71. Alving, C. R.; Beck, Z.; Matyas, G. R.; Rao, M., Liposomal adjuvants for human vaccines. *Expert opinion on drug delivery* **2016,** *13* (6), 807-16.
72. Teo, S. P., Review of COVID-19 mRNA Vaccines: BNT162b2 and mRNA-1273. *J Pharm Pract* **2021**, 8971900211009650.
73. Alving, C. R., Liposomes as carriers of antigens and adjuvants. *Journal of Immunological Methods* **1991,** *140* (1), 1-13.
74. Donnelly, J. J.; Wahren, B.; Liu, M. A., DNA vaccines: progress and challenges. *Journal of immunology (Baltimore, Md. : 1950)* **2005,** *175* (2), 633-9.
75. Boyle, J. S.; Silva, A.; Brady, J. L.; Lew, A. M., DNA immunization: induction of higher avidity antibody and effect of route on T cell cytotoxicity. *Proc Natl Acad Sci U S A* **1997,** *94* (26), 14626-31.
76. Buschmann, M. D.; Carrasco, M. J.; Alishetty, S.; Paige, M.; Alameh, M. G.; Weissman, D., Nanomaterial Delivery Systems for mRNA Vaccines. *Vaccines* **2021,** *9* (1), 65.
77. Tandrup Schmidt, S.; Foged, C.; Smith Korsholm, K.; Rades, T.; Christensen, D., Liposome-Based Adjuvants for Subunit Vaccines: Formulation Strategies for Subunit Antigens and Immunostimulators. *Pharmaceutics* **2016,** *8* (1), 7.
78. Shariat, S.; Badiee, A.; Jaafari, M. R.; Mortazavi, S. A., Optimization of a Method to Prepare Liposomes Containing HER2/Neu- Derived Peptide as a Vaccine Delivery System for Breast Cancer. *Iranian Journal of Pharmaceutical Research : IJPR* **2014,** *13* (Suppl), 15-25.
79. Eloy, J. O.; Claro de Souza, M.; Petrilli, R.; Barcellos, J. P.; Lee, R. J.; Marchetti, J. M., Liposomes as carriers of hydrophilic small molecule drugs: strategies to enhance encapsulation and delivery. *Colloids and surfaces. B, Biointerfaces* **2014,** *123*, 345-63.
80. Sur, S.; Fries, A. C.; Kinzler, K. W.; Zhou, S.; Vogelstein, B., Remote loading of preencapsulated drugs into stealth liposomes. *Proceedings of the National Academy of Sciences of the United States of America* **2014,** *111* (6), 2283-2288.
81. Badiee, A.; Khamesipour, A.; Samiei, A.; Soroush, D.; Shargh, V. H.; Kheiri, M. T.; Barkhordari, F.; Robert Mc Master, W.; Mahboudi, F.; Jaafari, M. R., The role of liposome size on the type of immune response induced in BALB/c mice against leishmaniasis: rgp63 as a model antigen. *Experimental parasitology* **2012,** *132* (4), 403-9.
82. Lee, S.; Nguyen, M. T., Recent advances of vaccine adjuvants for infectious diseases. *Immune network* **2015,** *15* (2), 51-7.

83. Giddam, A. K.; Zaman, M.; Skwarczynski, M.; Toth, I., Liposome-based delivery system for vaccine candidates: constructing an effective formulation. *Nanomedicine (London, England)* **2012,** *7* (12), 1877-93.
84. Venditto, V. J.; Watson, D. S.; Motion, M.; Montefiori, D.; Szoka, F. C., Jr., Rational design of membrane proximal external region lipopeptides containing chemical modifications for HIV-1 vaccination. *Clinical and vaccine immunology : CVI* **2013,** *20* (1), 39-45.
85. Venditto, V. J.; Wieczorek, L.; Molnar, S.; Teque, F.; Landucci, G.; Watson, D. S.; Forthal, D.; Polonis, V. R.; Levy, J. A.; Szoka, F. C., Jr., Chemically modified peptides based on the membrane-proximal external region of the HIV-1 envelope induce high-titer, epitope-specific nonneutralizing antibodies in rabbits. *Clinical and vaccine immunology : CVI* **2014,** *21* (8), 1086-93.
86. Coler, R. N.; Bertholet, S.; Moutaftsi, M.; Guderian, J. A.; Windish, H. P.; Baldwin, S. L.; Laughlin, E. M.; Duthie, M. S.; Fox, C. B.; Carter, D.; Friede, M.; Vedvick, T. S.; Reed, S. G., Development and characterization of synthetic glucopyranosyl lipid adjuvant system as a vaccine adjuvant. *PLoS One* **2011,** *6* (1), e16333.
87. McKee, A. S.; Marrack, P., Old and new adjuvants. *Current opinion in immunology* **2017,** *47*, 44-51.
88. Bal, S. M.; Hortensius, S.; Ding, Z.; Jiskoot, W.; Bouwstra, J. A., Co-encapsulation of antigen and Toll-like receptor ligand in cationic liposomes affects the quality of the immune response in mice after intradermal vaccination. *Vaccine* **2011,** *29* (5), 1045-52.
89. Rao, M.; Matyas, G. R.; Vancott, T. C.; Birx, D. L.; Alving, C. R., Immunostimulatory CpG motifs induce CTL responses to HIV type I oligomeric gp140 envelope protein. *Immunology and cell biology* **2004,** *82* (5), 523-30.
90. Van Dis, E.; Sogi, K. M.; Rae, C. S.; Sivick, K. E.; Surh, N. H.; Leong, M. L.; Kanne, D. B.; Metchette, K.; Leong, J. J.; Bruml, J. R.; Chen, V.; Heydari, K.; Cadieux, N.; Evans, T.; McWhirter, S. M.; Dubensky, T. W., Jr.; Portnoy, D. A.; Stanley, S. A., STING-Activating Adjuvants Elicit a Th17 Immune Response and Protect against Mycobacterium tuberculosis Infection. *Cell reports* **2018,** *23* (5), 1435-1447.
91. Dubensky, T. W., Jr.; Kanne, D. B.; Leong, M. L., Rationale, progress and development of vaccines utilizing STING-activating cyclic dinucleotide adjuvants. *Ther Adv Vaccines* **2013,** *1* (4), 131-43.
92. Alving, C. R.; Richards, R. L.; Guirguis, A. A., Cholesterol-dependent human complement activation resulting in damage to liposomal model membranes. *Journal of immunology (Baltimore, Md. : 1950)* **1977,** *118* (1), 342-7.
93. Christensen, D.; Korsholm, K. S.; Rosenkrands, I.; Lindenstrom, T.; Andersen, P.; Agger, E. M., Cationic liposomes as vaccine adjuvants. *Expert Rev Vaccines* **2007,** *6* (5), 785-96.
94. Lim, J.; Song, Y. J.; Park, W. S.; Sohn, H.; Lee, M. S.; Shin, D. H.; Kim, C. B.; Kim, H.; Oh, G. J.; Ki, M., The immunogenicity of a single dose of hepatitis A virus vaccines (Havrix(R) and Epaxal(R)) in Korean young adults. *Yonsei medical journal* **2014,** *55* (1), 126-31.
95. Chappuis, F.; Farinelli, T.; Deckx, H.; Sarnecki, M.; Go, O.; Salzgeber, Y.; Stals, C., Immunogenicity and estimation of antibody persistence following vaccination with an

inactivated virosomal hepatitis A vaccine in adults: A 20-year follow-up study. *Vaccine* **2017,** *35* (10), 1448-1454.
96. Herzog, C.; Hartmann, K.; Kunzi, V.; Kursteiner, O.; Mischler, R.; Lazar, H.; Gluck, R., Eleven years of Inflexal V-a virosomal adjuvanted influenza vaccine. *Vaccine* **2009,** *27* (33), 4381-7.
97. Gasparini, R.; Amicizia, D.; Lai, P. L.; Rossi, S.; Panatto, D., Effectiveness of adjuvanted seasonal influenza vaccines (Inflexal V (R) and Fluad (R)) in preventing hospitalization for influenza and pneumonia in the elderly: a matched case-control study. *Human vaccines & immunotherapeutics* **2013,** *9* (1), 144-52.
98. Conne, P.; Gauthey, L.; Vernet, P.; Althaus, B.; Que, J. U.; Finkel, B.; Glück, R.; Cryz, S. J., Immunogenicity of trivalent subunit versus virosome-formulated influenza vaccines in geriatric patients. *Vaccine* **1997,** *15* (15), 1675-1679.
99. Hasson, S. S. A. A.; Al-Busaidi, J. K. Z.; Sallam, T. A., The past, current and future trends in DNA vaccine immunisations. *Asian Pacific Journal of Tropical Biomedicine* **2015,** *5* (5), 344-353.
100. Lee, L. Y. Y.; Izzard, L.; Hurt, A. C., A Review of DNA Vaccines Against Influenza. *Frontiers in immunology* **2018,** *9*, 1568-1568.
101. Pardi, N.; Hogan, M. J.; Porter, F. W.; Weissman, D., mRNA vaccines — a new era in vaccinology. *Nature Reviews Drug Discovery* **2018,** *17*, 261.
102. Bramson, J. L.; Bodner, C. A.; Graham, R. W., Activation of host antitumoral responses by cationic lipid/DNA complexes. *Cancer gene therapy* **2000,** *7* (3), 353-9.
103. Lonez, C.; Vandenbranden, M.; Ruysschaert, J. M., Cationic lipids activate intracellular signaling pathways. *Advanced drug delivery reviews* **2012,** *64* (15), 1749-58.
104. Liu, J.; Wu, J.; Wang, B.; Zeng, S.; Qi, F.; Lu, C.; Kimura, Y.; Liu, B., Oral vaccination with a liposome-encapsulated influenza DNA vaccine protects mice against respiratory challenge infection. *Journal of medical virology* **2014,** *86* (5), 886-94.
105. Rodriguez, A. E.; Zamorano, P.; Wilkowsky, S.; Torra, F.; Ferreri, L.; Dominguez, M.; Florin-Christensen, M., Delivery of recombinant vaccines against bovine herpesvirus type 1 gD and Babesia bovis MSA-2c to mice using liposomes derived from egg yolk lipids. *Veterinary journal (London, England : 1997)* **2013,** *196* (3), 550-1.
106. Shlapobersky, M.; Marshak, J. O.; Dong, L.; Huang, M.-l.; Wei, Q.; Chu, A.; Rolland, A.; Sullivan, S.; Koelle, D. M., Vaxfectin-adjuvanted plasmid DNA vaccine improves protection and immunogenicity in a murine model of genital herpes infection. *The Journal of general virology* **2012,** *93* (Pt 6), 1305-1315.
107. Lin, W.-H. W.; Vilalta, A.; Adams, R. J.; Rolland, A.; Sullivan, S. M.; Griffin, D. E., Vaxfectin adjuvant improves antibody responses of juvenile rhesus macaques to a DNA vaccine encoding the measles virus hemagglutinin and fusion proteins. *Journal of virology* **2013,** *87* (12), 6560-6568.
108. Luo, K.; Zhang, H.; Zavala, F.; Biragyn, A.; Espinosa, D. A.; Markham, R. B., Fusion of antigen to a dendritic cell targeting chemokine combined with adjuvant yields a malaria DNA vaccine with enhanced protective capabilities. *PloS one* **2014,** *9* (3), e90413-e90413.
109. Kulkarni, V.; Rosati, M.; Valentin, A.; Jalah, R.; Alicea, C.; Yu, L.; Guan, Y.; Shen, X.; Tomaras, G. D.; LaBranche, C.; Montefiori, D. C.; Irene, C.; Prattipati, R.; Pinter, A.; Sullivan, S. M.; Pavlakis, G. N.; Felber, B. K., Vaccination with Vaxfectin(®)

adjuvanted SIV DNA induces long-lasting humoral immune responses able to reduce SIVmac251 Viremia. *Human vaccines & immunotherapeutics* **2013,** *9* (10), 2069-2080.
110. Smith, L. R.; Wodal, W.; Crowe, B. A.; Kerschbaum, A.; Bruehl, P.; Schwendinger, M. G.; Savidis-Dacho, H.; Sullivan, S. M.; Shlapobersky, M.; Hartikka, J.; Rolland, A.; Barrett, P. N.; Kistner, O., Preclinical evaluation of Vaxfectin-adjuvanted Vero cell-derived seasonal split and pandemic whole virus influenza vaccines. *Human vaccines & immunotherapeutics* **2013,** *9* (6), 1333-1345.
111. Coban, C.; Koyama, S.; Takeshita, F.; Akira, S.; Ishii, K. J., Molecular and cellular mechanisms of DNA vaccines. *Hum Vaccin* **2008,** *4* (6), 453-6.
112. Scorza, F. B.; Pardi, N., New Kids on the Block: RNA-Based Influenza Virus Vaccines. *Vaccines* **2018,** *6* (2).
113. Li, Y.; Hu, Y.; Jin, Y.; Zhang, G.; Wong, J.; Sun, L. Q.; Wang, M., Prophylactic, therapeutic and immune enhancement effect of liposome-encapsulated PolyICLC on highly pathogenic H5N1 influenza infection. *The journal of gene medicine* **2011,** *13* (1), 60-72.
114. Meyer, M.; Huang, E.; Yuzhakov, O.; Ramanathan, P.; Ciaramella, G.; Bukreyev, A., Modified mRNA-Based Vaccines Elicit Robust Immune Responses and Protect Guinea Pigs From Ebola Virus Disease. *The Journal of infectious diseases* **2018,** *217* (3), 451-455.
115. Baptista, B.; Carapito, R.; Laroui, N.; Pichon, C.; Sousa, F., mRNA, a Revolution in Biomedicine. *Pharmaceutics* **2021,** *13* (12).
116. Liu, M. A., A Comparison of Plasmid DNA and mRNA as Vaccine Technologies. *Vaccines* **2019,** *7* (2), 37.
117. Riley, M. K.; Vermerris, W., Recent Advances in Nanomaterials for Gene Delivery-A Review. *Nanomaterials (Basel, Switzerland)* **2017,** *7* (5).
118. Wood, H., FDA approves patisiran to treat hereditary transthyretin amyloidosis. *Nature reviews. Neurology* **2018,** *14* (10), 570.
119. Yin, H.; Kanasty, R. L.; Eltoukhy, A. A.; Vegas, A. J.; Dorkin, J. R.; Anderson, D. G., Non-viral vectors for gene-based therapy. *Nature reviews. Genetics* **2014,** *15* (8), 541-55.
120. Kanasty, R.; Dorkin, J. R.; Vegas, A.; Anderson, D., Delivery materials for siRNA therapeutics. *Nature Materials* **2013,** *12*, 967.
121. Zhao, Y.; Huang, L., Lipid Nanoparticles for Gene Delivery. *Advances in genetics* **2014,** *88*, 13-36.
122. Chakraborty, C.; Sharma, A. R.; Sharma, G.; Doss, C. G. P.; Lee, S.-S., Therapeutic miRNA and siRNA: Moving from Bench to Clinic as Next Generation Medicine. *Molecular Therapy. Nucleic Acids* **2017,** *8*, 132-143.
123. Second RNAi drug approved. *Nature Biotechnology* **2020,** *38* (4), 385-385.
124. Lv, H.; Zhang, S.; Wang, B.; Cui, S.; Yan, J., Toxicity of cationic lipids and cationic polymers in gene delivery. *Journal of Controlled Release* **2006,** *114* (1), 100-109.
125. Kaczmarek, J. C.; Kowalski, P. S.; Anderson, D. G., Advances in the delivery of RNA therapeutics: from concept to clinical reality. *Genome Medicine* **2017,** *9* (1), 60.
126. Garber, K., Worth the RISC? *Nature Biotechnology* **2017,** *35*, 198.
127. Zhang, S.; Xu, Y.; Wang, B.; Qiao, W.; Liu, D.; Li, Z., Cationic compounds used in lipoplexes and polyplexes for gene delivery. *Journal of Controlled Release* **2004,** *100* (2), 165-180.

128. Zabner, J., Cationic lipids used in gene transfer. *Advanced drug delivery reviews* **1997,** *27* (1), 17-28.
129. Al-Dosari, M. S.; Gao, X., Nonviral Gene Delivery: Principle, Limitations, and Recent Progress. *The AAPS journal* **2009,** *11* (4), 671.
130. Ramamoorth, M.; Narvekar, A., Non Viral Vectors in Gene Therapy- An Overview. *Journal of Clinical and Diagnostic Research : JCDR* **2015,** *9* (1), GE01-GE06.
131. Candiani, G., *Non-Viral Gene Delivery Vectors Methods and Protocols*. Humana Press: New York, 2016; Vol. 1, p 290.
132. Ulmer, J. B.; Geall, A. J., Recent innovations in mRNA vaccines. *Curr Opin Immunol* **2016,** *41*, 18-22.
133. Pardi, N.; Hogan, M. J.; Pelc, R. S.; Muramatsu, H.; Andersen, H.; DeMaso, C. R.; Dowd, K. A.; Sutherland, L. L.; Scearce, R. M.; Parks, R.; Wagner, W.; Granados, A.; Greenhouse, J.; Walker, M.; Willis, E.; Yu, J. S.; McGee, C. E.; Sempowski, G. D.; Mui, B. L.; Tam, Y. K.; Huang, Y. J.; Vanlandingham, D.; Holmes, V. M.; Balachandran, H.; Sahu, S.; Lifton, M.; Higgs, S.; Hensley, S. E.; Madden, T. D.; Hope, M. J.; Kariko, K.; Santra, S.; Graham, B. S.; Lewis, M. G.; Pierson, T. C.; Haynes, B. F.; Weissman, D., Zika virus protection by a single low-dose nucleoside-modified mRNA vaccination. *Nature* **2017,** *543* (7644), 248-251.
134. Pardi, N.; Tuyishime, S.; Muramatsu, H.; Kariko, K.; Mui, B. L.; Tam, Y. K.; Madden, T. D.; Hope, M. J.; Weissman, D., Expression kinetics of nucleoside-modified mRNA delivered in lipid nanoparticles to mice by various routes. *Journal of controlled release : official journal of the Controlled Release Society* **2015,** *217*, 345-351.
135. Song, X.; Wang, X.; Ma, Y.; Liang, Z.; Yang, Z.; Cao, H., Site-Specific Modification Using the 2'-Methoxyethyl Group Improves the Specificity and Activity of siRNAs. *Mol Ther Nucleic Acids* **2017,** *9*, 242-250.
136. Deleavey, G. F.; Watts, J. K.; Damha, M. J., Chemical modification of siRNA. *Current protocols in nucleic acid chemistry* **2009,** *Chapter 16*, Unit 16.3.
137. Wasungu, L.; Hoekstra, D., Cationic lipids, lipoplexes and intracellular delivery of genes. *Journal of Controlled Release* **2006,** *116* (2), 255-264.
138. Huth, U. S.; Schubert, R.; Peschka-Süss, R., Investigating the uptake and intracellular fate of pH-sensitive liposomes by flow cytometry and spectral bio-imaging. *Journal of Controlled Release* **2006,** *110* (3), 490-504.
139. Allen, T. M.; Cullis, P. R., Liposomal drug delivery systems: from concept to clinical applications. *Advanced drug delivery reviews* **2013,** *65* (1), 36-48.
140. Heath, T. D.; Lopez, N. G.; Papahadjopoulos, D., The effects of liposome size and surface charge on liposome-mediated delivery of methotrexate-gamma-aspartate to cells in vitro. *Biochimica et biophysica acta* **1985,** *820* (1), 74-84.
141. Dan, N.; Danino, D., Structure and kinetics of lipid–nucleic acid complexes. *Advances in Colloid and Interface Science* **2014,** *205*, 230-239.
142. Koynova, R., Analysis of Lipoplex Structure and Lipid Phase Changes. In *Liposomes: Methods and Protocols, Volume 2: Biological Membrane Models*, Weissig, V., Ed. Humana Press: Totowa, NJ, 2010; pp 399-423.
143. Gershon, H.; Ghirlando, R.; Guttman, S. B.; Minsky, A., Mode of formation and structural features of DNA-cationic liposome complexes used for transfection. *Biochemistry* **1993,** *32* (28), 7143-51.

144. Meunier-Durmort, C.; Picart, R.; Ragot, T.; Perricaudet, M.; Hainque, B.; Forest, C., Mechanism of adenovirus improvement of cationic liposome-mediated gene transfer. *Biochimica et Biophysica Acta (BBA) - Biomembranes* **1997,** *1330* (1), 8-16.
145. Nemerow, G. R.; Stewart, P. L., Insights into Adenovirus Uncoating from Interactions with Integrins and Mediators of Host Immunity. *Viruses* **2016,** *8* (12), 337.
146. Claassen, E., Detection, localization and kinetics of immunomodulating liposomes in vivo. *Research in Immunology* **1992,** *143* (2), 235-241.
147. Byrne, J. D.; Betancourt, T.; Brannon-Peppas, L., Active targeting schemes for nanoparticle systems in cancer therapeutics. *Advanced drug delivery reviews* **2008,** *60* (15), 1615-26.
148. Kullberg, M.; McCarthy, R.; Anchordoquy, T. J., Gene delivery to Her-2+ breast cancer cells using a two-component delivery system to achieve specificity. *Nanomedicine : nanotechnology, biology, and medicine* **2014,** *10* (6), 1253-62.
149. Hafez, I. M.; Maurer, N.; Cullis, P. R., On the mechanism whereby cationic lipids promote intracellular delivery of polynucleic acids. *Gene therapy* **2001,** *8* (15), 1188-96.
150. Sørensen, D. R.; Leirdal, M.; Sioud, M., Gene Silencing by Systemic Delivery of Synthetic siRNAs in Adult Mice. *Journal of Molecular Biology* **2003,** *327* (4), 761-766.
151. Zhang, Y.; Cristofaro, P.; Silbermann, R.; Pusch, O.; Boden, D.; Konkin, T.; Hovanesian, V.; Monfils, P. R.; Resnick, M.; Moss, S. F.; Ramratnam, B., Engineering mucosal RNA interference in vivo. *Molecular therapy : the journal of the American Society of Gene Therapy* **2006,** *14* (3), 336-42.
152. Aldayel, A. M.; O'Mary, H. L.; Valdes, S. A.; Li, X.; Thakkar, S. G.; Mustafa, B. E.; Cui, Z., Lipid nanoparticles with minimum burst release of TNF-α siRNA show strong activity against rheumatoid arthritis unresponsive to methotrexate. *Journal of Controlled Release* **2018,** *283*, 280-289.
153. Peer, D.; Park, E. J.; Morishita, Y.; Carman, C. V.; Shimaoka, M., Systemic leukocyte-directed siRNA delivery revealing cyclin D1 as an anti-inflammatory target. *Science (New York, N.Y.)* **2008,** *319* (5863), 627-30.
154. Katakowski, J. A.; Mukherjee, G.; Wilner, S. E.; Maier, K. E.; Harrison, M. T.; DiLorenzo, T. P.; Levy, M.; Palliser, D., Delivery of siRNAs to Dendritic Cells Using DEC205-Targeted Lipid Nanoparticles to Inhibit Immune Responses. *Molecular therapy : the journal of the American Society of Gene Therapy* **2016,** *24* (1), 146-55.
155. Feinberg, M. W.; Moore, K. J., MicroRNA Regulation of Atherosclerosis. *Circulation research* **2016,** *118* (4), 703-20.
156. Tessitore, A.; Cicciarelli, G.; Mastroiaco, V.; Vecchio, F. D.; Capece, D.; Verzella, D.; Fischietti, M.; Vecchiotti, D.; Zazzeroni, F.; Alesse, E., Therapeutic Use of MicroRNAs in Cancer. *Anti-cancer agents in medicinal chemistry* **2016,** *16* (1), 7-19.
157. Wang, W.-X.; Sullivan, P. G.; Springer, J. E., Mitochondria and microRNA crosstalk in traumatic brain injury. *Progress in Neuro-Psychopharmacology and Biological Psychiatry* **2017,** *73*, 104-108.
158. Wang, W.-X.; Springer, J. E., Role of mitochondria in regulating microRNA activity and its relevance to the central nervous system. *Neural regeneration research* **2015,** *10* (7), 1026-1028.
159. Lesizza, P.; Prosdocimo, G.; Martinelli, V.; Sinagra, G.; Zacchigna, S.; Giacca, M., Single-Dose Intracardiac Injection of Pro-Regenerative MicroRNAs Improves Cardiac Function After Myocardial Infarction. *Circulation research* **2017,** *120* (8), 1298-1304.

160. Ghatak, S.; Li, J.; Chan, Y. C.; Gnyawali, S. C.; Steen, E.; Yung, B. C.; Khanna, S.; Roy, S.; Lee, R. J.; Sen, C. K., AntihypoxamiR functionalized gramicidin lipid nanoparticles rescue against ischemic memory improving cutaneous wound healing. *Nanomedicine : nanotechnology, biology, and medicine* **2016,** *12* (7), 1827-1831.
161. Dinh, T. D.; Higuchi, Y.; Kawakami, S.; Yamashita, F.; Hashida, M., Evaluation of Osteoclastogenesis via NFκB Decoy/mannosylated Cationic Liposome-Mediated Inhibition of Pro-inflammatory Cytokine Production from Primary Cultured Macrophages. *Pharmaceutical research* **2011,** *28* (4), 742-751.
162. Wijagkanalan, W.; Kawakami, S.; Higuchi, Y.; Yamashita, F.; Hashida, M., Intratracheally instilled mannosylated cationic liposome/NFκB decoy complexes for effective prevention of LPS-induced lung inflammation. *Journal of Controlled Release* **2011,** *149* (1), 42-50.
163. Iwata, A.; Sai, S.; Nitta, Y.; Chen, M.; de Fries-Hallstrand, R.; Dalesandro, J.; Thomas, R.; Allen, M. D., Liposome-mediated gene transfection of endothelial nitric oxide synthase reduces endothelial activation and leukocyte infiltration in transplanted hearts. *Circulation* **2001,** *103* (22), 2753-9.
164. Chen, F.; Date, H., Update on ischemia-reperfusion injury in lung transplantation. *Current opinion in organ transplantation* **2015,** *20* (5), 515-20.
165. Guan, L.-Y.; Fu, P.-Y.; Li, P.-D.; Li, Z.-N.; Liu, H.-Y.; Xin, M.-G.; Li, W., Mechanisms of hepatic ischemia-reperfusion injury and protective effects of nitric oxide. *World journal of gastrointestinal surgery* **2014,** *6* (7), 122-128.
166. Furukawa, H.; Oshima, K.; Tung, T.; Cui, G.; Laks, H.; Sen, L., Liposome-Mediated Combinatorial Cytokine Gene Therapy Induces Localized Synergistic Immunosuppression and Promotes Long-Term Survival of Cardiac Allografts. *The Journal of Immunology* **2005,** *174* (11), 6983-6992.
167. Furukawa, H.; Oshima, K.; Tung, T.; Cui, G.; Laks, H.; Sen, L., Overexpressed Exogenous IL-4 And IL-10 Paradoxically Regulate Allogenic T-Cell and Cardiac Myocytes Apoptosis Through FAS/FASL Pathway. *Transplantation* **2008,** *85* (3), 437-446.
168. Tung, T. C.; Oshima, K.; Cui, G.; Laks, H.; Sen, L., Dual upregulation of Fas and Bax promotes alloreactive T cell apoptosis in IL-10 gene targeting of cardiac allografts. *American Journal of Physiology-Heart and Circulatory Physiology* **2003,** *285* (3), H964-H973.
169. Sen, L.; Hong, Y.-S.; Luo, H.; Cui, G.; Laks, H., Efficiency, efficacy, and adverse effects of adenovirus- vs. liposome-mediated gene therapy in cardiac allografts. *American Journal of Physiology-Heart and Circulatory Physiology* **2001,** *281* (3), H1433-H1441.
170. Oshima, K.; Sen, L.; Cui, G.; Tung, T.; Sacks, B. M.; Arellano-Kruse, A.; Laks, H., Localized interleukin-10 gene transfer induces apoptosis of alloreactive T cells via FAS/FASL pathway, improves function, and prolongs survival of cardiac allograft. *Transplantation* **2002,** *73* (7), 1019-1026.
171. Fabrega, A. J.; Fasbender, A. J.; Struble, S.; Zabner, J., Cationic lipid-mediated transfer of the hIL-10 gene prolongs survival of allogenic hepatocytes in nagase analmunemic rats. *Transplantation* **1996,** *62* (12), 1866-1871.
172. Duguay, B. A.; Huang, K. W.-C.; Kulka, M., Lipofection of plasmid DNA into human mast cell lines using lipid nanoparticles generated by microfluidic mixing. *Journal of Leukocyte Biology* **2018,** *104* (3), 587-596.

173. Gregoriadis, G., Liposomes in Drug Delivery: How It All Happened. *Pharmaceutics* **2016,** *8* (2), 19.
174. Adams, D.; Gonzalez-Duarte, A.; O'Riordan, W. D.; Yang, C. C.; Ueda, M.; Kristen, A. V.; Tournev, I.; Schmidt, H. H.; Coelho, T.; Berk, J. L.; Lin, K. P.; Vita, G.; Attarian, S.; Plante-Bordeneuve, V.; Mezei, M. M.; Campistol, J. M.; Buades, J.; Brannagan, T. H., 3rd; Kim, B. J.; Oh, J.; Parman, Y.; Sekijima, Y.; Hawkins, P. N.; Solomon, S. D.; Polydefkis, M.; Dyck, P. J.; Gandhi, P. J.; Goyal, S.; Chen, J.; Strahs, A. L.; Nochur, S. V.; Sweetser, M. T.; Garg, P. P.; Vaishnaw, A. K.; Gollob, J. A.; Suhr, O. B., Patisiran, an RNAi Therapeutic, for Hereditary Transthyretin Amyloidosis. *The New England journal of medicine* **2018,** *379* (1), 11-21.
175. Nardo, D.; Akers, C. M.; Cheung, N. E.; Isom, C. M.; Spaude, J. T.; Pack, D. W.; Venditto, V. J., Cyanuric chloride as the basis for compositionally diverse lipids. *RSC Adv* **2021,** *11* (40), 24752-24761.
176. Molla, M. R.; Böser, A.; Rana, A.; Schwarz, K.; Levkin, P. A., One-Pot Parallel Synthesis of Lipid Library via Thiolactone Ring Opening and Screening for Gene Delivery. *Bioconjugate Chemistry* **2018,** *29* (4), 992-999.
177. Zhou, C. Y.; Wu, H.; Devaraj, N. K., Rapid access to phospholipid analogs using thiol-yne chemistry. *Chemical science* **2015,** *6* (7), 4365-4372.
178. Alabi, C. A.; Love, K. T.; Sahay, G.; Yin, H.; Luly, K. M.; Langer, R.; Anderson, D. G., Multiparametric approach for the evaluation of lipid nanoparticles for siRNA delivery. *Proceedings of the National Academy of Sciences* **2013,** *110* (32), 12881-12886.
179. Miao, L.; Li, L.; Huang, Y.; Delcassian, D.; Chahal, J.; Han, J.; Shi, Y.; Sadtler, K.; Gao, W.; Lin, J.; Doloff, J. C.; Langer, R.; Anderson, D. G., Delivery of mRNA vaccines with heterocyclic lipids increases anti-tumor efficacy by STING-mediated immune cell activation. *Nature Biotechnology* **2019,** *37* (10), 1174-1185.
180. Watson, D. S.; Platt, V. M.; Cao, L.; Venditto, V. J.; Szoka, F. C., Antibody Response to Polyhistidine-Tagged Peptide and Protein Antigens Attached to Liposomes via Lipid-Linked Nitrilotriacetic Acid in Mice. *Clinical and Vaccine Immunology* **2011,** *18* (2), 289-297.
181. Alving, C. R.; Rao, M.; Steers, N. J.; Matyas, G. R.; Mayorov, A. V., Liposomes containing lipid A: an effective, safe, generic adjuvant system for synthetic vaccines. *Expert Rev Vaccines* **2012,** *11* (6), 733-44.
182. Fujii, G.; Ernst, W.; Adler-Moore, J., The VesiVax system: a method for rapid vaccine development. *Frontiers in bioscience : a journal and virtual library* **2008,** *13*, 1968-80.
183. Simanek, E. E.; Abdou, H.; Lalwani, S.; Lim, J.; Mintzer, M.; Venditto, V. J.; Vittur, B., The 8 year thicket of triazine dendrimers: strategies, targets and applications. *Proceedings of the Royal Society A: Mathematical, Physical and Engineering Sciences* **2010,** *466* (2117), 1445-1468.
184. Candiani, G.; Frigerio, M.; Viani, F.; Verpelli, C.; Sala, C.; Chiamenti, L.; Zaffaroni, N.; Folini, M.; Sani, M.; Panzeri, W.; Zanda, M., Dimerizable redox-sensitive triazine-based cationic lipids for in vitro gene delivery. *ChemMedChem* **2007,** *2* (3), 292-6.
185. Merkel, O. M.; Mintzer, M. A.; Librizzi, D.; Samsonova, O.; Dicke, T.; Sproat, B.; Garn, H.; Barth, P. J.; Simanek, E. E.; Kissel, T., Triazine dendrimers as nonviral

vectors for in vitro and in vivo RNAi: the effects of peripheral groups and core structure on biological activity. *Molecular pharmaceutics* **2010,** *7* (4), 969-83.
186. Watrelot, A. A.; Tran, D. T.; Buffeteau, T.; Deffieux, D.; Le Bourvellec, C.; Quideau, S.; Renard, C. M. G. C., Immobilization of flavan-3-ols onto sensor chips to study their interactions with proteins and pectins by SPR. *Applied Surface Science* **2016,** *371*, 512-518.
187. Ralston, E.; Hjelmeland, L. M.; Klausner, R. D.; Weinstein, J. N.; Blumenthal, R., Carboxyfluorescein as a probe for liposome-cell interactions effect of impurities, and purification of the dye. *Biochimica et Biophysica Acta (BBA) - Biomembranes* **1981,** *649* (1), 133-137.
188. Weinstein, J. N.; Blumenthal, R.; Klausner, R. D., Carboxyfluorescein leakage assay for lipoprotein-liposome interaction. *Methods in enzymology* **1986,** *128*, 657-68.
189. Jayaraman, M.; Ansell, S. M.; Mui, B. L.; Tam, Y. K.; Chen, J.; Du, X.; Butler, D.; Eltepu, L.; Matsuda, S.; Narayanannair, J. K.; Rajeev, K. G.; Hafez, I. M.; Akinc, A.; Maier, M. A.; Tracy, M. A.; Cullis, P. R.; Madden, T. D.; Manoharan, M.; Hope, M. J., Maximizing the potency of siRNA lipid nanoparticles for hepatic gene silencing in vivo. *Angew Chem Int Ed Engl* **2012,** *51* (34), 8529-8533.
190. Akbar, M. A.; Nardo, D.; Chen, M. J.; Elshikha, A. S.; Ahamed, R.; Elsayed, E. M.; Bigot, C.; Holliday, L. S.; Song, S., Alpha-1 antitrypsin inhibits RANKL-induced osteoclast formation and functions. *Molecular medicine (Cambridge, Mass.)* **2017,** *23*, 57-69.
191. Pineda-Torra, I.; Gage, M.; de Juan, A.; Pello, O. M., Isolation, Culture, and Polarization of Murine Bone Marrow-Derived and Peritoneal Macrophages. *Methods in molecular biology (Clifton, N.J.)* **2015,** *1339*, 101-9.
192. Inaba, K.; Swiggard, W. J.; Steinman, R. M.; Romani, N.; Schuler, G.; Brinster, C., Isolation of dendritic cells. *Current protocols in immunology* **2009,** *Chapter 3*, Unit 3.7.
193. Pitts, M. G.; Nardo, D.; Isom, C. M.; Venditto, V. J., Autoantibody Responses to Apolipoprotein A-I Are Not Diet- or Sex-Linked in C57BL/6 Mice. *ImmunoHorizons* **2020,** *4* (8), 455-463.
194. Watson, D. S.; Szoka, F. C., Jr., Role of lipid structure in the humoral immune response in mice to covalent lipid-peptides from the membrane proximal region of HIV-1 gp41. *Vaccine* **2009,** *27* (34), 4672-83.
195. Knudsen, K. B.; Northeved, H.; Kumar Ek, P.; Permin, A.; Gjetting, T.; Andresen, T. L.; Larsen, S.; Wegener, K. M.; Lykkesfeldt, J.; Jantzen, K.; Loft, S.; Møller, P.; Roursgaard, M., In vivo toxicity of cationic micelles and liposomes. *Nanomedicine: Nanotechnology, Biology and Medicine* **2015,** *11* (2), 467-477.
196. Lappalainen, K.; Jääskeläinen, I.; Syrjänen, K.; Urtti, A.; Syrjänen, S., Comparison of Cell Proliferation and Toxicity Assays Using Two Cationic Liposomes. *Pharmaceutical research* **1994,** *11* (8), 1127-1131.
197. Gustafson, H. H.; Holt-Casper, D.; Grainger, D. W.; Ghandehari, H., Nanoparticle Uptake: The Phagocyte Problem. *Nano Today* **2015,** *10* (4), 487-510.
198. Rawat, K.; Kumari, P.; Saha, L., COVID-19 vaccine: A recent update in pipeline vaccines, their design and development strategies. *Eur J Pharmacol* **2021,** *892*, 173751-173751.
199. Lechanteur, A.; Sanna, V.; Duchemin, A.; Evrard, B.; Mottet, D.; Piel, G., Cationic Liposomes Carrying siRNA: Impact of Lipid Composition on Physicochemical

Properties, Cytotoxicity and Endosomal Escape. *Nanomaterials (Basel, Switzerland)* **2018,** *8* (5), 270.
200. Du, Z.; Munye, M. M.; Tagalakis, A. D.; Manunta, M. D. I.; Hart, S. L., The Role of the Helper Lipid on the DNA Transfection Efficiency of Lipopolyplex Formulations. *Scientific Reports* **2014,** *4* (1), 7107.
201. Walsh, C. L.; Nguyen, J.; Tiffany, M. R.; Szoka, F. C., Synthesis, Characterization, and Evaluation of Ionizable Lysine-Based Lipids for siRNA Delivery. *Bioconjugate Chemistry* **2013,** *24* (1), 36-43.
202. Zhang, J.; Fan, H.; Levorse, D. A.; Crocker, L. S., Ionization Behavior of Amino Lipids for siRNA Delivery: Determination of Ionization Constants, SAR, and the Impact of Lipid pKa on Cationic Lipid−Biomembrane Interactions. *Langmuir* **2011,** *27* (5), 1907-1914.
203. Nardo, D.; Henson, D.; Springer, J. E.; Venditto, V. J., Chapter six - Modulating the immune response with liposomal delivery. In *Nanomaterials for Clinical Applications*, Pippa, N.; Demetzos, C., Eds. Elsevier: 2020; pp 159-211.
204. Li, J.; Wang, X.; Zhang, T.; Wang, C.; Huang, Z.; Luo, X.; Deng, Y., A review on phospholipids and their main applications in drug delivery systems. *Asian Journal of Pharmaceutical Sciences* **2015,** *10* (2), 81-98.
205. Daraee, H.; Etemadi, A.; Kouhi, M.; Alimirzalu, S.; Akbarzadeh, A., Application of liposomes in medicine and drug delivery. *Artificial cells, nanomedicine, and biotechnology* **2016,** *44* (1), 381-91.
206. Bangham, A. D.; Horne, R. W., Negative staining of phospholipids and their structural modification by surface-active agents as observed in the electron microscope. *Journal of Molecular Biology* **1964,** *8* (5), 660-IN10.
207. Bangham, A. D.; Hill, M. W.; Miller, N. G. A., Preparation and Use of Liposomes as Models of Biological Membranes. In *Methods in Membrane Biology: Volume 1*, Korn, E. D., Ed. Springer US: Boston, MA, 1974; pp 1-68.
208. Torchilin, V.; Weissig, V., *Liposomes : a practical approach*. 2nd ed. / ed.; Oxford ; New York : Oxford University Press: 2003.
209. Cullis, P. R.; Hope, M. J., Lipid Nanoparticle Systems for Enabling Gene Therapies. *Molecular Therapy* **2017,** *25* (7), 1467-1475.
210. Watson, D. S.; Endsley, A. N.; Huang, L., Design considerations for liposomal vaccines: influence of formulation parameters on antibody and cell-mediated immune responses to liposome associated antigens. *Vaccine* **2012,** *30* (13), 2256-2272.
211. Marasini, N.; Ghaffar, K. A.; Skwarczynski, M.; Toth, I., Chapter Twelve - Liposomes as a Vaccine Delivery System. In *Micro and Nanotechnology in Vaccine Development*, Skwarczynski, M.; Toth, I., Eds. William Andrew Publishing: 2017; pp 221-239.
212. Christensen, D.; Korsholm, K. S.; Andersen, P.; Agger, E. M., Cationic liposomes as vaccine adjuvants. *Expert Review of Vaccines* **2011,** *10* (4), 513-521.
213. Watson, D. S.; Endsley, A. N.; Huang, L., Design considerations for liposomal vaccines: influence of formulation parameters on antibody and cell-mediated immune responses to liposome associated antigens. *Vaccine* **2012,** *30* (13), 2256-72.
214. Alving, C. R.; Beck, Z.; Karasavva, N.; Matyas, G. R.; Rao, M., HIV-1, lipid rafts, and antibodies to liposomes: implications for anti-viral-neutralizing antibodies. *Molecular membrane biology* **2006,** *23* (6), 453-65.

215. Ferguson, S. W.; Nguyen, J., Exosomes as therapeutics: The implications of molecular composition and exosomal heterogeneity. *Journal of controlled release : official journal of the Controlled Release Society* **2016,** *228*, 179-190.
216. Nisini, R.; Poerio, N.; Mariotti, S.; De Santis, F.; Fraziano, M., The Multirole of Liposomes in Therapy and Prevention of Infectious Diseases. *Front Immunol* **2018,** *9*, 155.
217. Kohli, A. G.; Kierstead, P. H.; Venditto, V. J.; Walsh, C. L.; Szoka, F. C., Designer lipids for drug delivery: from heads to tails. *Journal of controlled release : official journal of the Controlled Release Society* **2014,** *190*, 274-87.
218. Murphy, K.; Weaver, C., *Janeway's Immunobiology, 9th edition*. CRC Press: 2016.
219. Karumanchi, D. K.; Skrypai, Y.; Thomas, A.; Gaillard, E. R., Rational design of liposomes for sustained release drug delivery of bevacizumab to treat ocular angiogenesis. *Journal of Drug Delivery Science and Technology* **2018,** *47*, 275-282.
220. Subramanian, N.; Atsmon-Raz, Y.; Tieleman, P. D., Characterization of the Physiochemical Interactions between LNPs and the Endosomal Lipids: A Rational Design of Gene Delivery Systems. *Biophysical Journal* **2017,** *112* (3), 43a.
221. Semple, S. C.; Akinc, A.; Chen, J.; Sandhu, A. P.; Mui, B. L.; Cho, C. K.; Sah, D. W. Y.; Stebbing, D.; Crosley, E. J.; Yaworski, E.; Hafez, I. M.; Dorkin, J. R.; Qin, J.; Lam, K.; Rajeev, K. G.; Wong, K. F.; Jeffs, L. B.; Nechev, L.; Eisenhardt, M. L.; Jayaraman, M.; Kazem, M.; Maier, M. A.; Srinivasulu, M.; Weinstein, M. J.; Chen, Q.; Alvarez, R.; Barros, S. A.; De, S.; Klimuk, S. K.; Borland, T.; Kosovrasti, V.; Cantley, W. L.; Tam, Y. K.; Manoharan, M.; Ciufolini, M. A.; Tracy, M. A.; de Fougerolles, A.; MacLachlan, I.; Cullis, P. R.; Madden, T. D.; Hope, M. J., Rational design of cationic lipids for siRNA delivery. *Nature Biotechnology* **2010,** *28*, 172.
222. Gause, K. T.; Wheatley, A. K.; Cui, J.; Yan, Y.; Kent, S. J.; Caruso, F., Immunological Principles Guiding the Rational Design of Particles for Vaccine Delivery. *ACS Nano* **2017,** *11* (1), 54-68.
223. Schwendener, R. A., Liposomes as vaccine delivery systems: a review of the recent advances. *Therapeutic Advances in Vaccines* **2014,** *2* (6), 159-182.
224. Allison, A. G.; Gregoriadis, G., Liposomes as immunological adjuvants. *Nature* **1974,** *252* (5480), 252.
225. De Serrano, L. O.; Burkhart, D. J., Liposomal vaccine formulations as prophylactic agents: design considerations for modern vaccines. *Journal of nanobiotechnology* **2017,** *15* (1), 83-83.
226. Alving, C. R.; Beck, Z.; Matyas, G. R.; Rao, M., Liposomal adjuvants for human vaccines. *Expert opinion on drug delivery* **2016,** *13* (6), 807-16.
227. Teo, S. P., Review of COVID-19 mRNA Vaccines: BNT162b2 and mRNA-1273. *J Pharm Pract* **2021**, 8971900211009650.
228. Alving, C. R., Liposomes as carriers of antigens and adjuvants. *Journal of Immunological Methods* **1991,** *140* (1), 1-13.
229. Donnelly, J. J.; Wahren, B.; Liu, M. A., DNA vaccines: progress and challenges. *Journal of immunology (Baltimore, Md. : 1950)* **2005,** *175* (2), 633-9.
230. Boyle, J. S.; Silva, A.; Brady, J. L.; Lew, A. M., DNA immunization: induction of higher avidity antibody and effect of route on T cell cytotoxicity. *Proc Natl Acad Sci U S A* **1997,** *94* (26), 14626-31.

231. Buschmann, M. D.; Carrasco, M. J.; Alishetty, S.; Paige, M.; Alameh, M. G.; Weissman, D., Nanomaterial Delivery Systems for mRNA Vaccines. *Vaccines* **2021,** *9* (1), 65.
232. Tandrup Schmidt, S.; Foged, C.; Smith Korsholm, K.; Rades, T.; Christensen, D., Liposome-Based Adjuvants for Subunit Vaccines: Formulation Strategies for Subunit Antigens and Immunostimulators. *Pharmaceutics* **2016,** *8* (1), 7.
233. Shariat, S.; Badiee, A.; Jaafari, M. R.; Mortazavi, S. A., Optimization of a Method to Prepare Liposomes Containing HER2/Neu- Derived Peptide as a Vaccine Delivery System for Breast Cancer. *Iranian Journal of Pharmaceutical Research : IJPR* **2014,** *13* (Suppl), 15-25.
234. Eloy, J. O.; Claro de Souza, M.; Petrilli, R.; Barcellos, J. P.; Lee, R. J.; Marchetti, J. M., Liposomes as carriers of hydrophilic small molecule drugs: strategies to enhance encapsulation and delivery. *Colloids and surfaces. B, Biointerfaces* **2014,** *123*, 345-63.
235. Sur, S.; Fries, A. C.; Kinzler, K. W.; Zhou, S.; Vogelstein, B., Remote loading of preencapsulated drugs into stealth liposomes. *Proceedings of the National Academy of Sciences of the United States of America* **2014,** *111* (6), 2283-2288.
236. Hasson, S. S. A. A.; Al-Busaidi, J. K. Z.; Sallam, T. A., The past, current and future trends in DNA vaccine immunisations. *Asian Pacific Journal of Tropical Biomedicine* **2015,** *5* (5), 344-353.
237. Lee, L. Y. Y.; Izzard, L.; Hurt, A. C., A Review of DNA Vaccines Against Influenza. *Frontiers in immunology* **2018,** *9*, 1568-1568.
238. Pardi, N.; Hogan, M. J.; Porter, F. W.; Weissman, D., mRNA vaccines — a new era in vaccinology. *Nature Reviews Drug Discovery* **2018,** *17*, 261.
239. Bramson, J. L.; Bodner, C. A.; Graham, R. W., Activation of host antitumoral responses by cationic lipid/DNA complexes. *Cancer gene therapy* **2000,** *7* (3), 353-9.
240. Christensen, D.; Korsholm, K. S.; Rosenkrands, I.; Lindenstrom, T.; Andersen, P.; Agger, E. M., Cationic liposomes as vaccine adjuvants. *Expert Rev Vaccines* **2007,** *6* (5), 785-96.
241. Lonez, C.; Vandenbranden, M.; Ruysschaert, J. M., Cationic lipids activate intracellular signaling pathways. *Advanced drug delivery reviews* **2012,** *64* (15), 1749-58.
242. Liu, J.; Wu, J.; Wang, B.; Zeng, S.; Qi, F.; Lu, C.; Kimura, Y.; Liu, B., Oral vaccination with a liposome-encapsulated influenza DNA vaccine protects mice against respiratory challenge infection. *Journal of medical virology* **2014,** *86* (5), 886-94.
243. Rodriguez, A. E.; Zamorano, P.; Wilkowsky, S.; Torra, F.; Ferreri, L.; Dominguez, M.; Florin-Christensen, M., Delivery of recombinant vaccines against bovine herpesvirus type 1 gD and Babesia bovis MSA-2c to mice using liposomes derived from egg yolk lipids. *Veterinary journal (London, England : 1997)* **2013,** *196* (3), 550-1.
244. Shlapobersky, M.; Marshak, J. O.; Dong, L.; Huang, M.-l.; Wei, Q.; Chu, A.; Rolland, A.; Sullivan, S.; Koelle, D. M., Vaxfectin-adjuvanted plasmid DNA vaccine improves protection and immunogenicity in a murine model of genital herpes infection. *The Journal of general virology* **2012,** *93* (Pt 6), 1305-1315.
245. Lin, W.-H. W.; Vilalta, A.; Adams, R. J.; Rolland, A.; Sullivan, S. M.; Griffin, D. E., Vaxfectin adjuvant improves antibody responses of juvenile rhesus macaques to a

DNA vaccine encoding the measles virus hemagglutinin and fusion proteins. *Journal of virology* **2013,** *87* (12), 6560-6568.
246. Luo, K.; Zhang, H.; Zavala, F.; Biragyn, A.; Espinosa, D. A.; Markham, R. B., Fusion of antigen to a dendritic cell targeting chemokine combined with adjuvant yields a malaria DNA vaccine with enhanced protective capabilities. *PloS one* **2014,** *9* (3), e90413-e90413.
247. Kulkarni, V.; Rosati, M.; Valentin, A.; Jalah, R.; Alicea, C.; Yu, L.; Guan, Y.; Shen, X.; Tomaras, G. D.; LaBranche, C.; Montefiori, D. C.; Irene, C.; Prattipati, R.; Pinter, A.; Sullivan, S. M.; Pavlakis, G. N.; Felber, B. K., Vaccination with Vaxfectin(®) adjuvanted SIV DNA induces long-lasting humoral immune responses able to reduce SIVmac251 Viremia. *Human vaccines & immunotherapeutics* **2013,** *9* (10), 2069-2080.
248. Smith, L. R.; Wodal, W.; Crowe, B. A.; Kerschbaum, A.; Bruehl, P.; Schwendinger, M. G.; Savidis-Dacho, H.; Sullivan, S. M.; Shlapobersky, M.; Hartikka, J.; Rolland, A.; Barrett, P. N.; Kistner, O., Preclinical evaluation of Vaxfectin-adjuvanted Vero cell-derived seasonal split and pandemic whole virus influenza vaccines. *Human vaccines & immunotherapeutics* **2013,** *9* (6), 1333-1345.
249. Coban, C.; Koyama, S.; Takeshita, F.; Akira, S.; Ishii, K. J., Molecular and cellular mechanisms of DNA vaccines. *Hum Vaccin* **2008,** *4* (6), 453-6.
250. Scorza, F. B.; Pardi, N., New Kids on the Block: RNA-Based Influenza Virus Vaccines. *Vaccines* **2018,** *6* (2).
251. Li, Y.; Hu, Y.; Jin, Y.; Zhang, G.; Wong, J.; Sun, L. Q.; Wang, M., Prophylactic, therapeutic and immune enhancement effect of liposome-encapsulated PolyICLC on highly pathogenic H5N1 influenza infection. *The journal of gene medicine* **2011,** *13* (1), 60-72.
252. Meyer, M.; Huang, E.; Yuzhakov, O.; Ramanathan, P.; Ciaramella, G.; Bukreyev, A., Modified mRNA-Based Vaccines Elicit Robust Immune Responses and Protect Guinea Pigs From Ebola Virus Disease. *The Journal of infectious diseases* **2018,** *217* (3), 451-455.
253. Baptista, B.; Carapito, R.; Laroui, N.; Pichon, C.; Sousa, F., mRNA, a Revolution in Biomedicine. *Pharmaceutics* **2021,** *13* (12).
254. Liu, M. A., A Comparison of Plasmid DNA and mRNA as Vaccine Technologies. *Vaccines* **2019,** *7* (2), 37.
255. Tazina, E.; Kostin, K.; Oborotova, N., Specific features of drug encapsulation in liposomes (A review). *Pharmaceutical Chemistry Journal* **2011,** *45* (8), 481-490.
256. Ventola, C. L., Progress in Nanomedicine: Approved and Investigational Nanodrugs. *Pharmacy and Therapeutics* **2017,** *42* (12), 742-755.
257. Song, G.; Wu, H.; Yoshino, K.; Zamboni, W. C., Factors affecting the pharmacokinetics and pharmacodynamics of liposomal drugs. *Journal of Liposome Research* **2012,** *22* (3), 177-192.
258. Bulbake, U.; Doppalapudi, S.; Kommineni, N.; Khan, W., Liposomal Formulations in Clinical Use: An Updated Review. *Pharmaceutics* **2017,** *9* (2).
259. Barenholz, Y., Doxil(R)--the first FDA-approved nano-drug: lessons learned. *Journal of controlled release : official journal of the Controlled Release Society* **2012,** *160* (2), 117-34.

260. Gabizon, A.; Catane, R.; Uziely, B.; Kaufman, B.; Safra, T.; Cohen, R.; Martin, F.; Huang, A.; Barenholz, Y., Prolonged Circulation Time and Enhanced Accumulation in Malignant Exudates of Doxorubicin Encapsulated in Polyethylene-glycol Coated Liposomes. *Cancer research* **1994,** *54* (4), 987-992.
261. Northfelt, D. W.; Martin, F. J.; Working, P.; Volberding, P. A.; Russell, J.; Newman, M.; Amantea, M. A.; Kaplan, L. D., Doxorubicin encapsulated in liposomes containing surface-bound polyethylene glycol: pharmacokinetics, tumor localization, and safety in patients with AIDS-related Kaposi's sarcoma. *Journal of clinical pharmacology* **1996,** *36* (1), 55-63.
262. Northfelt, D. W.; Dezube, B. J.; Thommes, J. A.; Miller, B. J.; Fischl, M. A.; Friedman-Kien, A.; Kaplan, L. D.; Du Mond, C.; Mamelok, R. D.; Henry, D. H., Pegylated-liposomal doxorubicin versus doxorubicin, bleomycin, and vincristine in the treatment of AIDS-related Kaposi's sarcoma: results of a randomized phase III clinical trial. *Journal of Clinical Oncology* **1998,** *16* (7), 2445-2451.
263. Kierstead, P. H.; Okochi, H.; Venditto, V. J.; Chuong, T. C.; Kivimae, S.; Frechet, J. M. J.; Szoka, F. C., The effect of polymer backbone chemistry on the induction of the accelerated blood clearance in polymer modified liposomes. *Journal of controlled release : official journal of the Controlled Release Society* **2015,** *213*, 1-9.
264. Dams, E. T. M.; Laverman, P.; Oyen, W. J. G.; Storm, G.; Scherphof, G. L.; van der Meer, J. W. M.; Corstens, F. H. M.; Boerman, O. C., Accelerated Blood Clearance and Altered Biodistribution of Repeated Injections of Sterically Stabilized Liposomes. *Journal of Pharmacology and Experimental Therapeutics* **2000,** *292* (3), 1071.
265. Ishida, T.; Atobe, K.; Wang, X.; Kiwada, H., Accelerated blood clearance of PEGylated liposomes upon repeated injections: effect of doxorubicin-encapsulation and high-dose first injection. *Journal of controlled release : official journal of the Controlled Release Society* **2006,** *115* (3), 251-8.
266. Besin, G.; Milton, J.; Sabnis, S.; Howell, R.; Mihai, C.; Burke, K.; Benenato, K. E.; Stanton, M.; Smith, P.; Senn, J.; Hoge, S., Accelerated Blood Clearance of Lipid Nanoparticles Entails a Biphasic Humoral Response of B-1 Followed by B-2 Lymphocytes to Distinct Antigenic Moieties. *ImmunoHorizons* **2019,** *3* (7), 282.
267. Laverman, P.; Carstens, M. G.; Boerman, O. C.; Dams, E. T.; Oyen, W. J.; van Rooijen, N.; Corstens, F. H.; Storm, G., Factors affecting the accelerated blood clearance of polyethylene glycol-liposomes upon repeated injection. *The Journal of pharmacology and experimental therapeutics* **2001,** *298* (2), 607-12.
268. Oja, C.; Tardi, P.; Schutze-Redelmeier, M.; Cullis, P. R., Doxorubicin entrapped within liposome-associated antigens results in a selective inhibition of the antibody response to the linked antigen. *Biochimica et biophysica acta* **2000,** *1468* (1-2), 31-40.
269. Tardi, P. G.; Swartz, E. N.; Harasym, T. O.; Cullis, P. R.; Bally, M. B., An immune response to ovalbumin covalently coupled to liposomes is prevented when the liposomes used contain doxorubicin. *Journal of immunological methods* **1997,** *210* (2), 137-48.
270. Shimizu, K.; Miyauchi, H.; Urakami, T.; Yamamura-Ichikawa, K.; Yonezawa, S.; Asai, T.; Oku, N., Specific delivery of an immunosuppressive drug to splenic B cells by antigen-modified liposomes and its antiallergic effect. *Journal of drug targeting* **2016,** *24* (9), 890-895.

271. Shek, P. N.; Lopez, N. G.; Heath, T. D., Immune response mediated by liposome-associated protein antigens. IV. Modulation of antibody formation by vesicle-encapsulated methotrexate. *Immunology* **1986,** *57* (1), 153-7.
272. van Rooijen, N.; van Nieuwmegen, R., Elimination of phagocytic cells in the spleen after intravenous injection of liposome-encapsulated dichloromethylene diphosphonate. An enzyme-histochemical study. *Cell and tissue research* **1984,** *238* (2), 355-8.
273. Van Rooijen, N.; Sanders, A., Liposome mediated depletion of macrophages: mechanism of action, preparation of liposomes and applications. *Journal of immunological methods* **1994,** *174* (1-2), 83-93.
274. Alves-Rosa, F.; Stanganelli, C.; Cabrera, J.; van Rooijen, N.; Palermo, M. S.; Isturiz, M. A., Treatment with liposome-encapsulated clodronate as a new strategic approach in the management of immune thrombocytopenic purpura in a mouse model. *Blood* **2000,** *96* (8), 2834-40.
275. Jordan, M. B.; van Rooijen, N.; Izui, S.; Kappler, J.; Marrack, P., Liposomal clodronate as a novel agent for treating autoimmune hemolytic anemia in a mouse model. *Blood* **2003,** *101* (2), 594-601.
276. Richards, P. J.; Williams, A. S.; Goodfellow, R. M.; Williams, B. D., Liposomal clodronate eliminates synovial macrophages, reduces inflammation and ameliorates joint destruction in antigen-induced arthritis. *Rheumatology* **1999,** *38* (9), 818-825.
277. Richards, P. J.; Williams, B. D.; Williams, A. S., Suppression of chronic streptococcal cell wall-induced arthritis in Lewis rats by liposomal clodronate. *Rheumatology (Oxford, England)* **2001,** *40* (9), 978-87.
278. Huitinga, I.; van Rooijen, N.; de Groot, C. J.; Uitdehaag, B. M.; Dijkstra, C. D., Suppression of experimental allergic encephalomyelitis in Lewis rats after elimination of macrophages. *J Exp Med* **1990,** *172* (4), 1025-33.
279. Allen, T. M.; Hansen, C. B.; Guo, L. S. S., Subcutaneous administration of liposomes: a comparison with the intravenous and intraperitoneal routes of injection. *Biochimica et Biophysica Acta (BBA) - Biomembranes* **1993,** *1150* (1), 9-16.
280. Riley, M. K.; Vermerris, W., Recent Advances in Nanomaterials for Gene Delivery-A Review. *Nanomaterials (Basel, Switzerland)* **2017,** *7* (5).
281. Wood, H., FDA approves patisiran to treat hereditary transthyretin amyloidosis. *Nature reviews. Neurology* **2018,** *14* (10), 570.
282. Yin, H.; Kanasty, R. L.; Eltoukhy, A. A.; Vegas, A. J.; Dorkin, J. R.; Anderson, D. G., Non-viral vectors for gene-based therapy. *Nature reviews. Genetics* **2014,** *15* (8), 541-55.
283. Kanasty, R.; Dorkin, J. R.; Vegas, A.; Anderson, D., Delivery materials for siRNA therapeutics. *Nature Materials* **2013,** *12*, 967.
284. Zhao, Y.; Huang, L., Lipid Nanoparticles for Gene Delivery. *Advances in genetics* **2014,** *88*, 13-36.
285. Chakraborty, C.; Sharma, A. R.; Sharma, G.; Doss, C. G. P.; Lee, S.-S., Therapeutic miRNA and siRNA: Moving from Bench to Clinic as Next Generation Medicine. *Molecular Therapy. Nucleic Acids* **2017,** *8*, 132-143.
286. Second RNAi drug approved. *Nature Biotechnology* **2020,** *38* (4), 385-385.

287. Lv, H.; Zhang, S.; Wang, B.; Cui, S.; Yan, J., Toxicity of cationic lipids and cationic polymers in gene delivery. *Journal of Controlled Release* **2006,** *114* (1), 100-109.
288. Kaczmarek, J. C.; Kowalski, P. S.; Anderson, D. G., Advances in the delivery of RNA therapeutics: from concept to clinical reality. *Genome Medicine* **2017,** *9* (1), 60.
289. Garber, K., Worth the RISC? *Nature Biotechnology* **2017,** *35*, 198.
290. Zhang, S.; Xu, Y.; Wang, B.; Qiao, W.; Liu, D.; Li, Z., Cationic compounds used in lipoplexes and polyplexes for gene delivery. *Journal of Controlled Release* **2004,** *100* (2), 165-180.
291. Zabner, J., Cationic lipids used in gene transfer. *Advanced drug delivery reviews* **1997,** *27* (1), 17-28.
292. Al-Dosari, M. S.; Gao, X., Nonviral Gene Delivery: Principle, Limitations, and Recent Progress. *The AAPS journal* **2009,** *11* (4), 671.
293. Ramamoorth, M.; Narvekar, A., Non Viral Vectors in Gene Therapy- An Overview. *Journal of Clinical and Diagnostic Research : JCDR* **2015,** *9* (1), GE01-GE06.
294. Candiani, G., *Non-Viral Gene Delivery Vectors Methods and Protocols*. Humana Press: New York, 2016; Vol. 1, p 290.
295. Ulmer, J. B.; Geall, A. J., Recent innovations in mRNA vaccines. *Curr Opin Immunol* **2016,** *41*, 18-22.
296. Pardi, N.; Hogan, M. J.; Pelc, R. S.; Muramatsu, H.; Andersen, H.; DeMaso, C. R.; Dowd, K. A.; Sutherland, L. L.; Scearce, R. M.; Parks, R.; Wagner, W.; Granados, A.; Greenhouse, J.; Walker, M.; Willis, E.; Yu, J. S.; McGee, C. E.; Sempowski, G. D.; Mui, B. L.; Tam, Y. K.; Huang, Y. J.; Vanlandingham, D.; Holmes, V. M.; Balachandran, H.; Sahu, S.; Lifton, M.; Higgs, S.; Hensley, S. E.; Madden, T. D.; Hope, M. J.; Kariko, K.; Santra, S.; Graham, B. S.; Lewis, M. G.; Pierson, T. C.; Haynes, B. F.; Weissman, D., Zika virus protection by a single low-dose nucleoside-modified mRNA vaccination. *Nature* **2017,** *543* (7644), 248-251.
297. Pardi, N.; Tuyishime, S.; Muramatsu, H.; Kariko, K.; Mui, B. L.; Tam, Y. K.; Madden, T. D.; Hope, M. J.; Weissman, D., Expression kinetics of nucleoside-modified mRNA delivered in lipid nanoparticles to mice by various routes. *Journal of controlled release : official journal of the Controlled Release Society* **2015,** *217*, 345-351.
298. Song, X.; Wang, X.; Ma, Y.; Liang, Z.; Yang, Z.; Cao, H., Site-Specific Modification Using the 2'-Methoxyethyl Group Improves the Specificity and Activity of siRNAs. *Mol Ther Nucleic Acids* **2017,** *9*, 242-250.
299. Deleavey, G. F.; Watts, J. K.; Damha, M. J., Chemical modification of siRNA. *Current protocols in nucleic acid chemistry* **2009,** *Chapter 16*, Unit 16.3.
300. Wasungu, L.; Hoekstra, D., Cationic lipids, lipoplexes and intracellular delivery of genes. *Journal of Controlled Release* **2006,** *116* (2), 255-264.
301. Huth, U. S.; Schubert, R.; Peschka-Süss, R., Investigating the uptake and intracellular fate of pH-sensitive liposomes by flow cytometry and spectral bio-imaging. *Journal of Controlled Release* **2006,** *110* (3), 490-504.
302. Allen, T. M.; Cullis, P. R., Liposomal drug delivery systems: from concept to clinical applications. *Advanced drug delivery reviews* **2013,** *65* (1), 36-48.

303. Heath, T. D.; Lopez, N. G.; Papahadjopoulos, D., The effects of liposome size and surface charge on liposome-mediated delivery of methotrexate-gamma-aspartate to cells in vitro. *Biochimica et biophysica acta* **1985,** *820* (1), 74-84.
304. Dan, N.; Danino, D., Structure and kinetics of lipid–nucleic acid complexes. *Advances in Colloid and Interface Science* **2014,** *205*, 230-239.
305. Koynova, R., Analysis of Lipoplex Structure and Lipid Phase Changes. In *Liposomes: Methods and Protocols, Volume 2: Biological Membrane Models*, Weissig, V., Ed. Humana Press: Totowa, NJ, 2010; pp 399-423.
306. Gershon, H.; Ghirlando, R.; Guttman, S. B.; Minsky, A., Mode of formation and structural features of DNA-cationic liposome complexes used for transfection. *Biochemistry* **1993,** *32* (28), 7143-51.
307. Meunier-Durmort, C.; Picart, R.; Ragot, T.; Perricaudet, M.; Hainque, B.; Forest, C., Mechanism of adenovirus improvement of cationic liposome-mediated gene transfer. *Biochimica et Biophysica Acta (BBA) - Biomembranes* **1997,** *1330* (1), 8-16.
308. Nemerow, G. R.; Stewart, P. L., Insights into Adenovirus Uncoating from Interactions with Integrins and Mediators of Host Immunity. *Viruses* **2016,** *8* (12), 337.
309. Claassen, E., Detection, localization and kinetics of immunomodulating liposomes in vivo. *Research in Immunology* **1992,** *143* (2), 235-241.
310. Byrne, J. D.; Betancourt, T.; Brannon-Peppas, L., Active targeting schemes for nanoparticle systems in cancer therapeutics. *Advanced drug delivery reviews* **2008,** *60* (15), 1615-26.
311. Kullberg, M.; McCarthy, R.; Anchordoquy, T. J., Gene delivery to Her-2+ breast cancer cells using a two-component delivery system to achieve specificity. *Nanomedicine : nanotechnology, biology, and medicine* **2014,** *10* (6), 1253-62.
312. Hafez, I. M.; Maurer, N.; Cullis, P. R., On the mechanism whereby cationic lipids promote intracellular delivery of polynucleic acids. *Gene therapy* **2001,** *8* (15), 1188-96.
313. Sørensen, D. R.; Leirdal, M.; Sioud, M., Gene Silencing by Systemic Delivery of Synthetic siRNAs in Adult Mice. *Journal of Molecular Biology* **2003,** *327* (4), 761-766.
314. Zhang, Y.; Cristofaro, P.; Silbermann, R.; Pusch, O.; Boden, D.; Konkin, T.; Hovanesian, V.; Monfils, P. R.; Resnick, M.; Moss, S. F.; Ramratnam, B., Engineering mucosal RNA interference in vivo. *Molecular therapy : the journal of the American Society of Gene Therapy* **2006,** *14* (3), 336-42.
315. Aldayel, A. M.; O'Mary, H. L.; Valdes, S. A.; Li, X.; Thakkar, S. G.; Mustafa, B. E.; Cui, Z., Lipid nanoparticles with minimum burst release of TNF-α siRNA show strong activity against rheumatoid arthritis unresponsive to methotrexate. *Journal of Controlled Release* **2018,** *283*, 280-289.
316. Peer, D.; Park, E. J.; Morishita, Y.; Carman, C. V.; Shimaoka, M., Systemic leukocyte-directed siRNA delivery revealing cyclin D1 as an anti-inflammatory target. *Science (New York, N.Y.)* **2008,** *319* (5863), 627-30.
317. Katakowski, J. A.; Mukherjee, G.; Wilner, S. E.; Maier, K. E.; Harrison, M. T.; DiLorenzo, T. P.; Levy, M.; Palliser, D., Delivery of siRNAs to Dendritic Cells Using DEC205-Targeted Lipid Nanoparticles to Inhibit Immune Responses. *Molecular therapy : the journal of the American Society of Gene Therapy* **2016,** *24* (1), 146-55.
318. Feinberg, M. W.; Moore, K. J., MicroRNA Regulation of Atherosclerosis. *Circulation research* **2016,** *118* (4), 703-20.

319. Tessitore, A.; Cicciarelli, G.; Mastroiaco, V.; Vecchio, F. D.; Capece, D.; Verzella, D.; Fischietti, M.; Vecchiotti, D.; Zazzeroni, F.; Alesse, E., Therapeutic Use of MicroRNAs in Cancer. *Anti-cancer agents in medicinal chemistry* **2016,** *16* (1), 7-19.
320. Wang, W.-X.; Sullivan, P. G.; Springer, J. E., Mitochondria and microRNA crosstalk in traumatic brain injury. *Progress in Neuro-Psychopharmacology and Biological Psychiatry* **2017,** *73*, 104-108.
321. Wang, W.-X.; Springer, J. E., Role of mitochondria in regulating microRNA activity and its relevance to the central nervous system. *Neural regeneration research* **2015,** *10* (7), 1026-1028.
322. Lesizza, P.; Prosdocimo, G.; Martinelli, V.; Sinagra, G.; Zacchigna, S.; Giacca, M., Single-Dose Intracardiac Injection of Pro-Regenerative MicroRNAs Improves Cardiac Function After Myocardial Infarction. *Circulation research* **2017,** *120* (8), 1298-1304.
323. Ghatak, S.; Li, J.; Chan, Y. C.; Gnyawali, S. C.; Steen, E.; Yung, B. C.; Khanna, S.; Roy, S.; Lee, R. J.; Sen, C. K., AntihypoxamiR functionalized gramicidin lipid nanoparticles rescue against ischemic memory improving cutaneous wound healing. *Nanomedicine : nanotechnology, biology, and medicine* **2016,** *12* (7), 1827-1831.
324. Dinh, T. D.; Higuchi, Y.; Kawakami, S.; Yamashita, F.; Hashida, M., Evaluation of Osteoclastogenesis via NFκB Decoy/mannosylated Cationic Liposome-Mediated Inhibition of Pro-inflammatory Cytokine Production from Primary Cultured Macrophages. *Pharmaceutical research* **2011,** *28* (4), 742-751.
325. Wijagkanalan, W.; Kawakami, S.; Higuchi, Y.; Yamashita, F.; Hashida, M., Intratracheally instilled mannosylated cationic liposome/NFκB decoy complexes for effective prevention of LPS-induced lung inflammation. *Journal of Controlled Release* **2011,** *149* (1), 42-50.
326. Iwata, A.; Sai, S.; Nitta, Y.; Chen, M.; de Fries-Hallstrand, R.; Dalesandro, J.; Thomas, R.; Allen, M. D., Liposome-mediated gene transfection of endothelial nitric oxide synthase reduces endothelial activation and leukocyte infiltration in transplanted hearts. *Circulation* **2001,** *103* (22), 2753-9.
327. Chen, F.; Date, H., Update on ischemia-reperfusion injury in lung transplantation. *Current opinion in organ transplantation* **2015,** *20* (5), 515-20.
328. Guan, L.-Y.; Fu, P.-Y.; Li, P.-D.; Li, Z.-N.; Liu, H.-Y.; Xin, M.-G.; Li, W., Mechanisms of hepatic ischemia-reperfusion injury and protective effects of nitric oxide. *World journal of gastrointestinal surgery* **2014,** *6* (7), 122-128.
329. Furukawa, H.; Oshima, K.; Tung, T.; Cui, G.; Laks, H.; Sen, L., Liposome-Mediated Combinatorial Cytokine Gene Therapy Induces Localized Synergistic Immunosuppression and Promotes Long-Term Survival of Cardiac Allografts. *The Journal of Immunology* **2005,** *174* (11), 6983-6992.
330. Furukawa, H.; Oshima, K.; Tung, T.; Cui, G.; Laks, H.; Sen, L., Overexpressed Exogenous IL-4 And IL-10 Paradoxically Regulate Allogenic T-Cell and Cardiac Myocytes Apoptosis Through FAS/FASL Pathway. *Transplantation* **2008,** *85* (3), 437-446.
331. Tung, T. C.; Oshima, K.; Cui, G.; Laks, H.; Sen, L., Dual upregulation of Fas and Bax promotes alloreactive T cell apoptosis in IL-10 gene targeting of cardiac allografts. *American Journal of Physiology-Heart and Circulatory Physiology* **2003,** *285* (3), H964-H973.

332. Sen, L.; Hong, Y.-S.; Luo, H.; Cui, G.; Laks, H., Efficiency, efficacy, and adverse effects of adenovirus- vs. liposome-mediated gene therapy in cardiac allografts. *American Journal of Physiology-Heart and Circulatory Physiology* **2001,** *281* (3), H1433-H1441.
333. Oshima, K.; Sen, L.; Cui, G.; Tung, T.; Sacks, B. M.; Arellano-Kruse, A.; Laks, H., Localized interleukin-10 gene transfer induces apoptosis of alloreactive T cells via FAS/FASL pathway, improves function, and prolongs survival of cardiac allograft. *Transplantation* **2002,** *73* (7), 1019-1026.
334. Fabrega, A. J.; Fasbender, A. J.; Struble, S.; Zabner, J., Cationic lipid-mediated transfer of the hIL-10 gene prolongs survival of allogenic hepatocytes in nagase analmunemic rats. *Transplantation* **1996,** *62* (12), 1866-1871.
335. Duguay, B. A.; Huang, K. W.-C.; Kulka, M., Lipofection of plasmid DNA into human mast cell lines using lipid nanoparticles generated by microfluidic mixing. *Journal of Leukocyte Biology* **2018,** *104* (3), 587-596.
336. Gregoriadis, G., Liposomes in Drug Delivery: How It All Happened. *Pharmaceutics* **2016,** *8* (2), 19.
337. Chappuis, F.; Farinelli, T.; Deckx, H.; Sarnecki, M.; Go, O.; Salzgeber, Y.; Stals, C., Immunogenicity and estimation of antibody persistence following vaccination with an inactivated virosomal hepatitis A vaccine in adults: A 20-year follow-up study. *Vaccine* **2017,** *35* (10), 1448-1454.
338. Lim, J.; Song, Y. J.; Park, W. S.; Sohn, H.; Lee, M. S.; Shin, D. H.; Kim, C. B.; Kim, H.; Oh, G. J.; Ki, M., The immunogenicity of a single dose of hepatitis A virus vaccines (Havrix(R) and Epaxal(R)) in Korean young adults. *Yonsei medical journal* **2014,** *55* (1), 126-31.
339. Gasparini, R.; Amicizia, D.; Lai, P. L.; Rossi, S.; Panatto, D., Effectiveness of adjuvanted seasonal influenza vaccines (Inflexal V (R) and Fluad (R)) in preventing hospitalization for influenza and pneumonia in the elderly: a matched case-control study. *Human vaccines & immunotherapeutics* **2013,** *9* (1), 144-52.
340. Herzog, C.; Hartmann, K.; Kunzi, V.; Kursteiner, O.; Mischler, R.; Lazar, H.; Gluck, R., Eleven years of Inflexal V-a virosomal adjuvanted influenza vaccine. *Vaccine* **2009,** *27* (33), 4381-7.
341. Saraswat, A.; Agarwal, R.; Katare, O. P.; Kaur, I.; Kumar, B., A randomized, double-blind, vehicle-controlled study of a novel liposomal dithranol formulation in psoriasis. *J Dermatolog Treat* **2007,** *18* (1), 40-5.
342. Adams, D.; Gonzalez-Duarte, A.; O'Riordan, W. D.; Yang, C. C.; Ueda, M.; Kristen, A. V.; Tournev, I.; Schmidt, H. H.; Coelho, T.; Berk, J. L.; Lin, K. P.; Vita, G.; Attarian, S.; Plante-Bordeneuve, V.; Mezei, M. M.; Campistol, J. M.; Buades, J.; Brannagan, T. H., 3rd; Kim, B. J.; Oh, J.; Parman, Y.; Sekijima, Y.; Hawkins, P. N.; Solomon, S. D.; Polydefkis, M.; Dyck, P. J.; Gandhi, P. J.; Goyal, S.; Chen, J.; Strahs, A. L.; Nochur, S. V.; Sweetser, M. T.; Garg, P. P.; Vaishnaw, A. K.; Gollob, J. A.; Suhr, O. B., Patisiran, an RNAi Therapeutic, for Hereditary Transthyretin Amyloidosis. *The New England journal of medicine* **2018,** *379* (1), 11-21.
343. Nardo, D.; Akers, C. M.; Cheung, N. E.; Isom, C. M.; Spaude, J. T.; Pack, D. W.; Venditto, V. J., Cyanuric chloride as the basis for compositionally diverse lipids. *RSC Adv* **2021,** *11* (40), 24752-24761.

344. Molla, M. R.; Böser, A.; Rana, A.; Schwarz, K.; Levkin, P. A., One-Pot Parallel Synthesis of Lipid Library via Thiolactone Ring Opening and Screening for Gene Delivery. *Bioconjugate Chemistry* **2018,** *29* (4), 992-999.
345. Zhou, C. Y.; Wu, H.; Devaraj, N. K., Rapid access to phospholipid analogs using thiol-yne chemistry. *Chemical science* **2015,** *6* (7), 4365-4372.
346. Alabi, C. A.; Love, K. T.; Sahay, G.; Yin, H.; Luly, K. M.; Langer, R.; Anderson, D. G., Multiparametric approach for the evaluation of lipid nanoparticles for siRNA delivery. *Proceedings of the National Academy of Sciences* **2013,** *110* (32), 12881-12886.
347. Miao, L.; Li, L.; Huang, Y.; Delcassian, D.; Chahal, J.; Han, J.; Shi, Y.; Sadtler, K.; Gao, W.; Lin, J.; Doloff, J. C.; Langer, R.; Anderson, D. G., Delivery of mRNA vaccines with heterocyclic lipids increases anti-tumor efficacy by STING-mediated immune cell activation. *Nature Biotechnology* **2019,** *37* (10), 1174-1185.
348. Watson, D. S.; Platt, V. M.; Cao, L.; Venditto, V. J.; Szoka, F. C., Antibody Response to Polyhistidine-Tagged Peptide and Protein Antigens Attached to Liposomes via Lipid-Linked Nitrilotriacetic Acid in Mice. *Clinical and Vaccine Immunology* **2011,** *18* (2), 289-297.
349. Alving, C. R.; Rao, M.; Steers, N. J.; Matyas, G. R.; Mayorov, A. V., Liposomes containing lipid A: an effective, safe, generic adjuvant system for synthetic vaccines. *Expert Rev Vaccines* **2012,** *11* (6), 733-44.
350. Fujii, G.; Ernst, W.; Adler-Moore, J., The VesiVax system: a method for rapid vaccine development. *Frontiers in bioscience : a journal and virtual library* **2008,** *13*, 1968-80.
351. Simanek, E. E.; Abdou, H.; Lalwani, S.; Lim, J.; Mintzer, M.; Venditto, V. J.; Vittur, B., The 8 year thicket of triazine dendrimers: strategies, targets and applications. *Proceedings of the Royal Society A: Mathematical, Physical and Engineering Sciences* **2010,** *466* (2117), 1445-1468.
352. Candiani, G.; Frigerio, M.; Viani, F.; Verpelli, C.; Sala, C.; Chiamenti, L.; Zaffaroni, N.; Folini, M.; Sani, M.; Panzeri, W.; Zanda, M., Dimerizable redox-sensitive triazine-based cationic lipids for in vitro gene delivery. *ChemMedChem* **2007,** *2* (3), 292-6.
353. Merkel, O. M.; Mintzer, M. A.; Librizzi, D.; Samsonova, O.; Dicke, T.; Sproat, B.; Garn, H.; Barth, P. J.; Simanek, E. E.; Kissel, T., Triazine dendrimers as nonviral vectors for in vitro and in vivo RNAi: the effects of peripheral groups and core structure on biological activity. *Molecular pharmaceutics* **2010,** *7* (4), 969-83.
354. Watrelot, A. A.; Tran, D. T.; Buffeteau, T.; Deffieux, D.; Le Bourvellec, C.; Quideau, S.; Renard, C. M. G. C., Immobilization of flavan-3-ols onto sensor chips to study their interactions with proteins and pectins by SPR. *Applied Surface Science* **2016,** *371*, 512-518.
355. Ralston, E.; Hjelmeland, L. M.; Klausner, R. D.; Weinstein, J. N.; Blumenthal, R., Carboxyfluorescein as a probe for liposome-cell interactions effect of impurities, and purification of the dye. *Biochimica et Biophysica Acta (BBA) - Biomembranes* **1981,** *649* (1), 133-137.
356. Weinstein, J. N.; Blumenthal, R.; Klausner, R. D., Carboxyfluorescein leakage assay for lipoprotein-liposome interaction. *Methods in enzymology* **1986,** *128*, 657-68.

357. Jayaraman, M.; Ansell, S. M.; Mui, B. L.; Tam, Y. K.; Chen, J.; Du, X.; Butler, D.; Eltepu, L.; Matsuda, S.; Narayanannair, J. K.; Rajeev, K. G.; Hafez, I. M.; Akinc, A.; Maier, M. A.; Tracy, M. A.; Cullis, P. R.; Madden, T. D.; Manoharan, M.; Hope, M. J., Maximizing the potency of siRNA lipid nanoparticles for hepatic gene silencing in vivo. *Angew Chem Int Ed Engl* **2012,** *51* (34), 8529-8533.
358. Akbar, M. A.; Nardo, D.; Chen, M. J.; Elshikha, A. S.; Ahamed, R.; Elsayed, E. M.; Bigot, C.; Holliday, L. S.; Song, S., Alpha-1 antitrypsin inhibits RANKL-induced osteoclast formation and functions. *Molecular medicine (Cambridge, Mass.)* **2017,** *23*, 57-69.
359. Pineda-Torra, I.; Gage, M.; de Juan, A.; Pello, O. M., Isolation, Culture, and Polarization of Murine Bone Marrow-Derived and Peritoneal Macrophages. *Methods in molecular biology (Clifton, N.J.)* **2015,** *1339*, 101-9.
360. Pitts, M. G.; Nardo, D.; Isom, C. M.; Venditto, V. J., Autoantibody Responses to Apolipoprotein A-I Are Not Diet- or Sex-Linked in C57BL/6 Mice. *ImmunoHorizons* **2020,** *4* (8), 455-463.
361. Watson, D. S.; Szoka, F. C., Jr., Role of lipid structure in the humoral immune response in mice to covalent lipid-peptides from the membrane proximal region of HIV-1 gp41. *Vaccine* **2009,** *27* (34), 4672-83.
362. Knudsen, K. B.; Northeved, H.; Kumar Ek, P.; Permin, A.; Gjetting, T.; Andresen, T. L.; Larsen, S.; Wegener, K. M.; Lykkesfeldt, J.; Jantzen, K.; Loft, S.; Møller, P.; Roursgaard, M., In vivo toxicity of cationic micelles and liposomes. *Nanomedicine: Nanotechnology, Biology and Medicine* **2015,** *11* (2), 467-477.
363. Lappalainen, K.; Jääskeläinen, I.; Syrjänen, K.; Urtti, A.; Syrjänen, S., Comparison of Cell Proliferation and Toxicity Assays Using Two Cationic Liposomes. *Pharmaceutical research* **1994,** *11* (8), 1127-1131.
364. Gustafson, H. H.; Holt-Casper, D.; Grainger, D. W.; Ghandehari, H., Nanoparticle Uptake: The Phagocyte Problem. *Nano Today* **2015,** *10* (4), 487-510.
365. Rawat, K.; Kumari, P.; Saha, L., COVID-19 vaccine: A recent update in pipeline vaccines, their design and development strategies. *Eur J Pharmacol* **2021,** *892*, 173751-173751.
366. Lechanteur, A.; Sanna, V.; Duchemin, A.; Evrard, B.; Mottet, D.; Piel, G., Cationic Liposomes Carrying siRNA: Impact of Lipid Composition on Physicochemical Properties, Cytotoxicity and Endosomal Escape. *Nanomaterials (Basel, Switzerland)* **2018,** *8* (5), 270.
367. Du, Z.; Munye, M. M.; Tagalakis, A. D.; Manunta, M. D. I.; Hart, S. L., The Role of the Helper Lipid on the DNA Transfection Efficiency of Lipopolyplex Formulations. *Scientific Reports* **2014,** *4* (1), 7107.
368. Walsh, C. L.; Nguyen, J.; Tiffany, M. R.; Szoka, F. C., Synthesis, Characterization, and Evaluation of Ionizable Lysine-Based Lipids for siRNA Delivery. *Bioconjugate Chemistry* **2013,** *24* (1), 36-43.
369. Zhang, J.; Fan, H.; Levorse, D. A.; Crocker, L. S., Ionization Behavior of Amino Lipids for siRNA Delivery: Determination of Ionization Constants, SAR, and the Impact of Lipid pKa on Cationic Lipid−Biomembrane Interactions. *Langmuir* **2011,** *27* (5), 1907-1914.
370. Hou, X.; Zaks, T.; Langer, R.; Dong, Y., Lipid nanoparticles for mRNA delivery. *Nature Reviews Materials* **2021,** *6* (12), 1078-1094.

371. Hirko, A.; Tang, F.; Hughes, J. A., Cationic lipid vectors for plasmid DNA delivery. *Curr Med Chem* **2003,** *10* (14), 1185-93.
372. Pennetta, C.; Bono, N.; Ponti, F.; Bellucci, M. C.; Viani, F.; Candiani, G.; Volonterio, A., Multifunctional Neomycin-Triazine-Based Cationic Lipids for Gene Delivery with Antibacterial Properties. *Bioconjugate Chemistry* **2021,** *32* (4), 690-701.
373. Akbar, M. A.; Cao, J. J.; Lu, Y.; Nardo, D.; Chen, M. J.; Elshikha, A. S.; Ahamed, R.; Brantly, M.; Holliday, L. S.; Song, S., Alpha-1 Antitrypsin Gene Therapy Ameliorates Bone Loss in Ovariectomy-Induced Osteoporosis Mouse Model. *Hum Gene Ther* **2016,** *27* (9), 679-86.
374. Geall, A. J.; Verma, A.; Otten, G. R.; Shaw, C. A.; Hekele, A.; Banerjee, K.; Cu, Y.; Beard, C. W.; Brito, L. A.; Krucker, T.; O'Hagan, D. T.; Singh, M.; Mason, P. W.; Valiante, N. M.; Dormitzer, P. R.; Barnett, S. W.; Rappuoli, R.; Ulmer, J. B.; Mandl, C. W., Nonviral delivery of self-amplifying RNA vaccines. *Proceedings of the National Academy of Sciences* **2012,** *109* (36), 14604-14609.
375. Kenjo, E.; Hozumi, H.; Makita, Y.; Iwabuchi, K. A.; Fujimoto, N.; Matsumoto, S.; Kimura, M.; Amano, Y.; Ifuku, M.; Naoe, Y.; Inukai, N.; Hotta, A., Low immunogenicity of LNP allows repeated administrations of CRISPR-Cas9 mRNA into skeletal muscle in mice. *Nature Communications* **2021,** *12* (1), 7101.
376. Song, S., Alpha-1 Antitrypsin Therapy for Autoimmune Disorders. *Chronic Obstr Pulm Dis* **2018,** *5* (4), 289-301.
377. Ehlers, M. R., Immune-modulating effects of alpha-1 antitrypsin. *Biol Chem* **2014,** *395* (10), 1187-1193.
378. Oppelt, K. A.; Kuiper, J. G.; Ingrasciotta, Y.; Ientile, V.; Herings, R. M. C.; Tari, M.; Trifirò, G.; Haug, U., Characteristics and Absolute Survival of Metastatic Colorectal Cancer Patients Treated With Biologics: A Real-World Data Analysis From Three European Countries. *Frontiers in Oncology* **2021,** *11*.
379. Selinger, D. C. P.; Carbery, D. I.; Al-Asiry, D. J., The role of biologics in the treatment of patients with inflammatory bowel disease. *British Journal of Hospital Medicine* **2018,** *79* (12), 686-693.
380. McGregor, M. C.; Krings, J. G.; Nair, P.; Castro, M., Role of Biologics in Asthma. *Am J Respir Crit Care Med* **2019,** *199* (4), 433-445.
381. Jawa, V.; Terry, F.; Gokemeijer, J.; Mitra-Kaushik, S.; Roberts, B. J.; Tourdot, S.; De Groot, A. S., T-Cell Dependent Immunogenicity of Protein Therapeutics Pre-clinical Assessment and Mitigation-Updated Consensus and Review 2020. *Front Immunol* **2020,** *11*, 1301.
382. Sethu, S.; Govindappa, K.; Alhaidari, M.; Pirmohamed, M.; Park, K.; Sathish, J., Immunogenicity to biologics: mechanisms, prediction and reduction. *Arch Immunol Ther Exp (Warsz)* **2012,** *60* (5), 331-44.
383. Dingman, R.; Balu-Iyer, S. V., Immunogenicity of Protein Pharmaceuticals. *Journal of pharmaceutical sciences* **2019,** *108* (5), 1637-1654.
384. Tonelli, A. R.; Brantly, M. L., Augmentation therapy in alpha-1 antitrypsin deficiency: advances and controversies. *Ther Adv Respir Dis* **2010,** *4* (5), 289-312.
385. Flotte, T. R.; Trapnell, B. C.; Humphries, M.; Carey, B.; Calcedo, R.; Rouhani, F.; Campbell-Thompson, M.; Yachnis, A. T.; Sandhaus, R. A.; McElvaney, N. G.; Mueller, C.; Messina, L. M.; Wilson, J. M.; Brantly, M.; Knop, D. R.; Ye, G. J.;

Chulay, J. D., Phase 2 clinical trial of a recombinant adeno-associated viral vector expressing α1-antitrypsin: interim results. *Hum Gene Ther* **2011,** *22* (10), 1239-47.
386. Aliño, S. F., Long-term expression of the human α1-antitrypsin gene in mice employing anionic and cationic liposome vector. *Biochemical Pharmacology* **1997,** *54* (1), 9-13.
387. Brigham, K. L.; Lane, K. B.; Meyrick, B.; Stecenko, A. A.; Strack, S.; Cannon, D. R.; Caudill, M.; Canonico, A. E., Transfection of nasal mucosa with a normal alpha1-antitrypsin gene in alpha1-antitrypsin-deficient subjects: comparison with protein therapy. *Hum Gene Ther* **2000,** *11* (7), 1023-32.
388. Kulkarni, J. A.; Cullis, P. R.; van der Meel, R., Lipid Nanoparticles Enabling Gene Therapies: From Concepts to Clinical Utility. *Nucleic Acid Therapeutics* **2018,** *28* (3), 146-157.
389. Inaba, K.; Swiggard, W. J.; Steinman, R. M.; Romani, N.; Schuler, G.; Brinster, C., Isolation of dendritic cells. *Current protocols in immunology* **2009,** *Chapter 3*, Unit 3.7.
390. Felgner, P. L.; Gadek, T. R.; Holm, M.; Roman, R.; Chan, H. W.; Wenz, M.; Northrop, J. P.; Ringold, G. M.; Danielsen, M., Lipofection: a highly efficient, lipid-mediated DNA-transfection procedure. *Proc Natl Acad Sci U S A* **1987,** *84* (21), 7413-7.
391. Kulkarni, J. A.; Myhre, J. L.; Chen, S.; Tam, Y. Y. C.; Danescu, A.; Richman, J. M.; Cullis, P. R., Design of lipid nanoparticles for in vitro and in vivo delivery of plasmid DNA. *Nanomedicine : nanotechnology, biology, and medicine* **2017,** *13* (4), 1377-1387.
392. Leung, A. K.; Tam, Y. Y.; Cullis, P. R., Lipid nanoparticles for short interfering RNA delivery. *Advances in genetics* **2014,** *88*, 71-110.
393. Kulkarni, J. A.; Darjuan, M. M.; Mercer, J. E.; Chen, S.; van der Meel, R.; Thewalt, J. L.; Tam, Y. Y. C.; Cullis, P. R., On the Formation and Morphology of Lipid Nanoparticles Containing Ionizable Cationic Lipids and siRNA. *ACS Nano* **2018,** *12* (5), 4787-4795.
394. Digiacomo, L.; Palchetti, S.; Pozzi, D.; Amici, A.; Caracciolo, G.; Marchini, C., Cationic lipid/DNA complexes manufactured by microfluidics and bulk self-assembly exhibit different transfection behavior. *Biochemical and Biophysical Research Communications* **2018,** *503* (2), 508-512.
395. Roces, C. B.; Lou, G.; Jain, N.; Abraham, S.; Thomas, A.; Halbert, G. W.; Perrie, Y., Manufacturing Considerations for the Development of Lipid Nanoparticles Using Microfluidics. *Pharmaceutics* **2020,** *12* (11).
396. Kulkarni, J. A.; Witzigmann, D.; Chen, S.; Cullis, P. R.; van der Meel, R., Lipid Nanoparticle Technology for Clinical Translation of siRNA Therapeutics. *Accounts of Chemical Research* **2019,** *52* (9), 2435-2444.
397. Blakney, A. K.; McKay, P. F.; Hu, K.; Samnuan, K.; Jain, N.; Brown, A.; Thomas, A.; Rogers, P.; Polra, K.; Sallah, H.; Yeow, J.; Zhu, Y.; Stevens, M. M.; Geall, A.; Shattock, R. J., Polymeric and lipid nanoparticles for delivery of self-amplifying RNA vaccines. *Journal of Controlled Release* **2021,** *338*, 201-210.
398. Zhang, R.; El-Mayta, R.; Murdoch, T. J.; Warzecha, C. C.; Billingsley, M. M.; Shepherd, S. J.; Gong, N.; Wang, L.; Wilson, J. M.; Lee, D.; Mitchell, M. J., Helper lipid structure influences protein adsorption and delivery of lipid nanoparticles to spleen and liver. *Biomater Sci* **2021,** *9* (4), 1449-1463.

399. Ambegia, E.; Ansell, S.; Cullis, P.; Heyes, J.; Palmer, L.; MacLachlan, I., Stabilized plasmid–lipid particles containing PEG-diacylglycerols exhibit extended circulation lifetimes and tumor selective gene expression. *Biochimica et Biophysica Acta (BBA) - Biomembranes* **2005,** *1669* (2), 155-163.
400. Ryals, R. C.; Patel, S.; Acosta, C.; McKinney, M.; Pennesi, M. E.; Sahay, G., The effects of PEGylation on LNP based mRNA delivery to the eye. *PLOS ONE* **2020,** *15* (10), e0241006.
401. Mui, B. L.; Tam, Y. K.; Jayaraman, M.; Ansell, S. M.; Du, X.; Tam, Y. Y. C.; Lin, P. J.; Chen, S.; Narayanannair, J. K.; Rajeev, K. G.; Manoharan, M.; Akinc, A.; Maier, M. A.; Cullis, P.; Madden, T. D.; Hope, M. J., Influence of Polyethylene Glycol Lipid Desorption Rates on Pharmacokinetics and Pharmacodynamics of siRNA Lipid Nanoparticles. *Molecular therapy. Nucleic acids* **2013,** *2* (12), e139-e139.
402. Tanaka, H.; Miyama, R.; Sakurai, Y.; Tamagawa, S.; Nakai, Y.; Tange, K.; Yoshioka, H.; Akita, H., Improvement of mRNA Delivery Efficiency to a T Cell Line by Modulating PEG-Lipid Content and Phospholipid Components of Lipid Nanoparticles. *Pharmaceutics* **2021,** *13* (12), 2097.
403. Francia, V.; Schiffelers, R. M.; Cullis, P. R.; Witzigmann, D., The Biomolecular Corona of Lipid Nanoparticles for Gene Therapy. *Bioconjug Chem* **2020,** *31* (9), 2046-2059.
404. Nakamura, T.; Kawai, M.; Sato, Y.; Maeki, M.; Tokeshi, M.; Harashima, H., The Effect of Size and Charge of Lipid Nanoparticles Prepared by Microfluidic Mixing on Their Lymph Node Transitivity and Distribution. *Molecular pharmaceutics* **2020,** *17* (3), 944-953.
405. Webb, C.; Khadke, S.; Schmidt, S. T.; Roces, C. B.; Forbes, N.; Berrie, G.; Perrie, Y., The Impact of Solvent Selection: Strategies to Guide the Manufacturing of Liposomes Using Microfluidics. *Pharmaceutics* **2019,** *11* (12).
406. Basha, G.; Novobrantseva, T. I.; Rosin, N.; Tam, Y. Y. C.; Hafez, I. M.; Wong, M. K.; Sugo, T.; Ruda, V. M.; Qin, J.; Klebanov, B.; Ciufolini, M.; Akinc, A.; Tam, Y. K.; Hope, M. J.; Cullis, P. R., Influence of Cationic Lipid Composition on Gene Silencing Properties of Lipid Nanoparticle Formulations of siRNA in Antigen-Presenting Cells. *Molecular Therapy* **2011,** *19* (12), 2186-2200.
407. Quagliarini, E.; Renzi, S.; Digiacomo, L.; Giulimondi, F.; Sartori, B.; Amenitsch, H.; Tassinari, V.; Masuelli, L.; Bei, R.; Cui, L.; Wang, J.; Amici, A.; Marchini, C.; Pozzi, D.; Caracciolo, G., Microfluidic Formulation of DNA-Loaded Multicomponent Lipid Nanoparticles for Gene Delivery. *Pharmaceutics* **2021,** *13* (8).
408. Crepso, J.; Blaya, C.; Crespo, A.; Aliño, S. F., Long-term expression of the human alpha1-antitrypsin gene in mice employing anionic and cationic liposome vectors. *Biochem Pharmacol* **1996,** *51* (10), 1309-14.
409. Stolk, J.; Tov, N.; Chapman, K. R.; Fernandez, P.; MacNee, W.; Hopkinson, N. S.; Piitulainen, E.; Seersholm, N.; Vogelmeier, C. F.; Bals, R.; McElvaney, G.; Stockley, R. A., Efficacy and safety of inhaled α1-antitrypsin in patients with severe α1-antitrypsin deficiency and frequent exacerbations of COPD. *European Respiratory Journal* **2019,** *54* (5), 1900673.
410. Campos, M.; Kueppers, F.; Stocks, J.; Strange, C.; Chen, J.; Griffin, R.; Wang-Smith, L.; Cruz, M.; Vandeberg, P.; Brantly, M., Safety, immunogenicity and pharmacokinetics (PK) of a 120 mg/kg/week dose of alpha₁-

proteinase inhibitor in alpha₁-antitrypsin deficiency. *European Respiratory Journal* **2013,** *42* (Suppl 57), P4151.
411. Vidal Pla, R.; Padullés Zamora, N.; Sala Piñol, F.; Jardí Margaleff, R.; Rodríguez Frías, F.; Montoro Ronsano, J. B., [Pharmacokinetics of alpha1-antitrypsin replacement therapy in severe congenital emphysema]. *Arch Bronconeumol* **2006,** *42* (10), 553-6.
412. Lu, Y.; Song, S., Distinct immune responses to transgene products from rAAV1 and rAAV8 vectors. *Proceedings of the National Academy of Sciences* **2009,** *106* (40), 17158.
413. Ogata, A. F.; Cheng, C.-A.; Desjardins, M.; Senussi, Y.; Sherman, A. C.; Powell, M.; Novack, L.; Von, S.; Li, X.; Baden, L. R.; Walt, D. R., Circulating Severe Acute Respiratory Syndrome Coronavirus 2 (SARS-CoV-2) Vaccine Antigen Detected in the Plasma of mRNA-1273 Vaccine Recipients. *Clinical Infectious Diseases* **2021**.
414. Habjanec, L.; Halassy, B.; Tomašić, J., Comparative study of structurally related peptidoglycan monomer and muramyl dipeptide on humoral IgG immune response to ovalbumin in mouse. *International Immunopharmacology* **2010,** *10* (7), 751-759.
415. Weeratna, R. D.; McCluskie, M. J.; Xu, Y.; Davis, H. L., CpG DNA induces stronger immune responses with less toxicity than other adjuvants. *Vaccine* **2000,** *18* (17), 1755-1762.
416. Moghimi, S. M.; Szebeni, J., Stealth liposomes and long circulating nanoparticles: critical issues in pharmacokinetics, opsonization and protein-binding properties. *Progress in lipid research* **2003,** *42* (6), 463-478.
417. Immordino, M. L.; Dosio, F.; Cattel, L., Stealth liposomes: review of the basic science, rationale, and clinical applications, existing and potential. *International journal of nanomedicine* **2006,** *1* (3), 297-315.
418. Martinez-Negro, M.; Barran-Berdon, A. L.; Aicart-Ramos, C.; Moya, M. L.; de Ilarduya, C. T.; Aicart, E.; Junquera, E., Transfection of plasmid DNA by nanocarriers containing a gemini cationic lipid with an aromatic spacer or its monomeric counterpart. *Colloids and surfaces. B, Biointerfaces* **2018,** *161*, 519-527.
419. Wong, P. T.; Choi, S. K., Mechanisms and implications of dual-acting methotrexate in folate-targeted nanotherapeutic delivery. *Int J Mol Sci* **2015,** *16* (1), 1772-1790.
420. Mohanty, J.; Barooah, N.; Dhamodharan, V.; Harikrishna, S.; Pradeepkumar, P. I.; Bhasikuttan, A. C., Thioflavin T as an Efficient Inducer and Selective Fluorescent Sensor for the Human Telomeric G-Quadruplex DNA. *Journal of the American Chemical Society* **2013,** *135* (1), 367-376.
421. Wilson, A. A.; Murphy, G. J.; Hamakawa, H.; Kwok, L. W.; Srinivasan, S.; Hovav, A. H.; Mulligan, R. C.; Amar, S.; Suki, B.; Kotton, D. N., Amelioration of emphysema in mice through lentiviral transduction of long-lived pulmonary alveolar macrophages. *The Journal of clinical investigation* **2010,** *120* (1), 379-89.
422. Huysmans, H.; Zhong, Z.; De Temmerman, J.; Mui, B. L.; Tam, Y. K.; Mc Cafferty, S.; Gitsels, A.; Vanrompay, D.; Sanders, N. N., Expression Kinetics and Innate Immune Response after Electroporation and LNP-Mediated Delivery of a Self-Amplifying mRNA in the Skin. *Molecular Therapy - Nucleic Acids* **2019,** *17*, 867-878.
423. Karadagi, A.; Cavedon, A. G.; Zemack, H.; Nowak, G.; Eybye, M. E.; Zhu, X.; Guadagnin, E.; White, R. A.; Rice, L. M.; Frassetto, A. L.; Strom, S.; Jorns, C.;

Martini, P. G. V.; Ellis, E., Systemic modified messenger RNA for replacement therapy in alpha 1-antitrypsin deficiency. *Scientific Reports* **2020,** *10* (1), 7052.
424. Lino, C. A.; Harper, J. C.; Carney, J. P.; Timlin, J. A., Delivering CRISPR: a review of the challenges and approaches. *Drug Delivery* **2018,** *25* (1), 1234-1257.
425. Wei, T.; Cheng, Q.; Min, Y.-L.; Olson, E. N.; Siegwart, D. J., Systemic nanoparticle delivery of CRISPR-Cas9 ribonucleoproteins for effective tissue specific genome editing. *Nature Communications* **2020,** *11* (1), 3232.
426. Hassett, K. J.; Higgins, J.; Woods, A.; Levy, B.; Xia, Y.; Hsiao, C. J.; Acosta, E.; Almarsson, Ö.; Moore, M. J.; Brito, L. A., Impact of lipid nanoparticle size on mRNA vaccine immunogenicity. *Journal of Controlled Release* **2021,** *335*, 237-246.
427. Cifuentes-Rius, A.; Desai, A.; Yuen, D.; Johnston, A. P. R.; Voelcker, N. H., Inducing immune tolerance with dendritic cell-targeting nanomedicines. *Nature Nanotechnology* **2021,** *16* (1), 37-46.
428. Manolova, V.; Flace, A.; Bauer, M.; Schwarz, K.; Saudan, P.; Bachmann, M. F., Nanoparticles target distinct dendritic cell populations according to their size. *Eur J Immunol* **2008,** *38* (5), 1404-13.
429. Hong, D. K.; Chang, S.; Botham, C. M.; Giffon, T. D.; Fairman, J.; Lewis, D. B., Cationic lipid/DNA complex-adjuvanted influenza A virus vaccination induces robust cross-protective immunity. *Journal of virology* **2010,** *84* (24), 12691-702.
430. Tseng, Y. S.; Agbandje-McKenna, M., Mapping the AAV Capsid Host Antibody Response toward the Development of Second Generation Gene Delivery Vectors. *Front Immunol* **2014,** *5*, 9.
431. Shirley, J. L.; de Jong, Y. P.; Terhorst, C.; Herzog, R. W., Immune Responses to Viral Gene Therapy Vectors. *Molecular Therapy* **2020,** *28* (3), 709-722.
432. Mingozzi, F.; High, K. A., Immune responses to AAV vectors: overcoming barriers to successful gene therapy. *Blood* **2013,** *122* (1), 23-36.
433. Russell, S.; Bennett, J.; Wellman, J. A.; Chung, D. C.; Yu, Z.-F.; Tillman, A.; Wittes, J.; Pappas, J.; Elci, O.; McCague, S.; Cross, D.; Marshall, K. A.; Walshire, J.; Kehoe, T. L.; Reichert, H.; Davis, M.; Raffini, L.; George, L. A.; Hudson, F. P.; Dingfield, L.; Zhu, X.; Haller, J. A.; Sohn, E. H.; Mahajan, V. B.; Pfeifer, W.; Weckmann, M.; Johnson, C.; Gewaily, D.; Drack, A.; Stone, E.; Wachtel, K.; Simonelli, F.; Leroy, B. P.; Wright, J. F.; High, K. A.; Maguire, A. M., Efficacy and safety of voretigene neparvovec (AAV2-hRPE65v2) in patients with RPE65-mediated inherited retinal dystrophy: a randomised, controlled, open-label, phase 3 trial. *Lancet (London, England)* **2017,** *390* (10097), 849-860.
434. Ferreira, V.; Petry, H.; Salmon, F., Immune Responses to AAV-Vectors, the Glybera Example from Bench to Bedside. *Frontiers in immunology* **2014,** *5*, 82-82.
435. Hoy, S. M., Onasemnogene Abeparvovec: First Global Approval. *Drugs* **2019,** *79* (11), 1255-1262.
436. Zhong, C.; Jiang, W.; Wang, Y.; Sun, J.; Wu, X.; Zhuang, Y.; Xiao, X., Repeated Systemic Dosing of Adeno-Associated Virus Vectors in Immunocompetent Mice After Blockade of T Cell Costimulatory Pathways. *Hum Gene Ther* **2022,** *33* (5-6), 290-300.
437. Ilyinskii, P. O.; Michaud, A. M.; Roy, C. J.; Rizzo, G. L.; Elkins, S. L.; Capela, T.; Chowdhury, A. C.; Leung, S. S.; Kishimoto, T. K., Enhancement of liver-

directed transgene expression at initial and repeat doses of AAV vectors admixed with ImmTOR nanoparticles. *Sci Adv* **2021,** *7* (9).
438. Meliani, A.; Boisgerault, F.; Hardet, R.; Marmier, S.; Collaud, F.; Ronzitti, G.; Leborgne, C.; Costa Verdera, H.; Simon Sola, M.; Charles, S.; Vignaud, A.; van Wittenberghe, L.; Manni, G.; Christophe, O.; Fallarino, F.; Roy, C.; Michaud, A.; Ilyinskii, P.; Kishimoto, T. K.; Mingozzi, F., Antigen-selective modulation of AAV immunogenicity with tolerogenic rapamycin nanoparticles enables successful vector re-administration. *Nature Communications* **2018,** *9* (1), 4098.
439. Gluck, T.; Kiefmann, B.; Grohmann, M.; Falk, W.; Straub, R. H.; Scholmerich, J., Immune status and risk for infection in patients receiving chronic immunosuppressive therapy. *The Journal of rheumatology* **2005,** *32* (8), 1473-80.
440. Engels, E. A.; Pfeiffer, R. M.; Fraumeni, J. F., Jr.; Kasiske, B. L.; Israni, A. K.; Snyder, J. J.; Wolfe, R. A.; Goodrich, N. P.; Bayakly, A. R.; Clarke, C. A.; Copeland, G.; Finch, J. L.; Fleissner, M. L.; Goodman, M. T.; Kahn, A.; Koch, L.; Lynch, C. F.; Madeleine, M. M.; Pawlish, K.; Rao, C.; Williams, M. A.; Castenson, D.; Curry, M.; Parsons, R.; Fant, G.; Lin, M., Spectrum of cancer risk among US solid organ transplant recipients. *JAMA* **2011,** *306* (17), 1891-1901.
441. Kishimoto, T. K., Development of ImmTOR Tolerogenic Nanoparticles for the Mitigation of Anti-drug Antibodies. *Frontiers in Immunology* **2020,** *11*.
442. Mima, Y.; Hashimoto, Y.; Shimizu, T.; Kiwada, H.; Ishida, T., Anti-PEG IgM Is a Major Contributor to the Accelerated Blood Clearance of Polyethylene Glycol-Conjugated Protein. *Molecular pharmaceutics* **2015,** *12* (7), 2429-2435.
443. Suzuki, T.; Ichihara, M.; Hyodo, K.; Yamamoto, E.; Ishida, T.; Kiwada, H.; Ishihara, H.; Kikuchi, H., Accelerated blood clearance of PEGylated liposomes containing doxorubicin upon repeated administration to dogs. *International journal of pharmaceutics* **2012,** *436* (1-2), 636-43.
444. Ichikawa, K.; Asai, T.; Shimizu, K.; Yonezawa, S.; Urakami, T.; Miyauchi, H.; Kawashima, H.; Ishida, T.; Kiwada, H.; Oku, N., Suppression of immune response by antigen-modified liposomes encapsulating model agents: a novel strategy for the treatment of allergy. *Journal of controlled release : official journal of the Controlled Release Society* **2013,** *167* (3), 284-9.
445. Henson, D., IDENTIFICATION AND CHARACTERIZATION OF EPITOPE SPECIFIC IMMUNE RESPONSES INN HUMANS AND MICE. *University of Kentucky Theses and Dissertations - Pharmacy.* **2021**.
446. Le, D. T.; Radukic, M. T.; Müller, K. M., Adeno-associated virus capsid protein expression in Escherichia coli and chemically defined capsid assembly. *Scientific Reports* **2019,** *9* (1), 18631.
447. Nielsen, U. B.; Kirpotin, D. B.; Pickering, E. M.; Drummond, D. C.; Marks, J. D., A novel assay for monitoring internalization of nanocarrier coupled antibodies. *BMC immunology* **2006,** *7*, 24-24.
448. Fritze, A.; Hens, F.; Kimpfler, A.; Schubert, R.; Peschka-Süss, R., Remote loading of doxorubicin into liposomes driven by a transmembrane phosphate gradient. *Biochimica et Biophysica Acta (BBA) - Biomembranes* **2006,** *1758* (10), 1633-1640.
449. Chan, K. Y.; Jang, M. J.; Yoo, B. B.; Greenbaum, A.; Ravi, N.; Wu, W. L.; Sánchez-Guardado, L.; Lois, C.; Mazmanian, S. K.; Deverman, B. E.; Gradinaru, V.,

Engineered AAVs for efficient noninvasive gene delivery to the central and peripheral nervous systems. *Nat Neurosci* **2017,** *20* (8), 1172-1179.
450. Wang, M.; Crosby, A.; Hastie, E.; Samulski, J. J.; McPhee, S.; Joshua, G.; Samulski, R. J.; Li, C., Prediction of adeno-associated virus neutralizing antibody activity for clinical application. *Gene therapy* **2015,** *22* (12), 984-92.
451. Li, C.; Wu, S.; Albright, B.; Hirsch, M.; Li, W.; Tseng, Y. S.; Agbandje-McKenna, M.; McPhee, S.; Asokan, A.; Samulski, R. J., Development of Patient-specific AAV Vectors After Neutralizing Antibody Selection for Enhanced Muscle Gene Transfer. *Molecular therapy : the journal of the American Society of Gene Therapy* **2016,** *24* (1), 53-65.
452. Chen, Z.; Moon, J. J.; Cheng, W., Quantitation and Stability of Protein Conjugation on Liposomes for Controlled Density of Surface Epitopes. *Bioconjug Chem* **2018,** *29* (4), 1251-1260.
453. Tombácz, I.; Laczkó, D.; Shahnawaz, H.; Muramatsu, H.; Natesan, A.; Yadegari, A.; Papp, T. E.; Alameh, M. G.; Shuvaev, V.; Mui, B. L.; Tam, Y. K.; Muzykantov, V.; Pardi, N.; Weissman, D.; Parhiz, H., Highly efficient CD4+ T cell targeting and genetic recombination using engineered CD4+ cell-homing mRNA-LNPs. *Molecular therapy : the journal of the American Society of Gene Therapy* **2021,** *29* (11), 3293-3304.
454. Lu, W. L.; Qi, X. R.; Zhang, Q.; Li, R. Y.; Wang, G. L.; Zhang, R. J.; Wei, S. L., A pegylated liposomal platform: pharmacokinetics, pharmacodynamics, and toxicity in mice using doxorubicin as a model drug. *J Pharmacol Sci* **2004,** *95* (3), 381-9.
455. Maldonado, R. A.; LaMothe, R. A.; Ferrari, J. D.; Zhang, A. H.; Rossi, R. J.; Kolte, P. N.; Griset, A. P.; O'Neil, C.; Altreuter, D. H.; Browning, E.; Johnston, L.; Farokhzad, O. C.; Langer, R.; Scott, D. W.; von Andrian, U. H.; Kishimoto, T. K., Polymeric synthetic nanoparticles for the induction of antigen-specific immunological tolerance. *Proc Natl Acad Sci U S A* **2015,** *112* (2), E156-65.
456. Pan, Y.; Ke, H.; Yan, Z.; Geng, Y.; Asner, N.; Palani, S.; Munirathinam, G.; Dasari, S.; Nitiss, K. C.; Bliss, S.; Patel, P.; Shen, H.; Reardon, C. A.; Getz, G. S.; Chen, A.; Zheng, G., The western-type diet induces anti-HMGB1 autoimmunity in Apoe(-/-) mice. *Atherosclerosis* **2016,** *251*, 31-38.
457. Boutin, S.; Monteilhet, V.; Veron, P.; Leborgne, C.; Benveniste, O.; Montus, M. F.; Masurier, C., Prevalence of Serum IgG and Neutralizing Factors Against Adeno-Associated Virus (AAV) Types 1, 2, 5, 6, 8, and 9 in the Healthy Population: Implications for Gene Therapy Using AAV Vectors. *Human Gene Therapy* **2010,** *21* (6), 704-712.
458. Wobus, C. E.; Hügle-Dörr, B.; Girod, A.; Petersen, G.; Hallek, M.; Kleinschmidt, J. A., Monoclonal antibodies against the adeno-associated virus type 2 (AAV-2) capsid: epitope mapping and identification of capsid domains involved in AAV-2-cell interaction and neutralization of AAV-2 infection. *Journal of virology* **2000,** *74* (19), 9281-9293.
459. Moskalenko, M.; Chen, L.; van Roey, M.; Donahue, B. A.; Snyder, R. O.; McArthur, J. G.; Patel, S. D., Epitope mapping of human anti-adeno-associated virus type 2 neutralizing antibodies: implications for gene therapy and virus structure. *Journal of virology* **2000,** *74* (4), 1761-1766.

460. Gurda, B. L.; Raupp, C.; Popa-Wagner, R.; Naumer, M.; Olson, N. H.; Ng, R.; McKenna, R.; Baker, T. S.; Kleinschmidt, J. A.; Agbandje-McKenna, M., Mapping a neutralizing epitope onto the capsid of adeno-associated virus serotype 8. *Journal of virology* **2012,** *86* (15), 7739-51.
461. Giles April, R.; Govindasamy, L.; Somanathan, S.; Wilson James, M.; Sandri-Goldin Rozanne, M., Mapping an Adeno-associated Virus 9-Specific Neutralizing Epitope To Develop Next-Generation Gene Delivery Vectors. *Journal of virology 92* (20), e01011-18.
462. Hui, D. J.; Edmonson, S. C.; Podsakoff, G. M.; Pien, G. C.; Ivanciu, L.; Camire, R. M.; Ertl, H.; Mingozzi, F.; High, K. A.; Basner-Tschakarjan, E., AAV capsid CD8+ T-cell epitopes are highly conserved across AAV serotypes. *Molecular therapy. Methods & clinical development* **2015,** *2*, 15029-15029.
463. Sabatino, D. E.; Mingozzi, F.; Hui, D. J.; Chen, H.; Colosi, P.; Ertl, H. C.; High, K. A., Identification of mouse AAV capsid-specific CD8+ T cell epitopes. *Molecular therapy : the journal of the American Society of Gene Therapy* **2005,** *12* (6), 1023-33.
464. Tellez, J.; Van Vliet, K.; Tseng, Y.-S.; Finn, J. D.; Tschernia, N.; Almeida-Porada, G.; Arruda, V. R.; Agbandje-McKenna, M.; Porada, C. D., Characterization of naturally-occurring humoral immunity to AAV in sheep. *PloS one* **2013,** *8* (9), e75142-e75142.
465. Govindasamy, L.; Padron, E.; McKenna, R.; Muzyczka, N.; Kaludov, N.; Chiorini John, A.; Agbandje-McKenna, M., Structurally Mapping the Diverse Phenotype of Adeno-Associated Virus Serotype 4. *Journal of virology* **2006,** *80* (23), 11556-11570.
466. Calcedo, R.; Vandenberghe, L. H.; Gao, G.; Lin, J.; Wilson, J. M., Worldwide epidemiology of neutralizing antibodies to adeno-associated viruses. *The Journal of infectious diseases* **2009,** *199* (3), 381-90.
467. Wilson, A. A.; Kwok, L. W.; Hovav, A. H.; Ohle, S. J.; Little, F. F.; Fine, A.; Kotton, D. N., Sustained expression of alpha1-antitrypsin after transplantation of manipulated hematopoietic stem cells. *American journal of respiratory cell and molecular biology* **2008,** *39* (2), 133-41.
468. Kruzik, A.; Fetahagic, D.; Hartlieb, B.; Dorn, S.; Koppensteiner, H.; Horling, F. M.; Scheiflinger, F.; Reipert, B. M.; de la Rosa, M., Prevalence of Anti-Adeno-Associated Virus Immune Responses in International Cohorts of Healthy Donors. *Mol Ther Methods Clin Dev* **2019,** *14*, 126-133.
469. Hecker, M.; Lorenz, P.; Steinbeck, F.; Hong, L.; Riemekasten, G.; Li, Y.; Zettl, U. K.; Thiesen, H.-J., Computational analysis of high-density peptide microarray data with application from systemic sclerosis to multiple sclerosis. *Autoimmunity Reviews* **2012,** *11* (3), 180-190.
470. Loeffler, F. F.; Pfeil, J.; Heiss, K., High-Density Peptide Arrays for Malaria Vaccine Development. *Methods in molecular biology (Clifton, N.J.)* **2016,** *1403*, 569-82.
471. Ruwona, T. B.; McBride, R.; Chappel, R.; Head, S. R.; Ordoukhanian, P.; Burton, D. R.; Law, M., Optimization of peptide arrays for studying antibodies to hepatitis C virus continuous epitopes. *Journal of immunological methods* **2014,** *402* (1-2), 35-42.

472. Melnyk, O.; Duburcq, X.; Olivier, C.; Urbès, F.; Auriault, C.; Gras-Masse, H., Peptide Arrays for Highly Sensitive and Specific Antibody-Binding Fluorescence Assays. *Bioconjugate Chemistry* **2002,** *13* (4), 713-720.
473. Opella, S. J.; Marassi, F. M., Applications of NMR to membrane proteins. *Arch Biochem Biophys* **2017,** *628*, 92-101.
474. Du, H.; Samuel, R. L.; Massiah, M. A.; Gillmor, S. D., The structure and behavior of the NA-CATH antimicrobial peptide with liposomes. *Biochimica et Biophysica Acta (BBA) - Biomembranes* **2015,** *1848* (10, Part A), 2394-2405.
475. Mäler, L., Solution NMR studies of peptide-lipid interactions in model membranes. *Molecular membrane biology* **2012,** *29* (5), 155-176.
476. van der Velden, V. H., Glucocorticoids: mechanisms of action and anti-inflammatory potential in asthma. *Mediators of inflammation* **1998,** *7* (4), 229-237.
477. Oh, Y. K.; Nix, D. E.; Straubinger, R. M., Formulation and efficacy of liposome-encapsulated antibiotics for therapy of intracellular Mycobacterium avium infection. *Antimicrobial Agents and Chemotherapy* **1995,** *39* (9), 2104-2111.
478. Murphy, B. S.; Sundareshan, V.; Cory, T. J.; Hayes, D., Jr.; Anstead, M. I.; Feola, D. J., Azithromycin alters macrophage phenotype. *The Journal of antimicrobial chemotherapy* **2008,** *61* (3), 554-60.
479. Al-Darraji, A.; Haydar, D.; Chelvarajan, L.; Tripathi, H.; Levitan, B.; Gao, E.; Venditto, V. J.; Gensel, J.; Feola, D. J.; Abdel-Latif, A., Azithromycin therapy reduces cardiac inflammation and mitigates adverse cardiac remodeling after myocardial infarction: Potential therapeutic targets in ischemic heart disease. *PLOS ONE* **2018,** *In press*.
480. Feola, D. J.; Garvy, B. A.; Cory, T. J.; Birket, S. E.; Hoy, H.; Hayes, D., Jr.; Murphy, B. S., Azithromycin alters macrophage phenotype and pulmonary compartmentalization during lung infection with Pseudomonas. *Antimicrob Agents Chemother* **2010,** *54* (6), 2437-47.
481. Zhang, B.; Bailey, W. M.; Kopper, T. J.; Orr, M. B.; Feola, D. J.; Gensel, J. C., Azithromycin drives alternative macrophage activation and improves recovery and tissue sparing in contusion spinal cord injury. *Journal of neuroinflammation* **2015,** *12*, 218.

VITA

David Nardo

EDUCATION

May 2016	**Doctor of Pharmacy** – University of Florida – Gainesville, FL
May 2012	**Bachelor's Degree in Biology** – Emory University – Atlanta, GA
May 2010	**Associate degree in Biology** – Miami Dade College – Miami, FL

RESEARCH AND WORK EXPERIENCE

Aug. 2017 – Present	**Graduate Research Assistant** – UK College of Pharmacy – Lexington, KY
Jul. 2016 – Jun. 2017	**Pharmacy Resident** – Newark Beth Israel Medical Center – Newark, NJ
May 2014 – Aug. 2014	**Research Intern** – UF College of Pharmacy – Gainesville, FL

TEACHING EXPERIENCE

May 2018 – Present	**Undergraduate Student Mentor** – University of Kentucky – Lexington, KY
Aug. 2017 – May 2019	**Teaching Assistant** – University of Kentucky – Lexington, KY

PUBLICATIONS

Nardo D, Kaur R, Pitts MG, Venditto VJ. Toxicity and immunogenicity of triazine based cationic lipids and their transgenes. Under review by Biomaterials Science.

Nardo D, Akers CM, Cheung NE, Isom CM, Spaude JT, Pack DW, Venditto VJ. Cyanuric chloride as the basis for compositionally diverse lipids. RSC Adv. 2021 Jul 15;11(40):24752-24761.

Pitts MG, **Nardo D**, Isom CM, Venditto VJ. Autoantibody Responses to Apolipoprotein A-I Are Not Diet- or Sex-Linked in C57BL/6 Mice. Immunohorizons. 2020 Aug 5;4(8):455-463.

Nardo D, David Henson, Joe E. Springer, Vincent J. Venditto. Chapter Six - Modulating the immune responses with liposomal delivery. Editor(s): Natassa Pippa, Costas Demetzos, In Micro and Nano Technologies, Nanomaterials for Clinical Applications, Elsevier, 2020, p. 159-211, ISBN 9780128167052.

Akbar MA, **Nardo D**, Chen MJ, et al. Alpha-1 antitrypsin inhibits RANKL-induced osteoclast formation and functions. Mol Med. 2017 Mar 21;23.

Akbar MA, Cao JJ, Lu Y, **Nardo D,** et al. Alpha-1 antitrypsin gene therapy ameliorates bone loss in ovariectomy-induced osteoporosis mouse model. Hum Gene Ther. 2016

Sep;27(9):679-86.

Liu L, **Nardo D**, Li E, Wang GP. CD4+ T-cell recovery with suppressive ART-induced rapid sequence evolution in hepatitis C virus envelope but not NS3. AIDS. 2016 Mar 13;30(5):691-700.

POSTERS AND PRESENTATIONS

Nov. 2021	Evaluation of immunity toward plasmid transgenes delivered via synthetic lipids. Autumn Immunology Conference. Chicago, IL.
Oct. 2020	Translational applications of triazine lipids. University of Kentucky Center for Clinical and Translational Science. Lexington, KY.
Aug. 2020	Introduction and survival guide to pharmaceutical sciences. UKY Pharmaceutical Sciences Clinical and Experimental Therapeutics Division. Lexington, KY.
Aug. 2020	Triazine lipids as therapeutic strategies. UKY Department of Pharmaceutical Sciences. Lexington, KY.
Oct. 2019	Synthesis of cyanuric chloride lipids for gene and vaccine delivery. UKY Department of Pharmaceutical Sciences. Lexington, KY.
Aug. 2019	Synthesis of triazine lipids and their applications in pharmaceutical delivery. UKY Pharmaceutical Sciences Clinical and Experimental Therapeutics Division. Lexington, KY.
Mar. 2018	Epitope specific suppression of ApoA-I peptide using liposomal doxorubicin. UKY Department of Pharmaceutical Sciences, Rho Chi Research Day poster presentation. Lexington, KY.

AWARDS

Feb. 2020	Peter G. Glavinos, Jr., Ph.D. Travel Award – Awardee
Jul. 2019 – May 2021	CCTS TL1 Fellowship – NIH Grant: 5TL1TR001997-03 – Awardee
Aug. 2017 – May 2019	Lyman T. Johnson Diversity Fellowship - Awardee

MEMBERSHIPS

May 2021	American Society of Virology – Student member
Jul. 2018 – Present	American Society of Gene and Cell Therapy – Student member
Sept. 2015 – Dec. 2018	American Society of Health System Pharmacists – Student member

ACADEMIC SERVICE

Jan. 2018 – Dec. 2020	Graduate student representative for UK College of Pharmacy Research Domain Advisory Committee
Sept. 2019 – Dec. 2020	Coordinator of Clinical and Experimental Therapeutics division of the UK College of Pharmacy graduate student track
Nov. 2018 – May 2020	Graduate student representative for the Inclusion and Diversity Task Force

VOLUNTEER EXPERIENCE

Jan. 2019 – Present	**Science Fair Judge** – KY School System – Lexington, KY
May 2021 – Jul. 2021	**Spanish Translator** – Wild Health – Lexington, KY
Oct. 2018 – Apr. 2022	**Pharmacy Preceptor** – Salvation Army Clinic – Lexington, KY
Jan. 2019 – May 2019	**SciCats** – University of Kentucky – Lexington, KY
May 2013 – Feb. 2015	**Volunteer Researcher** – UF College of Medicine – Gainesville, FL
Jan. 2013 – Feb. 2015	**Volunteer** – Florida Department of Health – Gainesville, FL

CERTIFICATIONS AND LICENSES

Jul. 2017	**Kentucky Pharmacist License (019298)**
Oct. 2021	**Methods to Promote Data Reproducibility in Laboratory Research**